Section 2.3 References

1. Bettinger et al. 2003. Bettinger, Jason, John Crane, and James Bulak. *Broad River Aquatic Resources Inventory Completion Report (Draft)*, Broad River Comprehensive Entrainment Mitigation and Fisheries Resources Enhancement Program, South Carolina Department of Natural Resources. January 28, 2003.

2. Brewer, K. E. and C. S. Sochor, 2002. *"Flow and Transport Modeling for D-Area Groundwater,"* Report Number WSRC-RP-2002-4166 prepared by Washington Savannah River Company for the DOE.

3. Childress, J. M. 2006. *South Carolina Ambient Groundwater Quality Report,* Technical Document Number 005-06, South Carolina Bureau of Water, South Carolina Department of Health and Environmental Control, Columbia, South Carolina, 23 pages, available at http://www.scdhec.gov/water/pubs/amb2004.pdf.

4. Childress, J. M., and A. Butler 2006. *South Carolina Water Use Report, 2005 Annual Summary,* Technical Document Number 006-06, South Carolina Bureau of Water, South Carolina Department of Health and Environmental Control, Columbia, South Carolina, 44 pages, available at http://www.scdhec.net/EQC/water/pubs/wtruse2005.pdf.

5. Cooney et al. 2006. Cooney, T. W., P. A. Drewes, S. W. Ellisor, T. H. Lanier and F. Melendez 2006. *Water Resources Data South Carolina: Water Year 2005,* Water-Data Report SC-05-1, U.S. Department of the Interior, U.S. Geological Survey, Columbia, South Carolina, 621 pages, available at http://pubs.er.usgs.gov/usgspubs/wdr/wdrSC051.

6. Craig, R. F. *Soil Mechanics, 6th Edition*, E & FN Spon, London, 1997 Page 25-26.

7. Devlin, R. 2006. Electronic Mail to J. Giles (SCE&G) regarding surface and groundwater withdrawals. Groundwater Management Section, South Carolina Department of Health and Environmental Control, December 8, 2006.

8. Fairfield County 1997. *Fairfield County Comprehensive Plan Update,* Winnsboro, South Carolina. April 1997.

9. FEMA (Federal Emergency Management Agency) Map Service Center. FEMA issued flood map (ID 4500750175B), Fairfield County, South Carolina, effective date: 07/19/1982, http://msc.fema.gov/webappp/wcs/stores/servlet/FemaWelcomeView?storeId=10001&catalogId=10001&landId=1.

10. Fetter, C.W. 1988. *Applied Hydrogeology, Second Edition*, Macmillan Publishing Company, New York.

11. Fogle, T. L. and K. E. Brewer 2001. *Groundwater Transport Modeling for Southern TCE and Tritium Plumes in the C-Area Groundwater Operable Unit,"* Report Number WSRC-TR-2001-00206 prepared by Washington Savannah River Company for the DOE 2001.

12. FPC (Federal Power Commission) 1974. Order Issuing New License (Major) Authorizing Project Redevelopment, Permitting Use of Project Waters for Condenser Cooling Purposes, Vacating Hearing Order, and Permitting Withdrawal of Intervention. Project No. 1894. Issued August 28, 1974.

13. Geotrans 1997. *Groundwater Flow and Solute Transport Modeling Report K-Area Burning Rubble Pit and Rubble Pile,"* Report Number WSRC-RP-98-5052 prepared by Washington Savannah River Company for the Department of Energy.

14. INTERA 2003. *"Groundwater Flow and Contaminant Transport Modeling in Support of the RRSB Operable Unit,"* Report Number WSRC-RP-2002-4081 prepared by Washington Savannah River Company for the DOE.

15. Julien, Pierre Y. 1998. *Erosion and Sedimentation*, Cambridge University Press, 1998.

16. Keyes and Radcliffe 2002. A Protocol for Establishing Sediment TDMLs developed by the Georgia Conservancy and the UGA Institute of Ecology, 2002.

17. MACTEC Engineering and Consulting 2007. Final Data Report, Results of Geotechnical Exploration and Testing, SCE&G COL Project, V.C. Summer Nuclear Station, Jenkinsville, Fairfield County, South Carolina, Revision 2, February 28.

18. de Marsily, G., 1986. *Quantitative Hydrogeology: Groundwater Hydrology for Engineers,* Academic Press, Inc., Orlando, Florida 1986.

19. Miller, J. A., 1990. *Ground Water Atlas of the United States*, Segment 6, Alabama, Florida, Georgia, and South Carolina, U.S. Geological Survey, Hydrologic Investigations Atlas 730-G, 1990.

20. NCDWQ (North Carolina Division of Water Quality) 1998. *Broad Basinwide Water Quality Management Plan,* North Carolina Division of Water Quality, July 1998. Available at: http://h2o.enr.state.nc.us/basinwide/Broad/broad_basinwide_water_quality_ma.htm. Accessed April 27, 2007.

21. Parker, G., 2007. *Transport of Gravel and Sediment Mixtures,* ASCE Manual 54, Sediment Engineering, Chapter 3Draft available at http://cee.uiuc.edu/people/parkerg/manual_54.htm. (in press).

22. Pettijohn, F. J., Potter, P.E. and R. Siever 1972. *Sand and Sandstone,* Springer, New York, 1972.

23. Purvis J. C. *Pan Evaporation Records for the South Carolina Area,* Department of Natural Resources of South Carolina, Southeast Regional Climate Center Columbia, South Carolina. Available at http://www.dnr.sc.gov/climate/sco/Publications/pan_evap_records.php. Accessed August 7, 2007.

24. SCDHEC (South Carolina Department of Health and Environmental Control) 1998. *Watershed Management Strategy for the Broad Basin,* 1998.

25. SCDHEC 2001. Bureau of Water, *Watershed Water Quality Assessment, Broad River Basin,* Bureau of Water, Technical Report No. 001-01, 2001.

26. SCDHEC 2003. *Source Water Protection, Source Water Assessment,* Bureau of Water. April 29, 2003. Available at http://www.scdhec.net/water.

27. SCDHEC 2004. *2004 303(d) List – State of South Carolina Integrated Report Part I: Listing of Impaired Waters.* Available at www.scdhec.gov/water/tmdl/index.html. Accessed July 17, 2006.

28. SCDHEC 2005. *South Carolina Water Use Report 2004 Summary,* Bureau of Water, Technical Document Number: 004-05. July 2005.

29. SCDHEC 2006a. *2006 305(b) Report – State of South Carolina Integrated Report Part II: Assessment and Reporting.* Available at www.scdhec.net/EQC/water/tmdl/index.html. Accessed July 17, 2006.

30. SCDHEC 2006b. Draft *2006 303(d) List – State of South Carolina Integrated Report Part I: Listing of Impaired Waters.* Available at www.scdhec.net/EQC/water/tmdl/index.html. Accessed May 2, 2006.

31. SCDHEC 2006c. FOIA Response: List of all surface water users (>100,000 gallons/day) downstream of the VCSNS. Response provided by Erica Johnson, Water Quality Modeling to Stephen E. Summer, SCE&G via e-mail Sept. 11, 2006.

32. SCDHEC 2006d. *South Carolina Ambient Groundwater Quality Report 2004 Summary*, February 2006.

33. SCDHEC 2007, Broad River Watershed 03050105-090, Available at http://www.scdhec.gov/environment/water/shed/text/50105-090.pdf. Accessed April 27, 2007.

34. SCDNR (South Carolina Department of Natural Resources) 2005. *The 100 Largest Water Supplies in South Carolina, Water Resources Report 37*, 2005.

35. SCE&G 1971. *Preliminary Safety Analysis Report: Virgil C. Summer Nuclear Station, Unit 1*, 1971.

36. SCE&G 1994. *Temperature and Dissolved Oxygen Monitoring in the Vicinity of the VCSNS Circulating Water Intake, Monticello Reservoir, Summer 1994*, 1994.

37. SCE&G 1995. *Water Quality Monitoring for the Monticello Reservoir*, March 1, 1996.

38. SCE&G 1996. *Water Quality Monitoring for the Monticello Reservoir, March 5, 1997.*

39. SCE&G 2001. *2000 Water Quality Monitoring Report For Monticello Reservoir*, Environmental Services SCE&G, February 14, 2001.

40. SCE&G 2002a. *Applicant's Environmental Report*, Operating License Stage Virgil C. Summer Nuclear Station, August 2002.

41. SCE&G 2002b. *2001 Water Quality Monitoring Report For Monticello Reservoir*, Environmental Services, SCE&G, February 28, 2002.

42. SCE&G 2002c. Virgil C. *Summer Nuclear Station Radiological Environmental Operating Report,* April 24, 2002.

43. SCE&G 2003a. *2002 Water Quality Monitoring Report For Monticello Reservoir*, Environmental Services, SCE&G, February 10, 2003.

44. SCE&G 2003b. *Virgil C. Summer Nuclear Station Radiological Environmental Operating Report*, April 14 3004.

45. SCE&G 2004a. *2003 Water Quality Monitoring Report For Monticello Reservoir*, Environmental Services, SCE&G, February 10, 2004.

46. SCE&G 2004b. *Virgil C. Summer Nuclear Station Radiological Environmental Operating Report,* April 30, 2004.

47. SCE&G 2005b. *V.C. Summer Nuclear Station FSAR*, last updated 2005.

48. SCE&G 2005a. *Virgil C. Summer Nuclear Station Radiological Environmental Operating Report*. April 20., 2005.

49. SCE&G 2006a. *Supporting Technical Information Document — Parr Shoals Hydroelectric Project P-1894 — Fairfield Development,* compiled by Devine Tarbell Associates, Charlotte, North Carolina, and published in May 2006.

50. SCE&G 2006b. *2005 Water Quality Monitoring Report For Monticello Reservoir*, Environmental Services, SCE&G, February 21, 2006.

51. SCE&G 2006c. *SCE&G Discharge Monitoring Reports for VCSNS 2001-2005,* 2006.

52. SCE&G 2006d, *Virgil C. Summer Nuclear Station Radiological Environmental Operating Report,* April 28, 2006.

53. SCE&G 2007a. *2006 Water Quality Monitoring for the Monticello Reservoir,* February 12, 2007.

54. SCE&G 2007b. *Estimate of Evaporation,* personal communication, Lisa Matis of TtNUS and Ray Ammarell of SCE&G, August 29, 2007.

55. Syvitski, J. P. M., Peckham, S. D., Hilberman, R., Mulder, T., 2003. *Predicting the Terrestrial Flux of Sediment to the Global Ocean: a Planetary Perspective*, 162, pp. 5-24, 2003.

56. Schumm, S. A. 1985. *"Patterns of Alluvial Rivers,"* Annual Review of Earth and Planetary Sciences 13: 5-27, 1985.

57. Trimble, S. W. 1974. *Man-Induced Soil Erosion on the Southern Piedmont 1700-1970.* Soil and Water Conservation Society of America, Ankenny, Iowa, 1974.

58. TtNUS (Tetra Tech NUS) 2007. *Mayo Creek Aquatic Survey,* Aiken, South Carolina. June 2007.

59. USACE (U.S. Army Corps of Engineers) 2002. T*hreatened & Endangered Species of the Upper Savannah River Basin – Southern Bald Eagle.* Available at http://www.sas.usace.army.mil/endspec.htm.

60. U.S. EPA 2005. *Safe Drinking Water Information System for South Carolina, List of Water Systems in SDWIS for Fairfield, Lexington, Newberry, and Richland Counties,* October 14. Available at http://oaspub.epa.gov/enviro/sdw.

61. U.S. EPA 2006. EPA STORET Data Warehouse, South Carolina Department of Health and Environmental Control Water Quality Data for Parr Reservoir and Monticello Reservoir, last updated 3/9/2006. Available at http://www.epa.gov/storet/dw_home.html. Accessed December 8, 2006.

62. U.S. EPA 2007. Ground Water Protection program database. Available at http://www.epa.gov/region4/water/groundwater/r4ssa.htm. Accessed April 18, 2007.

63. USGS (U.S. Geological Survey) 2006. *Surface-Water Data for the Nation.* Available at http://waterdata.usgs.gov/usa/nwis/sw. Accessed April 24, 2006.

64. USGS 2007. Letter from Toby D. Feaster, Hydrologist of the U.S. Geological Survey, South Carolina Water Science Center, Clemson Field Office to Steve Summer, dated March 6, 2007.

65. U.S. NRC 1981. *Final Environmental Statement related to the operation of Virgil C. Summer Nuclear Station Unit No. 1*, Office of Nuclear Reactor Regulation, Washington, D.C., 1981.

Sec 2.3 Ref 1

Broad River Comprehensive Entrainment Mitigation and Fisheries Resource Enhancement Program

Broad River Aquatic Resources Inventory Completion Report (DRAFT)

EG-040

Submitted by

Jason Bettinger, John Crane, and James Bulak

South Carolina Department of Natural Resources

January 28, 2003

EXECUTIVE SUMMARY

1. We evaluated the condition of 312 km of riparian habitat along the Broad River. Approximately 87% of the riparian area was in good condition, 12% was marginal, and only 1% was considered to be in poor condition. Poor bank stability was observed above Parr Shoals Reservoir.

2. We made 181 standardized boat electrofishing collections and 23 catfish electrofishing collections at 10 sites in the Broad River between January 2001 and May 2002. In addition, we made 676 standardized plot samples and 33 shoreline samples with backpack electrofishing gear at 9 sites in the Broad River between fall 2000 and spring 2002.

3. We collected 16,752 fish, comprising 51 species and nine families. No federally-listed threatened or endangered species were collected. Four species (including one hybrid) were not previously documented from the river. The species most commonly collected were redbreast sunfish, whitefin shiner and silver redhorse. Species richness and diversity tended to be higher at downstream locations. Species composition was comparable to that of similar-sized southern piedmont rivers.

4. Based on boat electrofishing collections, dams do not seem to prevent the distribution of resident species throughout the river; however, it's likely that a different community composition would exist in the absence of dams. Community composition differed between riverine sites and those located near hydroelectric operations.

5. In boat electrofishing collections, a significant relationship was observed between catch rates and distance from a dam. In backpack electrofishing collections, catch rates and species richness were related to physical habitat parameters.

6. The water quality parameters we measured were consistent with those expected for a piedmont river and did not affect species richness, species diversity or catch rates in backpack or boat electrofishing collections.

7. Redbreast sunfish and redear sunfish are long-lived in the Broad River. Growth rates of redbreast sunfish were slower than those reported from other southern rivers. Largemouth bass and smallmouth bass growth and longevity were typical of the region. Snail bullheads in the Broad River grow and live longer than reported elsewhere.

8. We investigated the health of largemouth bass at ten sites. Largemouth bass populations in the Broad River appear to be in good condition; however, our results suggested that condition was adversely affected by industrial effluent.

9. In 1996 Duke Power Company implemented minimum flows in the bypassed section of the Gaston Shoals Tailrace. Analysis of pre- and post-minimum flow fish community data indicated that minimum flows have had a positive impact on the fish community in the bypass. Species diversity was higher and pollution tolerance structure was markedly improved in the post-minimum flow fish community data.

10. We surveyed six sites for freshwater mussels and collected 315 live mussels, representing at least three species. Seven putative species were identified from relic shell collections. The native mussel fauna was more abundant and diverse in the lower section of the river.

TABLE OF CONTENTS

LIST OF TABLES

LIST OF FIGURES

INTRODUCTION

Background

The Broad River Trust Fund was established with money provided by the power companies that own and operate hydroelectric dams on the Broad River. The Trust Fund resulted from an agreement negotiated between SCDNR, USFWS, Duke Power Company, Lockhart Power Company, and South Carolina Electric & Gas Company, as a result of the FERC relicensing process. Funds in the Trust are administered by a board of trustees composed of representatives of each of the entities involved. The funds are intended to be used to enhance the fishery resources of the Broad River. The trustees decided that before any enhancement activity took place, a preliminary survey of the fish community was needed to determine its status and condition. The present study was undertaken to provide that information.

The purpose of this report is to present the findings of two years of baseline fish community, habitat and freshwater mussel data that were collected from the Broad River between October 2000 and September 2002. Objectives were addressed in five distinct study segments, detailed in separate sections of the report.

Objectives

The objectives of this study were to: (1) inventory the aquatic resources of the Broad River, with emphasis on fishes; (2) compare the fish community along the length of the river, examining the possibility of fish community fragmentation associated with dams; (3) compile habitat and natural resource data obtained in the current study and in previous efforts in a watershed-based database and investigate relationships between the status of the fish community and environmental variables; (4) examine the health of largemouth bass along the length of the river; (5) compare the fish community at the Gaston Shoals Bypass before and after the implementation of minimum flows; (6) inventory the mussel community residing in the Broad River; and (7) use the data collected from this effort to identify opportunities for protecting and enhancing the aquatic resources of the Broad River.

Study Area

The Broad River basin originates in North Carolina and dominates the central Piedmont of South Carolina. Within South Carolina, the river flows approximately 170 km until it merges with the Saluda River to form the Congaree River. The Broad River Basin, within South Carolina, encompasses 9,819 square km. Most of the basin is forested (70%); the remainder of the land is largely agricultural (13%) and urban (8%) (SCDHEC 2001). Average flow of the Broad River approximately 11 km downstream from the North Carolina state line (USGS gage # 1515) was 2,470 cfs, while average flow 16 km below Parr Reservoir (USGS gage #1615) was 6,250 cfs. In the upper part of the basin, where annual rainfall is highest, flows are well sustained and moderately variable; downstream, flows become more variable as rainfall and groundwater support decreases (Snyder et al. 1983). Seven hydropower dams are located on the South Carolina portion of the Broad River; these are Gaston Shoals, Cherokee Falls, Ninety-Nine Islands, Lockhart, Neal Shoals, Parr Shoals, and Columbia. Climatological, hydrological, and limnological differences along the river's course create a variety of habitat types for aquatic organisms residing in the Broad River.

The S.C. Department of Health and Environmental Control (SCDHEC) recently characterized water quality and the associated status of the aquatic community in the Broad River Basin, including nine assessment sites in the main stem of the Broad River (SCDHEC 2001). At all but one site, aquatic life use was fully supported. Excursions from aquatic life standards for dissolved oxygen and pH were ≤10% and acute aquatic life standards for toxins (heavy metals, priority pollutants, chlorine, and ammonia) were not exceeded. Aquatic life use not supported only in the Columbia Water Plant diversion canal, due to the occurrence of copper in excess of the acute aquatic life standards.

Sample Sites

Eleven sites distributed along the length of the river were selected for sampling (Figure 1) based on three primary criteria: access; variety of aquatic habitats (riffle, run and pool); and riverine character. Riverine character was defined as minimally impacted by hydroelectric operations. Most sites (1, 3, 5, 6, 8, and 9) were located far enough from hydroelectric operations that potential impacts from them were minimal. Two sites (2 and 11) that were upstream of dams were close enough to the dams to be influenced by reservoir ponding. Two other sites (4 and 7) were just downstream of dams, where fluctuations in discharge could affect aquatic habitat. Latitude and longitude coordinates of each area sampled are given in Table 1. Site 1, below Bookman Island, is the only site below Parr Reservoir. Sites 2 and 3 are between Neal Shoals and Parr reservoirs. Site 2 is directly below the confluence of the Tyger River, 22 km above Parr Shoals Dam. Ponding effects from Parr Reservoir are exacerbated by the operation of Monticello Reservoir as a pump-storage facility. Site 3 is above the confluence of the Tyger River, two km below the Sandy River boat access. Site 4 is two km below the Lockhart Power Canal. Sites 5 and 6 are located in the river reach from Ninety-Nine Islands to Lockhart Reservoir. Site 5 is directly below the Pacolet River and Site 6 is at Smiths Ford. Site 7 is two km below the Cherokee Falls Dam. Sites 8, 9, and 10 are located between the Gaston Shoals and Cherokee Falls hydropower dams. Site 8 is directly below Canoe Creek, 5 km above Cherokee Falls Dam. Site 9 is upstream of the confluence with Buffalo Creek, four km below

Gaston Shoals Dam. Site 10 is in the Gaston Shoals bypass. Site 11 is 5 km above Gaston Shoals Dam and is influenced by ponding from Gaston Shoals Reservoir.

Table 1. Sites sampled during the Broad River fisheries inventory October 2000 – June 2002.

Site #	Site coordinates	Habitat	Seasoned sampled	Electrofishing gear
1	34 13'46.8", 81 13'84.5"	Riverine	fall and spring	backpack/boat
2	34 43'15.1", 81 41'04.7"	Reservoir	fall and spring	backpack/boat
3	34 55'73.0", 81 42'27.3	Riverine	fall and spring	backpack/boat
4	34 75'89.9", 81 45'52.3"	Tailwater	fall and spring	backpack/boat
5	34 83'72.8", 81 45'80.3"	Riverine	fall and spring	boat
6	34 99'53.5", 81 48'42.2"	Riverine	fall and spring	backpack/boat
7	35 05'33.3", 81 53'82.5"	Tailwater	fall and spring	backpack/boat
8	35 09'96.1", 81 57'36.6"	Riverine	fall and spring	backpack/boat
9	35 11'79.0", 81 57'63.0"	Riverine	fall and spring	backpack/boat
10	35 16'84.6", 81 61'84.7"	Bypass	fall	backpack
11	35 13'73.9", 81 60'08.9"	Reservoir	fall and spring	boat

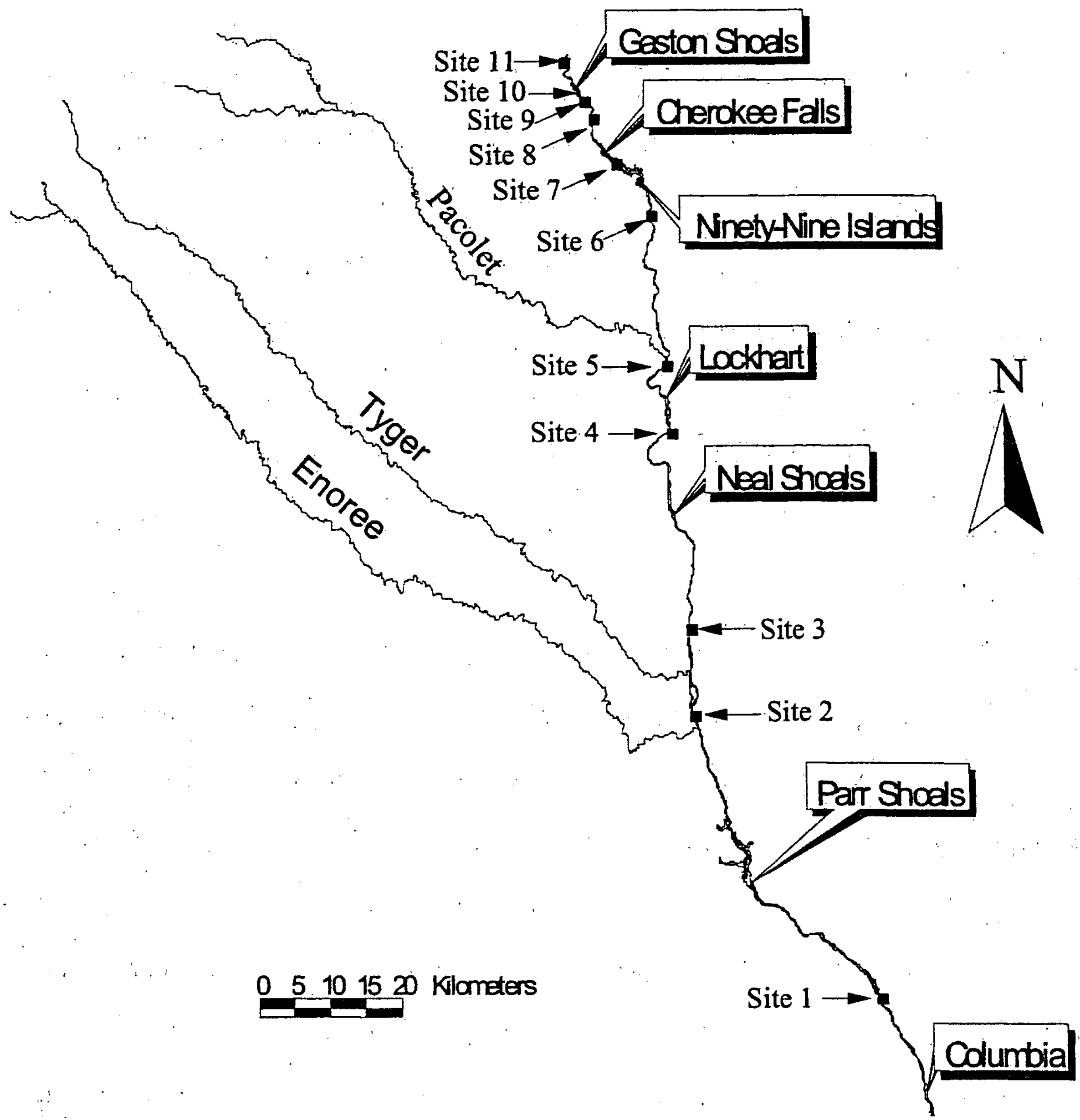

Figure 1. Sites sampled during the Broad River fisheries inventory October 2000 – June 2002. The location and name of hydropower dams is also shown.

HABITAT INVENTORY AND GIS DATABASE CONSTRUCTION

Preliminary reconnaissance of the Broad River was conducted by john boat during low water conditions in spring and summer, 2000, to collect habitat information and identify potential sample sites. Information derived from the survey was compiled in a geographic database using ArcView GIS software. Additional information obtained from a variety of sources was included as layers in the database. Fishery reports from earlier surveys were provided by Duke Power and South Carolina Electric & Gas, water quality monitoring sites and NPDES discharge sites were obtained from South Carolina Department of Health and Environmental Control (SCDHEC), and point locations for USGS gages were digitized from topographic maps.

During reconnaissance, we quantified mesohabitat in the riverine portions of the Broad River. Five categories of mesohabitat were defined: riffle, glide, run, pool, and shoal (Table 2). Upstream and downstream limits of each habitat unit were determined visually and recorded with a Trimble GeoExplorer[3] global positioning system (GPS). We also logged other landscape features, including riparian condition, bank stability, and potential access points using GPS. GPS locations were differentially corrected later using Pathfinder Office software and transferred to ArcView. Mesohabitat data were used to partition a digitized map of the Broad River into appropriate habitat units. We mapped 66 km of approximately 92 km of riverine habitat in the Broad River. Twenty-six km of habitat directly above the Columbia Dam were not mapped. Pools were the most common habitat type, accounting for 51% of the total area inventoried, followed by glides (28%) and shoals (18%)(Table 3). Runs (2%) and riffles (1%) were rare.

Digital orthophoto quarter quad (DOQQ) images downloaded from the SCDNR web page were imported into ArcView to quantify riparian condition. DOQQs were generated from photos taken in 1999. They had a resolution of 1 m, suitable for inventorying riparian vegetation. Riparian corridors were characterized as marginal if they were composed of mature trees but were less than 50 m wide. They were characterized as poor if they had few or no mature trees. Marginal and poor riparian areas on the Broad River were mapped in ArcView and measured. We evaluated 312 km of riparian corridor from the North Carolina state line to the Columbia Dam, excluding 99-Islands and Parr Shoals reservoirs. Approximately 11.5% of the riparian corridor was marginal and 1.3% was poor. Few long sections (>100 m) of riparian corridor in poor condition were identified. Such areas were generally associated with sand dredging operations, but occasionally with agricultural or forestry operations. There were numerous short sections (<100 m) of the riparian corridor in poor condition, however. Most were associated with power line or gas line crossings, or with private access areas (e.g., boat ramps). Almost all of the riparian habitat classified as marginal was associated with agricultural or forestry operations (94%).

The drought conditions during spring and summer, 2000, gave us an excellent opportunity to inventory the mesohabitats of the Broad River at base flows. It is important to recognize that the inventory we conducted was a gross evaluation of mesohabitat types. Shoals were the most complex habitat structure. Within a shoal most of the other habitat types were present, but were not delineated. Habitat classifications are subject to changes in flow. As flow increases the heterogeneous habitat units (i.e., riffles, runs and pools) we observed would likely change to a more homogenous run type habitat (Parasiewicz 2001). The mesohabitat information we collected could be used, with additional chemical and physical habitat data, in a model to predict the impacts of habitat alterations (e.g., impoundment) or the success of species introductions and reintroductions (e.g., robust redhorse and anadromous fish species).

Visual analysis of DOQQs indicated the riparian area along the Broad River is in relatively good condition. We recommend that habitat restoration efforts on the main stem be directed at rehabilitating riparian zones adjacent to sand mining operations, and at educating private landowners regarding the benefits of maintaining riparian buffers. Restoration of riparian areas on the tributaries might be a more effective way to improve conditions for aquatic life in the Broad River.

Sand mining poses other habitat concerns beyond those resulting from riparian zone degradation. Instream sand mining adversely affects physical and chemical habitat and can negatively affect biological communities (Nelson 1993) and recreational uses (Hartfield 1993). Physical impacts on instream habitat include increasing bedload materials and turbidity, changing substrate type and stability, and altering stream morphology (Nelson 1993). Physical habitat alterations associated with sand mining can adversely affect the biological community by impacting the reproduction and survival of fishes (Stuart 1953, Newport and Moyer 1974) and the distribution and composition of aquatic organisms (Buck 1956, Trautman 1957, Newport and Moyer 1974). Our inventory of the Broad River was not designed to evaluate the impacts of sand mining on the aquatic fauna; however, we did observe changes in the physical habitat near sand mining operations. The river downstream of sand mining operations appeared to be much more turbid than it was in areas directly above the activity. Further research to determine the impact of sand mining on the aquatic biota of the Broad River is recommended.

Cursory examination of riverbanks along the Broad River indicated that bank stability was not a major concern in most areas. One notable exception is an area above Parr Reservoir. From the Hwy 34 bridge approximately 7 km upstream the riverbanks are in poor condition with many long sections actively eroding and sloughing. The poor bank stability is probably attributable to large fluctuations in water elevations that occur daily because of Parr's operation as the lower reservoir in a pump storage hydroelectric power complex. Habitat restoration through bank stabilization in this degraded section could benefit aquatic resources.

Table 2. Mesohabitat unit definitions for visual assessment.

Habitat Type	Description
Riffle	Relatively shallow (<0.5m), swift flowing section of river where water surface is broken.
Glide	Relatively shallow (<1m); with visible flow but mostly laminar in nature; minimal observable turbulence; relatively featureless bottom.
Run	Deep (>1m), swift flowing sections with turbulent flow; surface generally not broken.
Pool	Deep (>1m) slow moving sections.
Shoals	Shoal area; which may contain a variety of habitat complexes.

Table 3. Results of the habitat inventory of the Broad River, spring and summer 2000.

Habitat Type	Number of Units	Mean Area (ha)	Total Area (ha)
Glide	71	3.0 (0.4 – 13.9)	214.1
Pool	68	5.7 (0.4 – 38.0)	384.5
Riffle	3	1.9 (0.8 – 3.3)	5.6
Run	8	1.8 (0.1 – 6.8)	14.7
Shoal	52	2.6 (0.2 – 20.3)	134.5
Total	202	3.7 (0.1 – 38.0)	753.3

FISH COMMUNITY

Boat electrofishing collections were made at 10 sites along the Broad River to collect baseline information on the fish community that inhabits pool/run habitat. The objectives of the boat electrofishing were to: (1) describe the fish community inhabiting pool/run habitat along the length of the Broad River; (2) examine the possibility of fish community fragmentation associated with dams; (3) examine the relationship between the fish community and physical and chemical habitat variables; and (4) describe the growth of selected species. Backpack electrofishing collections were made in shoal areas to augment fish community information.

Boat Methods

Fish collection

We conducted boat electrofishing during the winter (10 January – 2 February), 2001, spring (10 April – 3 May), 2001, fall (3 October – 14 November), 2001 and spring (8 April – 30 April), 2002. Boat electrofishing consisted of sampling at least three transects at each sample area: at least one transect along each bank in pool habitat and one mid-channel transect in glide/run habitat. We considered pool habitat to be areas that had little flow and a mean depth of at least one meter. Glide and run habitats were areas that had higher water velocities, more variable depths and were generally located in shoal areas. During the winter, each shoreline transect received ten minutes of continuous electrofishing effort in a downstream direction. Because of concerns about the effectiveness of this method in capturing fish, we modified our shoreline electrofishing techniques for the remaining sampling seasons. During those seasons we fixed the length of the shoreline transects at 150 m and shocked in an upstream direction. Shocking in an upstream direction gave us more control of the boat and allowed us to work the area more thoroughly. Electrofishing output was standardized by electrofishing at a frequency of 60 pulses per second (pps) and varying the voltage to achieve 3.5 – 4.0 amps of output.

At some sites during some seasons we sampled the catfish community with a catfish electrofishing transect. This sampling was conducted to augment fish community information collected with standard electrofishing techniques and to describe the composition of ictalurids in the Broad River. We also wanted to determine if flathead catfish were present in the system. Flathead catfish, a large ictalurid, has the potential to disrupt the aquatic communities of piedmont and coastal streams. Catfish electrofishing transects were conducted by slowly floating down the river mid-channel and operating the electrofisher at a low pulse frequency (7.5 pps).

Each fish collected during sampling was identified to species and, when practical, measured to the nearest mm total length (TL) and weighed to the nearest gram. Occasionally some species were too numerous to measure and weigh individually. In these instances, we enumerated the individuals by species, recorded lengths of 25 randomly selected individuals, and recorded a total batch weight. A reference collection of each species collected was maintained. Species identifications were verified by Fritz Rohde of the North Carolina Division of Marine Fisheries.

To assess age and growth of representative species, we collected otoliths during the spring from largemouth bass, smallmouth bass, redbreast sunfish, and redear sunfish. During the fall we collected the otoliths and opercle bones from silver redhorse and brassy jumprock. We also collected pectoral spines from snail bullheads during fall, 2001, at site 2. Aging structures were removed from individuals selected randomly from within predetermined length-groups. For largemouth bass, redear sunfish, brassy jumprock, silver redhorse, and snail bullheads, we attempted to collect aging structures from at least three individuals per 25-mm length group at each site. For redbreast sunfish, we used a 12-mm length interval. Whole otoliths were viewed in the lab with a microscope, using reflected light. When whole otoliths were difficult to read, they were broken in half near the nucleus, perpendicular to the sulcal groove, sanded smooth, and viewed in cross section microscopically, using a fiber optic light. One-mm sections of snail bullhead spines were cut through the articulating process, proximal to the basal recess. The sections were polished on both sides, mounted on glass slides and viewed under a microscope with transmitted light. To estimate age, two experienced readers read otoliths and spine sections independently. Results were compared. When readers did not agree on an age, they re-read the structure jointly. If agreement could not be reached, the structure was eliminated from analysis. Mean lengths-at-age were calculated for all species when enough data were available. Means for redbreast sunfish and largemouth bass were calculated by site. Means for redear sunfish and smallmouth bass were calculated for the entire river. Means for snail bullheads were calculated for Site 2.

Data obtained from boat electrofishing were used to calculate relative abundance (RA), relative biomass (RB) by family, species diversity (Simpson's diversity index, D), and species richness (total number of species, S) metrics for the fish community at each site during each season. Data collected from catfish electrofishing transects were not included in the calculation of community metrics. Relative abundance was calculated as

$$\mathrm{RA} = \frac{n_i}{N},$$

relative biomass was calculated as

$$\mathrm{RB} = \frac{w_i}{W},$$

and Simpson's diversity index was calculated as

$$D = \sum_{i=1}^{s} \left[\frac{n_i(n_i - 1)}{N(N-1)} \right],$$

where n_i = Number of individuals of species i in the sample
N = Total number of individuals in the sample
S = Number of species in the sample
w_i = Total weight of family i in the sample
W = Total weight of individuals in the sample.

The inverse of Simpson's diversity index (1/D) was used as a test statistic. Mean catch per unit effort (CPUE) was calculated as No./m for each boat electrofishing site during each season and year. Because catfish electrofishing transects were not conducted at every site during each season and year they were not included in calculating mean CPUE.

Water quality and habitat parameters collected

Water quality measurements were collected at each sample site. Water temperature, dissolved oxygen, and conductivity were measured using a YSI Model 85 handheld dissolved oxygen, conductivity, salinity, and temperature meter. pH was measured using a YSI Model 60 handheld pH/temperature meter. Turbidity was measured with a LaMotte 2020 turbidimeter.

Mean depth of each shoreline electrofishing transect was determined. Depth was measured with a wading rod at approximately 10 m intervals along the electrofishing transect with the boat positioned approximately 3 m from the bank.

Statistical Analysis

Differences in species richness were investigated using a two-way ANOVA by site and season. Differences in species diversity and CPUE among sites and seasons were evaluated with independent Kruskal-Wallis tests. Stepwise multiple linear regression was used to investigate the relationship between population and community descriptors such as mean CPUE (log 10) and species richness and habitat and water quality variables. Cluster analysis of relative abundance data was used to investigate longitudinal changes in the fish community and examine the possibility of fish community fragmentation associated with dams. The cluster analysis was performed with the simple average linkage method and the Bray-Curtis distance equation (McAleece et al. 1997). Differences in mean length-at-age, by site, for redbreast sunfish and largemouth bass were assessed using a Kruskal-Wallis test. When conducting non-parametric statistical analyses (e.g., Kruskal-Wallis) pairwise comparisons were not investigated. All statistical comparisons were calculated using SAS (SAS Institute 1989). Tests were considered statistically significant at $\alpha = 0.05$. Winter data were eliminated from all analyses because of the different electrofishing methods used in the winter.

Boat Results/Discussion

Fish sampling

One hundred and eighty-one transects covering approximately 27 km of river were sampled (Table 4). In all, 6,916 fish comprising 44 species were collected from shoreline and mid-channel electrofishing transects (Table 5). Common and scientific names of fishes used in this report are listed in Appendix 1. Overall, redbreast sunfish, bluegill sunfish, and silver redhorse were the most abundant species, comprising more than 50% of the total number of fish collected. Gizzard shad, whitefin shiner, sandbar shiner and brassy jumprock were also relatively common, each comprising more than 5% of all fish collected.

Relative abundance of fish species varied by site (Table 6). Silver redhorse was the only species collected at every site during each season and year. Bluegill and redbreast sunfish were collected at each site during every season and year, except during the winter at site 1. Rare species in the boat electrofishing transects included bluehead chub, fieryblack shiner, flier, green sunfish, golden shiner and rosyside dace; only one individual of each species was collected.

Some species had limited distribution in the river. White perch, white bass, pumpkinseed sunfish, yellow perch, yellowfin shiner, and longnose gar were only collected in the lower half of the river (site 4 and below), while V-lip redhorse and northern hogsucker were only collected in the upper half of the river (site 4 and above).

Twenty-three catfish electrofishing transects were conducted, during which 1,076 ictalurids comprising 5 species were collected (Table 7). Snail bullhead was the dominant species, representing more than 80% of the ictalurids collected at every site. The bullhead catfishes accounted for more than 98% of the ictalurids in the catfish samples. No flathead catfish were collected during our sampling efforts. Future efforts to restore anadromous fish may adversely affect the resident community if flathead catfish are introduced into the Broad River. The flathead catfish is a voracious predator, and has been shown to negatively impact native centrarchid, ictalurid and catostomid communities (Guire et al. 1984, Ashley and Buff 1986, Bart et al. 1994).

Catostomids dominated the boat electrofishing biomass, accounting for 51.2% of the total biomass in shoreline and mid-channel electrofishing samples (Table 8). Members of the centrarchid, cyprinid, and clupeid families were abundant, each comprising more than 11% of the biomass collected. The remaining families contributed little to the total biomass overall, but sometimes were locally important. For instance, ictalurids were an important component of the fish biomass at site 4, and gars were an important component at site 1. Catostomids were the dominant family by weight at every site, comprising 38% to 86% of the total biomass among sites.

Species richness and diversity varied by sample area and season; both tended to be higher at downstream locations (Table 9). Mean species richness among sites ranged from 11.0 to 20.0 and was significantly higher at sites 1-4 than site 11 (ANOVA, P = 0.003). No seasonal differences were detected (ANOVA, P = 0.23). No other significant differences were observed in species richness. Mean Simpson's inverse diversity index ranged from 3.37 to 9.06 among sites. Significant differences in diversity were observed among sites (Kruskal-Wallis, P = 0.05) and between seasons (Kruskal-Wallis, P = 0.05). Diversity was significantly greater during the spring (mean = 6.2) than fall (mean = 4.9).

Mean CPUE varied by season and site, ranging from 0.02 to 0.64 (Table 10). Mean CPUE was typically higher at the downstream sites during both spring and fall. The highest overall mean CPUE (0.61) occurred at site 1 and the lowest (0.20) occurred at site 6. There was a significant difference in CPUE among sites (Kruskal-Wallis, P = 0.04), but not between seasons.

Cluster analysis indicated the most similar sites were sites 8 and 9, and sites 3 and 4 (Figure 2). Two broad clusters were interpreted from the analysis, one containing sites 1, 6, 8, 9 and 5, the other containing sites 2, 3, 4, 7, and 11. There was no indication that dams fragment the current Broad River fish community. Based on cluster analysis, site 1 exhibited more similarity to upstream sites than to downstream sites. If dams fragmented the current Broad River fish community we would have expected the cluster analysis to group lower and upper river sites separately. The two large clusters generated by our analysis did suggest a difference in fish community composition between riverine sites and those impacted by hydroelectric operations. One cluster contained most of the more riverine sites (1, 5, 6, 8, 9) and the other contained sites that were considered tailwater areas (sites 4 and 7) or sites that were influenced from the ponding created by downstream dams (sites 2 and 11). The only site that did not fit this pattern was site 3, a riverine site clustered with those impacted by hydroelectric operations. Although our analysis did not indicate that dams fragment the current fish community, a different community composition would exist in the absence of dams. Dams along the Broad River have historically fragmented the fish community, preventing migrations of anadromous and catadromous species (e.g., American shad and American eel) that historically occurred in the river and currently exist in the Congaree River below the Columbia Dam.

During the two spring sampling periods we collected otoliths from 515 redbreast sunfish, 132 largemouth bass, 94 redear sunfish, and 49 smallmouth bass. During the fall we collected otoliths and opercle bones from 117 silver redhorse and 77 brassy jumprock. We also collected spines from 58 snail bullheads during the fall of 2001. Difficulties in determining a suitable method for aging moxostomid species precluded the inclusion of age data for silver redhorse and brassy jumprock in this report.

We aged 496 spring-collected redbreast sunfish, 35-76 per site. Estimated ages ranged from 1 to 8 years. At most sites at least 4 age classes were present. Age classes 2 and 3 predominated at all sites. Fish age-4 and older were more prevalent at upriver sites (sites 7-11). Differences in mean length of redbreast sunfish at ages 1, 2, and 3 were observed among sites (Kruskal-Wallis, $P<0.05$). Age-1 redbreast were longest at sites 6, 2 and 3; age-2 redbreast were longest at sites 6, 2 and 8; and age-3 redbreast were longest at sites 6, 2, and 9 (Table 11). Overall, sites 2 and 6 exhibited the best growth and sites 1, 4, and 7 exhibited the poorest growth over the three age classes. Redbreast sunfish that grew well in their first year generally exhibited good growth in their second and third years (Figure 3).

Redbreast sunfish in the Broad River are long-lived. The age-8 fish we collected equaled the maximum age reported by Carlander (1977) for redbreast sunfish. In surveys of six North Carolina coastal streams, redbreast sunfish did not exceed age-6 (Ashley and Rachels 1998). In the Edisto River, South Carolina, redbreast sunfish did not exceed age-3 (Thomason et al. 1993). Growth of redbreast sunfish in the Broad River was considerably slower than that reported for other southeastern rivers. Mean total length at age-3 in the Broad River was 130 mm, compared to 175 mm in other southeastern rivers (Ashley and Rachels 1998, Thomason et al. 1993).

We aged 126 spring-collected largemouth bass, 5-29 per site. The oldest individual was 12 years old. At most sites at least 4 age classes were present, but these were often represented by only one or two individuals. Mean length-at-age data are reported in Table 9. Because of the small numbers of fish aged at many sites, and the wide distribution of age classes, between-site comparisons of length-at-age and growth were not statistically meaningful. Largemouth bass at site 2 exhibited the fastest growth rate; mean lengths at ages 1, 2, and 3 were greater there than at any other site. Largemouth bass at sites 4, 6, and 11 exhibited relatively slow growth through age-3 (Table 12).

Life span and growth of largemouth bass in the Broad River was typical for the species in the Southeast. The average life span of largemouth bass in Virginia is 8-10 years (Jenkins 1993); in Tennessee, it's 10-12 years (Etnier and Starnes 1993). Growth of age 1–4 largemouth bass in the Broad River was similar to that reported for the Edisto River, South Carolina (Thomason et al. 1993).

We aged 92 redear sunfish and 42 smallmouth bass collected during spring 2001 and 2002. Numbers of aged fish were insufficient to make meaningful comparisons of growth between sites. Pooled mean lengths at age are reported in Table 13. We aged 54 snail bullheads collected during fall 2001 at site 2. Ten age classes were present. Mean length-at-age data are reported in Table 13.

Smallmouth bass in the Broad River appear to have a moderate life expectancy compared to those in some other Southeastern rivers. The oldest smallmouth bass we aged was 8, but fish as old as 15 have been documented in Virginia rivers (VDGIF, unpublished data). Growth of smallmouth bass in the Broad River was comparable to that of four piedmont rivers in Virginia (VDGIF, unpublished data). Based on growth rates in the Broad River, smallmouth bass could reach quality size (30 cm) in their fourth year, preferred size (35 cm) in their fifth year, and memorable size (40 cm) in their sixth year (Gabelhouse 1984).

Redear sunfish in the Broad River are long-lived; fish up to age-8, the maximum reported age for redear sunfish (Carlander 1977), were observed. Mean length-at-age of redear sunfish in the Broad River is comparable to that reported in Carlander (1977). Based on growth rates we calculated, redear sunfish in the Broad River could reach quality size (18 cm) in their third year, preferred size (23 cm) in their fourth year, and memorable size (28 cm) in their seventh or eighth year (Gabelhouse 1984).

The biology of the snail bullhead has received little attention (Jenkins1994). Snail bullheads in the Broad River, at least at site 2, are long–lived, attaining a maximum age of 9. No other studies that we're aware of have attempted to estimate snail bullhead age. Snail bullheads attain a larger size in the Broad River than reported in other systems. The longest reported snail bullhead had a standard length (SL) of 320 mm (Corcoran 1981); however, we collected numerous specimens longer than 400 mm TL, including one that was 448 mm. Snail bullheads in the Broad River reached approximately 100 mm during their first year and grew an average of 46 mm per year from age-1 through age-6.

Water quality and habitat parameters collected

Water quality and habitat data are reported in Table 14. No longitudinal or seasonal trends in water quality data were observed. Due to equipment problems, pH was only recorded during fall and winter sampling periods. In general, the water quality parameters we measured were consistent with those expected for a piedmont river. Conductivity tended to be lower at site 5, perhaps due to a dilution effect caused by the confluence of the Pacolet River just upstream of our sample site. pH values were somewhat higher than expected at sites 7 and 2, but as isolated data points, they are hard to interpret. During the winter 2001 sampling period, pH recorded hourly at the USGS monitoring station in the Broad River near Carlisle ranged from 6.7 to 8.0. During the fall 2001 sampling period, hourly pH values ranged from 5.1 to 7.6. Readings outside those ranges could have resulted from point or non-point source inputs. The USGS station near Carlisle is located well below site 7 and about 17 km above site 2. Sandy River and Tyger River both enter the Broad River between the gauge and site 2. Mean transect depth among sites ranged from 1.4 to 2.2 (mean = 1.7) m during winter, from 1.3 to 2.3 (mean = 1.7) m during spring, and from 1.0 to 2.2 (mean = 1.6) during fall.

Habitat and community relationship

A significant ($P = 0.0001$) positive relationship was observed between mean CPUE and distance from a dam and depth. No other variables were significant. Distance from a dam explained 46% of the variation in CPUE and depth explained 11%. There was not a significant relationship ($P = 0.13$) between species richness and habitat or water quality variables. It's important to recognize that our sampling strategy was not specifically designed to investigate the relationship between distance from a dam and catch rates. One possible explanation for the positive relationship we found is that areas located further from dams generally have more stable habitat and may support more individuals. Another possible explanation is that the relationship we observed was an artifact of our sampling design. The frequency of dams is greater in the upper reaches of the river and less in the in the lower reaches. Therefore, distance from dams was generally greatest at the lower sites. The lower sites may simply have greater catch rates due to the increased productivity one would expect in the lower reaches of a river.

Table 4. Numbers of electrofishing transects, by type, conducted at each site by season and year. Bank transects sampled pool habitat while mid-channel transects sampled glide/run habitat. Catfish transects were conducted in mid-channel using a low pulse frequency.

	2001									2002			
	Winter			Spring			Fall			Spring			
Site	Cat	Bank	Mid	Cat	Bank	Mid	Cat	Bank	Mid	Cat	Bank	Mid	Total
1	1	3	1		3	1		3	1		3	1	17
2	1	3	1		3	1	1	3	1	1	3	1	19
3		3	1		3	1		3	1	1	4	1	18
4		4	1		2	1		3	1	1	3	1	17
5	1	3	1	1	3		1	3	1	1	3	1	19
6		3	1	1	2	1	1	3	1	1	3	1	18
7	1	4	1	1	3	1	1	3	1	1	3	1	21
8		3	1	1	3	1		3	1	1	3	1	18
9	1	3	1		3	1		3	1	1	3	1	18
11	1	3	1	1	3			3	1		3		16
Total	6	32	10	5	28	8	4	30	10	8	31	9	181

Table 5. Relative percent abundance of fish species in Broad River boat electrofishing samples collected during winter, spring, and fall in 2001 and 2002.

Common Name	Winter 2001	Spring 2001	Fall 2001	Spring 2002	Grand Total
Longnose gar	0.8	0.2	0.1	0.2	0.2
Gizzard shad	17.9	4.1	11.2	6.3	8.8
Threadfin shad				0.6	0.2
Rosyside dace	0.1				>0.0
Greenfin shiner		0.6		0.6	0.3
Whitefin shiner	5.8	6.4	4	8.6	6.2
Fieryblack shiner	0.1				>0.0
Common carp	1.7	1.5	0.7	0.8	1.1
Eastern silvery minnow	0.4	0.1	0.1	0.1	0.1
Bluehead chub	0.1				>0.0
Golden shiner				>0.0	>0.0
Spottail shiner	11.8	1.4	0.2	1.2	2.3
Yellowfin shiner		0.1			>0.0
Sandbar shiner	5.6	2.4	4.3	8.5	5.3
Quillback			0.5	1.8	0.7
Highfin carpsucker				0.4	0.1
White sucker	0.1	0.2			0.1
Northern hogsucker	0.6	0.6	0.4	0.4	0.5
Smallmouth buffalo	0.2	0.7	>0.0		0.2
Silver redhorse	18.9	12.7	8.9	12.3	12.2
Shorthead redhorse	1.2	0.7	0.8	0.8	0.9
V-lip redhorse	0.4	0.2			0.1
Striped jumprock	0.2	1.7	1.2	1.2	1.2
Brassy jumprock	6.6	5	5.3	4.5	5.2
Snail bullhead	3.1	3	0.8	0.8	1.7
White catfish		0.1		0.5	0.2
Flat bullhead	0.2	0.6	>0.0	0.2	0.2
Channel catfish	0.1	1.8	1.3	1.2	1.3
Margined madtom		0.1	>0.0		>0.0
White Perch		1.9	2.8	3	2.3
White bass		0.2	>0.0	1.1	0.4
Flier			>0.0		>0.0
Redbreast sunfish	5.7	28.4	26.9	22.1	23.1
Green sunfish			>0.0		>0.0
Pumpkinseed	0.1	0.1	0.1	0.1	0.1
Warmouth		0.2	0.3	0.1	0.2
Bluegill	10.7	14.8	18.4	14.6	15.3
Redear sunfish	1.7	3.3	5.4	3.4	3.8
Smallmouth bass	0.7	1.7	1.3	0.8	1.2
Largemouth bass	4	3.9	3.6	3.0	3.5
Black crappie	0.4	1.0	0.5	0.2	0.5
Tessellated darter			0.1	0.1	0.1
Yellow perch	0.1	0.3	0.4	0.5	0.4
Piedmont darter	0.2	0.1			0.1
Total No. Collected	889.0	1744.0	2158.0	2125.0	6916.0

Table 6. Relative percent abundance of species in Broad River boat electrofishing samples, by site, collected during winter 2001, spring 2001, fall 2001, and spring 2002.

	Site										
Common name	1	2	3	4	5	6	7	8	9	11	Overall
Longnose gar	0.8	0.7	0.2								0.2
Gizzard shad	0.1	23.1	10.6	11.2	0.9	1.9	14.7	3.7	3.4	14.5	8.8
Threadfin shad	0.4	0.7					0.2				0.2
Rosyside dace								0.1			0.0
Greenfin shiner	0.1		0.8	0.2	0.4	0.2	0.6		0.9	0.2	0.3
Whitefin shiner	6.4	2.7	7.4	13.2	5.6	6.1	3.7	4.2	8.8	6.3	6.2
Fieryblack shiner									0.1		>0.0
Common carp	0.1	0.7	0.7	0.5		0.4	1.2	2.3	1.8	5.1	1.1
Eastern silvery minnow	0.1		0.2		0.7	0.4					0.1
Bluehead chub									0.1		>0.0
Golden shiner			0.1								>0.0
Spottail shiner	0.5	6.5	3.2	4.6	1.3	2.1	0.2	0.1	1.6		2.3
Yellowfin shiner	0.2										>0.0
Sandbar shiner	8.3	1.2	0.8	3.0	27.7	11.8		0.4	3.4	1.5	5.3
Quillback		0.1	0.1	0.2	2.0	1.9	4.5	0.4	0.1		0.7
Highfin carpsucker						1.7	0.2				0.1
White sucker						0.6			0.1		0.1
Northern hogsucker				0.9	1.1	0.4	0.8	1.0	1.0	0.2	0.5
Smallmouth buffalo		0.4	0.2	0.2		0.6	0.2	0.6			0.2
Silver redhorse	4.8	14.0	5.3	6.2	16.6	11.0	10.6	18.2	13.3	35.6	12.2
Shorthead redhorse	0.1	1.5	2.6	1.9	0.4	0.8					0.9
V-lip redhorse				0.2	0.2	0.2	0.2	0.1	0.4		0.1
Striped jumprock	0.2		0.3	3.2	0.2	1.9	1.0	1.7	3.6	1.9	1.2
Brassy jumprock	3.6	0.3	5.4	5.6	9.9	10.1	3.1	8.7	7.8	0.2	5.2
Snail bullhead	0.9	0.5	2.0	1.9	0.2	1.7	1.4	3.9	3.9	0.5	1.7
White catfish		1.1									0.2
Flat bullhead	0.6		0.3	0.2		0.4	0.2	0.3	0.3		0.2
Channel catfish	0.2	2.9	2.8	3.3	0.2	0.2	0.6		0.3	0.2	1.3
Margined madtom	0.2					0.2					>0.0
White perch	0.3	13.3	1.5								2.3
White bass	0.1	2.4	0.1	0.2							0.4
Flier	0.1										>0.0
Redbreast sunfish	41.8	8.4	11.3	13.5	22.4	27.4	27.1	31.4	31.6	18.4	23.1
Green sunfish								0.1			>0.0
Pumpkinseed	0.1	0.3	0.2								0.1
Warmouth	0.8			0.2	0.2			0.1	0.1		0.2
Bluegill	16.2	9.8	35.1	17.9	3.6	9.7	19.3	13.0	8.5	9.0	15.3
Redear sunfish	7.5	4.2	5.4	3.2	1.1	2.5	4.1	1.9	1.3	1.9	3.8
Smallmouth bass		0.5		0.9	1.3	2.3	0.6	4.0	3.0	0.5	1.2
Largemouth bass	4.2	3.0	2.6	6.0	3.6	2.3	4.3	2.9	3.6	3.6	3.5
Black crappie	0.4	0.6	0.1	1.4	0.2	0.8	1.2	0.4	0.4	0.2	0.5
Tessellated darter	0.1		0.1		0.4			0.1			0.1
Yellow perch	0.8	1.2	0.4	0.2							0.4
Piedmont darter	0.1		0.1	0.2				0.1			0.1
Total No. fish	1022	1054	974	569	553	474	491	698	668	413	6916

Table 7. Relative abundance of ictalurids collected in catfish electrofishing samples, by site, during winter 2001, spring 2001, fall 2001, and spring 2002.

	Site									
Common Name	2	3	4	5	6	7	8	9	11	Overall
Snail bullhead	93.9	95.6	100.0	92.0	90.2	95.2	99.2	98.7	84.0	95.0
White catfish	0.0	0.0	0.0	0.0	0.0	0.0	0.0	0.0	4.0	0.3
Flat bullhead	1.5	4.4	0.0	3.7	3.3	4.8	0.8	0.0	12.0	3.1
Channel catfish	3.0	0.0	0.0	0.0	0.0	0.0	0.0	0.0	0.0	0.4
Margined madtom	1.5	0.0	0.0	4.3	6.6	0.0	0.0	1.3	0.0	1.3
Total No. fish	132	136	70	162	61	125	240	75	75	1076

Table 8. Percent contribution of biomass, by family, at each Broad River boat electrofishing site.

	Site										
Family	1	2	3	4	5	6	7	8	9	11	Total
Catostomidae	49.5	48.9	37.5	38.5	86.1	65.2	53.6	53.3	55.4	45.0	51.2
Centrarchidae	28.2	8.8	10.1	21.7	10.2	15.8	24.2	18.1	15.1	8.8	14.9
Cyprinidae	7.3	12.4	16.1	11.1	0.6	9.4	11.8	16.1	17.2	36.7	14.6
Clupeidae	0.1	14.5	25.0	13.8	1.0	8.5	4.8	10.9	9.6	9.3	11.5
Ictaluridae	3.5	8.9	9.1	14.0	2.1	1.0	5.4	1.6	2.7	0.2	5.3
Lepisosteidae	11.3	1.2	1.5	0.0	0.0	0.0	0.0	0.0	0.0	0.0	1.2
Moronidae	0.1	5.0	0.6	0.8	0.0	0.0	0.0	0.0	0.0	0.0	1.2
Percidae	0.1	0.2	0.0	0.1	0.0	0.0	0.0	0.0	0.0	0.0	0.1
Grand Total	100.0	100.0	100.0	100.0	100.0	100.0	100.0	100.0	100.0	100.0	100.0

Table 9. Species richness and Simpson's inverse diversity index (1/D) for samples collected from the Broad River during 2001 and 2002. Means with similar letters were not significantly different (Tukeys, P> 0.05).

	Species Richness				Simpson's Inverse Diversity Index			
Site	Spring 01	Fall 01	Spring 02	Mean	Spring 01	Fall 01	Spring 02	Mean
1	19	18	18	18.3^{z}	3.5	2.9	6.1	4.17
2	20	13	21	18.0^{z}	10.9	6.0	10.3	9.06
3	19	21	20	20.0^{z}	5.8	4.9	5.8	5.50
4	20	17	18	18.3^{z}	9.6	9.2	6.6	8.46
5	14	17	11	14.0^{zy}	4.5	4.8	5.0	4.77
6	16	14	17	15.7^{zy}	6.2	3.3	9.4	6.30
7	18	15	15	16.0^{zy}	5.0	5.0	5.1	5.03
8	14	13	17	14.7^{zy}	7.2	5.0	4.9	5.70
9	17	14	17	16.0^{zy}	6.9	3.7	6.0	5.53
11	11	13	9	11.0^{y}	3.2	4.1	2.8	3.37
Total	34	33	33		6.3	4.9	6.2	

Table 10. Mean CPUE (No./m) for samples collected from the Broad River with boat electrofishing gear during 2001 and 2002. Winter data were not included in the overall mean or used in the analysis.

Area	Winter 2001	Spring 2001	Fall 2001	Spring 2002	Mean
1	0.05	0.55	0.64	0.63	0.61
2	0.31	0.32	0.44	0.38	0.38
3	0.09	0.45	0.47	0.34	0.41
4	0.09	0.28	0.27	0.26	0.27
5	0.03	0.33	0.33	0.26	0.30
6	0.15	0.18	0.21	0.21	0.20
7	0.03	0.16	0.29	0.31	0.25
8	0.14	0.23	0.25	0.38	0.29
9	0.16	0.30	0.25	0.27	0.27
11	0.02	0.27	0.15	0.32	0.24
Mean	0.11	0.31	0.33	0.33	0.32

Table 11. Mean length-at-age (number of observations in parentheses) of redbreast sunfish, collected by boat electrofishing in the Broad River, by site.

	Age							
Site	1	2	3	4	5	6	7	8
1	63 (4)	85 (29)	120 (31)	158 (9)	140 (3)			
2	83 (5)	102 (20)	141 (10)	136 (1)				
3	84 (5)	98 (19)	136 (18)	147 (2)	161 (2)			
4	64 (3)	88 (10)	119 (17)	137 (3)	143 (2)			
5	60 (7)	96 (16)	130 (21)	135 (1)	173 (3)	190 (1)		
6	85 (4)	103 (21)	140 (16)					
7	59 (4)	87 (10)	121 (19)	146 (5)	164 (3)	141 (1)		
8	66 (7)	100 (18)	132 (15)	154 (10)	172 (2)	183 (1)		
9	56 (3)	95 (26)	137 (27)	157 (11)	137 (2)			
11	59 (1)	93 (14)	128 (17)	146 (8)	166 (5)	148 (2)	146 (1)	185 (1)
Overall mean	69 (43)	95 (183)	130(191)	151 (50)	158 (22)	162 (5)	146 (1)	185 (1)

Table 12. Mean length-at-age (number of observations in parentheses) of largemouth bass, collected by boat electrofishing in the Broad River, by site.

	Age											
Site	1	2	3	4	5	6	7	8	9	10	11	12
1	101 (16)	265 (6)	351 (5)	353 (1)		436 (1)						
2	161 (3)	288 (3)	365 (3)									
3	110 (5)	252 (2)	336 (4)	351 (1)								
4	158 (2)	247 (4)	276 (6)	350 (1)	410 (1)							
5	115 (7)	250 (4)	314 (2)									
6		246 (2)	270 (1)			449 (1)	417 (1)					
7		235 (1)	285 (1)	295 (2)	446 (1)		481 (1)					
8	126 (1)	271 (1)	300 (2)	305 (2)	309 (1)			426 (1)	482 (1)	487 (2)	458 (2)	491 (1)
9	107 (4)	248 (4)	293 (3)	325 (3)	393 (1)							
11	128 (3)		273 (2)	303 (3)				470 (1)				
Overall mean	115 (41)	257 (27)	312 (29)	318 (13)	390 (4)	443 (2)	449 (2)	448 (2)	482 (1)	487 (2)	458 (2)	491 (1)

Table 13. Mean length-at-age (number of observations in parentheses), of redear sunfish (RES), smallmouth bass (SMB), and snail bullhead (SBH), collected from the Broad River by boat electrofishing. RES and SMB were collected during spring 2001 and 2002; SBH were collected during fall 2001.

Age	RES	SMB	SBH
0	--	--	80 (3)
1	74 (4)	129 (19)	111 (2)
2	135 (43)	229 (11)	134 (4)
3	188 (15)	272 (11)	187 (11)
4	234 (13)	298 (3)	255 (7)
5	244 (10)	--	312 (9)
6	264 (5)	432 (2)	340 (6)
7	255 (1)	--	404 (7)
8	301 (1)	465 (1)	405 (3)
9	--	--	397 (2)

Table14. Selected water quality and habitat data collected from the Broad River during boat electrofishing, by sample date in 2001 and 2002.

Date	Season	Site	Temp (C°)	DO (mg/L)	pH	Conductivity (hmos)	Turbidity (ntu's)	Mean depth (m)
01/12/01	Winter	1	6.1	11.4	7.7	100	10.4	--
02/07/01	Winter	2	8.8	11.9	8.2	121	8.0	1.8
01/10/01	Winter	3	4.6	13.5	7.8	120	6.6	1.9
01/11/01	Winter	4	3.8	12.3	7.5	97	9.3	1.9
01/23/01	Winter	5	5.5	11.4	6.5	62	15.0	1.4
01/30/01	Winter	6	8.6	12.6	7.9	114	8.7	1.4
01/16/01	Winter	7	8.0	12.2	6.4	130	13.5	1.5
02/06/01	Winter	8	7.7	11.3	7.8	119	24.0	1.4
01/26/01	Winter	9	5.2	12.0	7.4	71	9.9	--
01/25/01	Winter	11	4.6	11.9	7.7	69	9.3	2.2
04/10/01	Spring	1	19.9	10.5	--	98	--	2.0
04/19/01	Spring	2	15.7	8.7	--	90	10.2	1.7
04/18/01	Spring	3	18.8	9.3	--	107	7.7	1.9
04/16/01	Spring	4	20.1	7.4	--	92	11.3	1.9
04/23/01	Spring	5	18.9	7.6	--	80	7.5	1.4
04/24/01	Spring	6	21.4	7.4	--	122	12.0	1.4
04/17/01	Spring	7	16.6	7.9	--	106	11.5	1.6
05/01/01	Spring	8	19.5	7.5	--	136	10.0	1.3
05/03/01	Spring	9	22.8	7.2	--	101	7.2	1.4
04/30/01	Spring	11	18.6	7.4	--	90	3.9	2.3
10/31/01	Fall	1	14.5	8.5	7.8	110	4.9	1.7
11/05/01	Fall	2	15.6	9.1	8.3	133	15.6	1.3
11/14/01	Fall	3	11.3	8.5	7.8	137	--	1.8
10/17/01	Fall	4	17.4	6.8	7.6	136	18.9	1.9
10/18/01	Fall	5	15.6	7.7	7.6	45	14.0	1.0
10/29/01	Fall	6	14.2	11.1	--	129	6.5	1.2
10/03/01	Fall	7	20.7	9.6	8.4	136	14	1.6
10/30/01	Fall	8	12.2	9.2	7.9	118	5.3	1.4
10/16/01	Fall	9	19.6	7.9	7.4	100	10.3	--
10/18/01	Fall	11	11.4	8.8	7.7	88	5.5	2.2
04/08/02	Spring	1	16.5	8.2	--	87	8.6	2.0
04/09/02	Spring	2	16.8	9.0	--	91	11.7	1.6
04/10/02	Spring	3	16.7	8.8	--	93	12.5	1.8
04/11/02	Spring	4	18.5	8.2	--	96	9.8	1.9
04/15/02	Spring	5	18.9	7.6	--	77	10.9	1.3
04/17/02	Spring	6	24.7	8.8	--	92	9.6	1.4
04/16/02	Spring	7	20.9	8.5	--	98	9.9	1.6
04/30/02	Spring	8	20.2	7.8	--	127	9.8	1.3
04/18/02	Spring	9	23.9	8.4	--	76	10.7	1.3
04/22/02	Spring	11	24.2	6.0	--	92	6.2	2.2

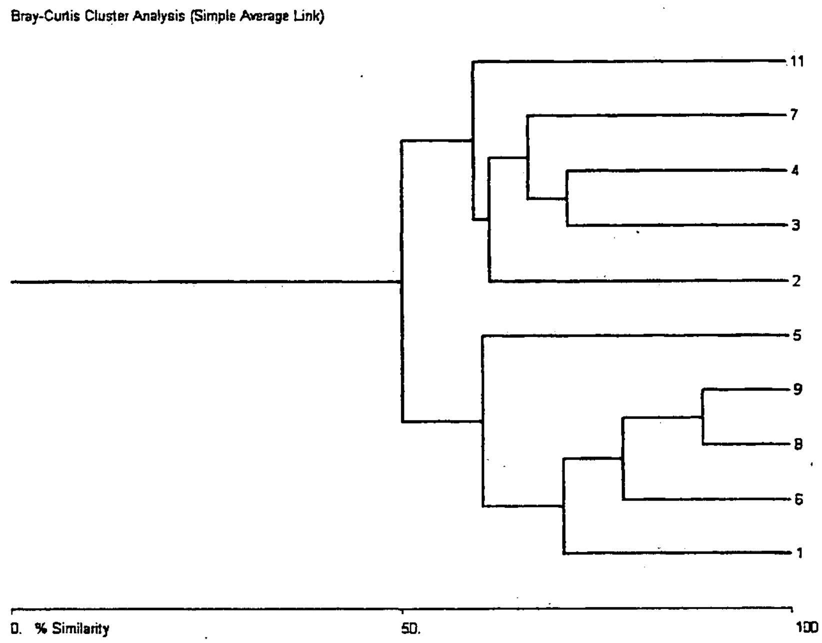

Figure 2. Bray-Curtis simple average cluster analysis of fish community relative abundance data for fish collected from the Broad River during fall 2001, spring 2001 and spring 2002.

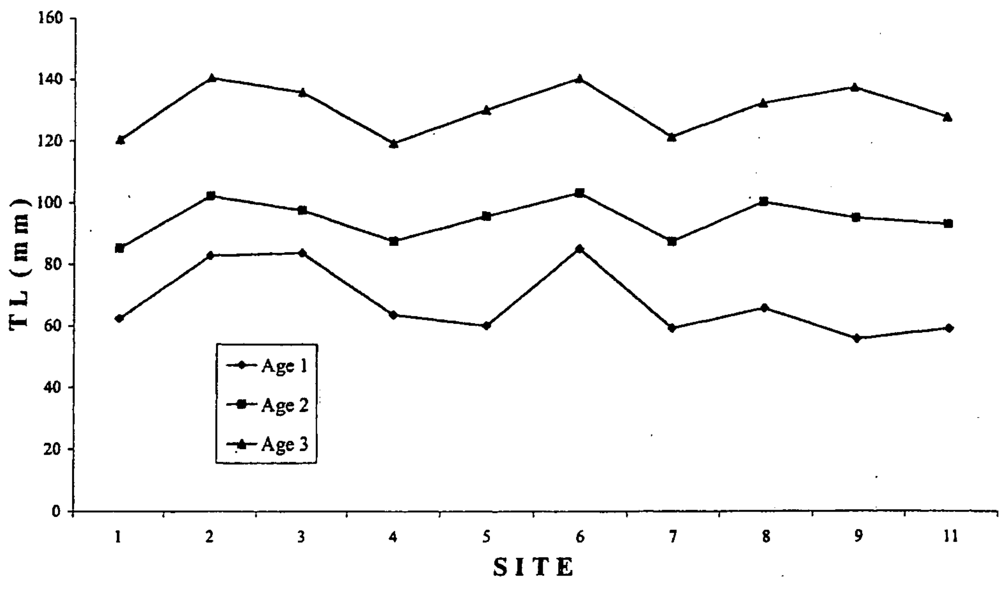

Figure 3. Mean length-at-age of redbreast sunfish collected during spring, 2001 and 2002, Broad River, SC.

Backpack Methods

Fish Collection

We conducted backpack electrofishing during fall 2000, spring and fall 2001, and spring 2002. A modification of the Tennessee index of biotic integrity (TIBI) protocol (TDEC 1995) was used for sampling complex habitat. The sampling protocol was designed to deplete species from dominant habitats (riffles, runs and shorelines). Riffles and runs were sampled until three consecutive units of effort produced no additional species for that habitat. Each unit of effort consisted of sampling a 30 m^2 plot (e.g., 6 x 5 m). A 6-m seine was positioned perpendicular to the current; one person outfitted with a backpack electrofishing unit began shocking 5 m above the seine and shocked downstream into the seine. Stunned fish were collected with dipnets when they were seen, but most fish were captured in the seine. At each sample area, shoreline habitat was sampled by backpack electrofishing a single pass along a 100 m wadeable transect.

Collected fish were identified to species and, when practical, measured (TL mm) and weighed (g). Occasionally some species were too numerous to measure and weigh individually. In these instances, we recorded lengths of 25 randomly selected individuals, then enumerated the fish and recorded a total batch weight by species. Each species collected was assigned to one of three pollution tolerance levels (tolerant, moderately tolerant, and intolerant) and one of five trophic levels (piscivore, insectivore, omnivore, specialized insectivore, and herbivore) (Barbour et al. 1999, NCDENR 2001). Representatives of each species collected were preserved in formalin and maintained in a reference collection. Species identifications were verified by Fritz Rohde of the North Carolina Division of Marine Fisheries.

Data obtained from backpack electrofishing were used to calculate relative abundance (RA), species diversity (Simpson's diversity index, D) and species richness (total # of species) for the fish community at each sample area during each season. Only data from plot samples were included in calculating species diversity and richness. Relative abundance was calculated as

$$\mathrm{RA} = \left(\frac{n_i}{N}\right) \times 100,$$

and Simpson's diversity index was calculated as

$$\mathrm{D} = \sum_{i=1}^{s}\left[\frac{n_i(n_i - 1)}{N(N-1)}\right],$$

where n_i = Number of individuals of species i in the composite sample for each site
N = Total number of individuals in the composite sample
s = Number of species in the sample.

The inverse of Simpson's diversity index (1/D) was used as a test statistic. Mean catch per unit effort (CPUE) was calculated for backpack electrofishing areas (N/plot) by sample area and season. Because only one shoreline section was sampled at each site, only fish collected from riffle and run samples were used in calculating mean CPUE.

Water quality and habitat parameters collected

Standard water quality parameters were measured and recorded at each sample site, as described previously.

Substrate, depth, and flow information were collected at each sample plot. Depth was measured at three points along each of three transects parallel to the seine; transects were at the upstream limit, middle and downstream limit of each sample plot. During fall 2000, substrate and flow were each characterized with a single observation per plot. Primary and secondary substrate components were described using a modified Wentworth scale (Table 15). Flow was categorized as low, moderate or swift. During spring 2001, fall 2001, and spring 2002, substrate and velocity information were collected at each point along each transect along with depth. Substrate was scored using the modified Wentworth scale and velocity was measured with a Marsh-McBirney model 201 flow meter. Percent contribution of each substrate type, mean depth sampled, and mean water velocity were calculated for each sample area. Qualitative data from fall 2000 were not used in these calculations.

Statistical Analysis

Differences in mean species richness and diversity were investigated by site and season with independent Kruskal-Wallis tests. Differences in mean CPUE were investigated using a two-way analysis of variance (ANOVA) by site and season. A logarithmic transformation (base 10) was used to normalize CPUE data. Chi-square analysis was used to evaluate differences in trophic composition and pollution tolerance structure among sites. Stepwise multiple linear regression was used to investigate relationships between normalized CPUE data and habitat and water quality variables. Stepwise multiple linear regression was also used to investigate relationships between species richness and habitat and water quality variables. All statistical comparisons were calculated using SAS (SAS Institute 1989). Tests were considered statistically significant at $\alpha = 0.05$.

Backpack Results/Discussion

Fish Sampling

During the study we made 676 standardized riffle and run backpack electrofishing collections. The mean number of run samples collected per site was 11.2 (range, 5 - 22) (Table

16). The mean number of riffle samples collected per site was 9.3 (range, 4 -15). In addition, one 100 m shoreline section was sampled at each site during each season and year.

A total of 9,836 fish, comprising 38 species, was collected during backpack electrofishing in the 3 habitat types (Table 17). Overall, whitefin shiner and redbreast sunfish were the most abundant species, together comprising more than 44% of the total number of fish collected. Spottail shiner, sandbar shiner, snail bullhead, and thicklip chub were relatively common; each comprised more than 5% of the total number of fish collected.

Relative abundance of fish species varied by site (Table 18). We collected whitefin shiner, snail bullhead, redbreast sunfish, and piedmont darter at every site during each season and year. Redbreast sunfish was the dominant species at sites 1 and 2, whitefin shiner was the dominant species at sites 3-9, and fieryblack shiner was the dominant species at site 10. Most species were relatively evenly distributed among the sites and throughout the river; however, the distributions of some fish were limited. Fantail darter was found only at site 6. Yellowfin shiner and seagreen darter were more common at site 1 than anywhere else. Yellowfin shiner was only collected at sites 1 and 6. Fieryblack shiner was only found above site 3 and was most prevalent at the uppermost sites; at site 10, fieryblack shiner represented 31% of the fish community.

Species richness and diversity computed from plot collection data varied by sample area and season (Table 19). Mean species richness among sites ranged from 10.8 to 16.3, but there were no significant statistical differences among sites (Kruskal-Wallis; $P = 0.06$) or between seasons (Kruskal-Wallis; $P = 0.22$). Mean Simpson's inverse diversity ranged from 3.1 (site 8) to 6.7 (site 1). There was a significant difference in mean species diversity among sites (Kruskal-Wallis; $P = 0.05$), but not between seasons (Kruskal-Wallis; $P = 0.23$). The low diversity of substrate material and the dominance of bedrock at site 8 may have contributed to the poor fish community diversity there.

Mean CPUE varied by site and season (Table 20). Mean catch per plot, among sites, ranged from 4.8 (site 2) to 16.3 (site 9), and there were significant differences among sites (ANOVA; P = 0.01), but not between seasons (ANOVA, P = 0.35). Mean catch per plot was significantly less at site 2 than at sites 4, 7 and 9. No other significant differences in catch per plot were observed. The low catch rates at site 2 may be related to unstable habitat. Site 2 was located at the first shoal area above Parr Reservoir, and may be inundated when the reservoir is at full pool. The frequent inundation of shoal habitat would not be conducive to the nongame communities that were targeted with backpack electrofishing gear.

The most abundant trophic guild in the Broad River was the Insectivores (67.7%), followed by the Specialized Insectivores (16.5%), and the Omnivores (15%). Herbivores and Piscivores were rare. Trophic composition differed among sites (χ^2, P = 0.0001), perhaps attributable to the dissimilar composition displayed at sites 1 and 10 (Figure 4). Insectivores comprised 50% or more of the trophic composition at all sites (Figure 4). In general, the trophic composition of the Broad River is indicative of a well-balanced fish community. Trophic generalists such as Omnivores were minimal at most sites. The paucity of Piscivores is not alarming, given the sampling gear. Backpack electrofishing into a seine in a large river is not very effective at sampling large predators.

The moderate pollution tolerance group was most abundant in the Broad River, comprising almost 80% of the fish collected. Intolerant individuals comprised 17.6% of the fish collected, while tolerant individuals comprised only 2.6%. The distribution of pollution tolerance levels was significantly different among sites (χ^2, P = 0.0001). Moderately tolerant fish dominated the fish community structure at all sites except 1 and 10, where large numbers of pollution-intolerant species were collected (Figure 5). The proportion of moderately tolerant individuals was greatest at site 7 and lowest at site 10. Conversely, the proportion of intolerant individuals was greatest at site 10 and lowest at site 7. Site 10 also had the highest proportion of tolerant individuals. At site 10 the pollution tolerance structure was greatly affected by the dominance of fieryblack shiner, an intolerant species that accounted for 31% of the total relative abundance. At site 1 seagreen and piedmont darters accounted for the increased proportion of intolerant species. Seagreen and piedmont darters accounted for 19% of the fish collected.

<u>Water quality and habitat parameters collected</u>

In general, the water quality parameters we measured were consistent with those expected for a piedmont river. Dissolved oxygen ranged from 6.1 to 9.9 ppm, pH values ranged from 6.3 to 8.5, conductivity ranged from 85 to 262 mhos and turbidity ranged from 3.2 to 24.4 NTU. Water quality data are reported in Table 21. No seasonal or longitudinal differences in water quality parameters were noted.

We recorded 4,306 depth and substrate measurements and 3,200 velocity measurements. The percent contribution of substrate types varied by site (Table 22). Overall, gravel, pebble and bedrock were the most common substrates. Gravel was the predominant substrate at sites 2, 3, and 7. Sand was a more important component of the substrate in the lower river than the upper. It dominated the substrate composition at sites 1 and 4. The primary substrate at sites 6 and 9 was pebble, and bedrock dominated the substrate composition at site 8. The average sample site depth ranged from 29 cm to 42 cm and the average water velocity ranged from 0.32 to 0.48 m/s.

Habitat and community relationship

The only habitat and water quality variables that significantly influenced CPUE were mean depth and turbidity (P = 0.01), which together explained 40% of the variation. There was a negative relationship between CPUE and depth, which explained 32% of the variation and a positive relationship between CPUE and turbidity, which explained 8% of the variation. The only habitat or water quality variables that significantly influenced the number of species captured were turbidity and depth (P = 0.004), which together explained 35% of the variation.. A positive relationship between turbidity and species richness was observed that explained 28% of the variation and a negative relationship between species richness and depth, which explained 7% of the variation. The relationships we identified between the fish community and physical habitat parameters may be artifacts of sampling. Backpack electrofishing into a seine was probably more effective in shallow, turbid water than in deep, clear water. Clear water likely made fish more wary and allowed them to spot us more easily, and greater depths provided them the opportunity to avoid capture.

Table 15. Size range of substrate components used for visual assessment, based on a modified Wentworth scale.

Particle type	Diameter
Bedrock	
Boulder	>256 mm
Cobble	65 – 256 mm
Pebble	17 – 64 mm
Gravel	2 – 16 mm
Sand	0.06 – 2 mm

Table 16. Number of plots sampled in the Broad River, by site, using backpack electrofishing, fall 2000 – spring 2002

	No. of riffle samples				No. of run samples				Total
Sample Area	Fall 00	Spring 01	Fall 01	Spring 02	Fall 00	Spring 01	Fall 01	Spring 02	Samples
1	11	11	5	10	10	13	6	7	73
2	11	8	8	10	12	13	12	7	81
3	4	7	8	8	11	11	9	15	73
4	12	10	6	11	5	10	10	11	75
6	11	9	15	9	14	13	12	8	91
7	12	11	9	10	14	12	12	11	91
8	10	6	8	13	18	8	22	17	102
9	11	7	9	9	7	11	8	10	72
10	6				12				18
Total	88	69	68	80	103	91	91	86	676

Table 17. Relative abundance, in percent, of fish collected in Broad River backpack electrofishing samples, by sample period.

Common Name	Fall 2000	Spring 2001	Fall 2001	Spring 2002	Overall
Gizzard shad	0.1	0.1	2.6	0.5	0.8
Threadfin shad				>0.0	>0.0
Greenfin shiner	3.4	5.7	2.4	6.1	4.3
Whitefin shiner	26.7	28.3	19.5	43.5	29.9
Fieryblack shiner	3.9	1.2	1.9	3.6	2.8
Eastern silvery minnow	0.2		0.4	0.1	0.2
Thicklip chub	8.2	7.3	3.4	3.5	5.5
Santee chub				>0.0	>0.0
Bluehead chub	2.4	2.8	4.0	1.3	2.6
Spottail shiner	6	7.6	11.1	10.9	9.0
Yellowfin shiner	0.2	0.3	0.2		0.1
Sandbar shiner	9.7	3	11.4	2.8	7.0
Northern hogsucker	0.6	0.6	1.2	1.3	1.0
Smallmouth buffalo			>0.0		>0.0
Silver redhorse				>0.0	>0.0
Shorthead redhorse	0.2			>0.0	0.1
V-lip redhorse		0.1			>0.0
Striped jumprock	1.2	1.4	1.4	1.3	1.3
Brassy jumprock	0.5	0.1	0.3	0.1	0.3
Snail bullhead	6.5	10.2	4.6	3.8	5.9
White catfish	0.1	0.1	>0.0		>0.0
Flat bullhead	0.7	0.8	0.5	0.4	0.6
Channel catfish	0.5	0.2	0.2		0.2
Margined madtom	4.4	6.1	4.8	1.8	4.1
Eastern mosquitofish	0.4	0.3	0.6	0.1	0.4
White perch				>0.0	>0.0
Redbreast sunfish	15.6	15.6	17.0	10.4	14.5
Green sunfish	0.1				>0.0
Pumpkinseed		0.1			>0.0
Warmouth		0.1	>0.0		>0.0
Bluegill	1.1	1.8	3.4	1.4	1.9
Redear sunfish	0.1	0.4	0.1	0.1	0.1
Smallmouth bass	0.5	1.1	0.7	0.5	0.7
Largemouth bass	0.1	0.1	0.3	>0.0	0.2
Fantail darter	0.2	0.1	>0.0	>0.0	0.1
Tessellated darter	0.9	0.7	1.2	1.1	1.0
Seagreen darter	1.0	0.8	1.9	0.7	1.1
Piedmont darter	4.4	3.0	4.5	4.5	4.2
Total No. of fish	2827	1778	2466	2765	9836

Table 18. Relative abundance, in percent, of fish collected in Broad River backpack electrofishing samples, by site, during fall 2000, spring 2001, fall 2001, and spring 2002.

	Site									
Common Name	1	2	3	4	6	7	8	9	10	Total
Gizzard shad		7.9	1.4	0.1		0.6				0.8
Threadfin shad						0.1				>0.0
Greenfin shiner	0.4	4.7	6.6	2.4	5.7	6.6	2.0	4.8	6.7	4.3
Whitefin shiner	9.0	13.3	21.2	39.6	17.5	43.6	26.9	46.2	17.8	29.9
Fieryblack shiner				0.1	1.7	0.2	8.9	6.5	31.1	2.8
Eastern silvery minnow		0.6	0.2	0.3	0.7		0.1			0.2
Thicklip chub	4.3	0.7	8.5	7.9	10.9	3.6	1.8	5.7	2.2	5.5
Santee chub				0.1						>0.0
Bluehead chub	1.7	0.0	0.1	1.2	7.9	1.4	4.0	3.4	1.1	2.6
Spottail shiner	0.9	11.3	3.2	6.0	10.6	19.8	6.9	8.5	1.1	9.0
Yellowfin shiner	1.3				0.1					0.1
Sandbar shiner	3.2	2.4	10.3	5.7	13.4	3.9	15.0	4.0	0.6	7.0
Northern hogsucker		0.6	0.3	0.4	1.6	2.4	0.7	0.7	1.7	1.0
Smallmouth buffalo					0.1					>0.0
Silver redhorse						0.1				>0.0
Shorthead redhorse		0.8			0.1					0.1
V-lip redhorse						0.1				>0.0
Striped jumprock		0.1	1.3	2.2	2.3	0.9	1.0	1.7	2.8	1.3
Brassy jumprock		0.0	0.7			0.3	0.3		4.4	0.3
Snail bullhead	7.7	6.2	14.0	6.6	4.6	2.2	7.2	2.6	9.4	5.9
White catfish		0.1	0.0		0.1					>0.0
Flat bullhead	1.0	0.8	1.0	0.7	0.9	0.2	0.4	0.2		0.6
Channel catfish	0.1	0.7	0.2	0.8			0.1			0.2
Margined madtom	13.6	6.2	4.8	2.1	8.2	0.5	1.8	1.2		4.1
Eastern mosquitofish			0.1	0.2	0.1	1.6	0.3			0.4
White perch		0.1								>0.0
Redbreast sunfish	35.9	26.3	13.7	11.6	6.9	6.3	17.5	10.7	17.2	14.5
Green sunfish							0.2			>0.0
Pumpkinseed		0.1								>0.0
Warmouth				0.1						>0.0
Bluegill	0.3	5.4	5.1	2.2	2.5	1.8	0.4	0.1		1.9
Redear sunfish		1.0		0.2		0.1		0.1	0.0	0.1
Smallmouth bass		0.4		0.1	0.8	0.9	1.2	1.1	2.2	0.7
Largemouth bass	0.5		0.4	0.4						0.2
Fantail darter					0.8					0.1
Tessellated darter	1.0	2.4	1.6	1.2	0.5	0.8	0.5	0.7		1.0
Seagreen darter	8.3		0.7	0.7	0.0		0.2	0.1	0.6	1.1
Piedmont darter	10.6	7.3	4.1	6.9	2.0	2.1	2.7	1.6	1.1	4.2
Total No. of fish	996	723	979	1445	1179	1723	1125	1486	180	9836

Table 19. Species richness and Simpson's inverse diversity index for plot samples collected with backpack electrofishing gear from the Broad River, SC, during 2000 – 2002.

	Species Richness					Simpson's (1/D)				
Site	Fall 00	Spring 01	Fall 01	Spring 02	Mean	Fall 00	Spring 01	Fall 01	Spring 02	Mean
1	12	13	9	9	10.8	7.8	7.4	5.3	6.2	6.7
2	14	11	11	9	11.3	6.1	6.8	4.8	5.4	5.8
3	9	11	14	14	12.0	5.8	4.6	4.5	7.3	5.6
4	14	12	12	13	12.8	5.5	5.8	2.9	1.9	4.0
6	19	14	19	13	16.3	9.1	5.6	6.6	2.7	6.0
7	13	14	14	18	14.8	2.9	2.5	4.2	2.9	3.1
8	15	6	14	15	12.5	4.2	2.7	5.7	3.5	4.0
9	16	15	16	13	15.0	5.0	3.5	4.9	1.9	3.8
10	14					4.8				

Table 20. Catch per plot for samples collected with backpack electrofishing gear from the Broad River, SC, during 2000 – 2002. Means with the same letter were not significantly different (Tukey, $P > 0.05$).

Site	Fall 00	Spring 01	Fall 01	Spring 02	Mean
1	8.1	6.8	14.8	7.1	9.2^{z}
2	4.4	3.1	6.9	4.9	4.8^{y}
3	6.4	8.7	11.7	8.2	8.7^{zy}
4	25.6	11.2	8.8	14.1	14.9^{z}
6	11.0	4.9	16.0	11.9	10.9^{zy}
7	10.1	12.3	11.2	30.7	16.1^{z}
8	8.6	4.0	7.6	8.7	7.2^{zy}
9	15.6	13.2	13.5	23.1	16.3^{z}
10	8.0				

Table 21. Water quality data collected from Broad River, SC, sample sites during backpack electrofishing.

Date	Season	Site	Temp (C°)	DO (mg/L)	pH	Conductivity (mhos)	Turbidity (NTU)
10/24/2000	Fall	1	19.5	8.1	7.1	136.3	5.2
10/25/2000	Fall	2	17.9	8.6	7.1	188.4	6.8
10/02/2000	Fall	3	19.3	8.0	6.7	147.0	--
10/05/2000	Fall	4	21.5	7.7	7.4	177.3	--
10/06/2000	Fall	6	20.7	6.9	7.4	262.0	--
10/10/2000	Fall	7	14.6	9.6	8.1	189.0	--
10/11/2000	Fall	8	15.2	9.2	--	178.0	--
10/26/2000	Fall	9	18.1	7.7	7.8	169.0	7.6
11/15/2000	Fall	10	11.6	9.5	6.3	84.6	11.9
5/08/2001	Spring	1	22.6	9.7	7.9	119.9	6.4
5/09/2001	Spring	2	23.5	8.5	8.4	145.8	5.5
5/14/2001	Spring	3	24.2	7.3	7.7	166.9	8.3
5/15/2001	Spring	4	26.8	7.8	7.8	166.2	7.8
5/16/2001	Spring	6	26.2	7.9	8.0	164.5	13.0
5/24/2001	Spring	7	28.9	7.2	--	143.1	19.7
6/07/2001	Spring	8	26.8	6.1	--	123.6	11.4
6/12/2001	Spring	9	26.8	6.7	7.7	117.1	18.9
9/24/2001	Fall	1	26.8	7.0	8.5	133.3	3.2
10/11/2001	Fall	2	18.7	8.4	8.2	132.0	9.9
10/10/2001	Fall	3	17.2	8.8	7.9	136.5	13.2
10/01/2001	Fall	4	20.5	9.6	8.4	100.0	20.6
10/02/2001	Fall	6	21.5	8.9	8.4	122.3	17.0
10/03/2001	Fall	7	20.7	9.6	8.4	136.0	14.0
10/08/2001	Fall	8	16.3		8.2	171.0	9.8
10/16/2001	Fall	9	19.6	7.9	7.4	99.7	10.3
5/29/2002	Spring	1	26.6	8.1	--	121.1	5.3
5/30/2002	Spring	2	25.4	7.0	8.2	148.5	6.5
6/04/2002	Spring	3	29.6	6.4	8.1	185.0	8.7
5/20/2002	Spring	4	22.3	9.5	--	119.8	11.1
5/22/2002	Spring	6	19.2	9.9	8.3	102.1	9.8
5/28/2002	Spring	7	25.1	6.8	7.7	156.8	24.4
5/23/2002	Spring	8	17.9	8.3	7.7	138.1	23.7
5/21/2002	Spring	9	20.5	7.6	7.7	97.0	15.8

Table 22. Percent contribution of substrate types, by site, with average depth and flow, during backpack electrofishing, 2000 – 2002, in the Broad River, SC.

Site	Sand	Gravel	Pebble	Cobble	Boulder	Bedrock	Depth (cm)	Flows (ft/s)
	Substrate							
1	36	29	12	8	9	7	42	0.42
2	18	27	21	9	11	13	38	0.43
3	18	24	15	8	15	20	40	0.33
4	35	12	17	11	15	10	36	0.42
6	4	17	43	17	6	13	29	0.48
7	7	44	21	2	4	22	37	0.39
8	9	14	10	9	18	41	40	0.32
9	8	17	29	9	18	19	32	0.38
Overall	16	23	21	9	12	19	37	0.39

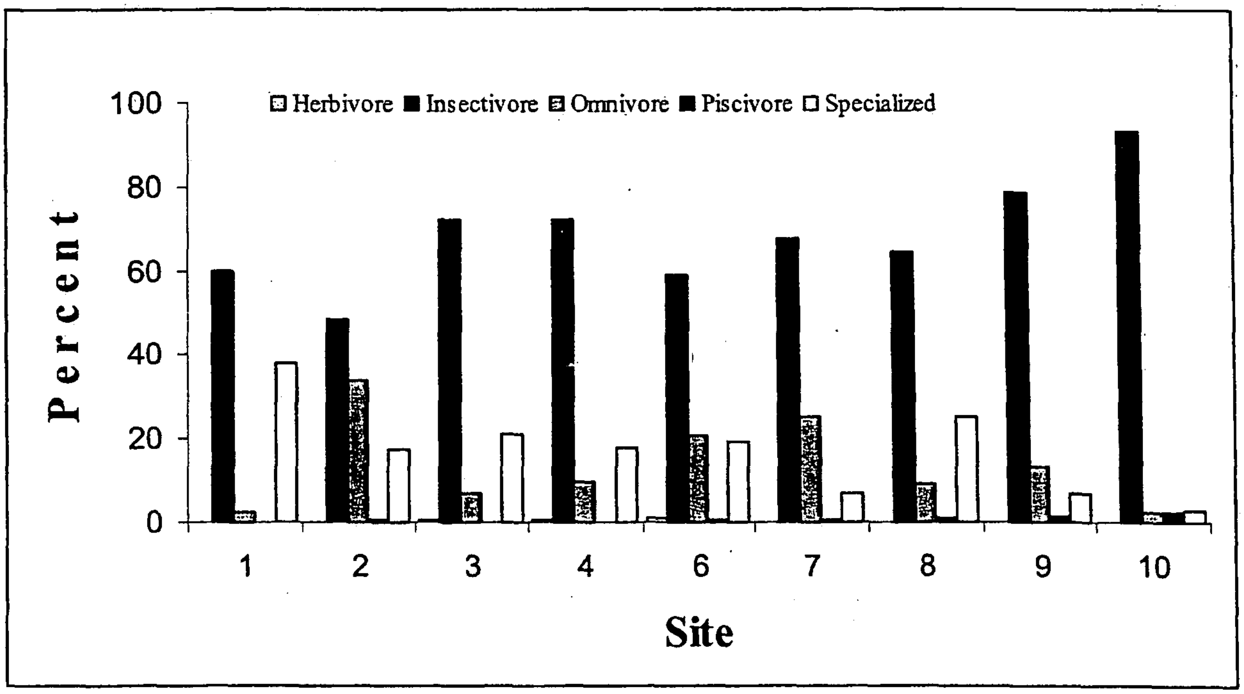

Figure 4. Relative abundance of five trophic groups of fish collected with backpack electrofishing gear from the Broad River, SC.

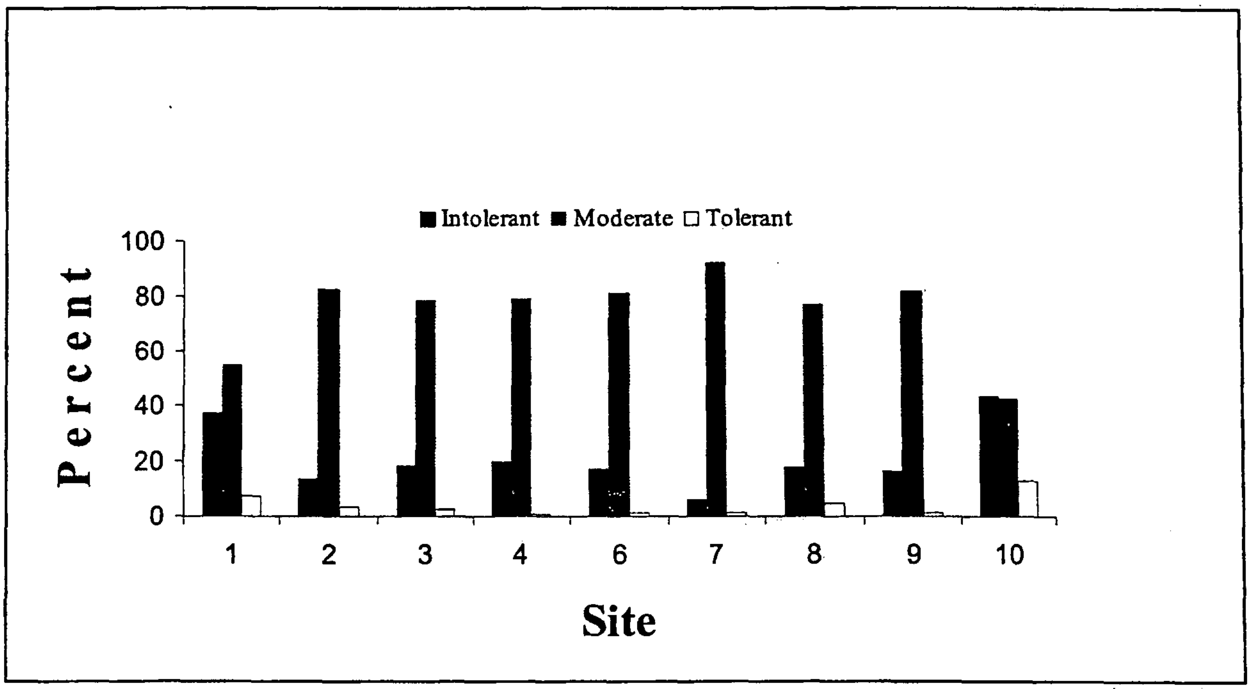

Figure 5. Relative abundance of three pollution tolerance groups of fish collected with backpack electrofishing gear from the Broad River, SC.

Discussion

The Broad River contains a rich and diverse fish community. Fifty-one species of fish representing nine families were collected from the Broad River during the present study (Appendix 1). Forty-seven species of fish were collected with boat electrofishing gear; 34 similar species and 4 additional species were collected with backpack electrofishing gear. We collected three species not previously documented from the Broad River, including an undescribed species similar to highfin carpsucker, smallmouth buffalo, and Santee chub. We also collected hybrid striped bass, not previously documented. The family Cyprinidae contributed the most species (14), followed by Centrarchidae (10 species) and Catostomidae (10 species). Overall, the most commonly collected fish were redbreast sunfish, whitefin shiner and silver redhorse. No federally-listed threatened or endangered species were collected. However, we did collect fantail darter, a species on the South Carolina Heritage Trust list of fishes of special concern.

The current species richness of the Broad River is comparable to what was previously known from the Broad River and similar-sized rivers in South Carolina. Previous sampling, conducted by various researchers (Kleinschmidt Associates 1995, Dames & Moore 1974, Duke Energy unpublished data), identified a total of 77 fish species occurring in the Broad River; however, the identifications of 22 of those species are questionable. Twelve of those 22 were almost certainly misidentified because the Broad River is far outside their known ranges (e.g. pallid shiner and spotted gar) (Appendix 1). A recent survey of the Catawba River documented 39 species (Dewitt 1998) and 59 freshwater fish species were documented in the Edisto River (Thomason et al. 1993).

Species richness and Simpson's inverse diversity index values varied among sites and between seasons. Longitudinal changes in mean species richness and mean diversity were observed in boat electrofishing collections. In general, species richness and diversity tended to be higher at downstream sites. Backpack electrofishing collections also indicated greater diversity at downstream sites, but species richness tended to be lower there. In undisturbed systems species richness normally increases downstream as drainage area increases. It is not clear why backpack electrofishing collections indicated higher mean species richness at upstream sites.

We did not observe any seasonal or longitudinal trends in water quality parameters. Water chemistry did not appear to affect CPUE, species richness or species diversity in backpack or boat electrofishing. Generally, it takes gross changes in water chemistry, such as with heavy pollution, to establish correlations with changes in fish communities (Moyle and Cech Jr. 1988).

Several species of interest were collected from the Broad River including "highfin" carpsucker, V-lip redhorse, and fantail darter. Our collection of "highfin" carpsucker represents only the third time it has been collected from the Atlantic Slope. Previous records for the species on the Atlantic Slope include one individual from the Catawba River, NC and one individual from the Pee Dee River, SC (person. comm., Robert Jenkins). The "highfin" carpsucker is native to the Interior Basin and its taxonomy and distribution along the Atlantic Slope are not known. The SCDNR is now supporting genetics work to investigate the relationship between the "highfin" carpsuckers of the Atlantic Slope and those from the Interior Basin.

The V-lip redhorse was very rare in our collections and was only found at middle and upstream sites. Although this species has been collected previously from the Broad River its occurrence does represent a range extension for the species (pers. comm., Wayne Starnes). It is not clear if there is a reproducing population of V-lip redhorse in the Broad River in South Carolina or if the adults we collected are simply displaced individuals from further up in the basin. The V-lip redhorse may be a candidate for inclusion on the South Carolina Heritage Trust list of fishes of special concern.

The fantail darter was only collected at site 6, a site that had the greatest mean species richness and the second highest mean species diversity in backpack electrofishing samples. Although this species is abundant throughout much of its range outside of South Carolina, we only found one population at one site in the Broad River. The rarity of this fish in our collections support its inclusion on the South Carolina Heritage Trust list of fishes of special concern.

The Broad River supports typical piedmont river sportfishing opportunities, comprising a variety of centrarchid species (e.g. largemouth bass and redbreast sunfish). The Broad River also boasts a smallmouth bass fishery, which is unique to piedmont rivers in South Carolina. Smallmouth bass were introduced into the South Carolina portion of the Broad River by the SCDNR in 1984 to increase and diversify sportfishing. Since their introduction a small but unique fishery has developed that is gaining local and regional attention annually. Based on anecdotal reports from anglers, the fishing for smallmouth bass is generally good. During our study we collected relatively few smallmouth bass; however, growth rates based on our data are comparable to other piedmont systems in the southeast. Additionally, we documented natural reproduction of smallmouth bass at sites 4, 7, and 8. We recommend that further efforts be directed at describing the life-history of the smallmouth bass population in the Broad River and that the economics of the SCDNR smallmouth bass stocking program be evaluated.

LARGEMOUTH BASS HEALTH

Introduction

We investigated the health of the largemouth bass (*Micropterus salmoides*) population in the Broad River, South Carolina, as part of the Comprehensive Broad River Aquatic Resources Inventory. We chose largemouth bass because they were readily available and we believed their condition would reflect the overall health of the aquatic community. The position of largemouth bass in the food chain, as a top predator, should integrate the effects of many biotic and abiotic variables that affect aquatic community health (Adams and McLean 1985). Largemouth bass have been used in Tennessee Valley Authority Reservoirs (Brown and Hickman 1990) and the Catawba River of North and South Carolina (Coughlan et al. 1996) to investigate fish health.

Largemouth bass health was determined by conducting a fish health assessment (FHA), an autopsy-based procedure in which organs, structures and blood parameters of individual fish are assessed and scored based on their deviation from normality (Table 23). Scores for organs, structures and blood parameters of individual fish are summed to calculate a fish health assessment index (FHAI) value. Fish with higher FHAI values are considered to be in poorer health than fish with lower values. The FHA was originally described by Goede and Barton (1990) and has been modified by Adams et al. (1993) and Coughlan et al. (1996).

Methods

Ten sites corresponding to current SCDNR fish community sampling sites were selected for conducting the FHA (Figure 1). Site numbers were assigned longitudinally with the most downstream site being site 1 and the most upstream being site 11. Each site was classified by what were perceived to be the most important anthropogenic impacts. Sites were classified as not impacted (N) or as impacted by industrial effluent (I), municipal/community effluent (M), or hydroelectric facilities (H). Industrial sites were defined as areas with one or more major industrial effluents within 4 km of the sample site. Municipal/community sites were those sites with municipal and community effluent within 4 km of the sample site. Sites classified as impacted by hydroelectric facilities were located within 2 km of an upstream hydroelectric facility.

Fifteen largemouth bass were collected at each site during November, 2001, and processed using the autopsy-based fish health assessment described by Adams (1993). Fish were captured during the day with boat mounted electrofishing gear. After capture, largemouth bass were anesthetized with 10% eugenol (Anderson et al. 1997) and held in an aerated live-well. The peritoneal and pericardial cavities were opened to expose the organs for visual assessment. Because liver coloration and blood parameters can change rapidly after death, liver coloration was evaluated and blood was collected from each fish before the other variables were assessed. Liver color was immediately recorded and blood was collected from the heart with a sharpened micro-hematocrit tube. Fish were then tagged and placed on ice until the other variables could be scored. Otoliths were collected from all fish to estimate age.

FHAI scores were calculated using the Adams scoring methodology (Adams et al. 1993) and the modified method suggested by Coughlan et al. (1996) (Table 23). Comparisons among sites were investigated using a Kruskal-Wallis Test (SAS 1989). Multiple comparisons were investigated using a Nemenyi Test (Zar 1996). Linear regression was used to determine if there was a relationship between average age or weight of fish and mean FHAI scores.

Results

We tried to follow the suggestions of Coughlan et al. (1996) and evaluate only fish that were between 250 mm and 450 mm total length (TL). However, occasionally fish outside the suggested size range were evaluated. Four fish greater than 450 mm TL (range 451-464 mm) and one fish 247 mm TL were scored. Estimated ages of largemouth bass ranged from 1 to 13. Mean estimated ages by site are reported in table 24.

Coughlan-modified FHAI scores (Coughlan et al. 1996) for individual fish ranged from 0 to 125. Mean Coughlan-modified scores by site ranged from 37 to 59 and averaged 45 (Table 25). The highest average scores, 59 and 54, were observed at sites 3 and 8, respectively and the lowest score (37) was observed at sites 1 and 7. The Adams scoring methodology resulted in FHAI scores ranging from 0 to 150 for individual fish. Mean scores by site ranged from 35 to 73 and averaged 57. The highest mean scores, 73 and 69, were observed at sites 3 and 8, respectively and the lowest score (35) was observed at site 6. There were no significant differences in the Coughlan-modified scores among sites (Kruskal-Wallis test; P = 0.18); however, there were significant differences among sites using the Adams scores (Table 25)(Kruskal-Wallis; P = 0.03). Significant differences were found between site 6 (lowest scoring non-impacted site) and all the sites impacted by industrial effluent (sites 3, 8 and 9). Significant differences were also found between sites 6 and 10, and between sites 3 and 4. There were no significant relationships (P> 0.05) between mean age or weight of largemouth bass and FHAI score using either the Adams or Coughlan scoring methodology.

Liver discoloration, poor relative weight (<85%), and skin anomalies were the most frequently observed abnormalities (Table 26). Anomalous livers were observed at every site and in 59% of the fish processed. Most abnormal livers (88%) were scored for moderate general discoloration of the whole liver. The frequency of anomalous livers was greatest at sites 1 and 8 where 12 of 15 fish had discolored livers. Site 6 had the fewest number of fish with anomalous livers (4 of 15). Poor relative weights were observed at every site and in 49% of the fish processed. At sites 4, 7, and 8, 11 of 15 fish had relative weights < 85%. Conversely, at sites 2 and 3 only 2 fish had poor relative weights. Mild hemorrhaging of the skin surface was observed at every site and in 47% of the fish processed. Hemorrhaging of the skin surface was most common at site 7 where 10 of 15 fish had mild hemorrhaging and least common at site 10 where only 3 fish had hemorrhagia on the skin surface.

Abnormalities of the gill rakers, trunk kidney and gills were common (Table 26). Gill raker abnormalities were observed at each site and in 33% of the fish processed. Most (96%) gill raker abnormalities consisted of slightly deformed rakers or gill arches missing 5 or fewer rakers. The frequency of gill raker deformities was rather consistent among sites. Abnormal trunk kidneys were observed in 32% of the fish processed. Most (47 of 48) trunk kidney abnormalities were due to swollen or enlarged trunk kidneys. One fish from site 6 had a trunk kidney that was gray in appearance and contained a milky fluid. The highest frequency of anomalous trunk kidneys was observed at site 3 where 10 of 15 fish had abnormal trunk kidneys. No trunk kidney abnormalities were observed at site 7. Gill abnormalities were observed in 20% of the fish processed and at every site. Most gill abnormalities were due to pale filaments and occasionally missing filaments.

Abnormal blood parameters were observed at each site (Table 27). Twenty-three percent of all fish processed had elevated plasma protein levels. Abnormal plasma protein levels were most common at site 3, where 9 of 15 fish had plasma protein levels above the normal range and least common at site 6 where none of the fish had elevated plasma protein levels. Atypical hematocrit levels were observed in 17% of the fish processed. Most (68%) deviant scores were due to hematocrit levels above the normal range. Atypical hematocrit levels were most frequent at site 4, where 6 of 15 fish had abnormal levels and least common at site 9 where one fish had below normal hematocrit levels. Only one of 150 fish processed had elevated leucocrit levels and it was collected at site 8.

The remainder of the metrics scored contributed little to the FHA. Four fish had mesenteric adhesions that were scored as gross abnormalities. Only three atypical spleens were observed: two were nodular and one was abnormally small; it appeared to be half the size of a normal spleen. We did not encounter an abnormal thymus, pseudobranch or hindgut.

Discussion

Largemouth bass populations in the Broad River appear to be in good condition based on the results of our FHA. Brown (1993) considered sites with average scores >90, using the Adams scoring methodology, to be areas in need of further study. Using the Coughlan-modified scoring method, areas of concern would have average index scores >75 (Coughlan et al. 1996). None of the Broad River sites had mean Adams scores > 73 or Coughlan-modified scores > 59.

Industrial effluent appears to adversely affect largemouth bass health. Sites located near industrial effluent scored higher than nearly all the other sites using both scoring methodologies. The next highest scores were observed at site 10. The high scores (Coughlan 49; Adams 66) at site 10 may have been confounded by the size and age of fish collected. Mean estimated age and weight were greater at site 10 than any of the other sites sampled. Although there was not a significant relationship between age or weight of fish and FHAI score in this study other studies have documented a positive relationship between largemouth bass age and FHAI score

(Coughlan et al. 1996). The other anthropogenic influences identified in this study (municipal impacts and hydropower operations) did not seem to adversely affect the health of largemouth bass.

Although none of the sites warrant further study based on the *a priori* concern levels a relationship between compromised largemouth bass health and industrial sites was identified. Further research is suggested to determine if the trend in largemouth bass health and proximity to industrial sites is consistent annually.

Table 23. Organs, structures and blood parameters scored during the Broad River largemouth bass FHA, associated condition, field designation and values used to calculate index scores using the Adams and Coughlan modified scoring criteria (modified from Adams et al. 1993 and Coughlan et al. 1996).

Tissue or Organ	Condition	Designation	Adams	Coughlan
Liver	Normal. Solid red or light red color.	A	0	0
	"Fatty" liver. Light tan color as "coffee with cream"			
	color moderate[a]	C1	30	15
	color severe	C	30	30
	Cysts/Nodules	D	30	30
	Focal discoloration - change of color in local areas or foci of liver.	E	30	30
	General discoloration of whole liver			
	color moderate[a]	F1	30	15
	color severe	F	30	30
	Other - any observation which does not fit above categories	OT	30	30
Gills	Normal with no apparent aberrations	N	0	0
	Frayed - erosion of tips of lamellae resulting in "ragged" appearing gills	F	30	30
	Clubbed - swelling of gill lamellae tips	C	30	30
	Marginate - light gill margin, discolored lamellar tips	M	30	30
	Pale - light, discolored gills (whole gills)	P	30	30
	Other - any observation which does not fit above categories			
	mild[a]	OT1		10
	moderate[a]	OT2		20
	severe	OT3	30	30
Gill Rakers[a]	Normal			0
	Slightly deformed or missing (<5 rakers)			10
	Moderately deformed or missing (5-10 rakers)			20
	Severely deformed or missing (>10 rakers)			30
Pseudobranch	Normal - flat with no aberrations	N	0	0
	Swollen - convex in appearance	S	30	30
	Lithic - mineral deposits (amorphous white spots)	L	30	30
	Swollen and lithic	X	30	30
	Inflamed	I	30	30
	Other - any observation which does not fit above categories	OT	30	30
Thymus	Normal appearance - no hemorrhage		0	0
	Mild hemorrhage		10	10
	Moderate hemorrhage		20	20
	Severe hemorrhage		30	30
Mesenteric Fat	No fat between pyloric ceca	0		
	Less than 50% of ceca covered with fat	1		
	50% of ceca covered with fat	2		
	More than 50% of ceca covered with fat	3		
	Ceca totally covered with fat	4		
Bile	Straw color, bladder empty	0		
	Straw color, bladder full	1		
	Grass green color, bladder full	2		
	Dark green color, bladder full	3		
Sex	Male	M		
	Female	F		

Table 23. Continued.

Tissue or Organ	Condition	Designation	Adams	Coughlan
Spleen	Normal - black, very dark red, or red	B	0	0
	Granular - rough appearance (normal)	G	0	0
	Nodular - nodules or fistulas of various sizes	N	30	30
	Enlarged	E	30	30
	Other - any observation which does not fit above categories	OT	30	30
Hindgut	Normal - no inflammation or reddening		0	0
	Slight inflammation or reddening		10	10
	Moderate inflammation or reddening		20	20
	Severe inflammation or reddening		30	30
Trunk Kidney	Normal - firm, lying relatively flat dorsally along the ventral surface of the vertebral column	N	0	0
	Swollen - enlarged or swollen, wholly or in part	S	30	30
	Mottled - gray discoloration	M	30	30
	Granular - granular appearance or texture	G	30	30
	Urolithic - white or cream-colored mineral deposits in kidney tubules (nephrocalcinosis)	U	30	30
	Other - any observation which does not fit above categories	OT	30	30
Opercles	Normal - no shortening, gills completely covered			0
	Slight shortening, a very small portion of the gills exposed			10
	Moderate shortening, a small portion of the gills exposed			20
	Severe shortening, a considerable portion of the gills exposed			30
Skin	Normal - no hemorrhagic areas			0
	Mild hemorrhagia on skin surface (<10 %)			10
	Moderate hemorrhagia on skin surface (10 - 60 %)			20
	Severe hemorrhagia on skin surface (>60 %)			30
Fins	Normal - no active erosion		0	0
	Light active erosion		10	10
	Moderate active erosion with some hemorrhaging		20	20
	Severe active erosion with hemorrhaging		30	30
Eye	Normal clear eyes (lens) - no aberrations	N	0	0
	Lenticular opacity (blind)			
	one eye	B1	30	15[a]
	both eyes	B2	30	30
	Exopthalmia - swollen or protruding eye			
	one eye	E1	30	15[a]
	both eyes	E2	30	30
	Hemorrhagic - bleeding			
	one eye	H1	30	15[a]
	both eyes	H2	30	30
	Missing			
	one eye	M1	30	15[a]
	both eyes	M2	30	30
	Other - any observation which does not fit above categories			
	one eye	OT1	30	15[a]
	both eyes	OT2	30	30

Table 23. Continued.

Tissue or Organ	Condition	Designation	Adams	Coughlan
Parasites	No observed parasites		0	0
	Few observed parasites, parasites in just one organ		10	10
	Moderate parasite infestation, parasites observed in several organs		20	20
	Numerous observed parasites, extensive infestation in several organs		30	30
Relative	≥85.00			0
Weight (%)[a]	≥70.00 and <85.00			15
	<70.00			30
Gross	No visible gross abnormalities	N		0
Abnormalities[a]	Tumors visible on external surfaces	E		30
	Tumors visible on internal surfaces	I		30
	Lordosis of vertebral column	L		30
	Scoliosis of vertebral column	S		30
	Skeletal deformities/broken bones of head and jaws	D		30
	Skeletal deformities/broken bones of remaining bony structures	B		30
	Other - any observation which does not fit above categories	OT		30
Hematocrit (%)	Normal range (30 - 45)		0	0
	Above normal range (>45)		10	10
	Below normal range (19 - <30)		20	20
	Well below normal range (<19)		30	30
Leucocrit (%)	Normal range (0 - <4)		0	0
	Above normal range (≥4)		30	30
Plasma	Normal range (3 - 7)		0	0
Protein (g/dL)	Above normal range (>7)		10	10
	Below normal range (<3)		30	30

[a] Parameters used to calculate Coughlan modified scores only.

Table 24. Mean estimated age, range in parentheses, and mean weight for largemouth bass collected from the Broad River during November 2001.

Site No.	Mean estimated age	Mean weight
1	1.9 (1-3)	394
2	3.5 (1-13)	595
3	2.5 (1-7)	647
4	2.7 (2-5)	448
5	2.7 (1-6)	468
6	3.8 (3-8)	586
7	2.7 (2-4)	372
8	2.9 (2-5)	302
9	2.9 (2-5)	390
11	4.1 (2-7)	737

Table 25. Mean Coughlan and Adams fish health assessment index (FHAI) scores and standard deviation for largemouth bass collected from the Broad River, SC, during November 2001. Mean scores with the same letter were not significantly different (Nemenyi Test; $P = 0.05$).

Site No.	Perceived Impact[a]	N	Coughlan	Adams
1	M	15	37 ± 20	$59^{xy} \pm 29$
2	N	15	39 ± 17	$52^{xy} \pm 29$
3	I	15	59 ± 24	$73^{x} \pm 28$
4	M, H	15	40 ± 20	$46^{yz} \pm 22$
5	N	15	45 ± 26	$60^{xy} \pm 34$
6	N	15	41 ± 34	$35^{y} \pm 39$
7	M, H	15	37 ± 17	$50^{xy} \pm 21$
8	I, M	15	54 ± 35	$69^{xz} \pm 42$
9	I	15	49 ± 20	$65^{xz} \pm 24$
11	N	15	49 ± 31	$66^{xz} \pm 39$
Mean			45 ± 26	57 ± 32

[a]Perceived impacts are classified as: (H) hydroelectric impacts; (I) industrial impacts; (M) municipal impacts; (N) not impacted.

Table 26. Percentage of fish with anomalous tissues, organs, and/or relative weight (Wr), collected from 10 sites in the Broad River, South Carolina during fall 2001.

	Percent atypical in					
Site	Liver	Wr	Skin	Gill rakers	Trunk kidney	Gills
1	80	40	60	13	13	13
2	53	13	40	27	47	7
3	73	13	60	33	67	13
4	60	73	47	33	7	13
5	53	40	47	47	33	33
6	27	60	33	40	33	13
7	47	73	67	40	0	27
8	80	73	60	33	20	20
9	53	60	40	33	47	40
10	67	40	20	27	53	20
All sites	59	49	47	33	32	20

Table 27. Percentage of fish with atypical blood parameters collected from 10 sites in the Broad River, South Carolina during fall 2001.

Site	Hematocrit	Leucocrit	Plasma Protein
1	13	0	33
2	13	0	40
3	20	0	60
4	40	0	0
5	20	0	13
6	13	0	0
7	13	0	7
8	13	7	13
9	7	0	27
10	13	0	40
All sites	17	1	23

GASTON SHOALS BYPASS

Introduction

In 1996 Duke Power Company (Duke) implemented minimum flows for the bypassed section of the Gaston Shoals Tailrace. The bypassed section is an area where water was diverted from the original river channel during dam construction. Before minimum flows were implemented the bypassed section received minimum flows from dam seepage and water running over the spillway during high flow events. We compared data collected before and after minimum flows were initiated to examine the effects of minimum flows on the fish community.

Methods

Pre-minimum flow fish community data were collected by Duke on 6 September 1989. Duke used rotenone and electrofishing to sample two sites located in the bypassed section of the Gaston Shoals Tailrace. Post-minimum flow fish community data were collected on 15 November 2000. Fish were collected with backpack electrofishing gear following the methods described previously.

We pooled the data by sampling year and calculated relative abundance (RA), species richness and Simpson's diversity metrics for the fish community before and after the implementation of minimum flows. Additionally, each species collected was assigned to one of three pollution tolerance levels (tolerant, moderately tolerant, or intolerant) and one of five trophic levels (piscivore, insectivore, omnivore, specialized insectivore, or herbivore) (EPA 1999, NCDENR 2001). We calculated the proportion of each trophic and tolerance group for the two samples.

Results

In 1989 a total of 541 fish comprising 16 species was captured (Table 28). Numerically redbreast sunfish dominated the catch, comprising 43% of all fish captured. The second most abundant species was the whitefin shiner comprising 17% of all fish captured. Bluegill, snail bullhead and greenfin shiner were common, each comprising more than 6% of all fish captured. The rarest fish collected was the tessellated darter; only one individual was collected.

In 2000 eighteen standardized riffle and run backpack electrofishing collections were made and one 100 m shoreline section was sampled. A total of 180 fish comprising 15 species was collected (Table 28). Numerically the most dominant fish was the fieryblack shiner, representing 31% of all fish captured. Whitefin shiner and redbreast sunfish were the second most abundant species, representing 18% and 17%, respectively, of all fish captured. Snail bullhead and greenfin shiner were common, each comprising more than 6% of all fish collected. The rarest fish in the sample included sandbar shiner and seagreen darter; only one of each species was collected.

Simpson's inverse diversity index was higher for the 2000 sample than for the 1989 sample (Table 29). Species richness (total number of species) was slightly higher in 1989 than in 2000.

Percent contribution of tolerance groups varied considerably between pre- and post-minimum flow collections. In the 1989 samples only moderately tolerant and tolerant individuals were collected and they were collected in nearly equal proportions (Figure 6). In the 2000 collections all three tolerance groups were collected. Moderately tolerant individuals were the most abundant followed by intolerant and tolerant individuals. Percent contribution of the five feeding groups did not vary greatly among the pre- and post-minimum flow samples (Figure

7). In both years insectivores were the most dominant trophic group representing more than 90% of the individuals collected. None of the remaining trophic groups represented more than 2% of the population in either 1989 or 2000. The only other notable observations were the slightly higher proportion of specialized insectivores and piscivores and the absence of herbivores in the 2000 collection.

Discussion

The various gear types used during the pre- and post-minimum flow sampling may have influenced the results. Several large bodied species were collected in 1989 that were not collected in 2000, including largemouth bass, silver redhorse and white sucker. The backpack electrofishing techniques used in 2000 are capable of collecting large bodied fish, but not as effectively as the rotenone sampling that was conducted in 1989. The change in species composition suggests that a more diverse community exists in the bypassed reach since minimum flows were introduced. In 2000 we collected four intolerant species: fieryblack shiner, thicklip chub, seagreen darter and piedmont darter. No intolerant species were collected in 1989, but in 2000 they represented 35 % of the fishes collected. The relative abundance of tolerant individuals was reduced during the 2000 sample. During 1989 the three tolerant species (white sucker, redbreast sunfish, and flat bullhead) collected represented 49% of the fish collected. During 2000 only one tolerant species (redbreast sunfish) was collected and it represented only 17% of the total fish collected.

The implementations of minimum flows in the Gaston Shoals bypass appear to have had a positive effect on the fish community residing in the bypass. The change in species composition, species diversity and tolerance composition all suggest a more diverse community residing in a more stable habitat.

Table 28. Number and relative abundance (RA, %) of each species collected for samples collected at the Gaston Shoals bypass before (1989) and after (2000) the implementation of minimum flows.

	1989		2000	
Common Name	No.	RA	No.	RA
Greenfin shiner	43	7.9	12	6.7
Whitefin shiner	93	17.2	32	17.8
Fieryblack shiner			56	31.1
Eastern silvery minnow	7	1.3		
Thicklip chub			4	2.2
Bluehead chub		0.0	2	1.1
Spottail shiner	2	0.4	2	1.1
Sandbar shiner			1	0.6
White sucker	10	1.8		
Northern hogsucker	4	0.7	3	1.7
Silver redhorse	14	2.6		
Striped jumprock	22	4.1	5	2.8
Brassy jumprock	3	0.6	8	4.4
Snail bullhead	33	6.1	17	9.4
Flat bullhead	23	4.3		
Redbreast sunfish	234	43.3	31	17.2
Bluegill	45	8.3		
Smallmouth bass	3	0.6	4	2.2
Largemouth bass	4	0.7		
Tessellated darter	1	0.2		
Seagreen darter			1	0.6
Piedmont darter			2	1.1
Total	541	100.0	180	100.0

Table 29. Species richness and Simpson's Inverse Diversity Index for samples collected at the Gaston Shoals bypass before (1989) and after (2000) the implementation of minimum flows.

Year	1989	2000
Simpson's	4.2	5.8
Richness	16.0	15.0

Figure 6. Percent contribution of three tolerance groups based on data collected from the Gaston Shoals bypass before (1989) and after (2000) the implementation of minimum flows.

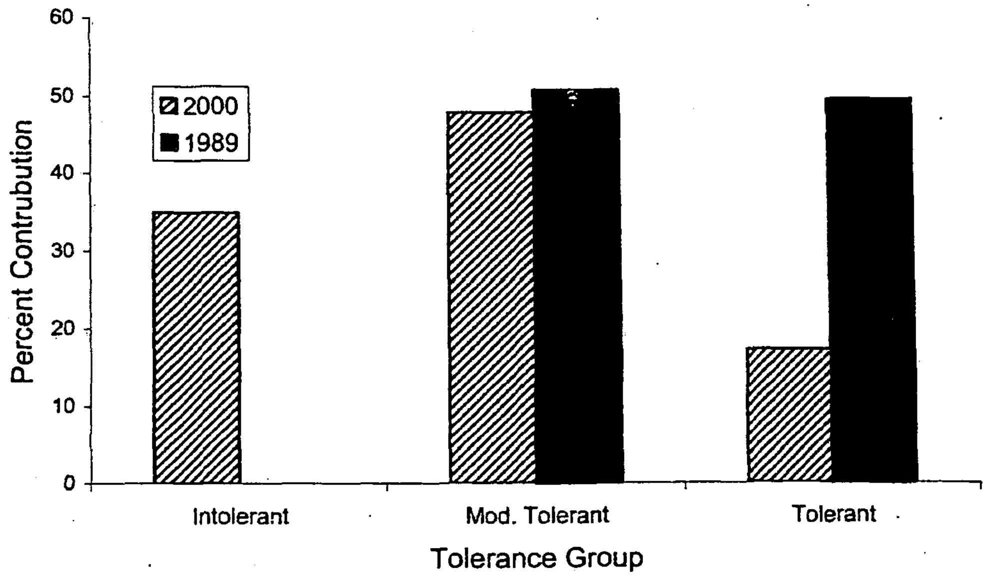

Figure 7. Percent contribution of five trophic groups based on data collected from the Gaston Shoals bypass before (1989) and after (2000) the implementation of minimum flows.

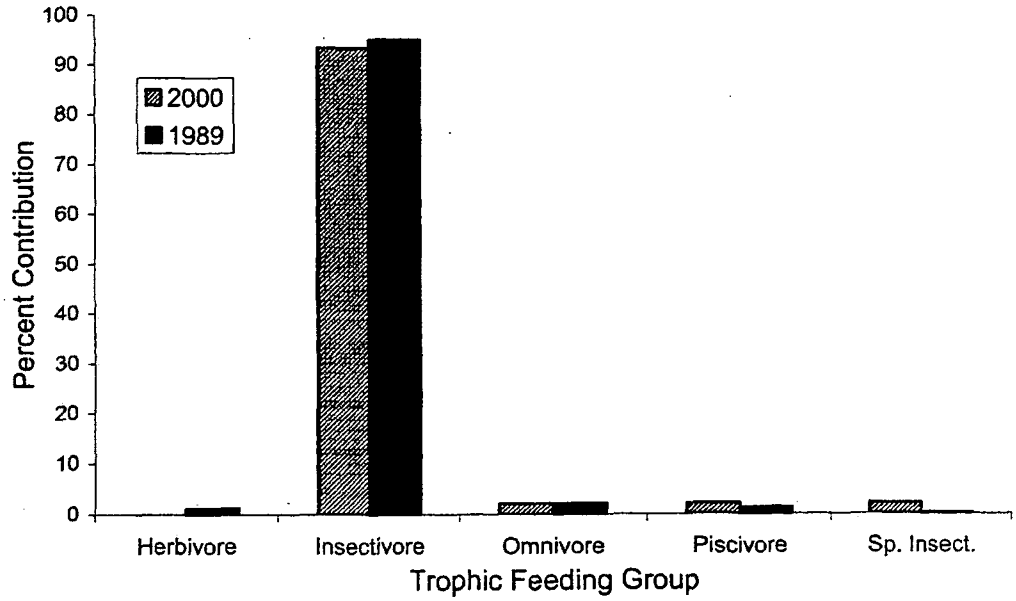

MUSSEL INVENTORY

Methods

We surveyed six sites for mussels during the summer 2002 (Figure 8). We surveyed two sites between Columbia Dam and Parr Shoals Dam, two sites between Lockhart and 99-Islands, and two sites between Cherokee Falls and Gaston Shoals. Latitude and longitude coordinates are provided in Table 30. At each site we conducted a qualitative mussel survey, where two people equipped with view buckets or snorkeling gear visually searched for live mussels. Search time was recorded to the nearest 0.1 hour. All live native mussels encountered were collected and, when possible, identified to species. Species identifications were facilitated with the illustrations and descriptions of Johnson (1970) and with the Workbook and Key to the Freshwater Bivalves of North Carolina (Bogan, 2002). We compiled species lists and computed catch per unit effort (CPUE) as number of live mussels per hour for each site.

Relic shell material was also collected at each site to construct a reference collection and verify species identifications. Relic shells were identified at the North Carolina Museum of Natural Sciences (NCMNS) by Dr. Arthur Bogan (Mussel Curator, NCMNS) using Johnson (1970) and by comparing relic material collected from the Broad River with type specimens held at NCMNS.

Results

At each site two people expended approximately 2 h of effort searching for live mussels (Table 30). We were unable to satisfactorily identify the species of the Elliptio genus in the field and were therefore only able to identify elliptio species as *E. complanata* or as a member of the *E. lanceolata* group. A total of 315 live mussels were collected during the mussel survey. Only two species, *E. complanata* and *Villosa delumbis* and one group of mussels (E. *lanceolata*), were collected. Eighty-seven percent of the mussels collected belonged to the *E. lanceolata* group, 9% were *E. complanata*, and 4% were *V. delumbis*. Catch rate of live native mussels ranged from 0.0 at sites 3 and 4 to 76.7 at site 2 (Table 31). Catch rate of mussels identified as belonging to the *E. lanceolata* group was higher at all sites than the catch rate of *V. delumbis* and *E. complanata*. Additionally, catch rate was much higher at the downstream sites (1 and 2) than the upstream sites.

From the relic shells collected in the Broad River we identified seven shell-forms, which we believe are seven different species (Table 32). Of those seven shell-forms only two, *E. complanata* and *V. delumbis*, could be identified with certainty. Three of the shell-forms likely belong to the *E. lanceolata* group. In that group the shell-forms we collected most resembled *E. gracilentus*, *E. angustata*, and *E. perlatus*. The other two shell-forms collected most resembled *E. icterina* and *Uniomerus carolinianus*.

Discussion

Native mussel fauna were more abundant and diverse in the lower river than in the upper section of the river. The collection gear used may have influenced our results. In the upper section of the river we used view buckets and unaided visual searches to locate live mussels and in the lower section we used snorkel gear. Snorkel gear is likely superior to view buckets and unaided visual searches for locating live mussels; however, it is doubtful that the gear type alone accounted for the differences in mussel catch rates between the upper and lower portions of the river. Physical habitat differences may have contributed to the disparate catch rates. The lower river is generally less turbid and has less silt than the upper sections of the Broad River (personal observation). Agricultural practices and multiple sand mining operations may contribute to the high level of siltation in the upper sections. Silt often causes freshwater mussels to suffocate by clogging their gills (Parmalee and Bogan 1998). Small and juvenile mussels can sink below the surface and suffocate in soft, freshly deposited silt (Williams and Schuster 1989). Silt deposits and shifting sand beds were abundant at sites 3 and 4 where no live native mussels were found. Fine sediment deposits were also common at sites 5 and 6 where few adult mussels and no juvenile mussels were collected. Additionally, the frequency of impoundments, which may have a deleterious effect on the mussel fauna, is greater in the upper section of the river. Dams negatively impact mussel communities by direct loss of habitat due to impoundment, altering flows and temperatures, and changing substrate composition (Parmalee and Bogan 1998).

To our knowledge, this limited mussel survey is the most intensive survey of its type conducted on the South Carolina portion of the Broad River. We identified seven distinct shell forms that we believe are seven different species; however, we are not certain of the identity of five of those species. The *Elliptio* species of the Southern Atlantic slope have received little attention and are among the least known mussels in North America (Arthur Bogan, personal communication). A concentrated study is needed not only in the Broad River, but also throughout the South Carolina portion of the Southern Atlantic slope to better understand the taxonomy and distribution of freshwater mussels in South Carolina.

Table 30. Location of each site sampled, gear used and the amount of effort in man-hours for the Broad River mussel survey, summer 2002.

Date	Site	Latitude	Longitude	Gear	Effort
9/16/2002	1	34 08' 39"	81 08' 46"	snorkel	3.1
9/16/2002	2	34 11' 64"	81 12' 44"	snorkel	2.8
6/20/2002	3	34 54' 38"	81 28' 18"	View bucket	4.0
6/20/2002	4	34 50' 48"	81 27' 11"	View bucket	4.0
9/11/2002	5	35 04' 45"	81 34' 02"	View bucket	4.0
9/11/2002	6	35 05' 18"	81 34' 18"	View bucket	3.9

Table 31. CPUE (No./h) of live mussels collected from six sites in the Broad River during the summer 2002.

	Species			
Site	*E. complanata*	*E. lanceolata group*	*V. delumbis*	All species
1	7.1	21.3	0.0	28.4
2	1.4	71.4	3.9	76.7
3	0.0	0.0	0.0	0.0
4	0.0	0.0	0.0	0.0
5	0.3	0.8	0.0	1.1
6	0.5	1.0	0.0	1.5

Table 32. Relic shells collected from six sites in the Broad River during the summer 2002.

	Site					
Species	1	2	3	4	5	6
Elliptio cf gracilentus	x	x			x	x
Elliptio cf angustata		x			x	
Elliptio cf perlatus	x	x				
Elliptio complanata	x	x			x	x
Elliptio cf icterina		x				
Villosa delumbis	x	x				
Uniomerus carolinianus		x				

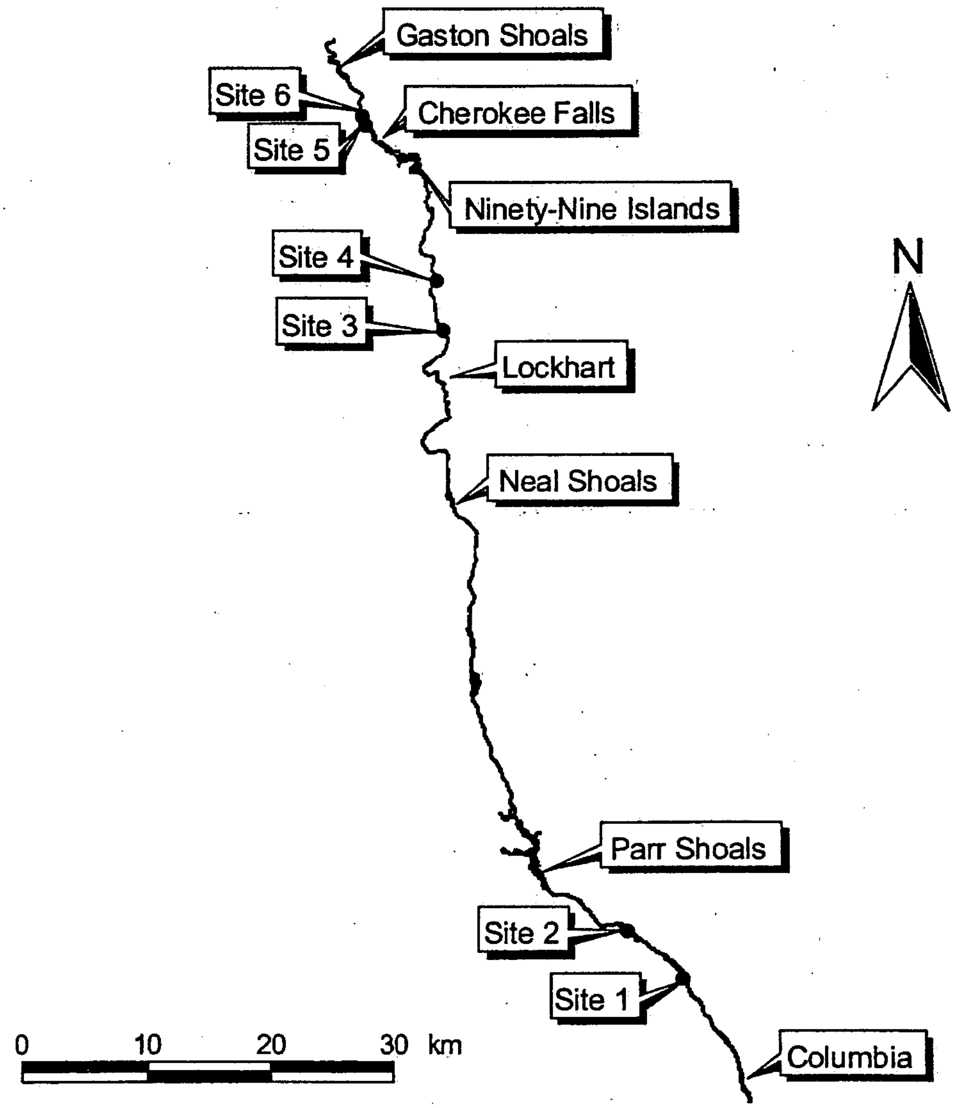

Figure 8. Sites surveyed during the summer 2002 for native mussels.

MANAGEMENT RECOMENDATIONS

1. **Habitat restoration:** Aquatic resources in several areas of the Broad River could benefit from habitat restoration. Efforts should be directed at improving riparian areas classified as "poor" and "marginal", and at addressing bank stability issues above Parr Reservoir.

2. **Minimum flows:** Minimum flows have had a positive affect on the fish community in the Gaston Shoals Tailrace. We recommend that minimum flows be implemented at all hydroelectric operations along the Broad River where appropriate (e.g. Lockhart Power Company).

3. **Sand mining:** Sand mining may have adverse effects on the biotic resources of the Broad River. We recommend that research be conducted to examine the nature and extent of such impacts, and to develop methods to minimize the operational impacts of sand dredging on aquatic biota.

4. **Recreational access:** The Broad River is a tremendous natural resource that would appeal to many outdoor enthusiasts, but recreational use of the river is restricted due to limited access. Additional access is needed to allow all users the opportunity to enjoy the river. Priority for the establishment of additional access should be directed at the river reach between Parr Shoals Dam and Columbia Dam and the river reach between 99-Islands Dam and Lockhart Dam.

5. **Industrial effluent:** Largemouth bass health in the Broad River appears to be adversely affected by industrial discharge. Further research is suggested to examine the effects of point source pollution on fish health.

6. **Fish passage:** Restoration of anadromous fish species to the Broad River could have a tremendous impact on the resident fish community. Although our survey was thorough, we used only one site to describe the fish community in the reach between Parr Shoals Dam and Columbia Dam. Before the installation of a fish passage facility at Columbia Dam, an intensive survey of current fishery resources in that reach is needed. Any fish passage facility installed at Columbia Dam should be designed expressly to prevent the passage of flathead catfish.

7. **Smallmouth bass:** Previous stockings of smallmouth bass have created a small but unique fishery. Creel and length restrictions are needed to protect this limited resource. The SCDNR Smallmouth Bass Management Plan and associated management recommendations are attached in Appendix 2.

8. **Freshwater mussels:** Native mussels in the Broad River are a poorly understood resource. We recommend that a concentrated study be undertaken to resolve questions about their taxonomy and distribution.

LITERATURE CITED

Adams, S.M., A.M. Brown, and R.W. Goede. 1993. A quantitative health assessment index for rapid evaluation of fish condition in the field. Transactions of the American Fisheries Society 122:63-73.

Adams, S.M., and R.B. McLean. 1985. Estimation of largemouth bass, Micropterus salmoides lacepede, growth using the liver somatic index and physiological variables. Journal of Fish Biology 26:111-126.

Anderson, W.G., R.S. McKinely, and M. Colavecchia. 1997. The use of clove oil as an anesthetic for rainbow trout and its effects on swimming performance. North American Journal of Fisheries Management 17:301-307.

Ashley, K. W., and B. Buff. 1986. Determination of current food habits of flathead catfish in the Cape Fear River. Final Report Submitted to the North Carolina Wildlife Resources Commission, Division of Boating and Inland Fisheries, Raleigh, NC. 19 pp.

Ashley, K.W., and R.T. Rachels. 1998. Changes in redbreast sunfish population characteristics in the Black and Lumbar Rivers, North Carolina. Proc. Annu. Conf. Southeast. Fish and Wildl. Agencies 52:29-38.

Barbour, M.T., J. Gerristen, B.D. Snyder, and J.B. Stribling. 1999. Rapid bioassessment protocols for use in streams and wadeable rivers: periphyton, benthic macroinvertebrates and fish, second edition. EPA 841-B-99-002. U.S. Environmental Protection Agency; Office of Water; Washington, D.C.

Bart, H. L., M. S. Taylor, J. T. Harbaugh, J. W. Evans, S. L. Schleiger, and W. Clark. 1994. New distribution records of Gulf Slope drainage fishes in the Ocmulgee River system, Georgia. Southeastern Fishes Council Proceedings, No. 30:4--9.

Bogan, A.E. 2002. Workbook and key to the freshwater bivalves of North Carolina. North Carolina Museum of Natural Sciences, Raleigh, North Carolina 101 pp.

Brown, A.M. 1993. Fish community health in four western North Carolina reservoirs utilizing the fish health assessment index. Report of Tennessee Valley Authority to Western Piedmont Council of Governments, Hickory, North Carolina.

Brown, A.M., and G.D. Hickman. 1990. Fish Health Program 1989. Tennessee Valley Authority, Knoxville.

Buck, H.D. 1956. Effects of turbidity on fish and fishing. Oklahoma Fish and Game Department. Twenty-first North American Wildlife Conference, New Orleans, LA.

Carlander, K.D. 1977. Handbook of freshwater fishery biology, volume 2. Iowa State University Press, Ames.

Corcoran, M.F. 1981. Geographic variation and evolutionary relationships of two species of bullhead catfishes (Siluriformes: Ictaluridae) in the southeastern United States. Doctoral dissertation. Duke University, Durham, North Carolina.

Coughlan, D.J. and three co-authors. 1996. Application and Modification of the Fish Health Assessment Index Used for Largemouth Bass in the Catawba River, North Carolina–South Carolina. American Fisheries Society Symposium 16:73-84.

Dames & Moore. 1974. Report on the baseline biotic survey, Broad River study area, Parr, South Carolina. Dames & Moore, consultants in the environmental and applied earth sciences, Atlanta, GA.

DeWitt. R.A. 1998. Fish community assessment of the Catawba River, South Carolina. Master's thesis. Clemson University, Clemson, South Carolina.

Etnier, D.A., and W.C. Starnes. 1993. The fishes of Tennessee. University of Tennessee Press, Knoxville. 681 pp. Fisheries Society, Bethesda. 1,079 pp.

Gabelhouse, D.W., Jr. 1984. A length categorization system to assess fish stocks. North American Journal of Fisheries Management 4:273-285.

Goede, R.W., and B.A. Barton. 1990. Organismic indices and an autopsy-based assessment as indicators of health and condition of fish. Pages 93-108 *in* S.M. Adams, editor. Biological indicators of stress in fish. American Fisheries Society Symposium 8.

Guire, C. R., L. E. Nichols, and R. T. Rachels. 1984. Biological investigations of flathead catfish in the Cape Fear River. Proceedings of the Southeastern Association of Fish and Wildlife Agencies 35(1981):607--621.

Hartfield, P. 1993. Headcuts and their effect on freshwater mussels. Pages 131-141 *in* K.S. Cummings, A.C. Buchanan, and L.M Kock, editors. Conservation and management of freshwater mussels. Proceedings of an Upper Mississippi River Conservation Committee (UMRCC) symposium, 12-14 October 1992, St. Louis, Missouri, UMRCC, Rock Island, IL.

Jenkins, R.E., and N.M. Burkhead. 1993. Freshwater fishes of Virginia. American Fisheries Society, Bethesda. 1,079 p.

Johnson, R.I. 1970. The systematics and zoogeography of the Unionidae (Mollusca: Bivalvia) of the southern Atlantic Slope Region. Bulletin of the Museum of Comparative Zoology 140(6):263-449.

Kleinshcimdt Associates. 1995. Lockhart Hydroelectric Project: Final fisheries baseline studies. Kleinschmidt Associates, consulting engineers, Columbia, SC.

McAleece, N. and three-coauthors. 1997. BioDiversity Pro software. The Natural History Museum, London.

Moyle, P.B. and J.J. Cech Jr. 1988. Fishes and introduction to Ichthyology. Prentice Hall, Englewood Cliffs, New Jersey.

Nelson, K.L. 1993. Instream sand and gravel mining. Pages 189-195. *In* C.F. Bryan and D.A. Rutherford, editors. Impacts on warmwater streams: Guidelines for evaluation, Second Edition. Southern Division, American Fisheries Society, Little Rock, Arkansas.

Newport, B.D., and J.E. Moyer. 1974. State-of-the-art: sand and gravel industry. U.S. Environmental Protection Agency Technical Series Report 660/2-74-066.

North Carolina Department of Environment and Natural Resources. 2001. Standard operating procedures stream fish community assessment and fish tissue. Environmental Sciences Branch Biological Assessment Unit, Raleigh, North Carolina.

Parasiewicz, P. 2001. MesoHABSIM: A concept for application of instream flow models in river restoration planning. Fisheries 26: 6-13.

Parmalee, P.W., and A.E. Bogan. 1998. Freshwater mussels of Tennessee. University of Tennessee Press, Knoxville.

Robins, C.R., and six coauthors. 1991. Common and scientific names of fishes from the United States and Canada, 5th edition. American Fisheries Society Special Publication 20.

SAS Institute. 1989. SAS/STAT user's guide, version 6, 4th edition. SAS Institute, Cary, North Carolina.

Snyder, H.S., and eight co-authors. 1993. South Carolina: State Water Assessment. South Carolina Water Resources Commission, Report No. 140. Columbia, SC.

South Carolina Department of Health and Environmental Control. 2001. Watershed Water Quality Assessment: Broad Basin. South Carolina Department of Health and Environmental Control, Technical Report No. xxx-01. Columbia, SC.

South Carolina Land Resources Conservation Commission. 1990. SPOT Satellite Image Based Land Use/Land Cover data.

Stuart, T.A. 1953. Spawning migration reproduction and young stages of loch trout (*Salmo trutta L.*). Freshwater and Salmon Fisheries Research 5:39, Edinburgh, United Kingdom.

Tennessee Department of Environment and Conservation. 1995. Draft Tennessee Standard Operating Procedures Manual: Protocol for Conducting an Index of Biotic Integrity Biological Assessment. Tennessee Department of Environment and Conservation, Division of Water Pollution Control. Nashville, Tennessee.

Thomas, S.T., D.E. Allen and J.S. Crane. 1993. A fisheries study of the Edisto River. South Carolina Wildlife and Marine Resources Department, Completion Report, Federal Aid Project F-30 and F-32. 84 pp.

Trautman, M.B. 1957. The fishes of Ohio. Ohio State University Press, Columbus.

Williams, J.C., and G.A. Schuster. 1989. Freshwater mussel investigations of the Ohio River. Kentcuky Department of Fish and Wildlife Resources, Frankfort, Kentucky.

Zar, J.H. 1996. Biostatistical Analysis, 3rd edition. Prentice Hall, Englewood Cliffs, New Jersey.

APPENDIX 1

Table 33. Fish species reported from the Broad River, South Carolina, during this and previous studies. Site numbers indicate locations where species were collected during our survey. Species not collected (NC) during our survey may have been present but not sampled, or they may have been misidentified originally. The probability that the original identification was correct, based on known species distributions, is characterized as (P) probable, (Q) questionable, or (N) not likely. Common and scientific names follow Robins et al. (1991) except where noted.

Family	Scientific Name	Common Name	Site	Probability
Lepisosteidae	*Lepisosteus oculatus*	Spotted gar	NC	N
Lepisosteidae	*Lepisosteus osseus*	Longnose gar	1-3	
Anguillidae	*Anguilla rostrata*	American eel	NC	P
Clupeidae	*Alosa aestivalis*	Blueback herring	NC	Q
Clupeidae	*Dorosoma cepedianum*	Gizzard shad	1-9 and 11	
Clupeidae	*Dorosoma petenense*	Threadfin shad	1,2 and 7	
Esocidae	*Esox masquinongy*	Muskellunge	NC	P
Cyprinidae	*Campostoma anomalum*	Central stoneroller	NC	P
Cyprinidae	*Clinostomus funduloides*	Rosyside dace	8	
Cyprinidae	*Ctenopharyngodon idella*	Grass carp[b]	1-3	
Cyprinidae	*Cyprinella analostana*	Satinfin shiner	NC	N
Cyprinidae	*Cyprinella chloristia*	Greenfin shiner	1-11	
Cyprinidae	*Cyprinella nivea*	Whitefin shiner	1-11	
Cyprinidae	*Cyprinella pyrrhomelas*	Fieryblack shiner	4 and 6-10	
Cyprinidae	*Cyprinella zanema*	Santee chub[a]	4	
Cyprinidae	*Cyprinus carpio*	Common carp	1-4, 6-9 and 11	
Cyprinidae	*Hybognathus regius*	Eastern silvery minnow	1-6 and 8	
Cyprinidae	*Hybopsis labrosa*	Thicklip chub	1-4 and 6-10	
Cyprinidae	*Nocomis leptocephalus*	Bluehead chub	1-4 and 6-10	
Cyprinidae	*Nocomis micropogon*	River chub	NC	N
Cyprinidae	*Notemigonus crysoleucas*	Golden shiner	3	
Cyprinidae	*Notropis amnis*	Pallid shiner	NC	N
Cyprinidae	*Notropis cummingsae*	Dusky shiner	NC	Q
Cyprinidae	*Notropis hudsonius*	Spottail shiner	1-11	
Cyprinidae	*Notropis hypselopterus*	Sailfin shiner	NC	N
Cyprinidae	*Notropis leedsi*	Bannerfin shiner	NC	N
Cyprinidae	*Notropis lutipinnis*	Yellowfin shiner	1 and 6	
Cyprinidae	*Notropis petersoni*	Coastal shiner	NC	P
Cyprinidae	*Notropis rubescens*	Rosyface chub	NC	N
Cyprinidae	*Notropis scepticus*	Sandbar shiner	1-11	
Cyprinidae	*Semotilus atromaculatus*	Creek chub	NC	P
Catostomidae	*Carpiodes carpio*	River carpsucker[d]	NC	N
Catostomidae	*Carpiodes cyprinus*	Quillback	2-9	
Catostomidae	*Carpiodes sp. cf. velifer*	Highfin carpsucker[a]	2[c], 3[c], 5[c] and 6-7	

Table 33. continued

Family	Scientific Name	Common Name	Site	Probability
Catostomidae	*Catostomus commersoni*	White sucker	6, 9 and 11	
Catostomidae	*Hypentelium nigricans*	Northern hogsucker	2-11	
Catostomidae	*Ictiobus bubalus*	Smallmouth buffalo[a]	2-4 and 6-8	
Catostomidae	*Minytrema melanops*	Spotted sucker	NC	Q
Catostomidae	*Moxostoma collapsum**	Silver redhorse	1-9 and 11	
Catostomidae	*Moxostoma duquesnei*	Black redhorse	NC	N
Catostomidae	*Moxostoma erythrurum*	Golden redhorse	NC	N
Catostomidae	*Moxostoma macrolepidotum*	Shorthead redhorse	1-6	
Catostomidae	*Moxostoma pappillosum*	V-lip redhorse	4-9	
Catostomidae	*Scartomyzon rupiscartes**	Striped jumprock	1-11	
Catostomidae	*Scartomyzon sp.**	"Brassy jumprock"	1-11	
Ictaluridae	*Ameiurus brunneus*	Snail bullhead	1-11	
Ictaluridae	*Ameiurus catus*	White catfish	2, 3, 6 and 11	
Ictaluridae	*Ameiurus melas*	Black bullhead	NC	Q
Ictaluridae	*Ameiurus natalis*	Yellow bullhead	NC	P
Ictaluridae	*Ameiurus nebulosus*	Brown bullhead	NC	P
Ictaluridae	*Ameiurus platycephalus*	Flat bullhead	1-9 and 11	
Ictaluridae	*Ictalurus punctatus*	Channel catfish	1-9 and 11	
Ictaluridae	*Noturus gyrinus*	Tadpole madtom	NC	Q
Ictaluridae	*Noturus insignis*	Margined madtom	1-9	
Ictaluridae	*Noturus leptacanthus*	Speckled madtom	NC	Q
Atherinidae	*Labidesthes sicculus*	Brook silverside	NC	Q
Poeciliidae	*Gambusia holbrooki*	Eastern mosquitofish	3, 4 and 6-8	
Moronidae	*Morone americana*	White perch	1-3	
Moronidae	*Morone chrysops*	White bass	1-4	
Moronidae	*Morone saxatilis*	Striped bass	NC	P
Moronidae	*Morone saxatilis x M. chrysops*	Hybrid striped bass[a]	2	
Centrarchidae	*Centrarchus macropterus*	Flier	1	
Centrarchidae	*Lepomis auritus*	Redbreast sunfish	1-11	
Centrarchidae	*Lepomis cyanellus*	Green sunfish	8	
Centrarchidae	*Lepomis gibbosus*	Pumpkinseed	1-3	
Centrarchidae	*Lepomis gulosus*	Warmouth	1, 4, 5, 8 and 9	
Centrarchidae	*Lepomis macrochirus*	Bluegill	1-9 and 11	
Centrarchidae	*Lepomis marginatus*	Dollar sunfish	NC	P
Centrarchidae	*Lepomis megalotis*	Longear sunfish	NC	N
Centrarchidae	*Lepomis microlophus*	Redear sunfish	1-9, and 11	
Centrarchidae	*Micropterus dolomieu*	Smallmouth bass	2-11	
Centrarchidae	*Micropterus punctulatus*	Spotted bass	NC	Q
Centrarchidae	*Micropterus salmoides*	Largemouth bass	1-9 and 11	
Centrarchidae	*Pomoxis annularis*	White crappie	NC	Q

Table 33. continued.

Family	Scientific Name	Common Name	Site	Probability
Centrarchidae	*Pomoxis nigromaculatus*	Black crappie	1-9 and 11	
Percidae	*Etheostoma flabellare*	Fantail darter	6	
Percidae	*Etheostoma fusiforme*	Swamp darter	NC	Q
Percidae	*Etheostoma olmstedi*	Tessellated darter	1-9	
Percidae	*Etheostoma thalassinum*	Seagreen darter	1, 3, 4, 6 and 8-10	
Percidae	*Etheostoma zonale*	Banded darter	NC	N
Percidae	*Perca flavescens*	Yellow perch	1-4	
Percidae	*Percina crassa*	Piedmont darter	1-4 and 6-10	

[a] Species not previously documented from the Broad River
[b] Species collected with sampling not associated with survey work
[c] Sites where a species was collected with sampling not associated with survey work
[d] Likely confused with *Carpiodes sp. cf. velifer*
* Expected common and/or scientific name change (R. Jenkins, person. comm.)

APPENDIX 2

Smallmouth Bass Management Plan – Broad River Drainage

Prepared by: Richard Christie, Willard "Gene" Hayes,
Hal Beard and Jason Bettinger

Introduction: Smallmouth bass (*Micropterus dolomieui*) were introduced into the South Carolina portion of the Broad River drainage in 1984 to increase the diversity of sport fishing opportunity. This was an experimental stocking of a non-native sportfish species into marginal habitat. The reproductive potential was considered to be low, and discontinuing the stocking program would control any un-anticipated negative impacts this stocking may have on native fish species.

Stocking smallmouth bass appears to have successfully created a small but unique sport fishery on the Broad River. This fishery is gaining prominence annually. Because of this gain in popularity, a management plan and recommended harvest regulations for smallmouth bass in the Broad River are needed to protect this limited resource.

Stocking History: The North Carolina Wildlife Resources Commission (NCWRC) first stocked smallmouth bass in the Broad River basin in May of 1941. They were stocked in a pond in Rutherford County. Stocking continued from the mid 1940's through the late 1960's in streams and ponds in all counties in the basin. Stocking rates are not known, however from 1,000 to 10,000 1-2 inch fingerlings were stocked at each site. Stocking was discontinued in 1985 and NCWRC currently has no plans for future stocking of this species in the Broad River basin.

Smallmouth bass were first introduced to the Broad River drainage in South Carolina in 1984. According to stocking records, 1339 6-inch sub-adults were stocked into several locations in Kings Creek. Since the initial stocking, fish have been stocked in 10 different years at seven different locations (Table 1). A total of 16,500 two-inch fingerlings were stocked just downstream from the Gaston Shoals Hydroelectric plant at Secondary Road 98, and 608 fingerlings were stocked in Bowen Creek. A total of 12,354 six-inch sub-adults were stocked at various bridge crossings on Kings Creek and in the Broad River.

In the summer of 1990, Fisheries District IV personnel surveyed potential stocking sites in tributaries to the Broad River. Sites were evaluated based on access, surface water temperature, turbidity, substrate, and existing sport and forage species. Five sites were identified in York County and seven sites were located in Cherokee County. Since 1990, stocking has been restricted to one or more of those sites and the upper Broad River near Gaston Shoals.

Life History: The following information is summarized from Black Bass Biology and Management, edited by Stroud and Clepper (1975). Smallmouth bass are native to the great Lakes and St. Lawrence River drainages in Canada south to northern Georgia, west to eastern Oklahoma, and north into Minnesota. The species has been introduced, and self-sustaining populations have been established across the United States, Canada, Hawaii, Asia and Africa. Smallmouth bass are found naturally in large, clear water lakes and cool, clear streams having a moderate current and rock substrate. A typical setting would be a stream that supports trout in the colder, upper reaches; smallmouth bass in the mid-section and largemouth bass in the slower, warmer waters. In streams, smallmouth bass usually avoid the stronger currents and inhabit the calmer waters behind structure or near the currents edge. They are not known to be migratory in nature and they have restricted home ranges. Smallmouth bass are active in a wide range of water temperatures but become less active when temperatures dip below 50° F or increase above 85° F. They may lose weight above 95° F. They are spring spawners and move into the spawning grounds when the water temperatures reach 60° F. Soon after they lose their yolksac, bass feed on insect larvae such as midges and mayflies. They are sight feeders, and water clarity is probably an important factor in the success of natural reproduction. Larger fish feed on insects, fish and crayfish. Smallmouth bass exhibit a wide range of growth rates. Smallmouth grow slower than largemouth bass, and age I, II and III fish average 3.7, 6.7, and 9.2 inches, respectively, in total length. One-year old fish grown at the Cheraw Fish Hatchery in South Carolina range from 3 to 7 inches (X=5 inches) and average about 0.1 pounds.

Management: Smallmouth bass were introduced into the Broad River drainage to increase the diversity of sport fishing opportunity. Although habitat is considered to be good in the Kings Creek tributary and satisfactory to marginal in the main river channel, habitat is limited by increased sediment and the resulting impact on turbidity and water temperature. Turbidity is thought to hinder the survival of the eggs by reducing their ability to respire, and to decrease survival of the post sac fry by reducing their ability to see and capture prey. In some years, high water temperature may also impact physiology. Based on limited aquatic surveys, food items do not appear to be a limiting factor in the success of this species. Insects (mayflies and midges), shiners (*Notropis* sp.) and crayfish are abundant in King's Creek but less numerous in the Broad River. Growth rates similar to those reported in the literature are expected. A 12 – 14 inch smallmouth (age V-VI) would be a quality fish and a 16-inch smallmouth would be a memorable fish.

Very little information is currently available regarding the distribution of smallmouth bass to judge the extent at which they will contribute to the sport fishery. A study to evaluate fish species abundance and distribution is ongoing in the Broad river system. Anecdotal information from anglers indicates that the species is concentrated in Kings Creek and above the Lockhart Hydroelectric facility, confined pretty much to where they were stocked. Some anglers have expressed an interest in wanting to "protect" this species before it becomes exploited. We have no estimates of angling effort, harvest, growth rates or mortality from the Broad River population. While the success of this introduction is evaluated, we need to protect smallmouth bass from over harvest. Thus, this proactive recommendation is offered.

Harvest Recommendation: Recommendations are based on the following set of assumptions. 1) the management objective of stocking smallmouth bass in the Broad River is to increase the number of sport species available for recreational fishing. 2) smallmouth bass are often sought by angling "purists" who use ultra-light tackle or fly rods and practice catch and release. A successful trip for most anglers will be determined by numbers of fish caught rather than the quality of the fish. 3) production of quality fish (> 16 in) may be limited by habitat. 4) some smallmouth bass anglers and fisheries managers think that the existing regulation of ten (10) black bass per day with no size limit is too liberal. 5) smallmouth bass handle well and non-harvest fishing mortality is less than 10%. 6) Broad River anglers and enforcement officers can differentiate between largemouth and smallmouth bass. **Based on these assumptions and the current management philosophy, a two (2) fish per day creel limit for smallmouth bass, of which only one may exceed 14 inches in total length, in Game zones 2, 3, and 4, should be imposed.**

Other management recommendations: the following additional recommendations are suggested in the order of their need:

1. Continue to stock smallmouth bass annually. Stocking rates will depend on the availability. Historically, 600-800 sub-adult fish have been stocked in the fall at several locations in Kings Creek. Up to 5,000 fingerlings have been stocked annually in the spring in the Gaston Shoals vicinity of the Broad River. All stocked fish should be marked. Stocking locations should be distributed between Parr reservoir and the Gaston Shoals Hydroelectric plant. Stocking should be confined to that area of the Broad River drainage upstream from Parr Reservoir.
2. Develop an anglers guide to differentiate largemouth and smallmouth bass and provide basic information.
3. Conduct a sport fish creel survey on the Broad River to estimate fishing pressure, harvest, success, and system specific angler information including the quality of fishing for smallmouth bass.
4. Collect life history data to include food habits, age and growth, and reproduction.
5. Establish a Broad River Smallmouth bass advisory council to solicit public input.

Sec 2.3 Ref 2

United States Department of Energy

Savannah River Site

Flow and Transport Modeling for D-Area Groundwater (U)

Kevin E. Brewer and Cynthia S. Sochor

WSRC–RP–2002-4166

Revision 0

October 2002

SRS
savannah river site ™

Prepared by:
Westinghouse Savannah River Company LLC
Savannah River Site
Aiken, SC 29808

Prepared for the U. S. Department of Energy Under Contract No. DE-AC09-96SR18500

DISCLAIMER

This report was prepared by Westinghouse Savannah River Company, LLC (WSRC) for the United States Department of Energy under Contract No. DE-AC00-96SR18500 and is an account of work performed under that contract. Reference herein to any specific commercial product, process, or services by trademark, name, manufacturer or otherwise does not necessarily constitute or imply endorsement, recommendation, or favoring of same by WSRC or the United States Government or any agency thereof.

Printed in the United States of America
Prepared for
U.S. Department of Energy
and
Westinghouse Savannah River Company LLC
Aiken, South Carolina

Technical Review and Approval Page

Date:____________________ Signature:____________________________________
Name: Kevin E. Brewer, Author
Hydrogeological Analysis and Evaluation Group

Date:____________________ Signature:____________________________________
Name: Cynthia S. Sochor, Author
Hydrogeological Analysis and Evaluation Group

Date:____________________ Signature:____________________________________
Name: Tamara L. Fogle, Technical Reviewer
Hydrogeological Analysis and Evaluation Group

Date:____________________ Signature:____________________________________
Name: Elizabeth G. Topp, Manager
Hydrogeological Analysis and Evaluation Group

This page has been intentionally left blank

EXECUTIVE SUMMARY

This document summarizes the development of a baseline groundwater flow and transport model for the D-Area Expanded Operable Unit. The objectives of the modeling were: (1) to ensure that the data quality objectives for the groundwater characterization have been accomplished, (2) to show the future nature and extent of existing groundwater plumes in the event no remedial action is conducted, and (3) to perform the baseline modeling which will establish the modeling approach for assessing effectiveness of remedial alternatives.

D-Area is located on an alluvial terrace near the western border of the Savannah River Site, east of the Savannah River, and is at an elevation of approximately 125 ft above mean sea level (amsl). Local topography is relatively flat with a general slope from the northeast to southwest. A portion of the Savannah River flood plain lies immediately west of the D-Area at an elevation of about 90 ft amsl.

The unconsolidated materials beneath D-Area can be divided into two main aquifer systems: a deep aquifer system and a shallow aquifer system. The shallow aquifer system is divided into two aquifers: a semi-confined aquifer (Gordon Aquifer) and an unconfined aquifer (Upper Three Runs Aquifer). The Gordon Confining Unit is the semi-confining layer within the shallow aquifer system. Since the deep aquifer system is separated from the shallow aquifer system by a competent confining layer (Crouch Branch Confining Unit) which was assumed to not allow significant flow between the two systems, the deep aquifer system was not included in this modeling effort. The hydrogeologic conceptual model of the D-Area shallow aquifer system is presented in Figures ES-1 and ES-2.

The Groundwater Modeling System, version 3.1, was selected for use in this modeling effort. The primary modeling codes used in this effort included MODFLOW (3-D finite-difference groundwater flow model), MODPATH (semi-analytic, 3-D particle-tracking), and MT3DMS (3-D contaminant transport code for the simulation of advection, dispersion, and chemical reactions of contaminants in groundwater).

The conceptual model process was used in development of the D-Area model. For example, borehole data were used to create major hydrostratigraphic surfaces, which ultimately resulted in a 3-D grid of material types. Hydraulic properties for each "material" were approximated from recent aquifer tests and modeling efforts, with final values based on model calibration.

This modeling study used a regional-to-local model development process. The regional flow model was constructed using natural groundwater boundaries: Upper Three Runs, Fourmile Branch, and the Savannah River. The local flow and transport model was constructed using the results from the regional flow model to determine appropriate boundaries around the immediate D-Area. (Figure ES-3)

The regional flow model was constructed with five layers to represent the shallow aquifer system and a lateral uniform grid spacing of 250 feet. The local flow model consisted of eight layers and a lateral uniform grid spacing of 100 feet. The calibration of both the regional and local flow models was within goals, with the root mean square error equal to three feet and the stream fluxes within calibration target ranges.

The model results show that the shallow groundwater system is generally flowing west towards the Savannah River, with some discharge to local D-Area streams/channel. The flow budget across the Gordon Confining Unit shows that a significant volume of water in the Upper Three Runs Aquifer is leaking through the Gordon Confining Unit into the Gordon Aquifer, which ultimately discharges to the Savannah River. In addition, the flow model achieved a reasonable match to the southwest flow directions at the D-Area Oil Seepage Basin consistent with known plume orientation, and flow paths indicate an approximate 20-year travel time across D-Area, which is consistent with known source timings and current plumes.

Transport modeling was performed for five constituents: TCE, tritium, beryllium, nickel, and total uranium. For TCE and tritium no current sources are contributing to groundwater contamination. The current plumes were constructed from monitoring data and used as initial conditions for 100-year simulations. The metal contaminants (beryllium, nickel, and uranium) have continuing sources. To achieve a qualitative calibration of the metal sources, various constant source concentrations were evaluated and a two-fold comparison was made. First, a mass balance calculation was made to determine rough estimates of the required contaminant loadings to achieve the assumed 2001 concentrations at the source locations. The second comparison involved running the model with constant source terms to recreate the current plumes. The best qualitative fit of continuous sources to current monitoring data was determined and used.

Metal sorption is highly dependent on pH. Therefore, a pH distribution and pH/Kd relationships were developed for use in the metal transport runs. The model only simulated metal contaminant transport until 2015 (15 years), because powerhouse operation is expected to cease around 2015 at which time flow and source conditions are expected to change significantly.

The results from the transport modeling show that the calculated TCE and tritium flux to the Savannah River is expected to peak in 25 years at 3 kg/yr and 3.5 Ci/yr, respectively. Maximum TCE concentrations discharging to the Savannah River are expected to be less than 25 ug/L, with maximum tritium discharges to the Savannah River at less than 60 pCi/mL. The model shows the highest concentrations/activities discharging to the D-Area Rubble Pit stream boundary, with TCE concentrations less than 50 ug/L between 15 to 35 years, and tritium activities less than 250 pCi/mL in 10 to 15 years. Figure ES-4 summarizes TCE and tritium fluxes to the Savannah River and the D-Area streams/channel.

Since metal transport is significantly retarded at higher pH in the wetland, there is no mass discharged directly to the Savannah River within the timeframe of the modeling for any of the metals studied. The maximum plume concentrations are not expected to change significantly over time since these concentrations are near the source at the D-Area Coal Pile Runoff Basin with near equilibrium conditions achieved during the timeframe of the modeling. The maximum discharge concentration does not change significantly over time, because the discharge location, the powerhouse effluent channel, is close to the source.

Sensitivity analyses on the flow models indicate that the model is most sensitive to changes in general recharge, aquifer horizontal hydraulic conductivity, and aquitard vertical hydraulic conductivity. With respect to particle track analysis, only a few test cases resulted in flow solutions where particles terminated in areas other than the calibrated discharge location, which indicates that the model flow directions are not very sensitive to the parameters tested.

The transport sensitivity analysis shows that tritium and TCE transport results are not highly affected by changes in dispersivity. Peak concentration timings are not affected, and as expected, lower peak concentrations are observed with higher dispersivities. The metals and pH transport results are very sensitive to changes in sorption parameters. Use of a single distribution coefficient proved insufficient to adequately model the transport of these constituents.

A number of uncertainties were identified during this modeling effort; however, the quality of the flow model calibrations and the ability of the transport model to recreate current contaminant plumes indicates that the results from this effort can be used as intended.

The objectives of this modeling effort have been achieved as follows:

- No data gaps associated with the definition of the nature and extent of the groundwater contamination were identified. The TCE and tritium simulations are consistent with the conceptual model and currently defined metal plumes were successfully recreated from known source areas. However, modeling uncertainty could be reduced with additional data.

- The successful calibration of the flow models indicates that the basic hydrostratigraphy and flow system hydraulics have been adequately characterized. The only area where additional information may prove useful for this scale of investigation is with the thickness of the Gordon Confining Unit immediately north of D-Area.

- The transport modeling provides predictions of future plume nature and extent in the event of no remedial action. These predictions include calculated fluxes and concentrations to surface water bodies. The models documented in this effort can be used as the framework for future modeling evaluations of remedial alternatives.

Figure ES-1. Hydrogeologic Conceptual Model Cross Section

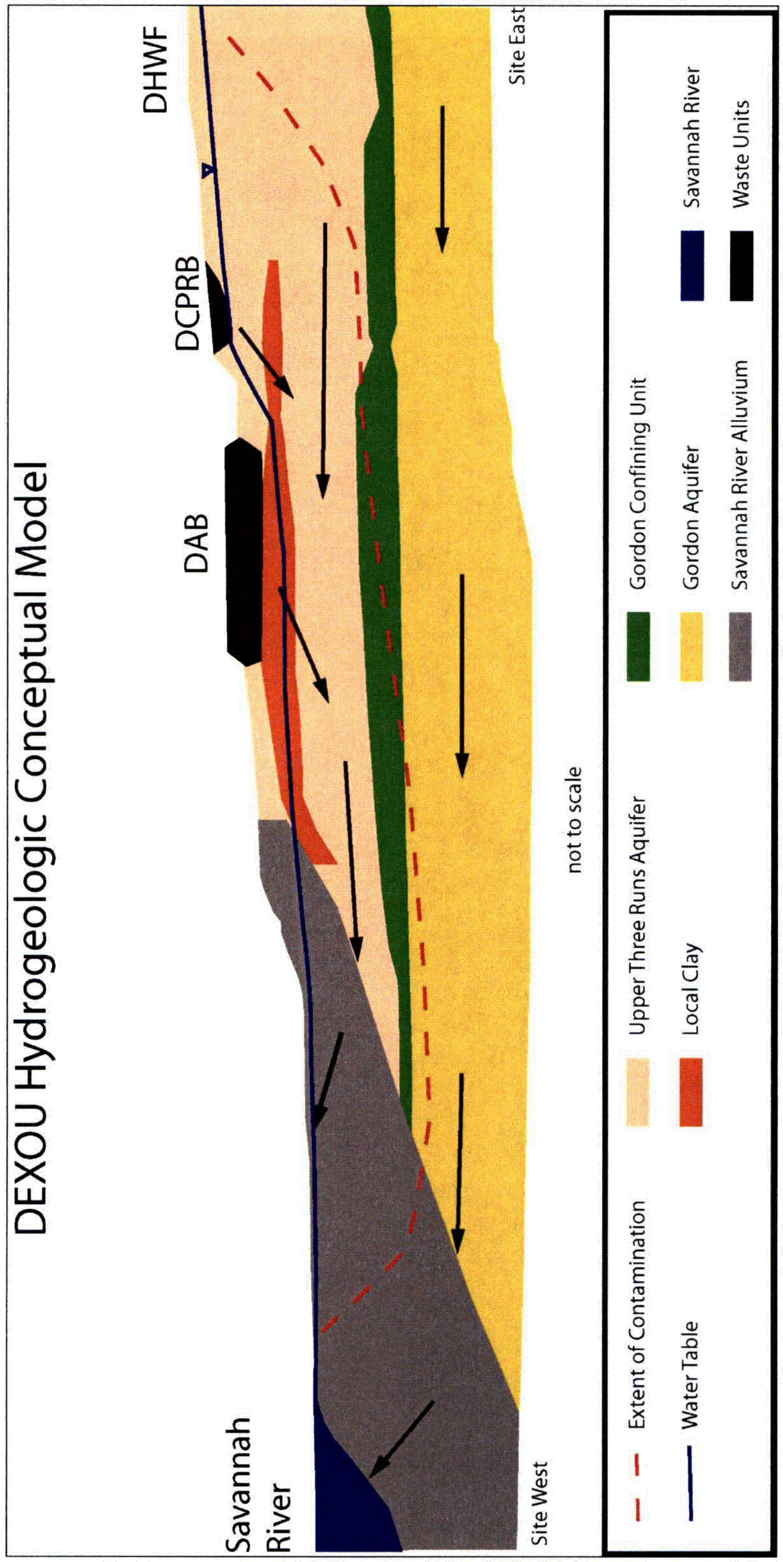

Figure ES-2. Oblique, Conceptual View of D-Area

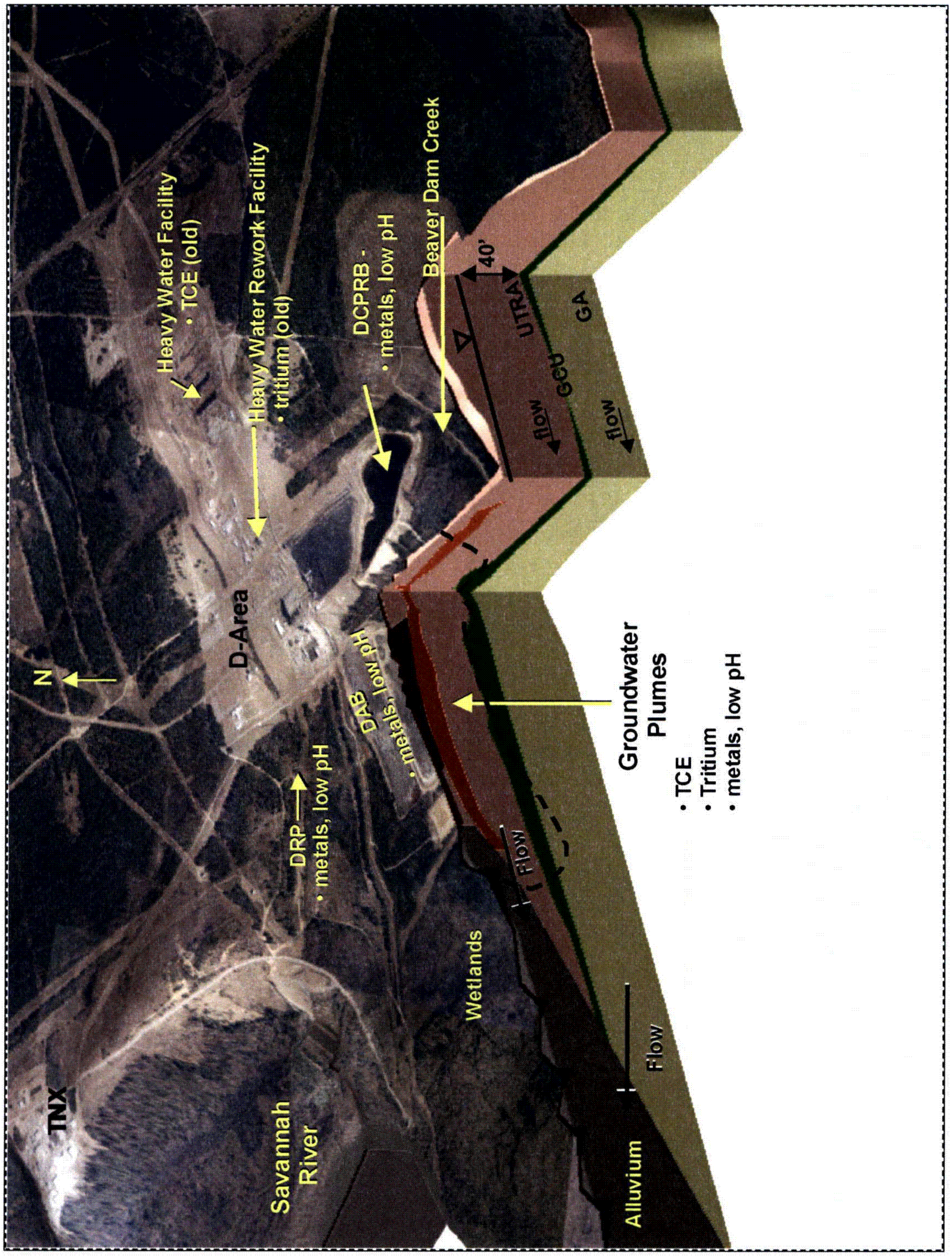

Figure ES-3. Map View of Regional and Local Model Domains

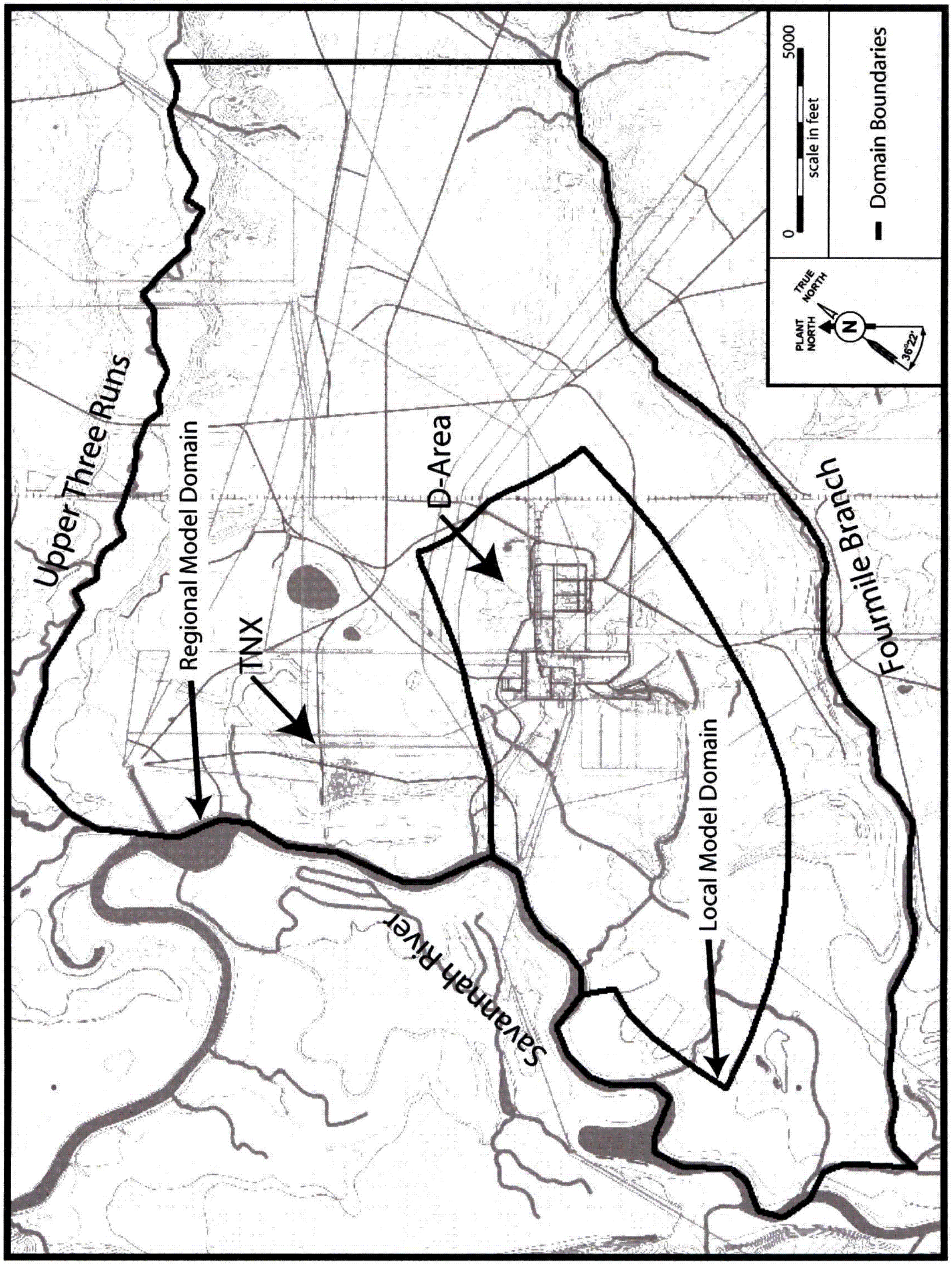

Figure ES-4. TCE and Tritium Transport Model Results Summary

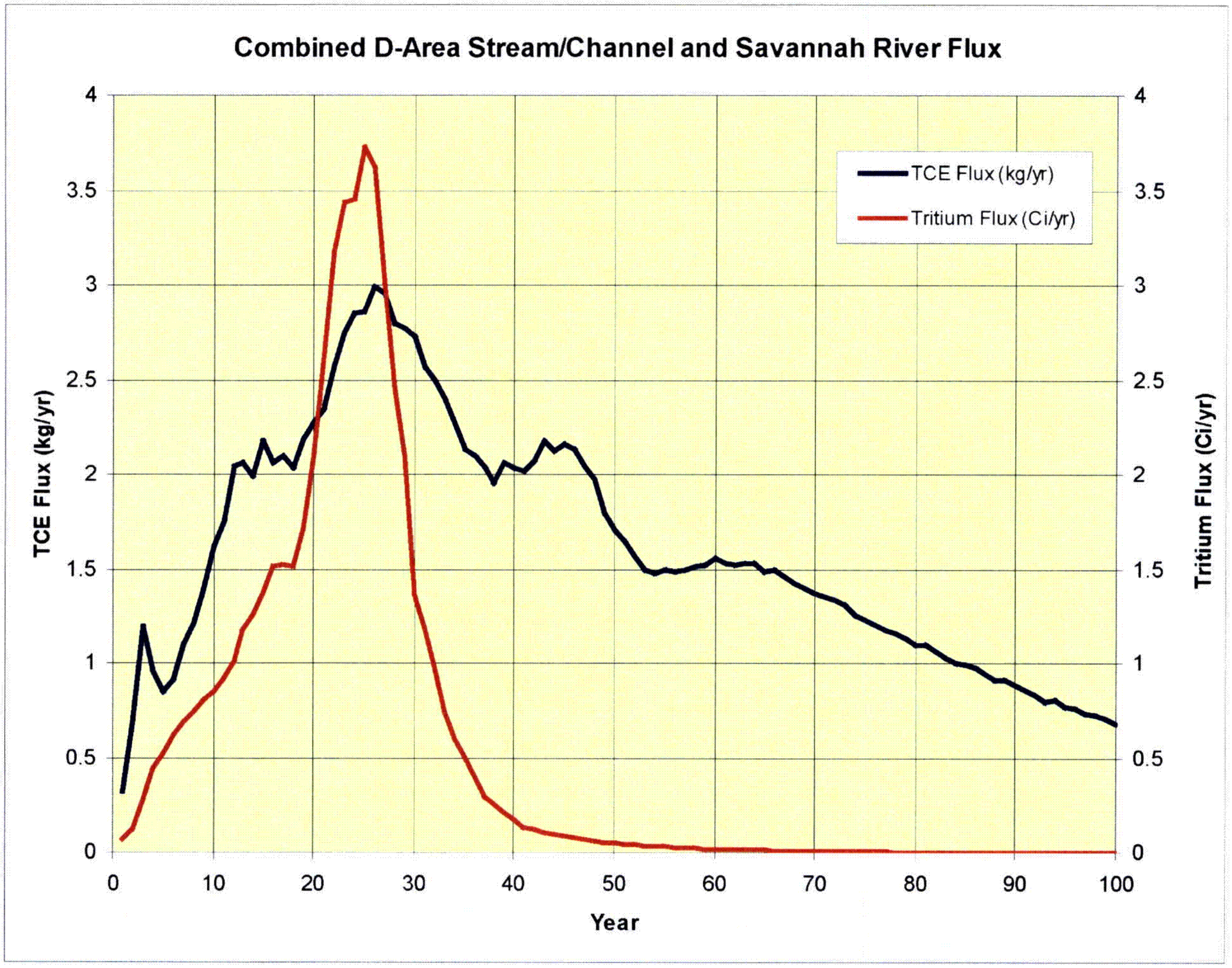

TABLE OF CONTENTS

LIST OF FIGURES

LIST OF TABLES

LIST OF ACRONYMS AND ABBREVIATIONS

3-D	three-dimensional
amsl	above mean sea level
BDC	Beaver Dam Creek
CBCU	Crouch Branch Confining Unit
cfd	Cubic feet per day
cfs	cubic feet per second
Ci	Curie
CERCLA	Comprehensive Environmental Response Compensation Liability Act
Ci/yr	Curies per year
COC	constituent of concern
CPT	cone penetrometer technology
DAB	D-Area Ash Basin
DCDP	D-Area Cinder Disposal Pit
DCPRB	D-Area Coal Pile Runoff Basin
DEXOU	D-Area Expanded Operable Unit
DHWF	D-Area Heavy Water Facility
DHWRF	D-Area Heavy Water Re-work Facility
DOSB	D-Area Oil Seepage Basin
DRP	D-Area Rubble Pit
DWOF	D-Area Waste Oil Facility
ERDMS	Environmental Restoration Data Management System
FMB	Fourmile Branch
ft	feet
ft/d	feet per day
GA	Gordon Aquifer
GCU	Gordon Confining Unit
GIS	Geographical Information System
GMS	Groundwater Modeling System
gpm	gallons per minute
HCM	hydrogeologic conceptual model
HFO	hydrousferric oxide
Kd	distribution coefficient or linear partitioning coefficient
kg	kilogram
kg/yr	kilograms per year
K_h	horizontal saturated hydraulic conductivity
K_v	vertical saturated hydraulic conductivity
LC	Local Clay
m	meter
MAE	mean average error
MCL	maximum contaminant level
ME	mean error
mg/L	milligrams per liter (ppm)

μg/kg	micrograms per kilogram
μg/L	micrograms per liter (ppb)
mg/L	milligrams per liter
MODFLOW	Modular Three-Dimensional Finite-Difference Groundwater Flow Model (Code)
MODPATH	a particle tracking post-processing package for MODFLOW (Code)
MT3DMS	transport modeling code
OU	Operable Unit
PAH	polycyclic aromatic hydrocarbon
pCi/mL	picoCuries per milliliter
ppm	parts per million (mg/L)
ppb	parts per billion (μg/L)
PRG	Preliminary Remediation Goals
QAP	Quality Assurance Plan
RCRA	Resource Conservation and Recovery Act
RFI/RI/BRA	RCRA Facility Investigation/Remedial Investigation/Baseline Risk Assessment
RMS	root mean square (error)
SCDHEC	South Carolina Department of Health and Environmental Control
SCE&G	South Carolina Electric and Gas
SGS	Site Geotechnical Services
SOI	Southern Oscillation Index
SR	Savannah River
SRA	Savannah River Alluvium
SRS	Savannah River Site
TCE	trichloroethylene
TINs	triangulated irregular networks
USDOD	United States Department of Defense
USDOE	United States Department of Energy
USEPA	United States Environmental Protection Agency
USGS	United States Geologic Survey
UTR	Upper Three Runs
UTRA	Upper Three Runs Aquifer
WSRC	Westinghouse Savannah River Company, LLC

1.0 INTRODUCTION

This document summarizes the development of a baseline groundwater flow and transport model for D-Area which will be included in the DEXOU Remedial Feasibility Investigation/Remedial Investigation/Baseline Risk Assessment (RFI/RI/BRA) document.

1.1 Modeling Objectives

The following objectives have been developed for this groundwater modeling analysis (WSRC 2002):

- *ensure that the data quality objectives for the groundwater characterization have been accomplished, namely: (a) defining the extent and nature of groundwater contamination, (b) defining the hydrostratigraphy, and (c) defining the flow system (hydraulics);*
- *show the future nature and extent of an existing groundwater plume in the event no remedial action is conducted; and*
- *perform the baseline modeling which will establish the modeling approach for assessing effectiveness of remedial alternatives in the FS report.*

1.2 Process History and Unit Description

D-Area is located in the southwest quadrant of the Savannah River Site (SRS), approximately 915 meters east of the Savannah River (Figure 1-1). The D-Area has been investigated as an integrated Resource Conservation and Recovery Act (RCRA)/Comprehensive Environmental Response Compensation Liability Act (CERCLA) unit. The D-Area operable unit consists of contaminated groundwater and source areas that are potential contributors to groundwater contamination.

Contaminants in the groundwater that are above maximum contaminant levels (MCLs) include tritium, trichloroethylene (TCE), and metals. Coal-related radionuclides are also contaminants of concern. Additionally, infiltration of low pH surface runoff and leachate has led to exceedances of South Carolina Secondary Drinking Water Standards for pH and has resulted in impacts to surface waters and wetlands.

The 488-D Ash Basin (488-DAB) and the D-Area Coal Pile Runoff Basin (489-D) (DCPRB) (Figure 1-2) were addressed in the DEXOU RFI/RI work plan prepared in 1998. The 488-DAB started receiving ash-sluice water from the 484-D powerhouse around the fall of 1952. In approximately 1978, ash-sluice water was directed from the 488-D to other ash basins and the 488-DAB waste stream changed from ash-sluice to dry ash and coal reject material. The 488-DAB received waste until the early to mid 1990s and is no longer in operation. The DAB contains coal-related constituents of concern (COCs) such as metals, radionuclides, and polycyclic aromatic hydrocarbons (PAHs); and pooled, low pH surface water may contribute to groundwater contamination. The DCPRB was constructed in 1978 to collect surface runoff from the coal pile that is used as a temporary storage location for coal to be used in the powerhouse. Recent maintenance activities taken by South Carolina Electric and Gas (SCE&G) include an approximate 50 percent reduction in the size of the coal pile in 1995 and removal of about 10,000 cubic yards of coal fines from the bottom of the basin since 2000. These operational changes and maintenance activities are expected to reduce the flux of leachate to groundwater. DCPRB COCs include low pH and coal-related metals and radionuclides that have impacted groundwater above MCLs.

The characterization of 488-DAB and DCPRB suggested that some additional upgradient sources might be contributing to groundwater contamination. An addendum to the original work plan was completed in 2001 that included investigation of additional facilities including the D-Area Waste Oil Facility (484-10D) (DWOF), the D-Area Rubble Pit (431-2D) (DRP) and the D-Area Cinder Disposal Pit (ECODS D-1) (DCDP).

The DWOF was suspected as a historical source of TCE. The DWOF serves as a temporary storage area for used oil before it is burned in the D-Area boilers. However, recent characterization data indicate that the DWOF is not contributing to groundwater contamination.

The DRP and ECODS D-1 DCDP were also investigated as possible sources of groundwater contamination. The DRP covers approximately eight acres and is located north of the DAB and southeast of the D-Area Burning Rubble Pit (DBRP) (Figure 1-2). Groundwater downgradient of the DRP has a low pH and beryllium concentrations which exceed the MCL. Aerial photography and historical records indicate that waste disposal began in the early 1950s and continued intermittently through 1989. A large volume of waste and debris appear to have been in place by about 1975. Operational procedures indicate that the DRP was used for disposal of non-hazardous materials. The DCDP is composed of two elongated trenches and was opened in 1951 and operated until late 1952 to early 1953 when it was back-filled. Aerial photography suggests that the DCDP contains miscellaneous debris. The presence of blackened material indicates that debris may have been burned in at least one of the trenches. Interviews with site personnel indicate that the trenches may also have been used for disposal of coal cinder, prior to construction of the D-Area ash basins.

Based on characterization, a decision was made to remove the DCDP from the DEXOU and list the unit as a Site Evaluation Area (USDOE, 2002) because groundwater data indicated it is not a source of groundwater contamination. This decision was made per the work plan addendum and in meetings held with South Carolina Department of Health and Environmental Control (SCDHEC) and the United States Environmental Protection Agency (USEPA) on July 16 and 26, 2001. Recently, at the post characterization scoping meeting in March 2002, several sub-units were removed from the DEXOU. The DCPRB and DWOF were removed from the DEXOU, because these subunits are active facilities and will continue to operate until powerhouse operations terminate at a projected date of 2015.

Figure 1-2 also shows the location of the D-Area Heavy Water Facility (DHWF) and Heavy Water Rework Facility (DHWRF) which produced heavy water for use in SRS reactors, but are no longer in operation. These two areas have been implicated as historical sources of TCE and tritium contamination to groundwater. Additional characterization at D-Area just north of the D-Area Heavy Water Facility was conducted at the request of Don Hunter of the US Environmental Protection Agency following the March scoping meeting. Vadose zone soil gas and soil sampling was performed and showed no significantly elevated levels of TCE in the vadose zone. The results of the additional characterization are consistent with an assumption that the TCE source is historical.

1.3 Summary of Approach

Determination of appropriate boundary conditions near a specific study area is often difficult because natural boundaries (streams and rivers, groundwater divides, outcrops, and natural barriers) are frequently at some distance from the study area. Without defined boundaries, model uncertainty is great. This uncertainty can be reduced by performing the modeling in two segments (phases). The first phase is focused on constructing a regional model, incorporating as many natural boundary conditions as possible. This phase involves looking beyond the immediate study area, to nearby streams, barriers, etc. to use as the model domain boundaries. Although larger than the immediate area of interest, the regional model incorporates appropriate hydrostratigraphy and hydraulic properties, but at a coarse grid and layer discretization.

The second phase of the modeling effort involves constructing a local model, focusing on the specific problem area, but with boundaries that are based on the regional head results. Typically, no-flow boundaries are determined from regional flowpaths, with constant head boundaries along regional equipotential lines. More detail is included in the local model (pumping/injecting wells, engineered barriers, etc.), and the model uses a fine grid and layer discretization. Properties and parameters for the local model are typically derived from the regional model. The regional to local model conversion is often referred to as "telescopic grid refinement."

This modeling study uses a regional to local model process. The regional model was constructed using the following natural groundwater boundaries: Upper Three Runs (UTR), Fourmile Branch (FMB), and the Savannah River (SR). The local flow and transport model used the regional results for construction of boundaries around the immediate D-Area.

1.4 Sources of Information

The following sources of information were used in this effort:

- Environmental Restoration Data Management System (ERDMS) for water-level, analytical, and field data; well information; and regulatory limits,
- Access database maintained by the project team for analytical and field measurements,
- Excel spreadsheets with reference elevations and codes maintained by the project team,
- USGS daily streamflow measurements,

- LANDMARK database for well and stratigraphic picks,
- ArcView site coverages and project specific coverages maintained for D-Area,
- Savannah River Technology Center data for metal/pH sorption modeling (Powell 2002),
- Groundwater modeling reports for TNX, DOSB, and C-Area, and
- RCRA RFI/RI Work Plan and Addendum.

2.0 HYDROGEOLOGIC CONCEPTUAL MODEL

The first step in the modeling process is formulation of the hydrogeologic conceptual model (HCM), which is a representation of the groundwater flow system pertaining to the field problem. The HCM incorporates a description of the geologic setting, hydrostratigraphic units, hydraulic parameters, and system boundaries. System boundaries include external boundaries, wells, and sources/sinks. In addition, the HCM serves to organize the dimensions and grid design of the numerical model.

2.1 Geologic and Hydrogeologic Setting

The SRS is underlain by Atlantic Coastal Plain sediments (interbedded sands, silts, and clays) that thicken to the southeast. These sediments range in age from Late Cretaceous to Recent and are approximately 900 ft thick at SRS (Aadland et al. 1995, Fallaw and Price 1995). The stratigraphy beneath D-Area consists of the Snapp, Fourmile Branch, Congaree, Warley Hill, Tinker/Santee, and Clinchfield Formations. A local veneer of Quaternary stream terrace deposits exists at D-Area, with more extensive reworking of the shallow material near the current SR.

D-Area is located on an alluvial terrace near the western border of the SRS, east of the SR. D-Area is at an elevation of approximately 125 ft above mean sea level (amsl). Local topography is relatively flat with a general slope from the northeast to southwest. A portion of the SR flood plain lies immediately west of the D-Area at an elevation of about 90 ft amsl.

A more extensive discussion of the D-Area geology can be found in Chapter 3 of the RFI/RI/BRA for the DEXOU (WSRC 2002b).

The unconsolidated materials beneath D-Area can be divided into two main aquifer systems: a deep aquifer system and a shallow aquifer system. The Meyers Branch confining unit, a confining layer consisting of thick sequences of interbedded silts and clays, separates the two systems. The deep aquifer system below the Meyers Branch confining system is composed of sands and clays and is approximately 450 ft thick in the vicinity of the SRS. The shallow aquifer system above the confining unit can be divided into several layers depending on the location within the SRS. At D-Area, the shallow aquifer system is divided into two aquifers: a semi-confined aquifer and an unconfined aquifer. The semi-confined aquifer, consisting of about 50 ft of fine- to medium-grained sand, is known as the Gordon Aquifer (GA). The Gordon Confining Unit (GCU), a 10 ft layer of clayey silt, is the semi-confining layer above the GA. The GCU is overlain by the Upper Three Runs Aquifer (UTRA), an unconfined system that varies in thickness from 40 to 60 ft beneath D-Area. The hydrogeologic conceptual model of the D-Area shallow aquifer system is presented in Figure 2-1.

The water table in the UTRA, which is also referred to as the water table aquifer, is about 25 ft below ground surface throughout much of the D-Area. Regionally, the UTRA has been divided into three zones: upper, "tan clay", and lower. The upper zone and the "tan clay" have been eroded in the immediate vicinity of D-Area, though the "tan clay" is thought to exist in the higher ground east of D-Area.

The lower zone of the UTRA (just UTRA in this report) consists of sands, silts, and clays which are interbedded and laterally discontinuous, causing variable hydraulic properties. Beneath 488-DAB and vicinity, there exists a dense, locally continuous clay layer that roughly corresponds to the Clinchfield aquitard. In this report, this layer is referred to as the "local clay" (LC).

Beneath D-Area, the shallow groundwater system generally flows from east to west, and eventually discharges to the floodplain/wetlands and the SR. Near UTR and FMB, groundwater flows north to UTR and south to FMB. The UTRA has been eroded along UTR and local groundwater typically flows downward through the GCU into the GA, eventually discharging into the stream. FMB incises the UTRA, causing local groundwater discharge. In addition to the general westward progression, downward movement of shallow unconfined groundwater is observed.

The GCU is informally referred to as the "green clay" at SRS, and separates the GA from the overlying UTRA. The GCU consists of fine-grained glauconitic clayey sand interbedded with lenses of green and gray clay that thicken and pinch-out. The GCU is a relatively competent confining unit, with approximately 2 ft of head difference across the unit. Flow through the unit is generally downward.

The GA consists of sands and clayey sands, of relatively uniform thickness, with relatively uniform hydraulic properties. Regional flow in the GA is from the southeast to the west, and is controlled by discharges to UTR and the SR. Near the SR, considerable reworking of the sediments from the GA and the UTRA has occurred, resulting in an alluvium deposit consisting of a variety of materials from coarse sand to clay. The Crouch Branch Confining Unit (CBCU) defines the bottom of the aquifer, and is assumed in this effort to be impermeable

2.2 Selection of Computer Codes

GMS (Groundwater Modeling System, version 3.1) was selected for the regional groundwater flow model and for the local flow and transport model. The U.S. Department of Defense (USDOD) in partnership with the U.S. Department of Energy (USDOE), the USEPA, Cray Research, the Environmental Modeling Research Laboratory at Brigham Young University, and 19 other academic partners, developed this software. GMS was created for use at USDOD and USDOE sites but is used throughout the commercial groundwater modeling community as well. GMS is a graphical user environment and contains analysis codes for performing groundwater simulations. GMS has been validated following the SRS Procedure Manual E-7, Revision 30, *Conduct of Engineering and Technical Support* (WSRC 1998) and is in compliance with Quality Assurance Plan (QAP) 20-1 for software per the WSRC 1Q Quality Assurance Manual.

The GMS flow, particle-tracking, and contaminant transport programs include MODFLOW, MODPATH, and MT3DMS. These programs are commonly used throughout the groundwater modeling community for solving groundwater flow problems. MODFLOW is a modular, 3-D finite difference groundwater flow model (McDonald and Harbaugh 1988). MODPATH (Pollock 1994) is a 3-D, particle-tracking and post-processing package for MODFLOW. MODPATH uses a semi-analytical, particle-tracking scheme that allows an analytical expression of the flow path to be obtained for each finite difference grid cell. MT3DMS is a 3-D transport model for the simulation of advection, dispersion, and chemical reactions of contaminants in groundwater (Zheng and Wang 1999).

2.3 Hydrostratigraphy

There are a number of different techniques for building groundwater models. In GMS, the grid approach and the conceptual model approach are both supported. For very simple models, the grid approach is commonly used. This approach starts with the creation of a grid. The hydraulic parameters, source/sink data, and boundary conditions are then assigned directly to the cells of the grid. Finally, the model input files are generated and the model is run. Since any changes to boundaries, parameters, or other model data have to be performed on individual cells, complexity is difficult to implement with this approach.

The most efficient approach for building realistic, complex models is the conceptual model approach. With this approach, a conceptual model is created using graphical information system (GIS) objects, including points, arcs, and polygons. The conceptual model is constructed independently of a grid and is a high-level description of the site including sources/sinks, the boundary of the domain to be modeled, recharge and evapotranspiration zones, and material zones within each of the layers. Once the conceptual model is complete, a grid is constructed and the model data are converted from the conceptual model to the cells of the grid.

For this effort, the conceptual model process was used within GMS. The general process to create the hydrostratigraphy was as follows:

- *Define regional groundwater flow model extent.* The regional groundwater flow model extent was used to constrain the extrapolation of the surfaces. The boundaries of the model extent were selected to match physical boundaries of groundwater flow systems near D-Area. The chosen boundaries for the regional model were: UTR (northern), SR (western), FMB (southern), and an arbitrary eastern limit connecting the UTR and FMB systems. The model extent is shown in Figure 2-2.

- *Import hydrostratigraphic picks into GMS boreholes.* The picks for the major hydrostratigraphic surfaces were obtained from the Site Geotechnical Services (SGS) Landmark database and are given in Table A-1 in Appendix A. Not all surfaces were defined for each borehole, as not all boreholes were drilled to the same depth. As discussed below, it was assumed that all surfaces were continuous through the model extent (except the LC), so "missing" surfaces did not have to be considered. Each borehole was augmented with an artificial bottom two feet below the bottom-most pick to facilitate easier contact selection. To smooth the interpolated surfaces and allow for proper extrapolation, a number of "artificial" boreholes were created. These are listed in Table A-2 in Appendix A. Five major materials/surfaces were defined: UTRA (essentially the ground surface), LC, GCU, GA, and CBCU. The borehole locations are provided in Figure 2-3.

- *Interpolate picks to triangulated irregular networks (TINs) for each major surface.* Using the GMS triangulation algorithm, a TIN was created from each set of contacts/surfaces. The GCU, GA and CBCU surfaces were assumed continuous throughout the model domain. Based on evaluation of the LC thickness, a separate, smaller boundary area was created (see Figure 2-2). The top and bottom of the LC were assumed continuous in this small area, and the picks were interpolated/triangulated accordingly.

- *Import ground surface to TIN.* Each of the aquifer and aquitard units outcrops within the model extent. To create the appropriate outcrops for the surfaces, a TIN representing the surface is needed to limit/constrain the units. The 10-foot surface contour lines (5 feet in the immediate D-Area) in the SRS GIS system were converted to scatter points, and input into GMS (see Figure 2-4). The scatter points were then converted to TIN vertices. These vertices were automatically triangulated in GMS to form a TIN representing the ground surface.

- *Create solids from TINs.* With all the TINs created, the next step was to create solids to represent the various aquifer and aquitard units (material types). The generation of the LC, GA, and the GCU solids was accomplished by a straightforward application of the GMS transformation of filling between two TINs. The UTRA was created between the surface TIN and the GCU TIN, with the additional removal of the LC. All solids were further modified by removing all volumes above the surface TIN using a set operation (subtraction) between each solid and an "above ground" solid created from the surface TIN. A three dimensional representation of the resulting solids and associated material types is given in Figure 2-5.

- *Interpolate to grid from solids.* The final step in the generation of the basic hydrostratigraphy was the generation of appropriate MODFLOW arrays to represent the constructed solid geometry. This transfer of information can be automated in GMS in two basic ways: boundary matching or grid overlay. Boundary matching honors the surface elevations of each material by layer, whereas grid overlay uses a predefined vertical discretization and assigns material types (or equivalents) to each cell.

  The method used in this effort was boundary matching as it was adequate in representing the hydrostratigraphy, and resulted in the simplest grid assignments (e.g., all GCU cells would be in the same layer). Boundary matching begins with the creation of a generic three-dimensional grid.

  For the regional model, a five layer grid with a uniform x-y grid size of approximately 250 feet was used (see Section 3.1 for further details). After grid creation, layer assignments were made for each of the solids. The D-Area regional flow model has 5 layers: the first three layers are of the UTRA, the fourth layer represents the GCU, and the bottom layer is the GA. The LC was simulated as a portion of the second layer within the UTRA. Where the LC was not defined, the GMS algorithm smoothly transitions the surfaces so that the three layers of the UTRA are uniformly vertically distributed.

The final layer elevations and thickness for the regional model are given in Figures 2-6 through 2-10.

The regional model hydrostratigraphy (layer elevations and thickness) were transferred to the local model using the scatter-point method. This method involved creating scatter point sets of the gridded regional model layer tops and bottoms. After the local model grid was created (see discussion below), the scatter point sets were interpolated to the new grid using the inverse-distance weighted routine.

2.4 Hydraulic Properties

Hydraulic properties were assigned using the GMS "materials" method. In this method, each cell is assigned a material and each material has a unique set of hydraulic properties defined. In this effort, the major material definitions were for the UTRA, the LC, the GCU, the GA, and the Savannah River Alluvium (SRA). To facilitate better calibration, the UTRA was defined using two material types (labeled: "UTRA" and "UTRA Zone 2"). The definition of the boundaries for the "Zone 2" material was chosen to optimize the calibration and does not directly relate to defined geology. However, the hydraulic property differences between these two materials are relatively minor.

Materials for a leakier zone of the GCU and a higher vertical conductivity zone beneath FMB in the UTRA (i.e., "UTRA Zone 3") were used to support simulation of proper seepage faces and flow to surface streams. Further, a tighter zone was defined in the GCU during regional model calibration, as discussed in Section 3.3.4. The final distributions of materials for each layer in the regional model are given in Figures 2-11 through 2-15. No significant changes in the regional model distributions were made for the local model.

To simplify the model, the ash basins and LC directly beneath the basins were not simulated. Recharge through the LC from the ash basins was treated as a recharge boundary condition. As such, the grid cells for layers including and above the LC at the ash basins were made inactive, as shown on Figures 2-11 and 2-12.

Table 2-1 summarizes applicable hydraulic properties for recent aquifer tests and modeling efforts. For most units/zones, there is a significant range in values. Table 2-2 provides the hydraulic properties for the material types used in this modeling effort. The values were based on those given in Table 2-1, and adjusted during the calibration process.

Table 2-1 **Summary of Hydraulic Property Values**

Hydrologic unit	K_h (ft/day)	K_v (ft/day) or (K_v:K_h)	Test type	Test location
Upper Aquifer Zone	40-44	1:3 - 1:17	extraction	well FSB-PD (F-area)
	35-40	1:100	extraction	well HSB-PD (H-area)
	37-63	56:442	injection	well FIW-1ID (F-area)
	24-44	10:34 - 14:102	injection	well HIW-1ID (H-area)
C-model transmissive zone	4.06-6.74		slug	well CSB-8D
C-model transmissive zone	1.90-2.33		slug	well CSB-9D
	5.62		slug (n=190)	
	0.67		short-duration single-well pump (n=14)	
	5.09		short-duration single-well pump (n=38)	
	13		long-duration multiple-well pump (n=1)	
	12.6		minipermeameter (n=317)	
	55.6-143	1:59	injection	FIN 10 test, injection side of F-area
	44.8-130	1:100	extraction	extraction side of F-area
	14.8-48.8	1:10 - 1:100	injection	injection side of H-area
	17.5-82.6	1:100 - 1:1000	extraction	extraction side of H-area
		5.68e-6 - 2.77e-1	lab (n=17)	CKLP
	3.12e-5 -6.04		lab (n=14)	CKLP
	0.0632-12.2		slug (n=11)	CKLP
A/AA+A54	1.6, 1.7		short duration multiple-well pump	R area, RPT-30PZ
Transmissive zone	24.8, 25.4		short duration multiple-well pump	R Area, RPC 2PR
	2.3, 4.2		short duration multiple-well pump	R-Area, RPT-2PW
UTRA(9 zones)	13-55	.05-1.2	calibrated model value	C-Area
Tan Clay		5.0e-4 - 5.03e-3	extraction	F and H
		2.4e-4 - 8.6e-4	injection	well FIW-2IC (F-area)
		7.1e-4 - 2e-3	injection	well HIW-2IC, full screen (H-area)
		7.2e-4 - 1.2e-3	injection	well HIW-2IC, upper screen (H-area)
		1.8e-3 - 4.5e-3	injection	well HIW-2IC, lower screen (H-area)
	1.45e-5 - 2.04e-1	3.7e-8 - 2.39e-1	lab	cores across SRS
(4 zones)	.4-18	.0025-.06	calibrated model value	C-Area

Table 2-1 Summary of Hydraulic Property Values (continued)

Hydrologic unit	K_h (ft/day)	K_v (ft/day) or (K_v:K_h)	Test type	Test location
Lower Aquifer Zone	.7-1.4 (10 at > distance)		extraction	well FSB-PC (F-area)
	1.3		extraction	well HSB-PC (H-area)
	8-11		injection	well FIW-2IC (F-area)
	4-6		injection	well HIW-2IC, full screen (H-area)
	8-11		injection	well HIW-2IC, upper screen (H-area)
	.8-1.4		injection	well HIW-2IC, lower screen (H-area)
	5.62		slug (n=173)	
	0.91		short-duration single-well pump (n=51)	
	33.3		short-duration single-well pump (n=7)	
	1.06		long-duration single-well pump (n=4)	
	10		long-duration multiple-well pump (n=1)	
	19		pump (n=1)	
	23.8		minipermeameter (n=199)	
	3.62-17.5		injection	injection side of F-area
		4.54e-6 - 3.42	lab (n=30)	CKLP
	1.59e-5 - 11.1		lab (n=26)	CKLP
	0.13–24.4		slug (n=31)	CKLP
	1.23-2.1		multiple-well pump (n=2)	CKLP
	22, 27.9		short duration multiple-well pump	R area, RPC-3PW
	2.9, 1.0		short duration multiple-well pump	R Area, RPT-3PW
Aquifers 1 and 2 (above and below Clinchfield aquitard)	10-24		slug test	DOSB
Aquifer 3 (below Tinker/Santee aquitard)	3.9		slug test	DOSB
Aquifer 3 (below Tinker/Santee aquitard)	4	.004	estimated	DOSB
	.5-100		calibrated model value	DOSB
Layer 1 (Above "Tan Clay")	25		model value	DOSB
Layer 2("Tan Clay")		.3	model value	DOSB
Layer 3(Below "Tan Clay")	10		model value	DOSB
Unconfined Aquifer Zone	9.2-73.2		Single well/Interference/SVE Interference Pumping	TNX
Unconfined Aquifer Zone	18-65		model value	TNX
Local Confining Zone	.01	.005	calibrated model value	TNX
LUTR (4 zones)	6-45	6-25	calibrated model value	TNX
Middle Aquifer Zone (5 zones)	10-60	.05-.7	calibrated model value	C-Area
Lower Confining Unit (4 zones)	2.2-2.5	.0008-.025	calibrated model value	C-Area
Lower UTRA (below Clinchfield aquitard where it exists)	.29-144		slug test	D-Area
Lower UTRA (below Clinchfield aquitard where it exists)	1.35-25	.098-.144	step and constant pumping tests	D-Area

In the 2001 DOSB MZ annual report the upper clay was renamed AT1; the "Tan Clay" is thought to be absent from the DOSB area.

Table 2-1 Summary of Hydraulic Property Values (continued)

Hydrologic unit	K_h (ft/day)	K_v (ft/day) or (K_v:K_h)	Test type	Test location
Gordon Confining Unit	5.4e-6 - 1.22e-1		lab (n=30)	CKLP
		1.14e-6 - 4.27e-1	lab (n=47)	CKLP
		2.9e-3 *	multiple-well pump (n=2)	well HSB-69A (H-area)
Clayey Sand	5.24e-4 - 1.5e-1	5.7e-4 - 1.59e-1	lab (n=4)	wells P-13, P-15, P-20, P-28
Sandy Clay	3.15e-1	2.24 e-4 - 3.68e-4	lab (n=2)	wells P-23 and P-25
	.005	.001	calibrated model value	TNX
	.01	.0001	calibrated model value	C-Area
		* local leakage observed through Gordon Confining Unit		
Gordon Aquifer	4.9		slug (n=41)	
	13.8		short-duration single-well pump (n=10)	
	1.86e-4 - 45		multiple-well pump (n=3)	wells in the GSA
	8.2e-1 - 143		single-well pump (n=10)	across SRS
	35 (24-41)		long-duration single- and multiple-well pump (n=8)	
	5.00e-3 - 33.1		slug (n=50)	CKLP
	6.6, 22.6		short duration multiple-well pump	R area, RPT-4PW
	20	2	calibrated model value	C-Area
	12	4	calibrated model value	TNX
	1.87-5.67		slug test	D-Area
Crouch Branch Confining Unit	.5	.01	calibrated model value	TNX

Table 2-2. **Hydraulic Property Summary**

Aquifer/Aquitard Units/Zones	Property[1]	Expected Value[2]	Minimum Value	Maximum Value	Units
UTRA	K_h	18	1	60	ft/day
	K_v	1	0.001	10	ft/day
UTRA Zone 2	K_h	10	1	60	ft/day
	K_v	.5	0.001	10	ft/day
Local Clay	K_h	.5	.001	1.8	ft/day
	K_v	.005	.00001	.01	ft/day
Tan Clay	K_h	5	.01	18	ft/day
	K_v	.05	.0001	.1	ft/day
Gordon Confining Unit	K_h	.1	.005	.15	ft/day
	K_v	.005	.0001	.05	ft/day
Gordon Aquifer	K_h	20	5	45	ft/day
	K_v	2	1	4	ft/day
Savannah River Alluvium	K_h	70	10	70	ft/day
	K_v	7	1	7	ft/day
"Leaky" GCU	K_h	1	.01	10	ft/day
	K_v	.1	.001	1	ft/day
"Tight" GCU	K_h	.01	.001	.1	ft/day
	K_v	.0001	.00001	.001	ft/day
UTRA at FMB (Zone 3)	K_h	18	10	70	ft/day
	K_v	3	1	7	ft/day
All	porosity	0.3	0.15	0.45	unitless
	dispersivity	5	1	500	ft

Notes: [1]K_h and K_v are horizontal and vertical saturated hydraulic conductivity, respectively.
[2]The expected value is the regional and local flow model calibrated value.

3.0 REGIONAL FLOW MODEL

This section documents the development of the D-Area regional flow model. The regional model is used to provide boundary conditions for the local flow and transport model.

3.1 Discretization of Regional Model Domain

The regional flow model used a nominal uniform cell size of 250 ft by 250 ft (Figure 3-1), oriented with Site North, with an origin (SW corner) of 5,500 (SRS E), 55,800 (SRS N). The actual grid created in GMS has cells 249.2 ft by 248.45 ft, due to an inadvertent slight reduction in the overall grid domain that occurred during grid development. The resulting grid included 5 layers, 97 rows and 126 columns giving a total of 61,110 cells (though not all active in the model domain). Vertically, the five layer regional model was composed of three layers representing the UTRA, a single layer for the GCU, and a single layer for the GA. The LC was simulated in the second model layer (i.e., the middle UTRA layer).

3.2 Regional Boundary Conditions

Boundary conditions are statements specifying the dependent variable (head) or the derivative of the dependent variable (flux) at the boundaries of the problem. Proper definition of boundaries is particularly important for steady-state flow systems because of the influence of the boundaries on the solution. Where possible, model boundaries are best selected to match physical boundaries of groundwater flow systems. Although sometimes considered a source/sink, recharge in the D-Area regional flow model will be discussed at the end of this section.

Three types of boundary conditions were used for the D-Area regional flow model: specified head (Dirichlet conditions), specified flow (Neumann conditions), and head-dependent flow (Cauchy or mixed boundary conditions). All boundaries were specified using Map Module Coverages in GMS. All the specified flow boundaries were of the special condition of no-flow (zero flux).

To simulate specified head boundaries with GMS coverages, the head at the beginning and ending points of the boundary arc are specified. GMS linearly interpolates the appropriate heads for cells along the arc. To simulate no-flow boundaries, no special designation is needed for a boundary arc.

Two types of head-dependent flow boundaries were used: drains and rivers. For drains, the beginning and ending drain elevations are specified, with GMS linearly interpolating along the arc. The drain conductance is specified for each arc. For rivers, the beginning and ending river bottom and stage (river elevation) are specified. Again, GMS linearly interpolates along the arc to each appropriate cell. The riverbed conductance is specified independently for each arc.

Figures 3-2 through 3-6 show the boundary condition arcs for the regional model and the resulting MODFLOW cell designations. Note that due to the interpolation and conversion scheme in GMS, not all cells along a boundary become the designated boundary type. For the regional model, this slight inconsistency is not significant and does not impact the model results.

For the UTRA (Layers 1 through 3), the stream boundary along FMB only occurs in Layer 1, with flow from Layers 2 and 3 ultimately moving upward to the stream (see Figure 3-7). For the portion of the Savannah River boundary south of TNX, boundaries were set in the same manner. Along the Savannah River north of TNX, and along UTR, the UTRA is absent at the boundary (see Figure 3-7).

Due to the low hydraulic properties, no-flow boundaries were used for the GCU. For the GA, a regional groundwater flow direction was assumed based on prior work in C-Area, and based on outcrop and discharge locations. Constant head boundaries were set at values consistent with those used for C-Area, and consistent with D-Area monitoring. Drain boundaries were used to simulate the natural discharge of the GA along UTR and the exposed portion of the GA north of TNX at the Savannah River.

Various surface features in the regional model domain were simulated with boundary conditions that were assigned to appropriate layers. The Carolina Bay north of D-Area was simulated as a river boundary with constant head (stage). This type of boundary seemed to best fit the limited monitoring data at DOSB and TNX.

Generally, stream conductances were set at arbitrarily high levels so as not to impede the groundwater discharge to streams and rivers. However, for the local surface streams and reaches at D-Area, lower conductances were assumed to support the observed head differences between surface features and groundwater levels. Elevations for all streams/drains/rivers were determined by examination of the local topography elevations.

Recharge was specified using a MODFLOW/MT3DMS Areal Attributes coverage in the GMS Map Module. In GMS, the Map module provides a suite of tools for using GIS objects to build conceptual models. Similar types of model information can be organized into separate coverages. Figure 3-8 shows the zones for recharge. The zones were determined by evaluating the topography, likely groundwater discharge and recharge areas, and surface structures (basins, drain pipes, etc).

As discussed above, for both the regional and local models, the ash basins and LC cells (immediately below the ash basins) were excluded from the model domain. The infiltration through the bottom of the basins was simulated as a recharge flux. As shown on Figure 3-8, recharge/infiltration below the northern two basins was simulated as 2 in/yr, with 22 in/yr below the southern two basins. These rates are somewhat different from the computed infiltration rates in Chapter 6 of the RFI/RI/BRA for D-Area (WSRC 2002b). The following discussion clarifies the reasons behind the difference.

Per the RFI/RI/BRA, Section 6.2.2.2, the average vertical conductivity of the "Clinchfield clay" (which is the clay sitting below the ash basins, equivalent to the Local Clay in this model) is given as 0.0777 ft/yr (0.00022 ft/day), based on vertical hydraulic conductivity measurements in four soil borings. A reasonable upper limit to actual flow through the clay is equal to the vertical hydraulic conductivity. Therefore, Chapter 6 assumed about 1 in/yr infiltration through the basin bottom.

In this effort, the calibrated vertical conductivity of the LC is 0.005 ft/day. The difference between this value and the Chapter 6 value is due to model calibration needs and is likely due to scale issues (i.e., in the model, the conductivity represents a much larger volume than a soil boring) and undefined spatial variability. The model calibrated recharge through the LC at the two northern (dry/inactive) ash basins is 2 in/yr. This value is close to the Chapter 6 value.

The model calibrated recharge through the LC at the two southern (wet/active) ash basins is 22 in/yr. This latter value is equal to the vertical hydraulic conductivity for the LC in the model, which as stated above, is a reasonable upper limit to actual flow through the clay. Thus, the modeled recharge occurring at the basins is less than what the hydraulic properties would indicate using the conservative analysis of Chapter 6.

3.3 Calibration

The purpose of model calibration is to establish that the model reproduces field-measured heads and flows within a reasonable margin of error. Calibration may be accomplished by trial-and-error adjustment of parameters or by using automatic parameter estimation techniques (such as inverse modeling). In this study, the automatic technique using the PEST code available within the GMS environment was used to augment the trial-and-error technique. PEST is a general purpose parameter estimation utility developed by John Doherty of Watermark Computing (Watermark 2000).

Through either an automated or manual trial-and-error process, calibration is achieved by adjusting selected input parameters (hydraulic conductivities, recharge, etc.) until the optimization is complete. In general, calibration is considered complete when all pre-defined calibration goals have been met. Nevertheless, calibration to a single set of field measurements does not guarantee a unique solution.

3.3.1 Calibration Goals

Calibration is often quantitatively evaluated through error in head residuals – the differences between field-measured values and model simulated values. The root mean square (RMS) residual error, the mean error (ME), and the mean absolute error (MAE) are typical measures of model error. The RMS (or standard deviation) is the average of the squared differences in measured and simulated heads. The ME is the average of the errors. The MAE is the absolute residual mean (variance). The equations for calculating RMS, ME, and MAE are as follows:

$$RMS = \left[\frac{1}{n} \sum_{i=1}^{n} (h_s - h_m)^2 \right]^{0.5} \tag{3-1}$$

$$ME = \frac{1}{n} \sum_{i=1}^{n} (h_s - h_m) \tag{3-2}$$

$$MAE = \frac{1}{n} \sum_{i=1}^{n} |h_s - h_m| \tag{3-3}$$

where

h_m = measured head,

h_s = simulated head, and

n = number of observations.

There are several opinions about how to establish quantitative calibration goals. In general, the magnitude of the error to the total head loss in the area of interest should be small (Anderson and Woesnner 1992, ASTM 1996). Rumbaugh has suggested (1998) that the minimum acceptable criteria is 5% for the ME ratio (ideally 2%), and 10% for the RMS error ratio (ideally 5%).

For this study, the Rumbaugh suggested criteria were used. With a head difference of 55 feet across the D-Area water table aquifer (145 ft to 90 ft), the quantitative calibration goals for head become:

- *RMS – 5.50 feet*
- *ME – 2.75 feet*
- *MAE – 2.75 feet.*

In addition to head goals, flux goals were specified for UTR and FMB. As discussed in Section 3.3.3, the uncertainty of the values for the flux targets was significant. Therefore, the goals were set to match the flux targets within +/- 2x.

Besides quantitative goals, qualitative calibration goals can also be set. For the D-Area model, two qualitative goals were used: matching the DOSB plume direction, and matching the general plume timing for tritium at D-Area (see Figure 3-9). The results of the matches are discussed in Section 3.4.

3.3.2 Head Calibration Targets

Typically, groundwater models of SRS waste sites are developed to represent the long-term steady-state groundwater flow system. A significant step in this development is model calibration to known field conditions -- called calibration targets. The most common calibration target is head, and the use of numerous, spatially distributed head targets is desired. Target values are developed by examining the historical monitoring data for each well, and for the case of a steady-state flow system, an average value is calculated from the historical data. To represent the long-term average steady-state flow system, each target value should be representative of the long-term head at that location. At SRS this is often not possible, and less-than-ideal calibration targets are developed and used, resulting in additional uncertainty in the groundwater modeling results. The two primary causes for less-than-ideal calibration targets is a lack of a monitoring well distribution throughout the model domain, and the lack of long-term historical head values at the monitoring wells.

Figure 3-10 gives a composite view of the available historical head data for D-Area monitoring wells. Each square indicates that at least one head measurement was obtained during the quarter. Historical head data were obtained from the Environmental Restoration Data Management System (ERDMS) and project maintained Excel/Access data files. Note that the earliest monitoring data available are from 1985, and that a large number of wells only have a few (recent) years of data. Figure 3-11 shows where the monitoring wells are located. As these figures show, there are few long-term monitoring wells and there is a poor spatial distribution around the greater D-Area.

This D-Area distribution (spatial and temporal) of historical groundwater head data is typical of SRS waste sites. Most groundwater monitoring wells are not installed until late in the RCRA/CERCLA characterization time-line, which means only one or two year's worth of monitoring data will be available for the baseline groundwater model.

Because a number of the D-Area monitoring wells are relatively new, a major problem in establishing realistic head calibration targets was determining long-term (baseline) head values for D-Area monitoring wells with limited historical data. Another major issue was ensuring that the long-term head values from older wells and the short-term head values from newer wells were appropriately compared and combined. Consequently, a technique was developed to improve the determination of a long-term head value for each well. This technique involved evaluation of long-term correlations between groundwater levels and surface water and precipitation records to facilitate development of adjustment factors. These quarterly adjustment factors were then applied to the measured data prior to calculation of the individual well statistics.

Streamflow records exist for about 25 years at UTR (at Road A, north of D-Area) from a United States Geologic Survey (USGS) station (#02197315). The daily streamflows were smoothed by first calculating monthly averages from the daily flows, then by using a 12-month moving average (Figure 3-12). Monthly rainfall at SRS has been collected for about 50 years at A/M area (Figure 3-13), with more recent (and partial) precipitation records existing for other areas around SRS. Because of the relatively small distances between areas (compared to weather systems) and consideration of the long-term record rather than daily events, it is assumed that the A/M area precipitation record is representative for all areas at SRS. The monthly rainfall was smoothed by using a 12-month moving average to minimize short-term variability and highlight longer-term trends.

Correlations between streamflow, precipitation, select long-term historical water table levels, and long-term climate indicators were investigated. Figure 3-14 shows the expected positive correlation between streamflow and rainfall. Due to natural hydrologic processes, there can be delays between precipitation events and corresponding responses in streams or in groundwater monitoring wells. To quantitatively define the delay between rainfall and streamflow, various "lags" were statistically assessed. Table 3-1 gives the correlation statistics, where correlation was calculated as:

$$r = \frac{Cov(x,y)}{s_x \cdot s_y} \tag{3-4}$$

$$Cov(x,y) = \frac{1}{n}\sum_{i=1}^{n}(x_i - \bar{x})(y_i - \bar{y}) \tag{3-4a}$$

$$s_x = \sqrt{\frac{1}{n-1}\sum_{i=1}^{n}(x_i - \bar{x})^2} \tag{3-4b}$$

$$s_y = \sqrt{\frac{1}{n-1}\sum_{i=1}^{n}(y_i - \bar{y})^2} \tag{3-4c}$$

where x_i and y_i represent the rainfall and streamflow data for each time period, i, n is the total number of sampled time periods, and r is the correlation coefficient. The best correlation (i.e., the highest correlation coefficient, see Table 3-1) was achieved with a four-month lag (delay rainfall), possibly indicating the effects of near surface natural hydrologic processes (interflow).

Table 3-1. Correlation Statistics Between Rainfall and Streamflow

Rainfall Delay (months)	Correlation Coefficient
0	0.415463
1	0.474196
2	0.511283
3	0.529511
4	0.538527
5	0.537119
6	0.522869
7	0.501741
8	0.466734
9	0.422438

The correlation between precipitation and select long-term D-Area water table wells was also examined using Equation 3-4, but without any rainfall delay (also see Figure 3-15 and Table 3-

2). The relatively poor correlation level is likely due to individual well factors, and the variable timing of the water levels during each quarter.

Table 3-2. Correlation Statistics Between Select Water Table Elevations and Rainfall

Well	Correlation Coefficient
DBP1	0.290242
DCB1A	0.400866
DCB3A	0.194568
DOB1	0.153315
TNX8D	0.361323
XSB4D	0.242439

Although the SRS precipitation, UTR streamflow, and D-Area groundwater levels appear to be reasonably correlated, each of the historical records, in their own way, show impacts (increases and decreases) from large-scale climatological phenomena. The most obvious (and most recent) impact can be seen in each record near the years 1997-98. Although there appear to be consistently high precipitation, streamflow, and groundwater levels for all of the 1990's, there is a short period during 1997-98 with significantly higher levels, followed by decreasing precipitation, streamflow and groundwater levels over the last few years. Local opinion is that a drought has been occurring since 1998. Examination of the precipitation record (Figure 3-13) shows that the precipitation for the last few years has been below average, but not unlike previous "drought" periods (namely, during the fifties and sixties). The streamflow and groundwater level records show that abnormally high values were seen during the nineties.

The "El-Niño/La-Niña" climatological phenomenon has been shown to have a significant large-scale climatic impact on North American hemispheric weather. The El-Niño/La-Niña is the result of warming and cooling of the near-surface water in the central and eastern Pacific Ocean. Under normal circumstances, the ocean water is colder than its equatorial location would suggest, (due to the influence of trade winds, a cold ocean current, and upwelling of cold, deep water). When the influences wane, the surface water of the eastern and central Pacific Ocean warms under the tropical sun, resulting in an El-Niño event. Cyclically, the influences of cold water become more intense, causing the surface of the eastern Pacific to cool, resulting in a La-

Niña event. Large-scale climatic events from this ocean water warming and cooling occur from Australia to the Americas.

A distinctive measure of the El-Niño has been determined to be the Southern Oscillation Index (SOI) (Figure 3-16). The SOI is a measure of the surface atmospheric pressure difference between Darwin and Tahiti. When the SOI is positive, a La-Niña (or ocean cooling) occurs, and when the number is negative, an El-Niño (or ocean warming) occurs. A slight correlation was found between streamflow/precipitation and SOI (Figure 3-17). When the SOI is negative (El-Niño), precipitation/streamflow is higher, and when the SOI is positive (La-Niña), precipitation/streamflow at SRS is lower.

As has been shown, precipitation, streamflow, and head are correlated but can vary significantly from year to year. The SOI indicates that fluctuations have occurred for many years. Thus, groundwater head data from just one or two years would be inadequate to determine a representative long-term average head value. Therefore, an adjustment technique for historical water table head measurements was developed to account for the short-term fluctuations in wells with limited historical data.

The adjustment technique used "adjustment factors" for each quarter which adjust each quarterly value closer to the well's theoretical long-term average. The key to this technique is developing appropriate adjustment factors for each quarter. Due to less-than-perfect correlation between heads and either the SOI, precipitation, or streamflow, the adjustment factors were based on head measurements in wells with long-term records.

The adjustment factors were created from examining quarterly variations in twelve water table monitoring wells for D-Area (DBP1, DBP2, DOB1, DOB2, DOB3, DOB4, DCB1A, DCB2A, DCB3A, DCB5A, DCB6, and DCB7) and twelve water table monitoring wells for the TNX-Area (XSB3A, XSB4D, TNX8D, TBG5, TBG7, TNX11D, TNX12D, TNX4D, TNX7D, TNX9D, TNX6D, and TNX1D) with long-term records. GA monitoring wells were not adjusted because it was assumed that there would be only minor head change impacts from precipitation to the deeper GA water levels, and that even short-term records would be representative of long-term conditions.

The idea behind the quarterly adjustment factors is to provide a multiplier for each quarter which reflects the general relationship of that quarter's value to a long-term average, in an effort to adjust each quarterly value towards the long-term average. Then, when an average of the adjusted quarterly values is calculated, that average is closer to the (unknown) long-term average. For some quarters, that adjustment would be positive (i.e., the quarterly value would be adjusted upwards toward the long-term average), and for some quarters, the adjustment would be negative.

The quarterly adjustment factor was determined by first calculating the normalized quarterly variation from the long-term average for each well in each twelve-well set. This normalized quarterly variation is calculated by taking the variation from the average and dividing it by the sample value. The overall adjustment factor for each area was then calculated by taking the average of the twelve-well normalized quarterly variations. In equation form, this adjustment factor determination from the twelve-well set was as follows:

$$f_i = \sum_{j=1,n_i} \left(\left(h_{ij} - \bar{h}_j \right) / h_{ij} \right) \Big/ n_i \tag{3-5}$$

where

f_i is the adjustment factor for quarter i;

h_{ij} is the measured value for well j for quarter i;

$\bar{h}_j$ is the long-term average for well j; and

n_i is the number of wells with data for quarter i.

The resulting adjustment factors are given in Table B-1 in Appendix B. Note that separate adjustment factors generated for D-Area wells and TNX area wells, and that the recent adjustments are all positive, indicating recent groundwater levels are 1 to 2 feet lower than historical long-term averages.

Then, the adjustment process for each monitoring well simply involves using the adjustment factors in the following equation:

$$\hat{h}_{ij} = h_{ij} \times (1 - f_i) \tag{3-6}$$

where $\hat{h}_{ij}$ is the adjusted value in well j for quarter i, h_{ij} is the measured value, and f_i is the adjustment factor for the sampling quarter. The hydrographs in Appendix B show the unadjusted values and the adjusted values. Table B-2 in Appendix B gives the summary statistics for unadjusted and adjusted head calibration targets. Table B-3 in Appendix B provides the final target list data for all wells. The impact of using the adjustment factors can be seen in Table B-2, where the spread from the average (as indicated by the magnitude of the standard deviation) is generally less for the adjusted data, compared with the unadjusted data. This is expected, as the adjustment process is intended to bring each individual sample value closer to the estimated long-term average value. Hydrographs for each well are provided in Appendix C, and show the original sample value and average, as well as the adjusted value and average, if applicable.

Because the wells were centered around D-Area and TNX, use of all the wells during regional flow model calibration may incorrectly bias the results to areas with a dense target spacing. Therefore, a select subset of all wells was used for the regional model. This subset was determined by deleting "duplicate" wells and ensuring a relatively, evenly distributed spacing for the remaining wells. The targets used for the regional model are indicated on Table B-3 in Appendix B and shown on Figure 3-18.

3.3.3 Flux Calibration Targets

Perhaps as important as head targets, flux targets are used during calibration to provide control of the overall flow system. Since head measurements alone do not provide a unique view on a flow system (i.e., the rate at which flow is moving through a system is not reflected in head measurements), flux targets are used to calibrate the flow through the system. The flux targets are derived from field baseflow measurements on boundary streams/rivers. Baseflow is measured during periods of no rainfall and is assumed to reflect a near steady-state between the groundwater and surface water. Comparison of baseflows from different points along stream reaches reflects the groundwater discharge (recharge) to the stream. This steady-state condition for groundwater discharge along specified reaches is the basis of flux calibration targets.

Three major streams/rivers border the regional flow model: FMB, UTR, and the SR. Since groundwater flux into the SR along the regional model domain is small compared to the total river flow, and since no historical stream flow measurements have been made near the upstream and downstream boundaries of the model, useful baseflow measurements cannot be estimated, consequently, no SR flux calibration targets were developed.

Two long-term USGS stream gauges exist on UTR (at Road A [02197315] and at Road C [02197310]), and two long-term USGS stream gauges exist on FMB (at Road A12.2 [2197344] and at Site 7 [2197342]). The locations of these gauges are shown on Figure 3-19. The long-term average baseflow measurements at these locations was determined using the "local minimum" method available in USGS's hydrograph separation program, HYSEP (Sloto and Crouse 1996).

The three hydrograph separation techniques available in HYSEP were developed by Pettyjohn and Henning (1979). They include *fixed interval*, *sliding interval*, and *local minimum* techniques. Prior to the development of HYSEP, hydrograph separation techniques were traditionally implemented manually with inconsistent results. The objective of the HYSEP program is to automate the process of calculating baseflow and to provide consistency in calculation results. USGS acknowledges that although "HYSEP consistently applies various algorithms that are commonly used for hydrograph separation, hydrograph separation remains a subjective process." Notwithstanding individual preferences in hydrograph separation methods, it is agreeable that long-term station readings are desirable to afford less weight to extremes in weather conditions that can bias the calculation of an average baseflow measurement. Fortunately, the USGS provides long historical records of daily streamflow measurements, which lend credence to the baseflow calculations. Furthermore, the methodology proposed by the program is a commonly accepted approach for the calculation of baseflow and is sufficient for the purposes of model calibration.

A time interval is calculated by HYSEP that is based on the drainage area corresponding to the sample location. Once the interval is calculated, the *direct method* assigns a baseflow value corresponding to the lowest streamflow measurement in the interval to every day in that interval. The *sliding interval* calculates a daily baseflow by centering the interval on the day to be evaluated. The day with the lowest streamflow measurement in that interval is assigned to that day. The interval is shifted over one day at a time until the entire time period is evaluated. The *local minimum* method identifies local minimums in the streamflow data and assigns values to the days by linear interpolation between the local minimum values.

The baseflow values in Table 3-3 were obtained by averaging the 1985-2000 data for years where all of the data were available for each of the stations evaluated (anomalous years were removed).

Table 3-3. Baseflow Measurements

Station Name	Station ID	Baseflow (cfs)
UTR @ Road A	02197315	193.0
UTR @ Road C	02197310	178.4
FMB @ Road 12.2	2197344	25.8
FMB @ Site 7	2197342	11.5

To calculate the flux target values for each stream, the first step is to determine the total groundwater flux to streams between the gauges. For UTR, the value is 15 cubic feet per second (cfs); and for FMB, the value is 14 cfs (see Table 3-3). Those values are reduced to account for the portions of the stream reaches that are within the regional model domain. It was determined that 5 cfs was entering FMB immediately prior to the model domain (3 cfs from Castor Creek and 2 cfs from FMB, see Figure 23 in Bills et al. 2000), so the FMB flux in the regional model domain was 9 cfs. For UTR, it was determined that only 1/3 of the reach was within the model domain (5 cfs). These values are further reduced in half to account for groundwater flux from only one side of the stream, resulting in the UTR flux target of 2.5 cfs (2.2×10^5 cubic feet per day (cfd)), and the FMB flux target of 4.5 cfs (3.9×10^5 cfd).

Due to the assumptions used in the generation of these flux targets, there is significant uncertainty in the values. The groundwater contribution is likely not equal for both sides of UTR or FMB. The assumption of ½ is likely adequate, but may be optimistic (i.e., more water being contributed from the non-model domain side of the stream). In addition, the estimates for contributions to the stream prior to the model domain are highly uncertain, particularly for UTR.

Overall, it was assumed that a reasonable range for acceptable flux values should be +/- factor of two around the target value.

3.3.4 Adjustments During Calibration

During calibration, various parameters are adjusted in an effort to reduce the head and flux errors. The primary parameters adjusted are horizontal and vertical hydraulic conductivities, and recharge. In addition to parameter adjustment, the spatial distribution of the parameters can be altered (for example, zone with differing recharge values are added) to further reduce the error. The parameters were generally altered within the ranges as given in Table 2-2. Recharge was kept within an arbitrary, but reasonable range of less than 25 inches per year.

Slight adjustments in the material zones were made in the UTRA near FMB, and in the GCU near UTR, both to facilitate more realistic vertical flow near groundwater discharge locations. A plausible explanation for these "leaky" zones could be that the near-surface aquifer material has been reworked near these surface drainage features.

The most significant adjustment during the calibration was the addition of a "tight" zone within the GCU, just north of D-Area. During the calibration process, it became evident that although the head and flux targets were acceptable, the qualitative goal of correct flow direction in the UTRA in the vicinity of DOSB was not being met. Examination of the hydrostratigraphy in the vicinity of DOSB showed an atypically thin GCU zone occurring just north of D-Area, which was solely the result of the interpolation – no actual wellbore data exists in this area. The thinner zone was allowing higher vertical leakage from the UTRA to the GA, causing UTRA flow to be westerly at DOSB. Reducing the leakage in that area caused UTRA flow to be more southwesterly at DOSB, which is consistent with the known plume directions at DOSB based on the monitoring data.

As stated in Section 3.3, the primary method used for calibrating the regional model was manual trial-and-error. In addition, PEST was used throughout the process to refine the results and direct further manual adjustments. Over 200 separate model runs were performed during the calibration process.

3.4 Regional Flow Model Results

3.4.1 Calibration Results

The adequacy of calibration should be viewed through an analysis of residuals. Calibration may be viewed as a regression analysis designed to bring the mean of the residuals close to zero, with little or no bias. Qualitative analysis consists of assessing the distribution of error by comparing observed and computed heads and residuals. Figure 3-20 shows the observed heads versus the model computed heads, Figure 3-21 shows the observed heads versus the residuals, and Figure 3-22 shows the spatial distribution of the residuals. Table 3-4 gives the individual calibration target computed heads and residuals. As shown in the figures and tables, a good calibration was achieved, with low error. A slight spatial bias exists in some areas, particularly near the powerhouse effluent channel with modeled heads higher than observed values, which would lead to an overestimate of the flux to surface water in this area.

A slight bias in the residuals can also be seen in Figure 3-21 with the higher modeled head values being too low, and the lower modeled head values being higher than observed. This type of bias indicates a smaller gradient and would result in slightly longer travel times for groundwater flow. In this case, however, the bias is small and no significant impact should be expected.

A quantitative analysis consists of evaluating the statistics of the residuals, as discussed in Section 3.3.1. Table 3-5 gives the overall statistics summary and shows that all calibration goals were met. Besides the head targets, flux targets were also considered during model calibration. Table 3-6 shows the flux targets and computed values. Overall, the model meets the flux target goals.

Table 3-4. Regional Model Calibration Results for Individual Head Targets

Well Name	Observed Head (ft)	Model Head (ft)	Residual (ft)	Well Name	Observed Head (ft)	Model Head (ft)	Residual (ft)
DB10C	102.99	106.58	3.59	DCB47C	109.11	113.35	4.24
DB15C	107.54	107.06	-0.48	DCB48A	97.93	102.87	4.94
DBP1	119.09	114.96	-4.13	DCB4A	119.09	122.91	3.82
DBP2	116.72	112.64	-4.08	DCB51A	142.49	139.37	-3.12
DCB10	116.39	115.18	-1.21	DCB51D	137.62	137.04	-0.58
DCB12	109.53	112.49	2.96	DCB53	105.82	109.84	4.02
DCB15R	109.32	105.64	-3.68	DCB54	99.53	102.43	2.90
DCB16R	107.15	106.19	-0.96	DCB56	123.86	121.77	-2.09
DCB17B	119.25	116.15	-3.10	DCB59A	120.63	118.50	-2.13
DCB1A	115.44	115.30	-0.14	DCB5A	118.82	120.63	1.81
DCB20D	115.76	119.69	3.93	DCB6	116.76	117.23	0.47
DCB23C	111.28	117.39	6.11	DCB61	125.12	121.78	-3.34
DCB23D	112.63	117.08	4.45	DCB64	135.86	131.75	-4.11
DCB24C	118.49	120.12	1.63	DCB65A	103.45	105.68	2.23
DCB26AR	119.02	116.63	-2.39	DCB7	117.96	118.82	0.86
DCB28	96.06	99.83	3.77	DOB15	140.62	143.63	3.01
DCB2A	124.81	125.05	0.24	DOB15PZ	135.87	133.78	-2.09
DCB30	102.88	105.40	2.52	DOB21PZ	126.84	131.75	4.91
DCB31	109.89	111.02	1.13	DOB22	140.02	138.64	-1.38
DCB33B	135.01	129.64	-5.37	DOB3	142.79	145.84	3.05
DCB33D	132.26	127.89	-4.37	DWP1	92.86	95.00	2.14
DCB34A	119.44	121.93	2.49	DWP6	92.74	96.47	3.73
DCB35C	115.23	119.90	4.67	DWP7	95.19	96.11	0.92
DCB38C	110.20	115.74	5.54	DWP9	91.12	92.91	1.79
DCB39C	115.99	116.30	0.31	TNX12D	94.64	93.96	-0.68
DCB3A	120.70	124.82	4.12	TNX14D	94.09	93.14	-0.95
DCB40A	118.00	116.80	-1.20	TNX22D	92.48	91.97	-0.51
DCB41C	121.76	119.33	-2.43	XSB1B	102.00	100.05	-1.95
DCB45C	124.88	124.58	-0.30	XSB3A	99.28	100.37	1.09
DCB46C	109.79	112.58	2.79				

Table 3-5. Regional Model Head Calibration Statistics

Statistic	Goal	Result
Mean Error	2.75	0.67
Mean Absolute Error	2.75	2.59
Root Mean Squared Error	5.50	3.02

Table 3-6. Regional Model Flux Calibration Results

Flux Target	Target Value (cfd)	Target Range (cfd)	Model Result (cfd)
Upper Three Runs	$2.2x10^5$	$1.1x10^5$ to $4.4x10^5$	$2.2x10^5$
Fourmile Branch	$3.9x10^5$	$1.7x10^5$ to $7.8x10^5$	$1.7x10^5$

3.4.2 Heads

Figures 3-23 through 27 show the head contours for the calibrated model. In general, flow directions are reasonable, with a predominant westerly gradient in the UTRA, and a predominantly northwesterly gradient in the GA. Locally, FMB and UTR both significantly impact groundwater flow. Figure 3-28 provides a west-east cross section of heads.

3.4.3 Particle Tracks

Figure 3-29 shows particle tracks based on the calibrated regional model. Particles were started at the water table at various locations within the domain, and are plotted with five-year timing indicators. Note that the paths portrayed are planar projections of three-dimensional paths and reflect travel in both the UTRA and the GA. Figure 3-30 shows a representative cross section approximately along a suite of particle paths. Note again that the paths portrayed are projections of three-dimensional paths.

As discussed earlier, two qualitative calibration goals were to achieve reasonable flow directions at the DOSB (consistent with known plume orientation) and to achieve general flow timings at D-Area. Both of these goals were met as shown on Figure 3-30. The flow paths at DOSB are generally southwest in the UTRA, which is consistent with plume characterization information. The flow paths indicate an approximate 20-year travel time across D-Area for particles that travel in the UTRA, which is consistent with known source timings and current plumes (see Figure 3-9).

3.4.4 Water Balance

Table 3-7 and Figure 3-31 shows the water balance information for the calibrated regional model. The water budget balance is excellent (indicating no significant problems with model convergence in MODFLOW). The flow budget across the Gordon Confining Unit shows that a significant volume of water in the UTRA is leaking through the GCU into the GA, which ultimately discharges to UTR or the SR.

Table 3-7. Regional Model Water Budget Results

In	In Rate (cfd)	Out Rate (cfd)
Constant Head	477,785	374,310
Drains	0	751,650
River Leakage	35,014	60,140
Recharge	673,000	0
Total	1,185,681	1,186,100

3.5 Sensitivity Analysis

The purpose of a sensitivity analysis is to quantitatively evaluate the effect of uncertainty in model inputs on the calibration and results of a model. Uncertain model inputs include parameter values, boundary conditions, and the conceptual model. To simplify this sensitivity analysis, boundary conditions and the conceptual model were assumed to be relatively certain and only input parameter values were varied. The results of this sensitivity analysis can be used to make quantitative or qualitative judgements about the relative importance of individual parameter values, to provide information about the confidence in the model results, and to guide future data collection and expenditure of resources. The results of this sensitivity analysis should only be used to make general assumptions regarding the uncertainty in the model results, however, since all of the parameter values have some degree of uncertainty and some parameters may be correlated to one another. The cumulative effect of these uncertainties and parameter correlations cannot be estimated by a sensitivity analysis that varies only one parameter value at a time.

3.5.1 Methodology

Based on previous analyses conducted for similar SRS models, hydraulic conductivity, recharge, river/drain conductance, and porosity were selected as the more sensitive parameter values to be evaluated in this analysis. The range of values used were based on a review of literature values, model calibration results, and/or professional judgement. Section 3.5.2 lists specific information about the parameter groupings, calibrated values, and range of values used in this analysis. Individual parameter values or groups (zones) of similar parameter values were systematically varied, one at a time, through the range of possible values and selected model outputs were recorded for each sensitivity run or "iteration." Particle track runs were performed to determine the sensitivity of flow direction and travel time to parameter values. Particles were started at the water table at the DOSB, at the bottom of layer 1 at the DHWRF and DHWF, and in the middle of layer 2 at the DCPRB (Figure 3-32). The particle tracks from the calibrated model are presented in Figure 3-33, with five-year time increment markers.

Calibration statistics and convergence of individual sensitivity iterations are important model outputs that are considered to determine if the information obtained from the model for a particular run is "believable." This is not to state that if the calibration criteria are not met, that the parameter value itself is invalid, as it is possible that calibration criteria can be met if other parameter values are varied at the same time. To assess the relative importance of a particular parameter value to the model results, the parameter values were varied over a wide range of possible values that may or may not meet calibration criteria. The range of values used in this study was chosen to provide pertinent information regarding the importance of the parameter value; calibration statistics provide information regarding the validity of the model results.

Calibration statistics and other model outputs evaluated as part of the sensitivity analysis on the regional flow model include the following:

- Calibration statistics (RMS, MAE, and ME)
- Flux to surface water (total flux to UTR and FMB)
- Flux out of the bottom of layer 3 (mainly out of the UTRA)
- Particle track time to reach surface water
- Particle track direction

3.5.2 Parameters

Parameter values varied in this analysis included the following: K_h or K_v for specific material types, recharge rates, river/drain conductances, and porosity (only particle tracking results are evaluated). Table 3-8 provides the ranges for these parameter values.

Table 3-8 Parameter (Boundary Condition) Values Used in the Sensitivity Analysis

Parameter Value	Calibrated Model Value	Range
K_h for UTRA	18 ft/d	.1, .5, 2, 10 (factors)
K_v for UTRA	1 ft/d	.001, .01, .1, 10 (factors)
K_h for UTRA Zone 2	10 ft/d	.1, .5, 2, 10 (factors)
K_v for UTRA Zone 2	.5 ft/d	.001, .01, .1, 10 (factors)
K_v for Local Clay	.005 ft/d	.001, .01, .1, 2, 10 (factors)
K_v for the GCU (all GCU zones varied by the same factor)	.0001-.1 ft/d	.01, .1, 10, 100 (factors)
K_h for "SR Alluvium"	70 ft/d	.1, .5., 2 (factors)
K_v for "SR Alluvium"	7 ft/d	.1, .5, 2 (factors)
K_h for the GA	20 ft/d	.1, .5, 2, 10 (factors)
K_v for the GA	2 ft/d	.1, .5, 2, 10 (factors)
FMB, UTR, and SR conductances (varied by the same factor)	10,000 $ft^2/d/ft$	100, 1000, 100,000
D-Area rivers/drains conductances (not including FMB, UTR, and SR -- varied by same factor)	500, 1000, or 10,000 $ft^2/d/ft$	10, 100, 10,000
Porosity (homogeneous throughout model domain)	.3*	.1, .2, .4, .5
Recharge for the DCPRB, 488-D/488-4D ash basins, (varied by the same factor)	11 (DCPRB), 2 (ash basins) and 11 (west of 488-4D) in/yr	.5, 1.5, 2 (factors)
Recharge for 488-1D/2D	22 in/yr	.5, 1.5, 2 (factors)
Lowland recharge	8	.5, 1.5, 2 (factors)

*Porosity is not a parameter value in the flow model calibration; therefore, the "calibrated model" represents the best estimate of the parameter value.

3.5.3 Results

Table 3-9 contains the complete results of the sensitivity analysis. Figures 3-34 through 3-36 illustrate the results for selected parameter values. Model results and parameter values used in the sensitivity analysis were normalized to the calibrated model results and parameter values in the figures, to assist with evaluating the relative change in model output with respect to the change in model input. In cases where the model did not converge (200 iterations), the results provide valuable information; however, no final solution was obtained for these test cases.

The figures indicate that lowland recharge, UTRA Zone 2 K_h, GCU K_v, and GA K_h are the most sensitive parameter values used in the model. River and drain conductances are not sensitive for any of the model outputs analyzed.

The most sensitive parameter (greatest change in output for a given change in input) with respect to calibration statistics is lowland recharge. The RMS error more than doubled at twice the calibrated recharge values. The highest RMS errors occurred for the lowest values of GCU K_v and GA K_h (test cases 22 and 32, respectively) used in the analysis. Generally, the model is not very sensitive to calibration statistics. Most of the test cases are within calibration criteria. RMS errors generally increased for parameter values above and below the calibrated values, which supports the flow model calibration results.

The vertical hydraulic conductivity of the GCU is the most sensitive parameter value of this type. Interestingly, the maximum GCU K_v used in this study (.01 ft/d) led to increased flux to the UTR, FMB, and flux out of the UTRA (layer 3). Intuitively, one would expect flux to UTR and out of the UTRA to increase with increased flow into the GA, which partially discharges to UTRA; however, FMB flux also increased. The increased vertical hydraulic conductivity of the GCU changed the UTRA potentiometric surface such that a steeper hydraulic gradient towards FMB resulted, which increased flow to FMB.

A ten-fold increase in the GA K_h resulted in a factor of five increase in flux to UTR and an almost 50% reduction in the net flow out of layer 3. The reduced flux out of layer 3 is a result of increased discharge to UTR and the SR (more discharge flowed upwards towards these surface water bodies). On the other hand, increases to UTRA Zone 2 K_h resulted in increased discharge to FMB and flux out of the UTRA.

Major recharge zones are very sensitive parameter values. In these zones, higher recharge rates led to increased flux to UTR, FMB, and the GA. Changes to a group of recharge zones near the

DAB and DCPRB which cover a much smaller area had negligible impact on flux, as these recharge areas were too small in aerial extent to impact more global model outputs such as flux to surface water bodies. These recharge zones had a small but more noticeable impact on calibration statistics, as most of the calibration targets are concentrated near D-Area. Lower D-Area ash basin recharge led to a slightly improved RMS error, but the improvement is considered insignificant.

Particle track runs were performed for most of the flow model test cases to determine the sensitivity of parameter values to flow direction and travel times. The particle track directions in the flow model are generally not very sensitive to changes in the parameter values analyzed. The general direction for particles from the DHWRF was to the DRP stream boundary or to the Savannah River. On the other hand, particle tracks from the DHWF usually terminated at the D-Area powerhouse effluent channel that flows into Beaver Dam Creek, or traveled to the Savannah River. Particle tracks starting from the DCPRB almost always terminated at the powerhouse effluent channel. More rarely, particles discharged to the Savannah River from the DCPRB. Contamination from the DCPRB must be lower in the UTRA to have a higher probability of "escaping" the powerhouse effluent channel, i.e. most of the flow directly underneath the DCPRB is to the powerhouse effluent channel. Only a few test cases led to solutions where particles from the DOSB traveled in directions other than a westerly direction towards the Savannah River. These atypical particle directions resulted from reduced flow to the GA and consequently, increased discharge to D-Area streams/channel.

Porosity only effects travel times and not travel direction, because it is not a flow model parameter and does not effect volumetric flow rates or heads. Lower porosities resulted in higher average linear velocities and faster travel times, while higher porosities led to lower average linear velocities and longer travel times to discharge areas.

Higher UTRA K_h led to reduced travel times. Increases to the local clay K_v led to local effects near the DCPRB, including shorter paths and travel times to the powerhouse effluent channel where most of these particles usually terminated. Increases to the GCU K_v and GA K_h led to increased travel times and distances through the GA with more particles discharging to the Savannah River. Decreased alluvium horizontal hydraulic conductivity led to early discharge to the D-Area streams/channel for DHWRF particles, while flow directions and travel times appeared to be insensitive to alluvium K_v.

As expected, increases to recharge for the major recharge zones increased flow rates and shortened travel times to discharge areas. Changes to recharge rates for the smaller DAB and DCPRB zones had a much less noticeable effect on particle track directions and travel times.

In summary, lowland recharge, UTRA Zone 2 K_h, GCU K_v, and GA K_h are the most sensitive parameters used in the model, i.e. greatest change in model output for a given change in model input, (see Figures 3-32 through 3-34). Higher GCU K_v and GA K_h led to increased flow into the Gordon aquifer, longer travel times and distances to the SR, and less discharge to the D-Area streams/channel. Higher lowland recharge leads to increased flux to surface water with shorter travel times and is the most sensitive parameter with respect to calibration. Drain/stream/river conductances are insensitive parameters. Calibration and particle track direction model outputs are relatively insensitive to changes in parameter values.

Table 3-9 Regional Flow Model Sensitivity Analysis Results

Parameter	Material/Zone/Arc Groups	Calibrated Value	Test Number [a]	Test Value [b]	File Name	Iterations Required for Convergence	RMS Error	MAE Error	ME Error	Flux to UTR (cfd x 1E+05)	Flux to FMB (cfd x 1E+05)	Net Flux Out of Bottom of Layer 3 (cfd) (negative implies downward flux)	DOSB Particle Track Time and Direction*	HWF Particle Track Time and Direction*	HWRF Particle Track Time and Direction*	DCPRB Particle Track Time and Direction*
CALIBRATED RESULTS						**77**	**3.02**	**2.59**	**0.67**	**3.17**	**2.31**	**-633843**	**85 to SR**	**30 Drain**	**45-50 SR**	**5-15 Drain**
UTRA K_h	UTRA	18	1	1.8	run001	200/nc	6.31	4.85	4.48	3.19	1.95	-679833	85 to SR	40 to Drain >100 to SR	10 to Drain	25 to Drain 90 SR
ft/d			2	9	run002	14	3.79	3.1	1.92	3.79	2.19	-652810	85 to SR	30 to Drain	20 to Drain	15 to Drain
			3	36	run003	19	2.97	2.53	-0.44	3.76	2.43	-616908	85 to SR	50 to SR 25 to Drain	40 to SR	1-25 to Drain
			4	180	run004	25	5.55	4.66	-3.56	3.72	2.54	-581330	90 to SR	40 to SR	20 to SR	20 to SR 15 Drain
UTRA K_v	UTRA	1	5	0.001 .003	run005	200/nc	5.13	4.02	3.01	3.8	1.26	-735343	85 to SR	50- >100 to SR	20 to Drain	5-25 to Drain
ft/d	"leaky" UTRA	3	6	0.01 .03	run006	200/nc	4.24	3.44	2.23	3.79	1.6	-706375	80 to SR	55-95 to SR	15-20 Drain	10-20 Drain
			7	0.1 .3	run007	14	3.38	2.82	1.25	3.78	2.14	-652101	85 to SR	50- >100 SR	20 Drain 45 SR	5-15 Drain
			8a	2 6	run008a	200/nc	2.99	2.57	0.6	3.77	2.32	-632498	-	-	-	-
			8	10 30	run008	200/nc	3.03	2.66	0.52	3.77	2.33	-631347	-	-	-	-
UTRA Zone 2	UTRA Zone 2	10	9	1	run009	30	5.33	3.16	1.95	3.55	1.65	-518227	105 to SR	75-80 to SR	50-65 to SR 20 to Drain	1-15 to Drain
K_h			10	5	run010	34	3.25	2.71	0.89	3.64	2.02	-581301	105 to SR	>200 to Drain 75-85 SR	85 to SR	5-15 Drain
ft/d			11	20	run011	15	3.19	2.71	0.63	4.02	2.76	-706227	70 to SR	20 to Drain	35-45 to SR	15 to Drain
			12	100	run012	30	4	3.35	1.3	5.77	5.24	-1041108	20 to SR	40 to SR 10 to Drain	< 5 to Drain	5-10 to Drain
UTRA Zone 2	UTRA Zone 2	0.5	13	0.0005	run013	200/nc	9.27	5.7	2.65	2.64	2.64	-95123	-	-	-	-
K_v			14	0.005	run014	21	3.53	2.81	1.37	3.63	2.11	-397654	90 to SR	20-30 to Drain	40-50 to SR	5-10 to Drain
ft/d			15	0.05	run015	53	2.96	2.54	0.76	3.75	2.21	-580738	95 to SR	30-35 to Drain	45-60 to SR	>5-15 to Drain
			16	5	run016	82	3.03	2.6	0.65	3.77	2.33	-641259	85 to SR	30 to Drain	45-50 to SR	5-15 to Drain
Local Clay K_v	Local Clay	0.005	17	5.00E-06	run017	200/nc	8.45	4.44	2.77	3.77	2.32	-634607	-	-	-	-
ft/d			18	5.00E-05	run018	200/nc	5.12	3.45	1.79	3.77	2.32	-634558	85 to SR	30 to Drain	45-50 SR	<5-120 to Drain
			19	5.00E-04	run019	200/nc	3.25	2.74	1.1	3.77	2.32	-634435	-	-	-	-
			19a	1.00E-03	run019a	200/nc	3.11	2.6	0.95	3.77	2.32	-634350	-	-	-	-
			20	0.01	run020	154	2.96	2.52	0.48	3.77	2.31	-633380	-	-	-	-
			21	0.05	run021	14	2.94	2.5	0.2	3.77	2.3	-632061	85 to SR	30 to Drain	45-55 SR	<5-10 to Drain

Table 3-9 Regional Flow Model Sensitivity Analysis Results (con't)

Parameter	Material/Zone/Arc Groups	Calibrated Value	Test Number [a]	Test Value [b]	File Name	Iterations Required for Convergence	RMS Error	MAE Error	ME Error	Flux to UTR (cfd x 1E+05)	Flux to FMB (cfd x 1E+05)	Net Flux Out of Bottom of Layer 3 (cfd) (negative implies downward flux)	DOSB Particle Track Time and Direction*	HWF Particle Track Time and Direction*	HWRF Particle Track Time and Direction*	DCPRB Particle Track Time and Direction*
CALIBRATED RESULTS						**77**	**3.02**	**2.59**	**0.67**	**3.17**	**2.31**	**-633843**	**85 to SR**	**30 Drain**	**45-50 SR**	**5-15 Drain**
GCU K_v	"tight" GCU	1E-04	**22**	1E-06 5E-05 1E-03	run022	22	10.3	6.81	2.92	2.21	2.5	-74580	40 to Drain	15-20 Drain	5-15 to Drain	<5-10 Drain
ft/d	GCU	0.005	**23**	1E-05 5E-04 1E-02	run023	36	4.59	3.45	1.34	3.37	1.88	-351350	60 to Drain	20 to Drain	10 to Drain 45 to SR	<5-10 Drain
	"leaky" GCU	0.1	**24a**	.0005 .025 .5	run024a	200/nc	3.13	2.39	0.48	3.83	4.06	-969345	85 to SR	80 to SR 25-30 to Drain	45 to SR	5-15 to Drain
			24	1E-03 5E-02 1	run024	200/nc	3.18	2.65	0.4	3.85	5.42	-1188457	-	-	-	-
			25	1E-02 5E-01 10	run025	200/nc	3.19	2.68	0.42	3.97	11.19	-1820791	80 to SR	75 to SR 30 to Drain	50-65 to SR	75 to SR <5-15 to Drain
Alluvium K_h	SR Alluvium	70	**26**	7	run026	15	3.89	3.2	1.83	3.82	2.45	-643436	90 to SR	30 to Drain	20-40 to Drain	5-10 to Drain
ft/d			**27**	35	run027	200/nc	3.22	2.74	1.01	3.79	2.37	-636370	-	-	-	-
			27a	50	run027a	45	3.11	2.66	0.83	3.78	2.35	-635100	85 to SR	30 to Drain	45-50 to SR	5-15 to Drain
			28a	90	run028a	159	2.97	2.54	0.51	3.77	2.28	-633002	-	-	-	-
			28	140	run028	200/nc	2.91	2.48	0.34	3.76	2.24	-630777	-	-	-	-
Alluvium K_v	SR Alluvium	7	**29**	0.7	run029	53	3.04	2.6	0.76	3.8	2.33	-637266	90 to SR	30 to Drain	45-50 SR	<5-15 to Drain
ft/d			**30**	3.5	run030	73	3.02	2.59	0.68	3.78	2.32	-634360	-	-	-	-
			31	14	run031	80	3.02	2.59	0.66	3.77	2.31	-633546	85 to SR	30 to Drain	45-50 to Drain	5-15 to Drain
Gordon Aquifer K_h	Gordon Aquifer	20	**32**	2	run032	29	11.29	7.63	7.32	1.41	2.8	-397688	50 to Drain	15-20 to Drain	15 to Drain	5-10 to Drain
ft/d			**33**	10	run033	122	4.52	3.56	2.83	2.72	2.44	-593489	-	-	-	-
			34	40	run034	18	4.43	3.55	-1.6	5.45	2.26	-614335	70 to SR	50-55 to SR	40 to SR	<5-25 to Drain
			35	200	run035	24	7.45	5.54	-4.26	18.43	2.58	-354440	-	-	-	-
Gordon Aquifer K_v	Gordon Aquifer	2	**36**	0.2	run036	63	3.02	2.59	0.7	3.77	2.5	-578226	90 to SR	30 to Drain	45-50 to SR	<5-15 to Drain
ft/d			**37**	1	run037	74	3.02	2.59	0.67	3.77	2.31	-619476	-	-	-	-
			38	4	run038	80	3.02	2.59	0.66	3.77	2.32	-646410	-	-	-	-
			39	20	run039	79	3.02	2.59	0.66	3.77	2.32	-665997	80 to SR	30 to Drain	45-50 to SR	<5-15 to Drain

Table 3-9 Regional Flow Model Sensitivity Analysis Results (con't)

Parameter	Material/Zone/Arc Groups	Calibrated Value	Test Number [a]	Test Value [b]	File Name	Iterations Required for Convergence	RMS Error	MAE Error	ME Error	Flux to UTR (cfd x 1E+05)	Flux to FMB (cfd x 1E+05)	Net Flux Out of Bottom of Layer 3 (cfd) (negative implies downward flux)	DOSB Particle Track Time and Direction*	HWF Particle Track Time and Direction*	HWRF Particle Track Time and Direction*	DCPRB Particle Track Time and Direction*
CALIBRATED RESULTS						**77**	**3.02**	**2.59**	**0.67**	**3.17**	**2.31**	**-633843**	**85 to SR**	**30 Drain**	**45-50 SR**	**5-15 Drain**
River/Drain Conductance	FMB	10,000	40	100	run040	58	3.01	2.56	0.68	3.13	2.28	-686299	-	-	-	-
ft^2/d/ft	UTR	10,000	41	1000	run041	74	3.02	2.59	0.67	3.17	2.31	-634066	-	-	-	-
	SR	10,000	42	100,000	run042	77	3.02	2.59	0.67	3.18	2.28	-633833	-	-	-	-
River/Drain Conductance	Beaver Dam Creek	1000	43	10 5 100	run043	25	3.04	2.59	0.73	3.17	2.32	-633428	-	-	-	-
ft^2/d/ft	DRP Stream Boundary	500	44	100 50 1000	run044	41	3.01	2.58	0.69	3.17	2.31	-633309	-	-	-	-
	Unnamed Drain	10000	45	10000 5000 100,000	run045	84	3.01	2.58	0.62	3.17	2.31	-633062	-	-	-	-
Porosity	All layers	0.3	46	0.1	run046	NA	NA	NA	NA	NA	NA	NA	30 to SR	10 to Drain	15-20 SR	<5 to Drain
dimensionless			47	0.2	run047	NA	NA	NA	NA	NA	NA	NA	55 to SR	20 to Drain	30-35 to SR	<5-10 to Drain
			48	0.4	run048	NA	NA	NA	NA	NA	NA	NA	120 to SR	35-40 to Drain	55-65 to SR	<5-20 to Drain
			49	0.5	run049	NA	NA	NA	NA	NA	NA	NA	140 to SR	40-45 to Drain	70-80 to SR	<5-20 to Drain
Recharge	DAB (upper)	2	50	1 5.5 5.5	run050	200/nc	2.98	2.55	0.56	3.17	2.31	-633655	85 to SR	30 to Drain	45-50 to SR	<5-15 to Drain
in/yr	DAB (west end)	11	51	3 16.5 16.5	run051	18	3.06	2.62	0.74	3.17	2.23	-634043	85 to SR	30 to Drain	45-50 to SR	<5-15 to Drain
	DCPRB	11	52	4 22 22	run052	18	3.1	2.66	0.81	3.17	2.27	-634241	85 to SR	30 to Drain	45-50 to SR	<5-15 to Drain
Recharge	DAB (lower)	22	53	11	run053	14	2.88	2.51	0.31	3.17	2.31	-632840	85 to SR	30 to Drain	45-50 to SR	<5-15 to Drain
in/yr			54	33	run054	16	3.27	2.78	0.99	3.17	2.32	-634944	-	-	-	-
			55	44	run055	14	3.57	3.01	1.32	3.17	2.33	-636040	-	-	-	-
Recharge	Lowland	8	56	4	run056	26	4.7	3.63	-2.24	2.85	1.98	-555296	100 to SR	90 to SR	60-70 to SR	<5 to 25 to Drain
in/yr			57	12	run057	16	4.32	3.42	2.92	3.44	2.62	-707235	75 to SR	25 to Drain	<5-15 to Drain	<5-10 to Drain
			58	16	run058	200/nc	6.67	5.32	5.13	3.68	2.97	-780084	75 to SR	50 to SR 20 to Drain	<5-10 to Drain	<5-10 to Drain

Footnotes: [a] In some cases additional runs were made if planned runs did not converge. These additional runs are indicated with a suffix of "a" after the text number.
[b] When multiple test values are included in a single cell, the first number corresponds to the first material listed for the parameter and so on.
* The generic term "drain" is used for any interior drainage area in the model. HWRF particles drained to the DRP Stream Boundary. HWF and DCPRB particles drained to the D-Area powerhouse effluent channel adjacent to the DCPRB that flows into Beaver Dam Creek.

4.0 REGIONAL TO LOCAL CONVERSION

The local model for this effort focuses on the groundwater system in D-Area, including D-Area Oil Seepage Basin (DOSB), DRP, and the wetlands downgradient from D-Area. As such, the regional model to local model conversion was performed to create a flow and transport model that would adequately reproduce the groundwater system in this area. The local model domain was determined after examination of the regional flow model heads in the aquifers (UTRA and GA). As shown in Figure 4-1, the domain boundary was chosen to maximize use of (single-value) constant head and no-flow boundaries.

4.1 Discretization of Local Model Domain

To improve transport calculations, more layers were used in the local model, as shown in Figure 4-2. In general, the new layers were created by splitting the respective regional model layer. For example, the GCU (regional layer 4) was split into two equal thickness (at any particular location) layers for the local model. The local model cell size is 100 ft by 100 ft, as shown in Figure 4-3, oriented with Site North, with an origin (southwest corner) of 8,950 (SRS E), 59,150 (SRS N). The overall local model grid consists of 8 layers, 103 rows, and 175 columns for a total of 144,200 cells (though not all active in the domain).

4.2 Local Model Boundaries

Based on the regional flow model results, boundaries were determined for each of the local flow model layers. Figures 4-4 through 4-7 show the boundary conditions and resulting MODFLOW cell designations.

One major difference in the local model when compared to the regional model is the use of general head boundary cells instead of no-flow boundaries. The general head boundary cells used a zero value constant-head source and zero conductance to simulate no-flow boundary cells. This convention allowed GMS to create no-flow cells directly below drains and constant head boundary cells because of the way that GMS interprets boundary arcs in the map module when determining MODFLOW cell types. (If a cell is partially covered by a no-flow boundary arc, the cell is activated if the majority of the cell area is inside the coverage. Conversely, the cell is inactivated if the majority of the cell area is outside the coverage. If an arc on the boundary of the model domain has a head dependent attribute (such as drain, river, general head, or constant head) assigned to it, a different test is used. Any cell that intersects the arc is designated as active, regardless of what percentage of the cell is inside the model domain. Thus, use of general head boundaries allows GMS to assign cells using the same "test".)

5.0 LOCAL FLOW AND TRANSPORT MODEL

The local flow and transport model used the same parameter (material) distributions as that used in the regional model. See the figures from Section 2.4.

5.1 Calibration

The calibration goals for the local flow model were equivalent to the calibration goals for the regional flow model: ME less than 2.75, MAE less than 2.75, and RMS error less than 5.50. The calibration targets for the local flow model were essentially a subset of the regional targets, because the TNX wells are not within the local model domain. The targets used in the calculation of the local flow model calibration statistics are listed in Table B-3 in Appendix B.

Only minor recharge zone boundary adjustments were made to the local flow model since the initial converted model achieved acceptable calibration results (Figure 3-8 and Table 5-1). Due to the limited use of natural boundaries, flux targets were not considered during local flow model calibration. Some target wells show significant changes in model heads between the regional and local flow models. There are three likely causes for these differences. First, the changes in the recharge zone boundaries near the ash basins and DRP were made to account for the revised grid spacing and to account for the reduced recharge expected through the LC. The impacts of these recharge changes are expected to be minor. Second, because of the way the model heads are calculated for each target well location, changes in horizontal discretization could have impact to computed heads, particularly in areas of steeper flow gradients. Finally, the local flow model has additional layers, which can impact the calculation/interpolation of heads at target screen elevations. Overall, however, the differences between the regional and local model results are minor as evidenced by the similarity of the flow field contours.

Figure 5-1 shows the observed heads versus the computed heads, Figure 5-2 shows the observed heads versus the residuals, and Figure 5-3 shows the spatial distribution of the residuals for the local flow model calibration. Table 5-2 gives the individual calibration target computed heads and residuals. As shown in the figures and tables, a good calibration was achieved, with low error. Figure 5-3 shows some spatial bias, particularly near the powerhouse effluent channel with modeled heads higher than observed values, which will lead to increased flux to surface water.

As shown in Table 5-2, the observed GA "head reversal" (i.e., upward flow through the GCU) in the DCB23 cluster is not simulated in the local flow model. The model predicts the occurrence of the "head reversal" further west in the domain. The observed head difference across the GCU in the DCB23 cluster is only slightly more than one foot, and the model heads are relatively close. As stated above, the model heads near the DCB23 cluster will lead to a conservative transport prediction, with increase flux to surface water, and increased flux to deeper aquifers.

Although the DBP1 and DBP2 wells were included in the regional model calibration statistics, they were not included in the local model calibration results of Table 5-2. The local model predicted the water table below the screen elevation of these two monitoring wells. Consequently, no local model head values can be computed for these wells. As noted above, there are slight head differences between the local and regional model. The regional model results showed very low head values in these wells while the local model predicted even lower heads.

Table 5-1. Local Model Head Calibration Statistics

Statistic	Goal	Result
Mean Error	2.75	0.78
Mean Absolute Error	2.75	2.51
Root Mean Squared Error	5.50	2.97

Table 5-2. Local Model Calibration Results for Individual Head Targets

Well Name	Observed Head (ft)	Model Head (ft)	Residual (ft)	Well Name	Observed Head (ft)	Model Head (ft)	Residual (ft)
DB10C	102.99	106.55	3.56	DCB45C	124.88	124.92	0.04
DB15C	107.54	106.45	-1.09	DCB46C	109.79	112.30	2.51
DCB10	116.39	117.79	1.40	DCB47C	109.11	112.79	3.68
DCB12	109.53	110.59	1.06	DCB48A	97.93	101.68	3.75
DCB15R	109.32	104.71	-4.61	DCB4A	119.09	120.33	1.24
DCB16R	107.15	105.52	-1.63	DCB51A	142.49	138.93	-3.56
DCB17B	119.25	119.41	0.16	DCB51D	137.62	136.57	-1.05
DCB1A	115.44	118.92	3.48	DCB53	105.82	109.49	3.67
DCB20D	115.76	119.04	3.28	DCB54	99.53	101.97	2.44
DCB23C	111.28	117.66	6.38	DCB56	123.86	121.80	-2.06
DCB23D	112.63	116.45	3.82	DCB59A	120.63	118.20	-2.43
DCB24C	118.49	119.18	0.69	DCB5A	118.82	119.59	0.77
DCB26AR	119.02	116.99	-2.03	DCB6	116.76	119.91	3.15
DCB28	96.06	97.59	1.53	DCB61	125.12	121.80	-3.32
DCB2A	124.81	123.67	-1.14	DCB64	135.86	131.72	-4.14
DCB30	102.88	105.41	2.53	DCB65A	103.45	104.86	1.41
DCB31	109.89	110.87	0.98	DCB9	114.97	118.83	3.86
DCB33B	135.01	129.14	-5.87	DOB15	140.62	143.54	2.92
DCB33D	132.26	127.22	-5.04	DOB15PZ	135.87	133.70	-2.17
DCB34A	119.44	119.73	0.29	DOB21PZ	126.84	131.43	4.59
DCB35C	115.23	118.32	3.09	DOB22	140.02	138.64	-1.38
DCB38C	110.20	117.11	6.91	DOB3	142.79	145.86	3.07
DCB39C	115.99	118.02	2.03	DWP1	92.86	93.96	1.10
DCB3A	120.70	122.12	1.42	DWP6	92.74	96.45	3.71
DCB40A	118.00	116.93	-1.07	DWP7	95.19	94.65	-0.54
DCB41C	121.76	120.00	-1.76	DWP9	91.12	92.20	1.08

5.2 Flow Model Results

Figures 5-4 through 5-9 show the calculated head contours for the aquifer layers in the calibrated local flow model. As with the regional flow model, flow directions in the local model are reasonable, with a predominant westerly gradient in the UTRA and the GA. Figure 5-10 provides a west-east cross section of heads.

5.2.1 Water Balance

Table 5-3 provides the basic water balance information for the calibrated local model. The water budget balance is excellent, which indicates no significant problems with model convergence in MODFLOW.

Table 5-3. Local Model Water Budget Results

In	In Rate (cfd)	Out Rate (cfd)
Constant Head	30,078	46,316
Drains	0	83,749
River Leakage	32,218	57,009
Recharge	124,800	0
Total	187,096	187,074

5.2.2 Particle Tracking Results

Figure 5-11 shows particle tracks based on the calibrated local model. Particles were started at the water table at various locations within the domain, and are plotted with five-year timing indicators. Note that the paths portrayed are planar projections of three-dimensional paths and reflect travel in both the UTRA and the GA. Figure 5-12 shows a representative cross section along a single particle path. Note again that the paths portrayed are projections of three-dimensional paths.

5.3 Modeled Contaminants

The constituents modeled in this study are TCE, tritium, beryllium, nickel, and total uranium. Of the various metals (aluminum, beryllium, cadmium, chromium, nickel, radium, selenium, uranium, etc.) that have been found above MCLs or PRGs in the groundwater, beryllium, nickel and total uranium were selected for modeling based on expected mobility, higher human health risk, or more widespread distribution in the UTRA. In the case of aluminum, transport is thought to be solubility limited and although not specifically modeled in this study, aluminum is discussed further below. Transport parameters are summarized in Table 5-4.

Table 5-4. Transport Parameter Summary

	Modeled Constituent					
Parameter	**TCE**	**Tritium**	**pH**	**Be**	**Ni**	**U**
Dispersivity						
Longitudinal (ft)	5	5	5	5	5	5
Transverse (ratio)	.1	.1	.1	.1	.1	.1
Vertical (ratio)	.01	.01	.01	.01	.01	.01
Porosity	0.3	0.3	0.3	0.3	0.3	0.3
Bulk Density (kg/L)	na	na	1.6	1.6	1.6	1.6
Sorption Model	na	na	see Fig. 5-30	see Eqn. 5-5 & Fig. 5-35	see Eqn. 5-6 & Fig. 5-36	see Eqn. 5-7 & Fig. 5-37
Decay Coefficient (1/d)	na	1.56E-04	na	na	na	na

na = not applicable

5.3.1 TCE

To qualitatively evaluate the timing and location of TCE releases to the saturated zone at D-Area, TCE concentrations from well and cone penetrometer technology (CPT) sampling that was performed in D-Area were plotted versus time for each well series, single well, or CPT at various depths. Next, 2001 data were analyzed and averaged to create plume maps to produce initial starting concentrations for each model layer.

Each well screen and CPT sample was located within the local flow model domain and assigned to the appropriate model layer by comparing the grid elevations against the middle of the well screen or CPT depth. Scatter points were created for each model layer and assigned an average 2001 concentration for each CPT/monitoring well location. Plumes were hand-contoured by layer based on the scatter points values, flow contours, and the vertical profile of contamination. Plume contours for each layer were digitized in GMS using the TIN module, converted to scatter points, and interpolated to a 2D grid using various geostatistical methods including kriging. Each 2D grid interpolation was assigned to the appropriate layer in the 3D model as a starting concentration. The initial groundwater concentrations for TCE are shown in Figures 5-13 through 5-18. Note that the concentrations for layers 5 and 6 (GCU) are the same, and that there are no initial concentrations in the lower portion of the GA (layer 8).

Based on analysis of monitoring data and the conceptual model for the site, no additional sources of TCE were assumed, because there is currently no identifiable TCE concentration in the vadose zone, and the highest TCE concentrations are generally located lower in the UTRA. Recent evaluations at SRS have indicated that sorption for TCE is low; therefore, the transport model conservatively assumed no sorption for TCE.

5.3.2 Tritium

The initial tritium plume was developed and applied as described for TCE above. Tritium is a historical source (i.e., no current source) and a zero source term assumption was made. Tritium is assumed to have a distribution coefficient (sorption) of zero, because tritium is present as tritiated water and generally does not associate with the solid phase. A first order decay constant of 1.54E-04/d based on a tritium half-life of 12.3 years was used in the transport modeling. The initial groundwater activities for tritium are shown in Figures 5-19 through 5-23. Note that there are no initial activities in the lower portion of the GCU (layer 6), or in the GA (layers 7 and 8).

5.3.3 Metals

Sorption parameters for metals and radionuclides can vary orders of magnitude based on the geochemical conditions at a particular waste site; therefore, important mechanisms that may effect contaminant transport should be considered. In the case of D-Area, the D-Area ash basins, coal pile, and DCPRB are known sources of low pH leachate to groundwater. Furthermore, monitoring well data near the DRP also indicate elevated levels of acidity near this unit. A good understanding of the impact of these sources of acidity on the geochemistry at the site is very important to modeling the fate and transport of metals at D-Area, because sorption for inorganics is highly pH dependent. Hydrogen ions react with aquifer materials, which results in competition for sorption sites and changes to the surface charge of soils. Information about the acid plume at D-Area was evaluated for use in the transport modeling for the metals. First, historical pH data were analyzed and graphed. Based on this analysis, a conservative background pH of 5 (or $[H^+]$=10 ppb, where the pH is equal to the negative log of the hydrogen ion concentration in an infinitely dilute solution) was assumed in the modeling. The monitoring data show that background levels of acidity are present in the GCU and the GA; therefore, no pH "plume" is associated with the GA.

To model soil buffering of acidity and subsequent groundwater pH, aqueous concentration versus sorbed concentration data for hydrogen ion were provided by SRTC. These data are based on laboratory soil titration experiments conducted with SRS upland soils (Kaplan and Serkiz 2002). These data represent the equilibrium aqueous and solid phase concentrations over a pH range that incorporates all of the buffering reactions that occur with SRS soils. To use this information, a sorption isotherm was fit to the data. The best fit to the model was obtained using a linearized version of the non-linear Freundlich isotherm. The non-linear Freundlich isotherm and linearized version of the non-linear Freundlich isotherm are of the following form:

$$S = kC^n \tag{5-1}$$

$$\log[S] = \log[k] + n \times \log[C] \tag{5-2}$$

where

S = sorbed phase concentration,

k = Freundlich absorption constant,

C = aqueous phase concentration, and

n = Freundlich exponent.

Excel solver was used to further minimize the error between the isotherm and experimental data using the best fit parameters obtained from the fit to the linearized version of the Freundlich isotherm above. Each error was normalized by the observation value to give more weight to lower concentration values. A value of 0.38 for the exponent and 396 $L^{.38}ug^{.62}$/kg for the adsorption constant were the optimized parameter values. A "best-fit" distribution coefficient (Kd) was also calculated for comparison. It is significant to note that the Kd sorption model had a very poor fit to the data with an R-squared value around 0.5, while the non-linear Freundlich isotherm had a much better fit with an R-squared value greater than 0.95. The resulting Freundlich sorption isotherm for hydrogen ion is shown in Figures 5-24.

Transport of [H+] was simulated in the local model using the parameters listed in Table 5-4 and the recharge sources shown on Figure 5-25. To maintain a background pH of 5 (10 ppb [H+]), a constant background recharge concentration of 10 and a constant concentration boundary of 10 (see Figure 5-25) were used. Time-series monitoring data from the existing monitoring well network (Figure 5-26) and the pH transport modeling indicate that near the source areas, the current pH plume is not changing significantly through time. Therefore, to simplify modeling, sorption values for the metal contaminants were considered constant in time but spatially varying based on pH.

The resulting distributions of pH used to determine metal Kds are shown in Figures 5-27 through 5-30. These distributions were hand contoured by model layer and interpolated to a 2D grid for use in calculating sorption parameters for each metal on a grid cell by cell basis. The contours were primarily created from the pH transport modeling results; however, adjustments were made to the pH in the wetlands to account for additional buffering capacity and lower oxidation-reduction potentials in the wetland that were not considered in the pH transport modeling. These conditions were expected to lead to an increase in the pH in the wetlands. Thus, a background wetland pH of 5 (Kaplan et al, 2002, Kaplan and Serkiz 2002) was assumed when the pH distributions were constructed.. This adjustment is consistent with the field pH data in D-Area and other SRS wetland data (Dixon et al. 1997). Uncertainty with respect to the leading edge of the pH plume (wetland pH) is discussed in the sensitivity and uncertainty analysis sections.

SRTC performed MINTEQA2 (Allison et al. 1991) surface complexation modeling to estimate sorption parameters for Ni and Be to D-Area soils (Powell et al. 2002) over a range of pH. The surface complexation reactions and equilibrium constants used in the SRTC modeling were obtained from the literature. To simplify the modeling, it was assumed that hydrousferric oxide (HFO) is the only soil surface participating in sorption reactions. HFO binding site concentrations were calculated based on representative concentrations of extractable iron in D-Area soils using US EPA 3050B extraction. Various contaminant concentrations representative of field conditions were also evaluated in the modeling to investigate the impact of aqueous phase concentration on sorption. Variations in contaminant concentrations in the field were found to be insignificant with respect to sorption. Fraction sorbed versus pH data were provided. These data were converted to Kds for use in the transport modeling using the following equation:

$$K_d = \frac{f_s}{1 - f_s} \times \frac{\eta}{\rho} \tag{5-3}$$

where

K_d = distribution coefficient,

f_s = fraction sorbed,

η = porosity, and

ρ = bulk soil density.

For nickel, field data from D-Area were used to supplement the surface complexation modeling data (Powell et al. 2001). In-situ Kd values for Ni were essential, because the surface complexation modeling indicated insignificant sorption at the pH range used in the modeling, which is inconsistent with the field measurements and made calibration difficult. The extreme sensitivity of Ni sorption to the modeled result is discussed in the sensitivity analysis.

For uranium, field data from F- and H-Area seepage basins were provided that showed the relationship between Kd and pH for U-235 and U-238 (WSRC 1994). Since U-238 data covered a larger pH range and sorption does not vary for different isotopes of the same element, only U-238 data were used. Furthermore, data for pH values greater than five were not used, because the average sorption coefficient in this pH range are in excess of 10,000 L/kg. Use of these data would have provided additional weight in the curve fitting routine to higher pH values that are not expected to dominate the model geochemistry. The lowest pH represented by the data was 3; therefore, a minimum distribution coefficient was assumed below a pH of 3.

For all of the metals, a four-parameter logistic function or sigmoid (stretched out S-shape) of the following form was used to fit the data (see Figures 5-31 through 5-33):

$$f(x) = \frac{a - d}{1 + \left[\dfrac{x}{c}\right]^b} + d \tag{5-4}$$

where

a = maximum function evaluation,

b = slope parameter,

$c = x$ at the inflection point of the sigmoid, and

d = minimum function evaluation.

Equations 5-5 through 5-7 show the best-fit relationship between pH (hydrogen ion concentration in ppb) and Kd for each metal based on four-parameter logistic function fits to the sorption data and/or adjustments that were made to these fits based on subsequent metal transport modeling. For beryllium it was necessary to multiply the fitted sorption coefficients by 0.7 in order to get a closer match to 2001 monitoring data at D-Area. This adjustment is reflected in Equation 5-5 (the entire function is multiplied by 0.7 in the equation). For nickel it was necessary to fit the four-parameter logistic function to in-situ calculated Kds only, because the surface complexation modeling results appeared to underestimate the amount of sorption occurring at D-Area based on a comparison with monitoring well data

$$Kd_{Be} = \left[\frac{156 - 0.00004}{1 + \left[\frac{[H+]}{1} \right]^2} + 0.00004 \right] \times 0.7 \tag{5-5}$$

$$Kd_{Ni} = \frac{389 - .001}{1 + \left[\frac{[H+]}{9.2} \right]^{4.9}} + .001 \tag{5-6}$$

$$Kd_U = \frac{2000 - 1}{1 + \left[\frac{[H+]}{6} \right]^2} + 1 \tag{5-7}$$

Table 5-5 provides select values from these relationships. Conservative assumptions were made to limit the maximum Kd used in the curve-fits; however, it is significant to note that maximum Kds for all of the metals occurred at lower concentrations (higher pHs) than were represented in the pH distributions.

Table 5-5. pH – Kd Relationship

pH	[H+] ppb	Beryllium Kd (L/kg)	Nickel Kd (L/kg)	Uranium Kd (L/kg)
7	0.1	110	389	1998
6	1	55	389	1946
5	10	1	155	530
4	100	.014	.002	8.2
3	1000	.00014	.001	1.1
2	10000	3E-05	.001	1

Each metal has a different inflection point in the four parameter logistic function, above and below which sorption rapidly increases or decreases as determined by the slope parameter. For nickel, a five order of magnitude increase in the Kd between a pH of 4 and 5 occurs in the model fit. Similarly, uranium sorption increases dramatically (almost two orders of magnitude) between the pH range of 4-5. Beryllium sorption also increases two orders of magnitude over the pH range between 4 and 5; however, the Kd is much lower and is not significant until a pH of 5 is obtained. In the case of uranium, however, sorption is relatively high over most of the pH range represented in the transport modeling compared to nickel and beryllium which only have significant sorption above a pH of 4.

Distribution coefficient (Kd) values are generally not available for the lower pH range represented by the field data at D-Area (pH=2). EPA's soil screening guidance lists Kd versus pH for nickel and beryllium for pH values greater than 4 based on MINTEQ modeling (US EPA 1996). According to the EPA document, at a pH of 4 nickel and beryllium Kds are estimated to be around 4 and 6.3, respectively. These values are much higher than the values used in the metal transport modeling with a Kd of .002 for nickel and .014 for Be (see Table 5-5). At a pH of 5 the EPA document lists Kds of 16 and 25 for nickel and beryllium, respectively. The Kds used in the metal transport modeling are much lower (Kd=1) for beryllium and much higher (Kd=155) for nickel. The less conservative Kd values used for nickel occur only around a pH of 5 and are justified by actual field data that were used to calculate in-situ Kds, as opposed to empirically based surface complexation modeling results that appear inconsistent with the monitoring data. for nickel.

Plume maps showing average 2001 groundwater concentrations for beryllium, nickel, and uranium are provided in Figures 5-34 through 5-44. Note that there are no plume maps for any of the metals in the GCU (layers 5 and 6), or in the GA (layers 7 and 8), because all of the samples below the UTRA are either non-detect or well below the regulatory limits for these constituents. Furthermore, uranium concentrations in the lowest UTRA layer (layer 4) are not provided, because either the concentrations were non-detect or well below the MCL of 30 ug/L with no identifiable "plume".

A constant source term for the metals was assumed in the transport modeling. Mass was loaded into five source areas as a recharge concentration. The locations included the tip of the DCPRB adjacent to the D-Area coal pile, the DCPRB, the western edge of the 488-D and 488-4D ash basins, and the DRP. Although not a part of the DEXOU, a source area was included on the western end of the 488-4D, because monitoring wells in this area had elevated acidity and metals concentrations. These locations and corresponding calibrated recharge concentrations are shown on Figure 5-45. Although elevated levels of acidity and metal concentrations were present in a well near the dead and stressed vegetation area, this source area could not be considered in the modeling, because recharge was assumed to be zero in this area. The contaminant levels in this area are below regulatory limits; therefore, this source area is not considered significant for the purposes of transport modeling.

To achieve a qualitative calibration of the metal sources, various constant source concentrations were tested and a two-fold comparison was made. First, a mass balance calculation was made to determine a rough estimate of contaminant loadings to achieve the assumed constant 2001 concentrations at the source locations. The mass estimate of source loadings (from recharge) for a particular source area was determined by manipulating and solving a simple mass balance equation:

$$\sum_{i=1}^{5} Q_i C_i + Q_r C_r = 0 \qquad (5\text{-}8)$$

where

i = front, back, left, right, and bottom faces of group of cells in source area,

Q_i = volumetric flux through face i, in group,

C_i = concentration of flux through face i, in group,

Q_r = volumetric flux of recharge in entire source area, and

C_r = average concentration of recharge flux in source area.

The resulting source loading recharge concentrations are given in Table 5-6. The second comparison involved running the model with constant sources to recreate the current plumes. The model was run for a simulation time frame of 20 years with initial aquifer concentrations of zero. Comparisons of the simulated plumes to the 2001 actual concentration data (Figures 5-34 through 5-44) were made. Although the actual source timings are unknown, 20 years was assumed a reasonable source time because that is when the DCPRB began operation. The best qualitative fit of continuous sources to current monitoring data is given in Figure 5-45 and Table 5-6. Figures 5-34 through 5-44 show that there is very good agreement between the model predicted concentration after 20 years and the 2001 analytical data.

Table 5-6. Recharge Concentrations for Be, Ni, and U

	Beryllium (ug/L)		Nickel (ug/L)		Uranium (ug/L)	
Source Location	Mass Balance Derived Estimates	Model Source Values	Mass Balance Derived Estimates	Model Source Values	Mass Balance Derived Estimates	Model Source Values
Coal Pile	327	300	4316	4000	100	150
DCPRB	50	100	1195	1000	120	150
488-D DAB	0	100	1500	1000	80	100
488-4D DAB	207	100	910	1000	56	75
DRP	73	50	500	300	50	150

Powerhouse operations are expected to cease around 2015, at which time the flow and source conditions are expected to change significantly; therefore, the model only simulated metal contaminant transport until 2015 (15 years). Recent operational changes were made to reduce the amount of acid leachate emanating from the coal pile and DCPRB, including reduction in the size of the coal pile and periodic dredging of the DCPRB. These operational changes were not explicitly considered in the modeling.

Although aluminum was not modeled, the transport of aluminum is thought to be solubility controlled and a curve of aqueous solubility versus pH is presented in Figure 5-46. This curve is based on MINTEQA2 modeling performed by SRTC that considers only solubility of aluminum in contact with kaolinite over a range of pH (Powell et al. 2002). The maximum concentration predicted by solubility control at a background pH of 5, is around 40 ppb. Wetland pH in unimpacted areas is expected to be higher, which will further limit the aqueous solubility of aluminum. The field data suggest that kaolinite may be acting as a solubility control on groundwater aluminum concentrations as the data are slightly higher but follow the same general trend as the MINTEQ modeling as illustrated on Figure 5-46.

5.4 Transport Results

5.4.1 TCE

Figure 5-47 shows the total TCE flux to the SR and to D-Area streams/channel, as well as maximum discharge concentrations. As shown, the peak discharge is predicted to occur between 20-30 years from the present, with the maximum discharge concentration occurring within the 10-40 year timeframe. Because of the closer proximity of the D-Area streams/channel to the heart of the plume, the maximum discharge concentrations are generally higher than those expected at the SR. However, almost all of the mass flux discharges to the SR because more flow discharges to the SR than to the D-Area streams/channel. The maximum concentration predicted in the GA is approximately 20 ppb at 40 years, as the heart of the plume travels slowly down through the GCU.

Figure 5-48 shows the maximum plume concentration over time as well as the volume of fluid with concentrations above the MCL. The maximum plume concentration declines rapidly during the first 10 years of the simulation due to dispersion processes – which result in an increase in the plume volume above MCL. After about 20-30 years, the plume begins decreasing in size as the current plume "heart" reaches and discharges to the SR. Table 5-7 provides the total plume mass over time.

Table 5-7. TCE Plume Mass Balance

Year	Total Mass in Aquifer (kg)	Cumulative Discharge (kg)
0	172.5	-
10	162.3	10.2
20	141.6	30.9
30	114.0	58.5
40	91.9	80.6
50	71.8	100.7
60	56.5	116.0
70	41.7	130.8
80	29.5	143.0
90	19.7	152.8
100	12.0	160.5

Figure 5-49 provides a summary of the expected concentrations in selected monitoring wells. As shown, there are numerous monitoring wells in D-Area that are expected to show TCE above the MCL of 5 ug/L (blue dots). In general, the monitoring wells near the historical sources are expected to show a rapid decline in concentration, and the monitoring wells nearer the SR to show continued current concentration levels for many decades. Figure 5-50 shows a map view of the TCE plume (layer 3) at various simulated years.

5.4.2 Tritium

Figure 5-51 shows the total tritium flux to the Savannah River and to D-Area streams/channel, as well as the maximum discharge activity. As shown, the peak discharge is predicted to occur between 20-30 years from the present (similar to TCE), with the maximum discharge activity occurring within the 10-30 year timeframe. Because of the closer proximity of the D-Area streams/channel to the heart of the plume, the maximum discharge activities are generally higher than those expected at the SR, and occur sooner. However, almost all of the activity flux discharges to the SR because more flow discharges to the SR than to the D-Area streams/channel. As expected, tritium's short half-life results in a rapid drop in activity, with little flux occurring after 40-50 years. The maximum activity predicted in the GA is approximately 1 pCi/mL.

Figure 5-52 shows the maximum plume activity over time as well as the plume fluid volume with activities above the MCL. The maximum plume activity declines rapidly during the first 10 years of the simulation due to dispersion and decay processes. During the first 20 years, dispersion processes maintain the plume volume above MCL at a relatively constant level. After about 20-30 years, the plume begins to rapidly decrease in size as the current plume "heart" reaches and discharges to the SR. Table 5-8 shows the total plume activity over time.

Table 5-8. Tritium Plume Activity Balance

Year	Total Plume Activity (Ci)	Cumulative Plume Decay (Ci)	Cumulative Discharge (Ci)
0	212.0	-	-
10	116.3	90.5	5.1
20	54.7	138.0	19.2
30	9.0	154.8	48.2
40	1.3	157.2	53.5
50	0.1	157.5	54.4
51+	0.0	157.5	54.5

Figure 5-53 provides a summary of the expected activities in selected monitoring wells. As shown, due to the relatively small plume geometry, only a few monitoring wells in D-Area are expected to show tritium above the MCL of 20 pCi/mL (blue dots). As was the case for TCE, the monitoring wells near the historical sources are expected to show a rapid decline in activity. The monitoring wells nearer the SR are expected to show an increase in activity followed by a rapid decline. No monitoring wells are expected to show activities above the MCL within 40-50 years. Figure 5-54 shows a map view of the tritium plume (layer 3) at various simulation times.

5.4.3 Metals

As metal transport is significantly retarded at a higher pH expected in the wetland near the SR, there is no mass predicted to discharge directly to the SR within the timeframe of the modeling for any of the metals. The maximum plume concentrations in the UTRA are not expected to change significantly over time, because these concentrations are near the source at DCPRB with near equilibrium conditions achieved during the timeframe of the modeling. Figures 5-55 through 5-57 show the maximum discharge concentration that occurred during the simulation time frame and discharge flux to D-Area streams/channel for beryllium, nickel, and uranium, respectively. Table 5-9 provides the maximum discharge concentration and cumulative discharge to D-Area streams/channel for each metal at the end of the simulation. The maximum discharge concentration does not change significantly over time, because the discharge location, the powerhouse effluent channel leading into Beaver Dam Creek, is also close to the source.

Table 5-9. Metal Maximum Discharge Concentration and Cumulative Discharge (year 2015)

Constituent	Maximum Concentration (ppb)	Cumulative Discharge (kg)
Beryllium	170	35.2
Nickel	2200	476.2
Uranium	70	6.8

Figures 5-58 through 5-60 provide a summary of expected concentrations in select monitoring wells for the three metal forecasts. Figure 5-58 shows that for beryllium, several monitoring wells are above the MCL of 4 ug/L. Some of these wells are at the western boundary of the monitoring well network near the SR. The lower regulatory threshold for beryllium has made the mobility of this particular metal more problematic. In fact, at the end of the simulation the beryllium plume has concentrations near the MCL just east of the SR. Beryllium is much more mobile than nickel and uranium at the background pH in the wetland and is expected to travel faster through the wetland to the SR. Little dilution occurs in the wetland, because this area is a discharge area simulated in the model with no recharge. Furthermore, at the modeled hydraulic gradient, the relatively high horizontal hydraulic conductivity of the alluvium (70 ft/d) results in fairly rapid transport through the wetland. For example, particles started near the tip of the DCPRB have an advective transport time through the wetland of approximately 15-20 years.

As shown in Figures 5-59 and 5-60, there are only a few monitoring wells in D-Area that are expected to show concentrations above the preliminary remediation goal (PRG) of 730 ug/L (blue dots) for nickel and the MCL of 30 ug/L for uranium. All of the wells above the MCL for uranium are located in close proximity to the DCPRB as retardation (pH-driven sorption) has considerably slowed the transport of uranium away from the source. Uranium exhibits significant retardation even at low pH and is the most immobile metal of the contaminants studied. This is confirmed by the data, which shows a rapid decline in concentration at close distances away from the source. Although nickel is more mobile than uranium and the nickel plume covers a much larger area than the uranium plume, only those wells close to the source have concentrations greater than the PRG of 730 ug/L for nickel. It is important to note that there is no significant concentration predicted for any of the metals in the GA during the timeframe of the modeling.

A comparison of the retardation factors for the metal contaminants provides valuable information regarding their mobility at D-Area. Retardation for an equilibrium, linear model would usually be constant; however, for the metal transport conducted in this study, the distribution coefficients were considered variable with pH. Therefore, retardation is also a function of pH. The data and transport modeling results show that pH is depressed on the flowpath from the DCPRB to an area west of 488-D DAB and 488-4D ash basin. Sorption near these source areas can be considered insignificant for beryllium and nickel with only advection and dispersion processes significantly affecting the transport of these contaminants from the DCPRB to the wetlands. However, when these contaminants reach the wetland, retardation starts to differentiate the travel times between the metal types. Beryllium transport has a retardation factor of approximately 9 in the wetland, while nickel has a retardation factor close to 828. Thus, beryllium is significantly more mobile than nickel in the wetland.

In the case of uranium, sorption is significant near the source with a retardation factor greater than 6; therefore, the uranium plume does not move a significant distance away from the DCPRB during the timeframe of the modeling, which is consistent with the 2001 concentration data. If any significant amount of uranium were transported to the wetland, its mobility would be severely limited with a retardation factor in the wetland for uranium around 2500. As discussed further in the sensitivity and uncertainty sections that follow, the transport of the metals is very sensitive to changes in pH.

5.5 Sensitivity Analysis

The purpose of the sensitivity analysis on the local flow and transport model was to quantitatively evaluate the effect of uncertainty in model inputs on the calibration and results of the model. As discussed above, results of this sensitivity analysis should only be used to make general assumptions regarding the uncertainty in the model results, because all of the model inputs have some degree of uncertainty and some parameters may be correlated to one another. The cumulative effect of these uncertainties and correlations cannot be estimated by a sensitivity analysis that varies one parameter value at a time.

5.5.1 Methodology

The sensitivity analysis on the local flow and transport model was conducted in the same manner as the regional flow model as described in Section 3.5. Calibration statistics and other flow and transport model outputs were evaluated. Particle track runs were performed for most of the flow model test cases to determine the sensitivity of parameter values to flow direction and travel times. Particles were started at the bottom of layer 1 at the DHWRF and DHWF, in the middle of layer 2 at the DCPRB, and in the middle of layer 3 at the northern tip of the DCPRB. Figure 5-68 shows the particle track starting locations.

5.5.2 Parameters

Parameter values varied in this analysis included the following:

- K_h or K_v for specific material types
- Recharge rates
- Porosity (only particle tracking (MODPATH) results are evaluated)
- Dispersivity (only transport (MT3DMS) results are evaluated)
- Sorption (only metal transport (MT3DMS) results are evaluated)

As the list indicates, the parameters varied in this sensitivity analysis are similar to those varied previously; however, based on "insensitive" results in the regional model sensitivity analysis, LC K_v, SR Alluvium K_v, GA K_v, river/drain conductance, and Upper Ash Basin/DCPRB recharge were not varied in the local model sensitivity analysis. Table 5-10 presents the ranges for the parameter values.

Table 5-10 Parameter Values Used in the Local Model Sensitivity Analysis

Parameter Value	Calibrated Model Value	Range
LOCAL FLOW MODEL		
K_h for UTRA	18 ft/d	.1, .5, 2, 10 (factors)
K_v for UTRA	1 ft/d	.001, .01, .1, 2, 10 (factors)
K_h for UTRA Zone 2	10 ft/d	.1, .5, 2, 10 (factors)
K_v for UTRA Zone 2	0.5 ft/d	.001, .01, .1, 10 (factors)
K_v for the GCU (all GCU zones varied by the same factor)	.0001-.005 ft/d	.01, .1, 5, 10, 100 (factors)
K_h for "SR Alluvium"	70 ft/d	.1, .5., .71, 1.3, 2 (factors)
K_h for the GA	20 ft/d	.1, .5, 2, 10 (factors)
Porosity (homogeneous throughout model domain)	.3*	.1, :2, .4, .5
Recharge for the lower ash basins recharge zone	22 in/yr	.5, 1.5, 2 (factors)
Recharge for lowland	8	.5, 1.5, 2 (factors)
LOCAL TRANSPORT MODEL		
Dispersivity (tritium and TCE only)	5	.2, 10 (factors)
pH sorption	$S=396[C]^{.38}$	0 L/kg (no sorption), 400 L/kg (pH 6)
Uranium Kd	see equation 5-7 (between 1 and 530)	0 L/kg, 40 L/kg^, +
Beryllium Kd	see equation 5-5 (between 3E-05 and 1)	0 L/kg, 790 L/kg^, +
Nickel Kd	see equation 5-6 (between .001 and 155)	0 L/kg, 65 L/kg^, +

*Porosity is not a flow model parameter, therefore, the "calibrated model" represents the best estimate of the parameter value.

^Vadose Zone Contaminant Migration Multi-Layered Model (VZCOMML) default values (Rucker 1999) (from US EPA's Soil Screening Guidance (USEPA 1996) for Be and Ni and from W. Johnson (1995) for U).

+The final simulation involves use of the results of the pH transport simulation at 20 years, which shows a conservatively lower pH in the wetland.

5.5.3 Results

Flow Model Sensitivity Results

Table 5-11 contains the complete results of the local flow model sensitivity analysis. Figures 5-62 through 5-64 illustrate the results for selected parameters. Model results and parameter values used in the sensitivity analysis were normalized to the calibrated model results and parameter values in the figures, to assist with evaluating the relative change in model output with respect to the change in model input. In cases where the model did not converge (100 iterations), the results provide valuable information; however, no final solution was obtained for these test cases. The figures indicate that GCU K_v, GA K_h, SR Alluvium K_h, and lowland recharge are the most sensitive parameter values in the local flow model.

Changes to UTRA K_h led to the highest RMS errors; RMS error more than doubled at the highest (ten) and lowest (one-tenth) multipliers for UTRA K_h. The figures show that RMS errors generally increase at multipliers above and below one for the parameter values varied in this analysis, which further supports local flow model calibration results.

As SR Alluvium K_h and GA K_h were increased, flux to the SR also increased. This increase is expected as these materials are adjacent to the SR and higher hydraulic conductivities are expected to lead to increased flux to the SR.

Flux out of layer 4 (mainly out of the UTRA) increased with increased lowland recharge with higher recharge rates driving more flow into the GA. As expected, a higher flux through the GCU, facilitated by a higher K_v, also resulted in a higher flux out of the UTRA and into the GA. On the other hand, increases to GA K_h led to a net gain to the UTRA through the bottom of layer 4 with an increase in hydraulic head in the GA at D-Area and a decrease in the hydraulic gradient between the aquifers. For this test case most of the gain to layer 4 from the GA takes place near the SR where the hydraulic head is reversed.

Flux to D-Area streams/channel associated with the DRP stream boundary increased with lower GCU K_v and UTRA Zone 2 K_v. A stream reach downgradient from the DRP stream boundary loses close to the wetland area in the calibrated model, resulting in a net loss to the stream or a net gain to the UTRA. Limiting vertical flow through the UTRA, which sources the GA, should result in a higher flux and head in the UTRA, leading to increased discharge to streams/drains. In fact, the heads near the DRP stream boundary were higher than the calibrated model for these test cases. Similarly, increased lowland recharge and UTRA Zone 2 K_h led to a net gain to the D-Area streams/channel, as higher heads resulted from increases to these two parameter values, particularly for higher UTRA K_h values

Flux to Beaver Dam Creek and the powerhouse effluent channel increased with increased lowland recharge, which resulted in higher modeled heads at calibration targets than the calibrated model shows. It is significant to note, however, that the calibrated model has higher than observed heads near these drains and already overestimates the flux to the powerhouse effluent channel and Beaver Dam Creek. Higher lowland recharge resulted in model results that were even further out of calibration and more grossly overestimated flux to surface water at D-Area.

Particle track runs were performed for most of the local flow model test cases to determine the sensitivity of parameter values to flow direction and travel times. Results of the calibrated local flow model particle track runs are presented in Figure 5-65. Each dot along the particle track represents 5 years. The particle track directions are generally not very sensitive to changes in the parameters analyzed. Particles from the DHWRF usually terminate at the SR or more rarely at the D-Area streams/channel associated with the DRP stream boundary. Particles from the DHWF usually travel to the SR and more rarely terminate at the DRP stream boundary. Most of the particles from the DCPRB terminate at the powerhouse effluent channel adjacent to the DCPRB or flow to Beaver Dam Creek. The particle started at the tip of the DCPRB in layer 3 usually discharges to the SR, which is consistent with the regional particle track results. These results suggest that particles lower in the UTRA near the DCPRB are more likely to "escape" the powerhouse effluent channel.

Again, porosity only effects travel time and not travel direction, as it is not a flow model parameter and does not effect volumetric flow rates or heads. Lower porosities resulted in higher average linear velocities and faster travel times, while higher porosities led to lower average linear velocities and longer travel times to discharge areas, as expected.

Higher K_h for the UTRA led to reduced travel times. Increases to K_v generally led to more particles discharging to the SR, with fewer particles "captured" by D-Area streams/channel. Higher SR Alluvium K_h led to reduced travel times or in some cases longer travel distances and times to the SR, while decreased SR Alluvium K_h led to early discharge to D-Area streams/channel for DHWRF and DHWF particles.

As expected, increases to recharge for the lowland recharge zone, increased flow rates and shortened travel time to discharge areas. Changes to recharge rates for the smaller DAB lower recharge zone had a much less noticeable effect on particle track directions and times, as it covers a much smaller area and does not effect heads and groundwater flow to as great an extent.

In summary, the local flow model is very sensitive to GA K_h with over a factor of three increase in flux to the SR and a factor of fourteen decrease in flux out of layer 4 (mainly out of the UTRA) with a factor of ten increase in this parameter value. GCU K_v is also a sensitive parameter value, with increased flux to D-Area streams/channel at lower values and increased flux out of layer 4 (UTRA) and more particles discharging to the SR at higher values. Higher lowland recharge results in greater flux to D-Area streams/channel and the SR. Changes to UTRA K_h result in the greatest increase in RMS error because most of the calibration targets are located in the UTRA at D-Area. Calibration and particle track direction are relatively insensitive to changes in parameter values.

Transport Model Sensitivity Results

As illustrated on Figures 5-66 and 5-67, at a factor of ten times the dispersivity value used in the transport modeling, the peak concentration for tritium was lower and occurred at around the same time as the calibrated model. The higher dispersion coefficient caused additional spreading of the leading edge of the plume and resulted in lower concentrations spread over a larger area. At a dispersivity value of 20 percent of the calibrated model, several wells indicated insignificant variations in the maximum concentration versus time. For TCE, the higher dispersivity value resulted in lower maximum concentrations that occurred earlier for wells at the leading edge of the plume. A well closer to the source, which reached its maximum concentration prior to the beginning of the simulation, had a more rapid decline in concentration on the tail end of the plume. Again, the lower dispersivity value used for TCE modeling had no significant impact on the timing or magnitude of the maximum concentration.

With regard to sorption sensitivity, the metal concentrations and pH are very sensitive to changes in sorption parameters. As the range of sorption parameter values vary several orders of magnitude over the range of pH represented by the data and the modeling, use of a single Kd or distribution coefficient in the sensitivity runs proved insufficient to adequately model the transport of these constituents. Figure 5-68 shows results for the beryllium sensitivity runs.

With a Kd of 400, corresponding to a pH of 6 in the Freundlich isotherm for hydrogen ion sorption, the pH plume was almost completely attenuated. At a Kd of 0 for hydrogen ion, the plume traveled quickly to the Savannah River at concentrations around 50 ppb (pH=4.3).

Because there is limited information available with respect to sorption for metals at a pH of 2 (lowest observed pH at D-Area), an assumption of no sorption would be a conservative approach for modeling the metals at D-Area. Therefore, a sensitivity run was performed with a distribution coefficient of zero (no sorption) for beryllium, nickel, and uranium. Each constituent traveled to the Savannah River within the timeframe of the simulation (2015), as expected. However, only beryllium concentrations were above regulatory limits (greater than 4 ppb) prior to discharging in the Savannah River. Although nickel concentrations were still increasing, the concentrations were well below the PRG. Using the same recharge concentrations (mass flux) as the calibrated model, the metal concentrations near the source were higher for all of the metals. This is due to the fact that sorption was not simulated; therefore, all of the mass was associated with the aqueous phase leading to increased concentrations. Concentrations deeper in the aquifer, however, were lower than observed concentrations. Based on these results, it is clear that the "no sorption" scenario is insufficient to adequately model the transport of these constituents in the UTRA.

Default Kds for U, Be, and Ni found in VZCOMML, a screening code used in leachability assessments (Rucker 1999), were also simulated in the sensitivity analysis. There was minimal transport for the metals and reduced aqueous concentrations near the source. The source term would have to be adjusted to better match the field data. Reduced concentrations near the source are due to the fact that the default Kds are for neutral pH or higher (around a pH of 6.8 for Be and Ni), allowing increased sorption and lower aqueous phase concentrations than are actually occurring in the aquifer. Again, a single, default Kd approach is insufficient to model these constituents in the UTRA.

Finally, sorption runs that use realistically conservative pH transport results, that neglect the additional buffering capacity of wetland soils, to calculate the sorption parameters, reveal that the beryllium and nickel plumes reach the SR by 2015. However, only beryllium reaches the SR above the MCL (4 ppb) (see Figure 5-68) at concentrations of about 10 ppb, while nickel is well below the PRG. Uranium transport is virtually unaffected, as the uranium plume does not travel to the wetland within the timeframe of the model simulation where the sorption coefficients differ between the calibrated model and the realistically conservative pH metal transport simulation. This scenario uses the spatially varying Kd approach and is adequate to model the transport of metals at D-Area; however, this scenario is more conservative and may over-predict the concentrations discharging to the SR and predict early discharge of metal contamination to the SR.

Table 5-11 Local Model Sensitivity Analysis Results

Parameter	Material/Zone/Arc Groups	Calibrated Value	Test Value	File Name	Iterations Required for Convergence	RMS Error	MAE Error	ME Error	Flux to SR	Flux to Beaver Creek	Flux to D-Area Drainage	Net Flux Out of Bottom of Layer 4 (cfd) (negative implies downward flux)	HWRF Particle Track Time and Direction	HWF Particle Track Time and Direction	DCPRB Particle Track Time and Direction
CALIBRATED RESULTS					**14**	**2.97**	**2.51**	**0.78**	**72484**	**37904**	**-1849**	**-14885**	**40 to SR**	**105-120 SR**	**35 to SR 10-20 BDC**
UTRA K_h	UTRA	18	**1.8**	run001	35	6.28	5.16	4.72	66521	27428	1934	-26677	5-15 to Drain	30 to Drain 65-95 to SR	<5-30 to Drain 90 to SR
ft/d			**9**	run002	20	3.79	3.23	2.03	69323	36286	-658	-18497	10 to Drain 60 to SR	70-95 to SR	10-20 to Drain 55 to SR
			36	run003	25	3.01	2.51	-0.66	77722	35900	-2183	-11588	30-35 to SR	50 to SR	20-40 to Drain 25-45 to SR
			180	run004	100/nc	6.83	5.79	-4.73	100100	28620	-4159	1844	15 to Drain 20 to SR	25 to Drain 30 to SR	15 to Drain 15-20 to SR
UTRA K_v	UTRA	1	**0.001**	run005	100/nc	4.75	3.81	2.56	72660	31371	457	-17627	20 to Drain 40 to SR	75-190 to SR	<5-30 to Drain 35 to SR
ft/d			**0.01**	run006	100/nc	3.69	3.15	1.76	73077	31933	-408	-17646	20 to Drain 40 to SR	75-125 to SR	10-20 to Drain 35 to SR
			0.1	run007	16	3.15	2.69	1.19	72938	35109	-1235	-16115	40 to SR	115 to SR	10-20 to Drain 35 to SR
			2	run008a	17	2.95	2.48	0.73	72403	38397	-1970	-14677	40 to SR	115 to SR	5-20 to Drain 35 to SR
			10	run008	17	2.92	2.45	0.66	72300	38973	-2106	-14435	45 to SR	110-115 SR	15-20 to Drain 35 to SR
UTRA Zone 2	UTRA	10	**1**	run009	14	2.85	2.35	0.38	70497	30789	-6542	-20010	70-75 to SR	75-85 to SR	15-50 to Drain 35-70 to SR
K_h	Zone 2		**5**	run010	18	2.78	2.3	0.44	71396	34747	-4135	-16200	55-80 to SR	75-115 to SR	10-25 to Drain 45 to SR
ft/d			**20**	run011	51	3.31	2.84	1.24	73858	42385	3827	-14538	10 to Drain 35 to SR	45-55 to SR	10-15 to Drain 35 to SR
			100	run012	21	4.73	4.02	3.1	78952	57419	63565	-20737	5 to Drain	10 to Drain	5-10 to Drain 35 to SR
UTRA Zone 2	UTRA	0.5	**0.0005**	run013	18	3.87	2.98	1.59	71642	38707	14385	16054	5 to Drain 40 to SR	65-185 to SR	10-20 to Drain 35 to SR
K_v	Zone 2		**0.005**	run014	14	2.95	2.44	1.27	72286	38424	5230	123	35-40 to SR	60-185 to SR	10-20 to Drain 35 to SR
ft/d			**0.05**	run015	14	2.9	2.43	0.87	72463	37969	-907	-12592	40 to SR	70-110 to SR	10-20 to Drain 35 to SR
			5	run016	14	2.98	2.52	0.76	72472	37900	-1836	-15066	40 to SR	100-115 to SR	10-20 to Drain 35 to SR
GCU K_v	"tight" GCU	0.0001	**1E-06 5E-05**	run022	19	3.82	3.12	1.77	71627	46467	11865	24582	<5 to Drain 40 to SR	50-55 to SR	<5-15 to Drain 35 to SR
ft/d	GCU	0.005	**1E-05 5E-04**	run023	33	3.29	2.73	1.4	72406	41523	8149	11802	<5 to Drain 40 to SR	55-65 to SR	10-15 to Drain 35 to SR
			.0005 .025	run024a	15	3.22	2.64	0.24	72008	38255	-4673	-32354	-	-	-
			1E-03 5E-02	run024	15	3.26	2.65	0.2	71947	38416	-4745	-41504	-	-	-
			1E-02 5E-01	run025	18	3.41	2.74	-0.08	72778	38653	-4430	-97579	50-120 to SR	65-70 to SR	10-30 to Drain 40 to SR

Table 5-11 Local Model Sensitivity Analysis Results (con't)

Parameter	Material/Zone/Arc Groups	Calibrated Value	Test Value	File Name	Iterations Required for Convergence	RMS Error	MAE Error	ME Error	Flux to SR	Flux to Beaver Creek	Flux to D-Area Drainage	Net Flux Out of Bottom of Layer 4 (cfd) (negative implies downward flux)	HWRF Particle Track Time and Direction	HWF Particle Track Time and Direction	DCPRB Particle Track Time and Direction
CALIBRATED RESULTS					**14**	**2.97**	**2.51**	**0.78**	**72484**	**37904**	**-1849**	**-14885**	**40 to SR**	**105-120 SR**	**35 to SR 10-20 BDC**
Alluvium K_h	SR Alluvium	70	**7**	run026	34	4.03	3.42	2.1	34159	61024	16678	-16004	20-35 to Drain	120 to Drain 130-150 to SR	10-20 to Drain 35 to SR
ft/d			**35**	run027	100/nc	3.24	2.75	1.11	54596	47382	10452	-14717	-	-	-
			50	run027a	14	3.08	2.6	0.99	62669	42926	3977	-14747	45 to SR	75-120 to SR	10-20 to Drain 35 to SR
			90	run028a	18	2.9	2.44	0.63	81652	33521	-7510	-15030	-	-	-
			140	run028	18	2.83	2.33	0.37	102490	23884	-20683	-15495	40 to SR	40-115 to SR	10-20 to Drain 30 to SR
Gordon Aquifer K_h	Gordon Aquifer	20	**2**	run032	17	3.78	3.06	2.29	50050	43834	3683	-19193	5 to Drain 40 to SR	55-60 to SR	10-15 to Drain 35 to SR
ft/d			**10**	run033	14	3.1	2.61	1.38	60231	40565	-680	-22425	-	-	-
			40	run034	17	2.98	2.46	0.3	95326	35578	-900	8247	-	-	-
			200	run035	13	3.38	2.71	-0.07	238450	44895	13555	203239	30-40 to Drain	45-50 to SR	15-45 to Drain
Porosity	All layers	0.3	**0.1**	run046	NA	NA	NA	NA	NA	NA	NA	NA	15 to SR	35-40 to SR	<5-10 to Drain 15 to SR
dimensionless			**0.2**	run047	NA	NA	NA	NA	NA	NA	NA	NA	30 to SR	70-85 to SR	5-15 to Drain 25 to SR
			0.4	run048	NA	NA	NA	NA	NA	NA	NA	NA	55 to SR	140-160 to SR	10-25 to Drain 40 to SR
			0.5	run049	NA	NA	NA	NA	NA	NA	NA	NA	70 to SR	175-190 to SR	15-30 to Drain 60 to SR
Recharge	DAB (lower)	22	**11**	run053	14	2.81	2.35	0.46	71917	33878	-2841	-14090	40-45 to SR	70-130 to SR	10-50 to Drain 40 to SR
in/yr			**33**	run054	100/nc	3.18	2.68	1.1	73023	42112	-875	-15651	-	-	-
			44	run055	15	3.42	2.88	1.45	73585	46265	111	-16414	40-45 to SR	100-110 to SR	10-15 to Drain 35 to SR
Recharge	Lowland	8	**4**	run056	13	3.32	2.6	-0.77	69705	17171	-8290	885	45-50 to SR	70-75 to SR	15-75 to Drain 40 to SR
in/yr			**12**	run057	13	3.41	2.86	1.94	74823	58241	7638	-28232	5 to Drain 40 to SR	70-95 to SR	10-15 to Drain 35 to SR
			16	run058	16	4.25	3.52	3.22	77148	78553	17525	-41278	5 to Drain 40 to SR	55-85 to SR	5-15 to Drain 35 to SR

Note: The generic term "drain" is used for any interior drainage area in the model. HWRF and HWF particles usually drained to the DRP stream boundary, while DCPRB particles usually drained to the D-Area powerhouse outfall adjacent to the DCPRB that flows into Beaver Dam Creek.

6.0 LIMITATIONS AND UNCERTAINTY

Uncertainty is inherent in any modeling process, and the uncertainties associated with this modeling task have been managed by using conservative assumptions, obtaining a good calibration, and analyzing a wide range of possible parameter values in the sensitivity analysis. As new hydrogeological data become available, the HCM can be updated and new modeling performed, which will reduce the uncertainty of model predictions.

The following is a summary of the reliability of the flow model calibration and the limitations of model predictions that arise from uncertainties in the modeling approach and data used for this modeling task. These limitations require consideration if the model is to be used in the remedial decision process.

Flow Model Uncertainty

The use of simplistic boundary conditions, homogeneous hydraulic parameter zones, and a simplistic hydrostratigraphic representation of the subsurface aquifer/aquitard zones introduces uncertainty into the flow model results. This representation of reality is a gross simplification of real world conditions. The uncertainties that arise from using this approach have been managed by choosing conservative values for model parameters, performing sensitivity analyses, and by analyzing a wide range of hydrogeologic parameter information.

Uncertainty in the flow model also results from the calibration targets. Although the wells used as targets are distributed across the area of interest, there are a limited number of GA wells and there are no wells outside the TNX and D-Areas. Most of the wells have been installed recently and have limited time-series data. The uncertainty has been reduced by the application of the calibration head adjustment scheme. The flow model calibration to the selected calibration targets is reasonable for the area of interest near the waste units. The use of flux calibration targets to Fourmile Branch and Upper Three Runs increases the confidence in the calibration of the model.

TCE and Tritium Transport Model Uncertainty

Although a significant amount of characterization data has been obtained, when compared to the model domain and potential flow history, the tritium and TCE plumes associated with D-Area have incomplete configuration and concentration estimations through time. Most of the plume configuration information is based on single point-in-time CPT data or long-term data in areas outside of the "hot spot" areas of the plume. The complexity of modeling multiple sources with unknown locations and release histories further complicated estimates of the current plume configurations. .However, the use of CPT data to re-create present day plumes is expected to be a conservative approach leading to higher transport modeling results. The conservatism inherent in this approach is supported by the data with maximum observed concentrations in groundwater monitoring wells much lower than the CPT data indicate.

Metal Transport Model Uncertainty

There are several buffering reactions that were generically represented in the pH modeling with a Freundlich isotherm. These reactions include surface complexation reactions with HFO, gibbsite, and kaolinite; dissolution reactions; and to a lesser extent, carbonate buffering. The isotherm was used to describe these reactions for simplicity, but the surface complexation reactions occurring are much more complicated. Furthermore, the data used in the sorption modeling were based on titration experiments that were conducted for upland soils and are not necessarily representative of wetland conditions. The buffering capacity for wetland soils is expected to be significantly higher with anaerobic conditions generally leading to increased pH. Therefore, the pH distribution that was used to calculate sorption coefficients for the metals assumed that the wetland pH was closer to the background pH. This assumption is consistent with the data and our knowledge about the contaminant distributions. The pH in the lower UTRA is uncertain; however, the background pH of 5 used in the modeling is considered conservative as many upland and wetland locations have pH in excess of 6.

While wetland wells located in the upper UTRA near the source areas indicate more neutral pH close to the expected path of the plume west of the ash basins, the western extent of the pH plume and vertical profile are not well-defined. The direction and western extent of the pH plume emanating from the source near the DRP is also not well-defined. Similarly, the transport modeling indicates significant transport of low pH groundwater to Beaver Dam Creek with little groundwater data in this area for comparison. Additional data collection in these areas, would assist with reducing these uncertainties

As discussed in the sensitivity analysis, metal sorption is extremely sensitive to pH in the wetlands as sorption dramatically increases between a pH of 4-5. While there is significant uncertainty with respect to the pH distribution in the wetland, realistically conservative metal transport simulations with lower pH in the wetland reveal that the levels of contamination that may discharge to the SR are below regulatory limits for uranium and nickel, as discussed in the sensitivity analysis. Only beryllium discharges to the Savannah River at a concentration of around 10 ppb, which is above the MCL of 4 ppb.

The modeling assumes that the buffering capacity of the aquifer at D-Area is sufficient to attenuate the pH plume through the timeframe of the simulation. In fact, the buffering capacity of the aquifer may be depleted along the flowpath of the plume, especially if the pH plume follows a narrow pathway to the Savannah River, as the conservative pH modeling runs indicate.

MINTEQA2 modeling performed by SRTC for Ni and Be only considered reactions with HFO for simplification of the surface complexation modeling effort. Other surface complexation reactions with kaolinite and gibbsite were not modeled. The equilibrium constants used in the modeling were obtained from the literature and have not been verified with field data for Be at D-Area. In the case of nickel, the surface complexation modeling were overly conservative and the in-situ Kds that were calculated from field data for nickel appear to be more representative of conditions at D-Area. The HFO binding site concentrations estimated using US EPA 3050B extraction are also subject to some uncertainty. The method used is expected to be conservative, in that a more aggressive approach such as total digestion could have been used to estimate the sites available for sorption.

Several assumption were made to fit the four parameter logistic function to data provided by SRTC. In some cases, a maximum and minimum Kd had to be chosen, because the data did not cover the range of pH and/or extreme values of Kds would compromise the results of the fit. Since the pH range used in the modeling was from 2 to 5, more weight was placed on this range in the curve by adjusting the figure of merit, i.e. non-weighted, or weighted least squares, or normalized error, by which the "goodness of fit" was measured in the curve fitting routine. In the case of Be and Ni, the pH range from 4 to 6 was extremely sensitive, because the sorption curve sharply increased with increasing pH. Therefore, care was taken to fit this portion of the curve to facilitate model calibration. Overly conservative fits to the data would have essentially eliminated any sorption from occurring in the transport modeling, which is inconsistent with the data. The sensitivity analysis emphasizes the importance of using site-specific and variable sorption parameters for the metal transport modeling. Without this approach, the field data could not be reproduced in a technically defensible manner.

There are many uncertainties associated with the metals source term, including the D-Area conceptual model. The data suggest that the D-Area ash basins are not contributing to low pH and metal contamination, as the bottom of the ash basins contain neutral pH groundwater. Therefore, the ash basin sources were assumed to be on the western boundary of the ash basins where low pH and metals contamination have been observed. The extent to which the D-Area coal pile contributes to low pH/metal contamination is uncertain; however, the pH/metals data suggested that the highest concentrations occurred at the northern tip of the DCPRB adjacent to the coal pile; therefore, a separate source area was created in this area and for the DCPRB footprint. The actual vadose zone source for the low pH/metals concentrations observed at DCB 31 near the DRP is unknown but was assumed to be related to waste coal rejects deposited at DRP. Therefore, a source area near the DRP was created close to this high concentration area.

The actual size, timing, and concentrations for all five source areas were simplified with one constant source term over a relatively large area with simulations beginning in 1980 when the DCPRB began operation. The actual source loading is much more complicated due to the chemical conditions, as well as operational/source variations over time. Although transient source loading scenarios were attempted, the complexity of modeling sorption parameters, source areas, and time-varying source concentrations made calibration difficult. Eventually, the source term was simplified to a constant source to facilitate calibration of the model. Furthermore, the initial source term assumed in the metal transport modeling was calculated using a simple mass balance calculation. This calculation was expected to be a rough estimate, but facilitated calibration and reduced some of the uncertainty in the source term.

Conclusion

Despite all of the uncertainties associated with the flow and transport modeling, the 2001 initialized plumes for TCE and tritium appeared to agree well with the 2001 data and were generally consistent with the HCM and expected flow conditions at the site. Uncertainty in the tritium and TCE modeling was managed through use of conservative assumptions including use of CPT data that are expected to overestimate the amount of mass in the aquifer and lead to higher model-predicted concentrations.

With regard to the metal transport modeling, the 2001 model simulated plumes based on the source terms in Table 5-6 and sorption parameters calculated using Equations 5-5 through 5-7 were in good agreement with the 2001 field data. The ability of the model to accurately reproduce current conditions, provides additional support for the metal transport results.

Finally, due to limitations and assumptions of the model (some of which are more fully discussed in other sections of this report), the results of this modeling should be considered as only representative of the large-scale (i.e. the scale of D-Area) groundwater flow system near the D-Area and should not be used to predict small-scale predictions of flow (or transport). Because of the conservative assumptions, however, the model can be used to predict general flow and transport directions and travel times, and can be used as a basis for future evaluation of remedial alternatives.

7.0 SUMMARY AND CONCLUSIONS

This modeling effort successfully developed a groundwater model that reproduces the groundwater flow system at D-Area. The regional flow and local D-Area flow models achieved excellent calibration to known head and flux measurements. The flow directions from the major source areas are adequately represented in the model.

The currently defined TCE and tritium plumes were simulated for 100-years with no current sources contributing to groundwater contamination. The peak fluxes to the SR are expected in 20 to 30 years, at concentrations/activities above the MCL. The model shows the highest concentrations/activities discharging to the DRP stream boundary with TCE concentrations less than 50 ug/L between 15 to 35 years, and tritium activities less than 250 pCi/mL in 10 to 15 years.

Three metal contaminants (beryllium, nickel, and uranium) were simulated for 15-years (end of powerhouse operation). Transport of each metal was simulated with pH dependent sorption relationships and continuing sources. A qualitative calibration of the metal sources was achieved through a mass balance calculation and comparison of model predictions to recreate the current plumes. Metal transport is significantly attenuated by natural processes in the wetland that reduce the concentrations discharging to the SR to acceptable levels. There is some uncertainty with respect to the vertical profile and western extent of the pH plume and its effect on metal attenuation in the wetland. Additional investigation of natural attenuation processes occurring in the wetland are ongoing and should reduce this uncertainty for future modeling (WSRC 2002a). Metal discharges to the powerhouse effluent channel are above MCLs/PRGs near the source area but are significantly diluted by process water discharging from the powerhouse.

Sensitivity analyses on the flow models indicated that the model is most sensitive to changes in general recharge, aquifer horizontal hydraulic conductivity, and aquitard vertical hydraulic conductivity. A sensitivity analysis on the transport model showed that the model results are relatively insensitive to changes in dispersion.

With regard to sorption sensitivity, the metals and pH transport modeling are very sensitive to changes in sorption parameters. A conservative no sorption (Kd = 0) run, a VZCOMML default value run with a spatially constant Kd, and a "realistically conservative" pH run (no consideration of additional wetland buffering) with spatially varying Kds based on pH were performed. The range of sorption parameter values vary several orders of magnitude over the range of pH represented by the data and the modeling; therefore, use of a single Kd or distribution coefficient in the sensitivity runs proved insufficient to adequately model the transport of these constituents.

The impact of the SR Alluvium is most noticeable in the transport simulations. When the plume reaches this material, the transport velocity increases due to the significantly higher hydraulic properties. There appears to be no increase in plume spreading or dilution in this material; conversely, the rapid transport appears to accelerate the leading edge reaching discharge locations along the Savannah River.

A number of uncertainties have been identified in the modeling effort. However, the excellent calibration of the flow model to known head and flux targets and the ability of the transport model to recreate the current contaminant plumes indicate that the results from this effort can be used as intended.

The objectives of this model effort have been achieved as follows:

- No data gaps with the definition of the nature and extent of the groundwater contamination were identified. The TCE and tritium simulations are consistent with the conceptual model and currently defined metal plumes were successfully recreated from known source areas. However, modeling uncertainty could be reduced with additional data.

- The successful calibration of the flow models indicates that the basic hydrostratigraphy and flow system hydraulics have been adequately characterized. The only area where additional information may prove useful for this scale of investigation is with the thickness of the Gordon Confining Unit immediately north of D-Area.

- The transport modeling provides predictions of future plume nature and extent in the event of no remedial actions. These predictions include calculated fluxes and concentrations to surface water bodies. The models documented in this effort can be used as the framework for future modeling evaluations of remedial alternatives.

The models documented in this effort are intended to be used as the framework for future modeling evaluations of remedial alternatives. The modeling can also assist with development of a groundwater monitoring plan.

8.0 REFERENCES

Aadland, R.K., Gellicic, J.A., and Thayer, P.A., 1995. *Hydrogeologic Framework of West-Central South Carolina*, Report 5, Water Resources Division, South Carolina Department of Natural Resources, Columbia, South Carolina.

Allison, J.D., D.S., Brown, K.J., Gradac, 1991. *MINTEQA2/PRODEFA2, A Geochemical Assessment Model for Environmental Systems: Version 3.0 Users Manual.* Washington, DC, US Government Printing Office, EPA/600/3-91/021

Bills, T.L., K.E. Brewer, A.L. Stieve, and M.S. Rabin, 2000. *Groundwater Flow Modeling for C-Area Groundwater Operable Unit (U).* WSRC-RP-2000-4096, Westinghouse Savannah River Company, Aiken, SC, November 2000

Brigham Young University (BYU), 2000. *The Department of Defense, Groundwater Modeling System (GMS) Version 3.5.* Brigham Young University Environmental Modeling Research Laboratory, September

Dixon, K.L., V.A. Rogers, S.P. Conner, C.L. Cummings, J.B. Gladden, and J.M. Weber. 1997. *Geochemical and Physical Properties of Wetland Soils at the Savannah River Site.* WSRC-TR-96-0115, Westinghouse Savannah River Company, Aiken, SC

Fallaw, W.C. and V. Price, 1995. *Stratigraphy of the Savannah River Site and Vicinity*, Southeastern Geology V35. N1, p. 21-58

Johnson, W.H., 1995. *Sorption Models for U, Cs, and Cd on Upper Atlantic Coastal Plan Soils,* PhD Thesis, Georgia Institute of Technology

Kaplan, D.I., A.S. Knox, J. Myers, 2002. *Mercury Geochemistry in Wetlands and Its Implications for In-Situ Remediation.* Journal of Environmental Engineering. 128:723-732

Kaplan, D.I., and S.M. Serkiz, 2002. *Influence of Surface Charge on Iodide and Pertechnetate Sorption to Soils Dominated by Fe-oxide or Organic Matter.* Radiochim. Acta (in press)

McDonald, M.G. and A.W. Harbaugh, 1988. *A Modular Three Dimensional Finite-Difference Groundwater Flow Model.* Techniques of Water Resources Investigations 06-A1, United States Geological Survey

Pollock, D.W., 1994. *User's Guide for MODPATH/MODPATH-PLOT Version 3: A Particle Tracking Post-Processing Package for MODFLOW, the U.S. Geological Survey Finite Difference Groundwater Flow Model, U.S. Geological Survey.* Open-File Report 94-464, Reston, VA

Powell, K.P., S.M. Serkiz, and D.I. Kaplan, 2001. *Evaluation of the D-Area Expanded Operable Unit for Monitored Natural Attenuation of Inorganic Constituents of Concern: Interim Report.* WSRC-TR-2001-00574, Savannah River Site, Aiken, South Carolina, December 2001.

Powell, K.P., S.M. Serkiz, and D.I. Kaplan, 2002. *Metal Distribution Coefficient for Transport Model Input.* WSRC-TR-2002-00406, Savannah River Site, Aiken, South Carolina, September 2002

Rucker, G., 1999. *Vadose Zone Contaminant Migration Multi-Layered Model,* Westinghouse Savannah River Company, Savannah River Site, Aiken, South Carolina

Rumbaugh, J., 1998. Applied Techniques for Model Calibration and Stochastic Simulation, Course Notebook, Environmental Simulations, Incorporated, Denver, Colorado.

Sloto, R. A., and Crouse M.Y., 1996. *HYSEP: A Computer Program for Streamflow Hydrograph Separation and Analysis,* USGS Water-Resources Investigations Report 96-4040, Lemoyne, PA.

US DOE, 2002, *DCDP Removed from the Investigation and Listed as a Site Evaluation Area,* Letter from Hennessey, B., to Gorman, C.M., and Feely, K.B., Savannah River Site, Aiken, South Carolina, letter dated May 9, 2002

US EPA, 1996, *Soil Screening Guidance: Technical Background Document*, Publication 9355.4-17A, United States Environmental Protection Agency, Office of Emergency and Remedial Response, Washington, DC, May, 1996

Watermark Numerical Computing, 2000. PEST Model-Independent Parameter Estimation, Fourth Edition, 2000.

WSRC, 1994. *Uranium Geochemistry in Soil and Groundwater at the F and H Seepage Basins (U)*, EPD-SGS-94-307

WSRC, 1998. *Conduct of Engineering and Technical Support (U),* Revision 30. SRS Procedure Manual E-7, Savannah River Site, Aiken, South Carolina

WSRC, 2002. *Technical Task Plan D-Area Expanded Operable Unit Groundwater Modeling for RFI/RI/BRA.* K-ESR-D-00002, Savannah River Site, Aiken, South Carolina, February

WSRC, 2002a. *Treatability Study Work Plan for Monitored Natural Attenuation of Inorganic Contaminants (U).* WSRC-RP-2002-4039, Revision 0, June, 2002

WSRC, 2002b. *RCRA Facility Investigation/Remedial Investigation/Baseline Risk Assessment (RFI/RI/BRA) for the D-area Expanded Operable Unit (U)*, Revision 0. WSRC-RP-2001-4162, Savannah River Site, Aiken, South Carolina, December 2002

Zheng, C. and P.P. Wang, 1999c. *MT3DMS, A Modular Three-Dimensional Multispecies Transport Model for Simulation of Advection, Dispersion and Chemical Reactions of Contaminants in Groundwater Systems (MT3DMS) (Release DoD_3.50.B).* Documentation and User's Guide, Department of Geological Sciences, Department of Mathematics, University of Alabama, Tuscaloosa, Alabama, November

Figure 1-1. D-Area Location Map

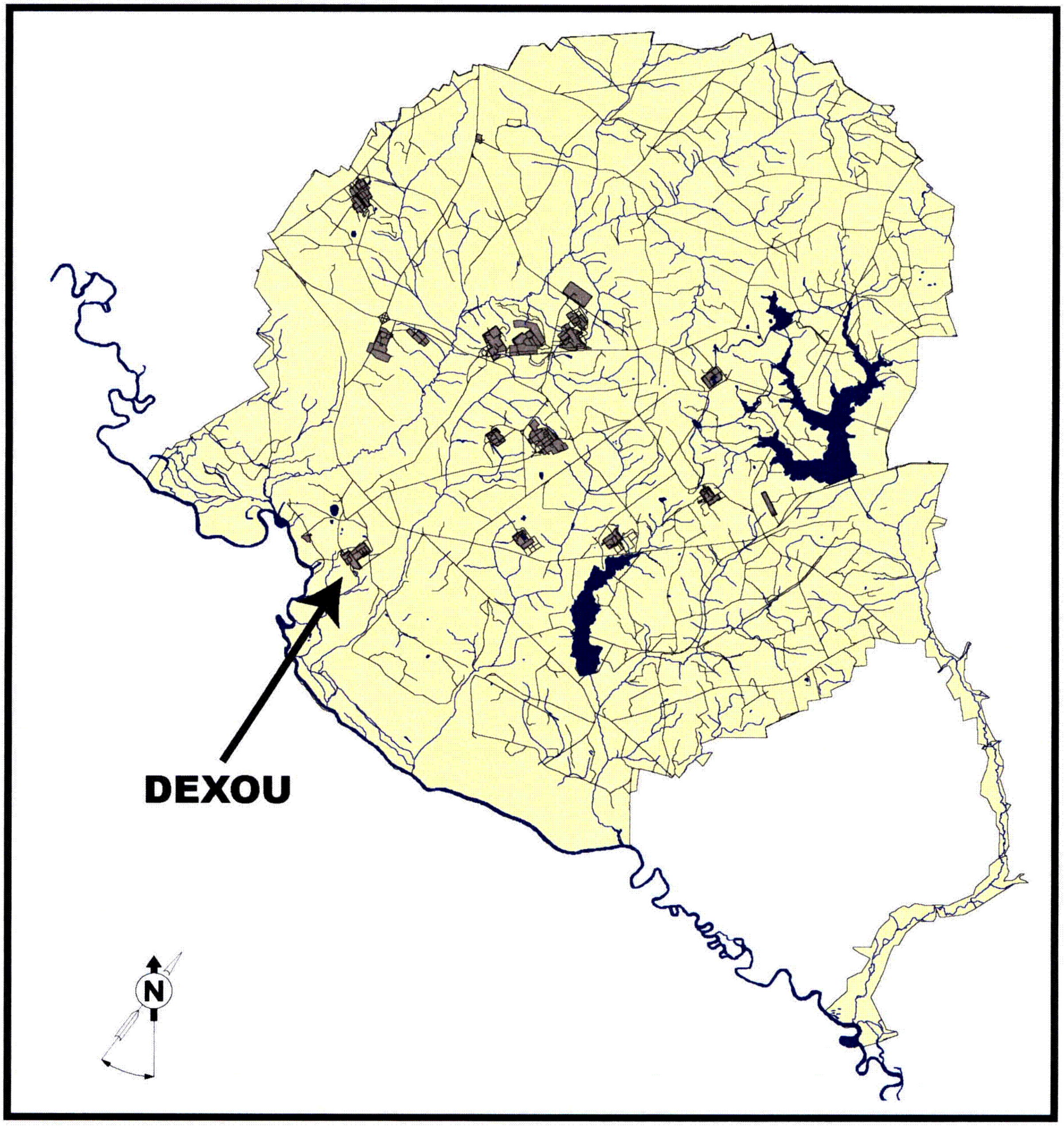

Figure 1-2. D-Area Facilities and Subunits

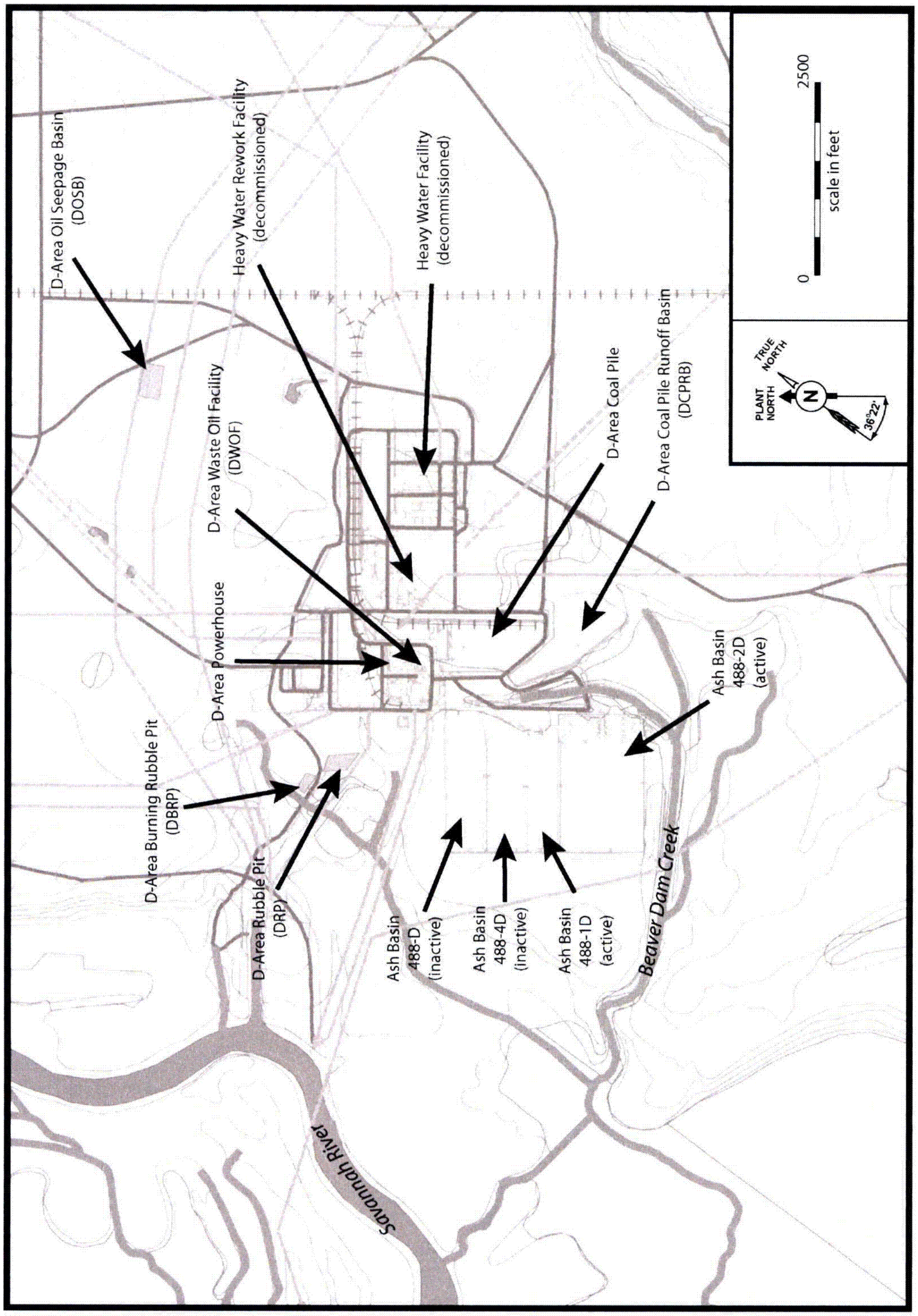

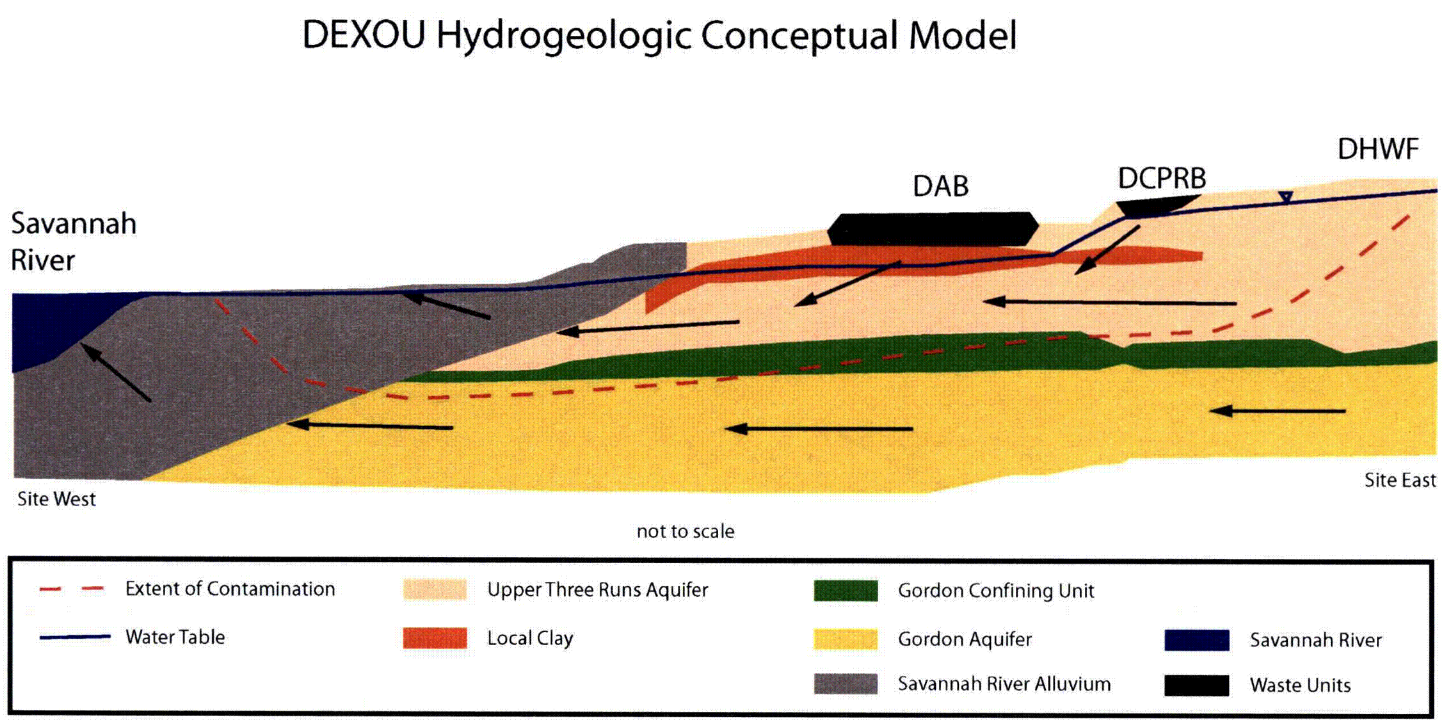

Figure 2-1. Hydrogeological Conceptual Model Cross Section

Figure 2-2. Regional Flow Model Extent

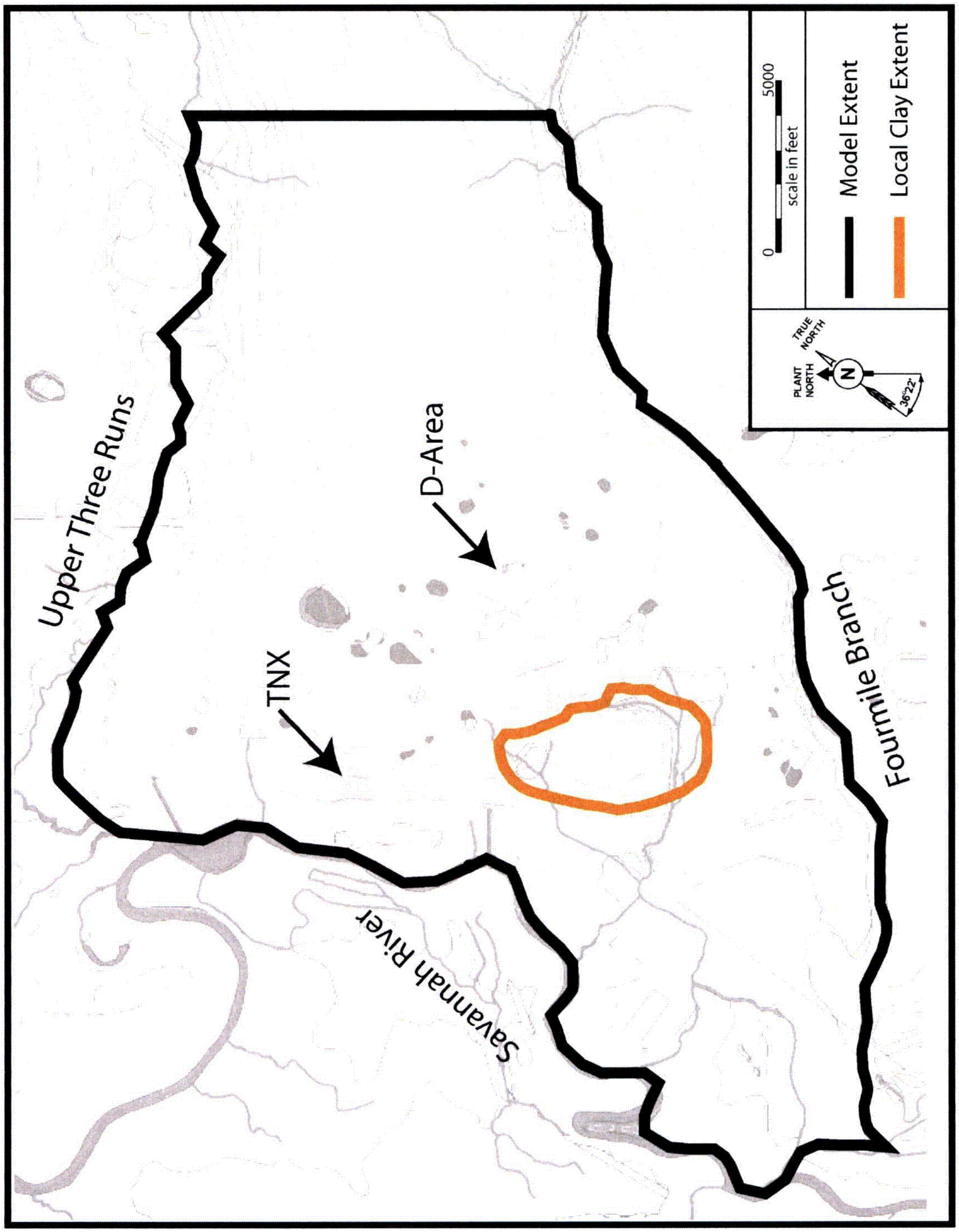

Figure 2-3. Borehole Locations

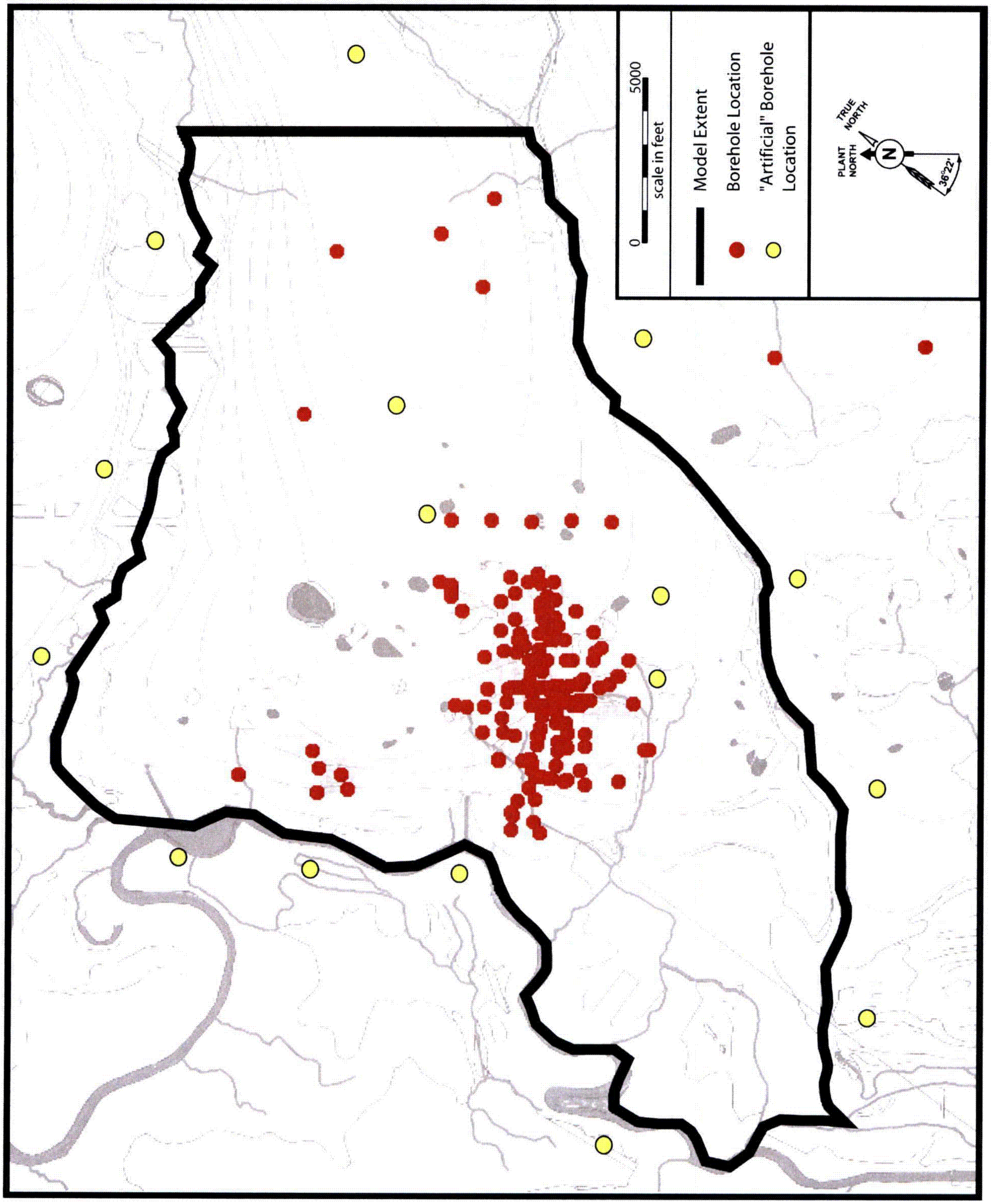

Figure 2-4. Ground Elevation Scatter Points

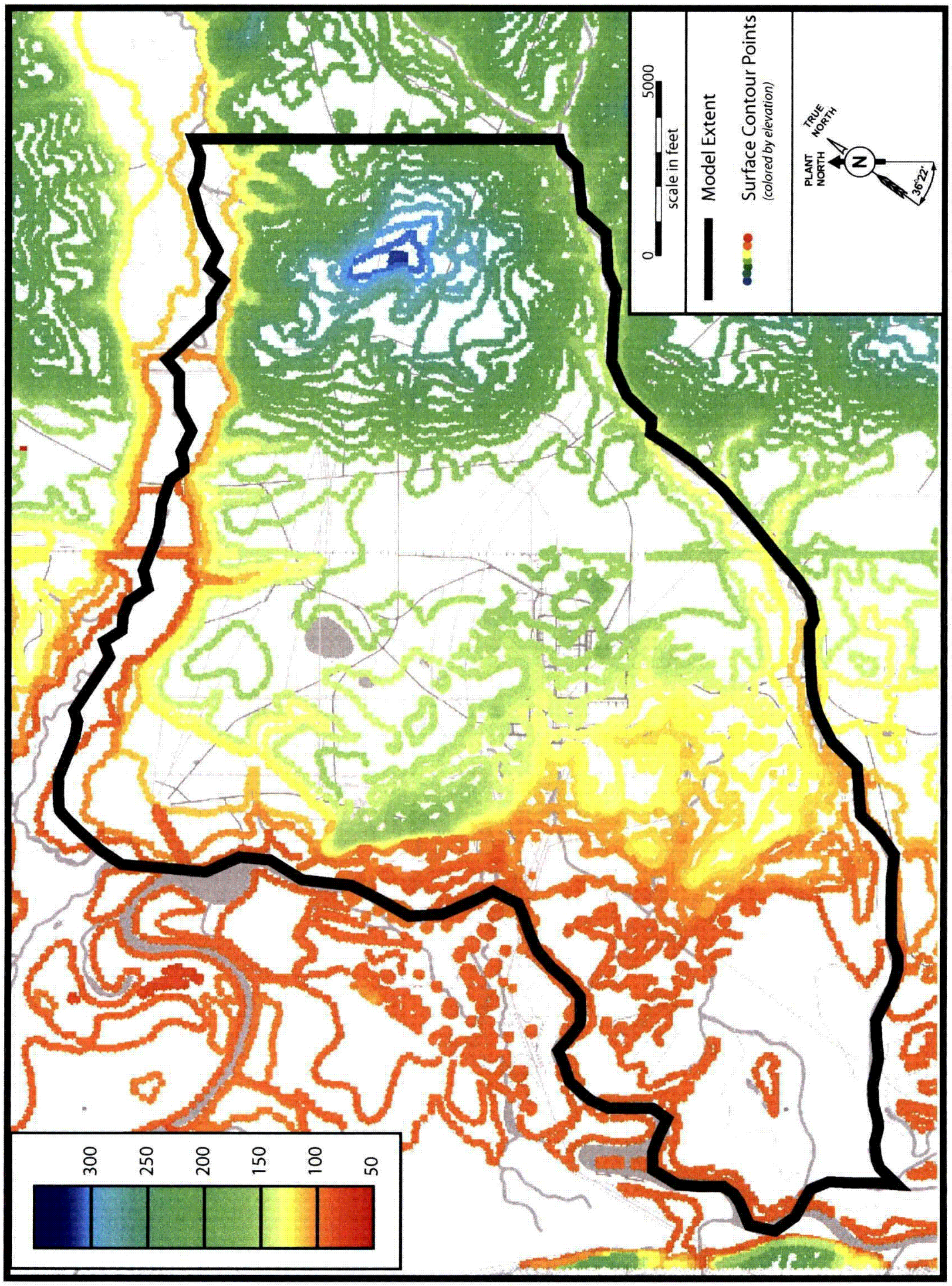

Figure 2-5. Regional Model Hydrostratigraphy Solids Model

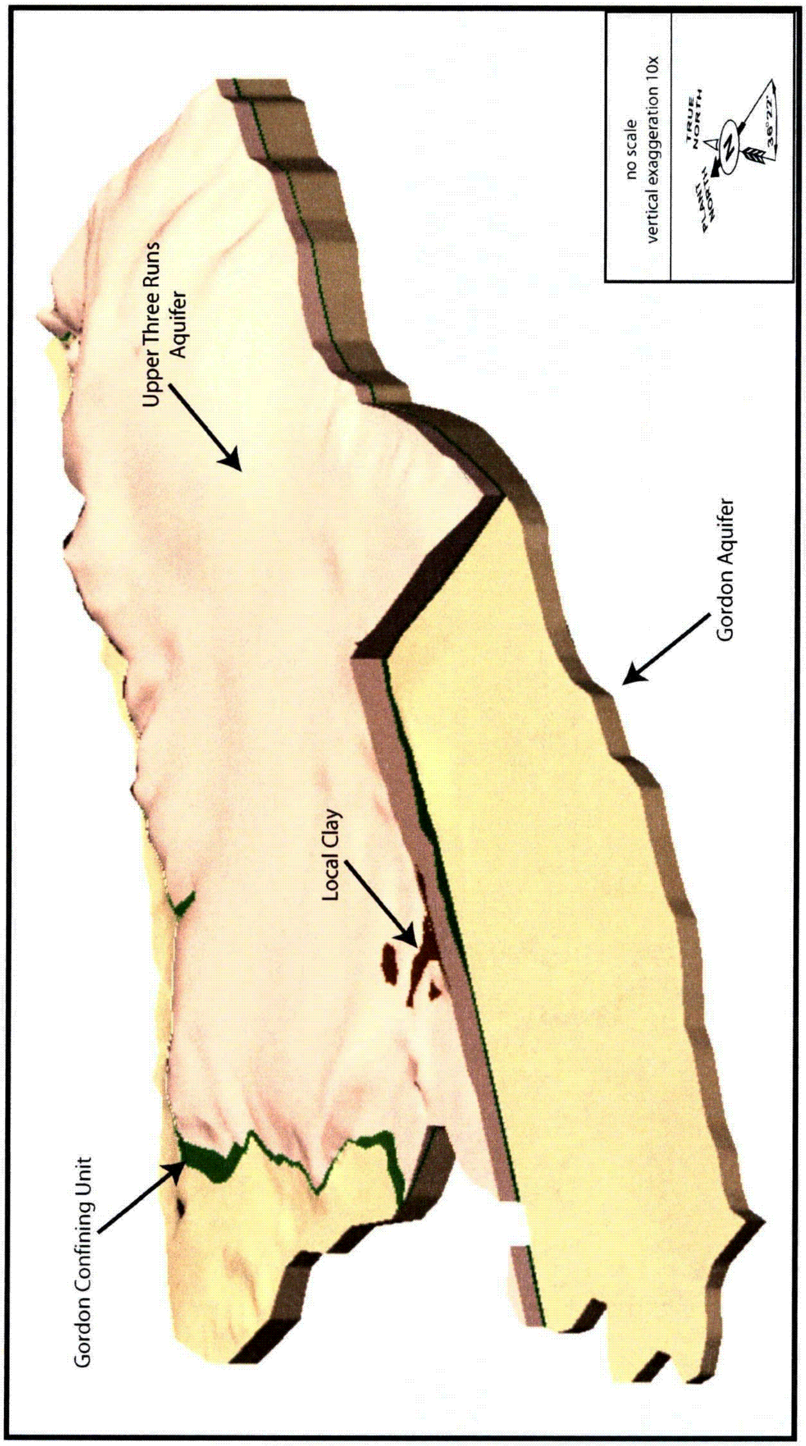

Figure 2-6. Regional Model Layer 1 (UTRA) Thickness and Top Elevation

(a) Layer Thickness (ft)

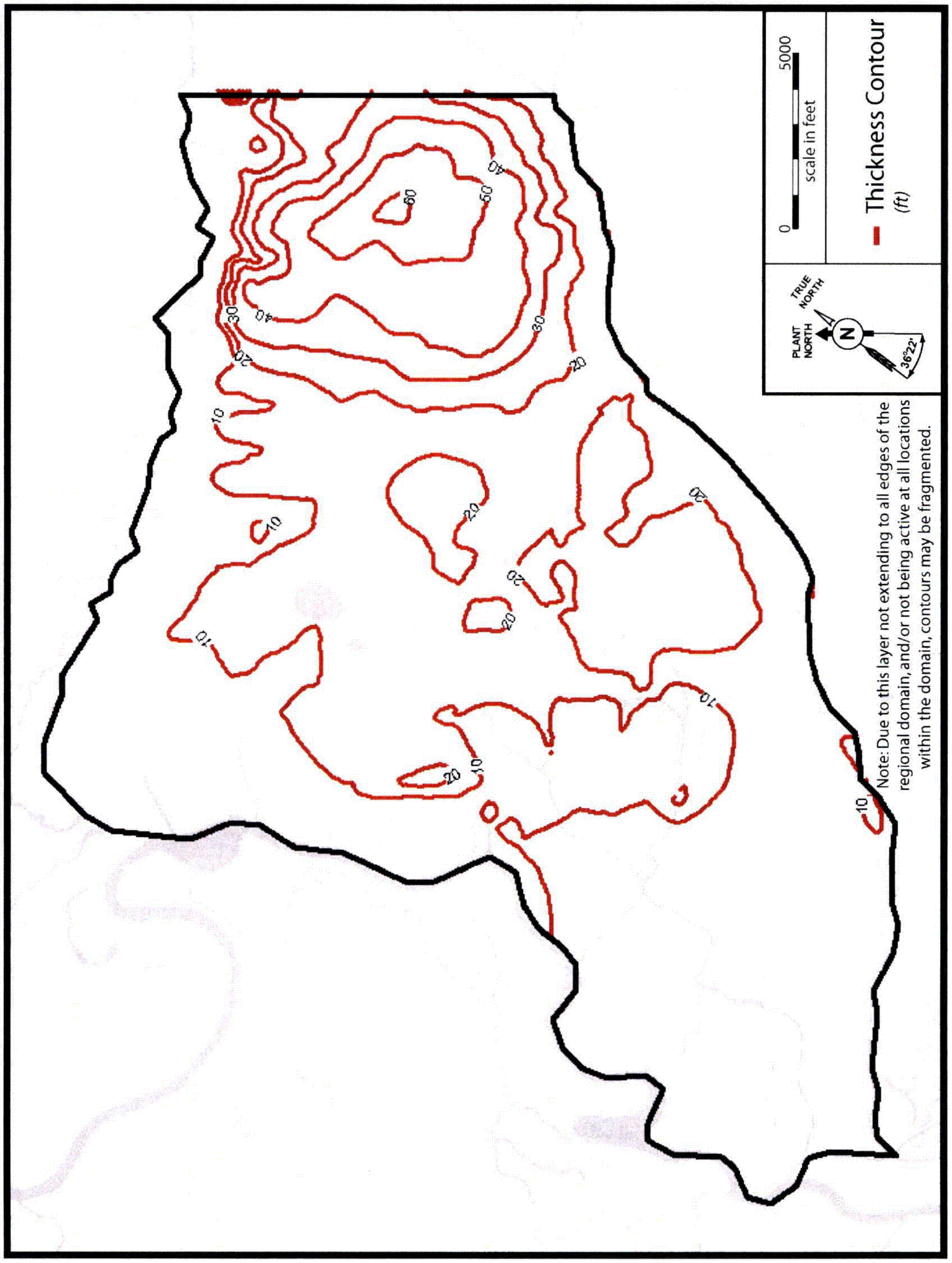

Figure 2-6. (con't) Regional Model Layer 1 (UTRA) Thickness and Top Elevation

(b) Layer Top Elevation (ft amsl)

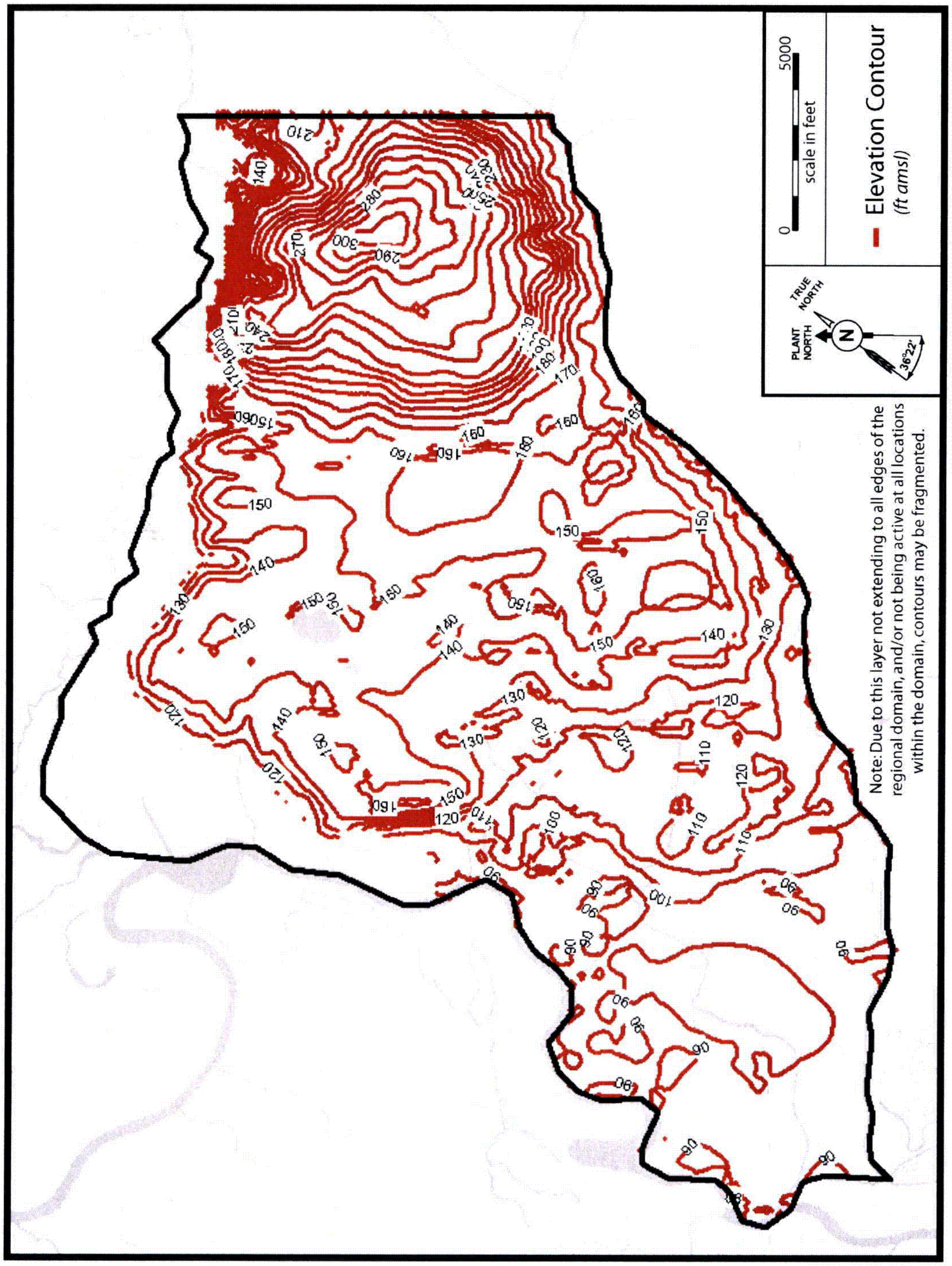

Figure 2-7. Regional Model Layer 2 (UTRA) Thickness and Top Elevation

(a) Layer Thickness (ft)

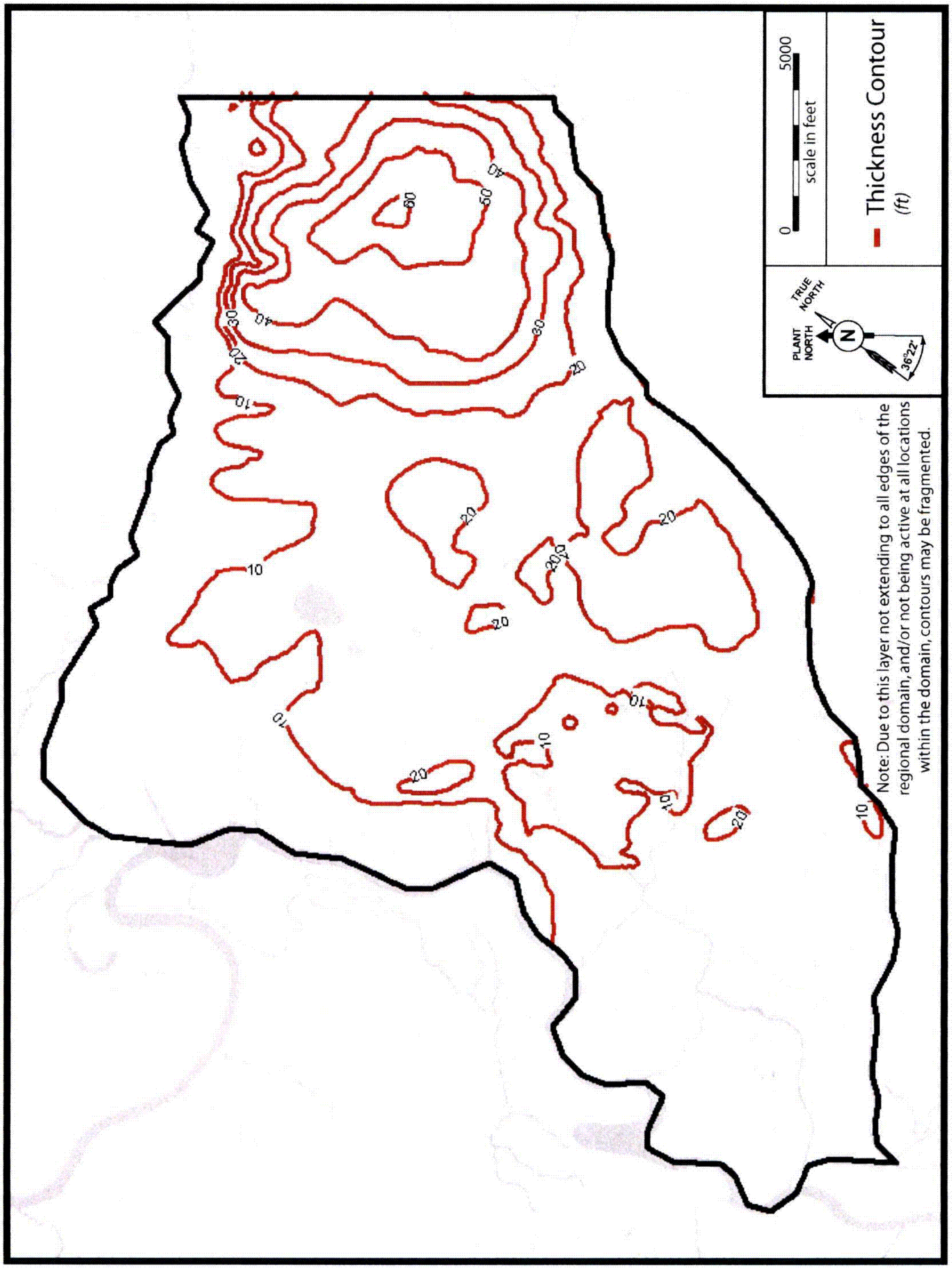

Figure 2-7. (con't) Regional Model Layer 2 (UTRA) Thickness and Top Elevation

(b) Layer Top Elevation (ft amsl)

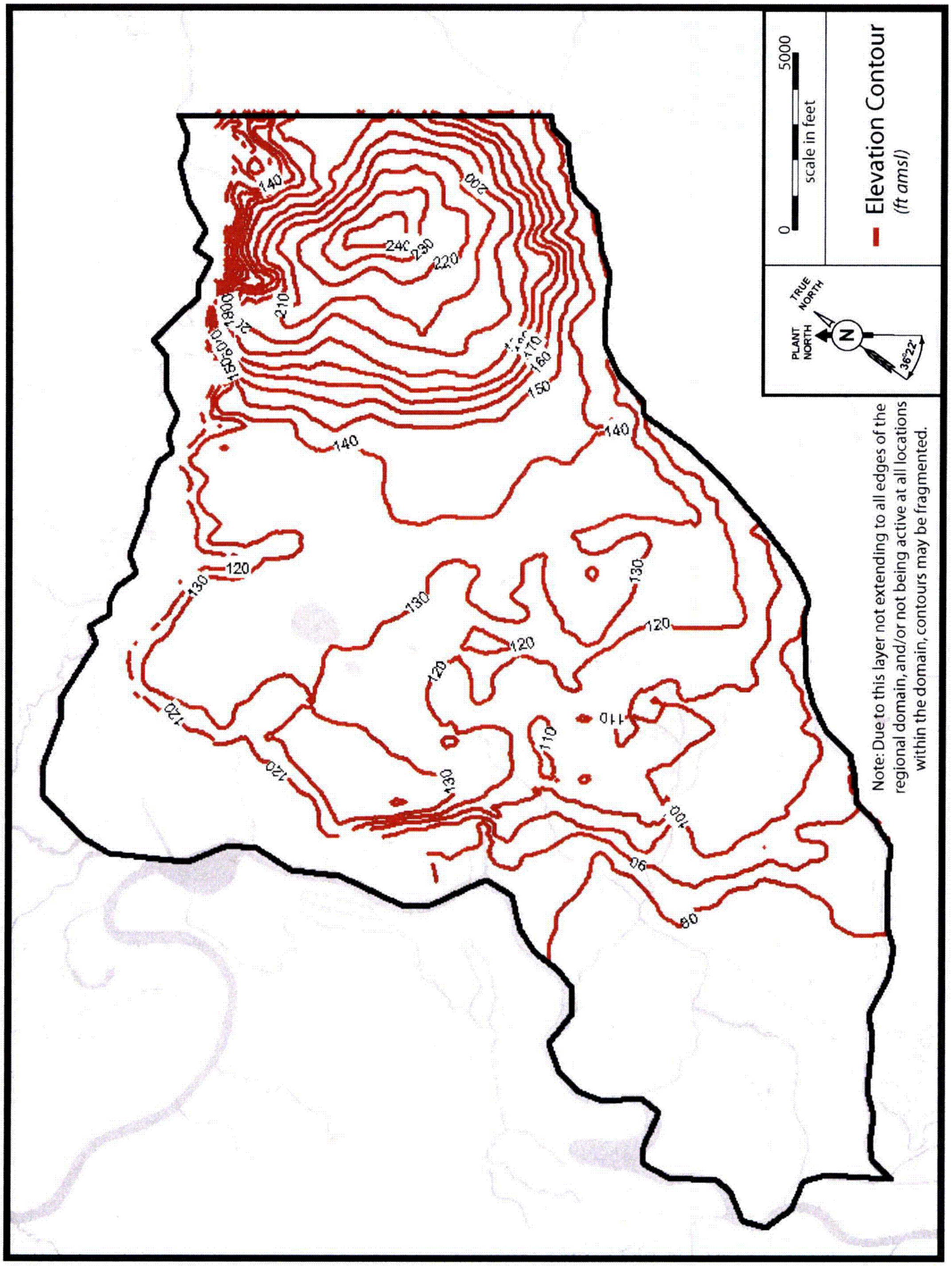

Figure 2-8. Regional Model Layer 3 (UTRA) Thickness and Top Elevation

(a) Layer Thickness (ft)

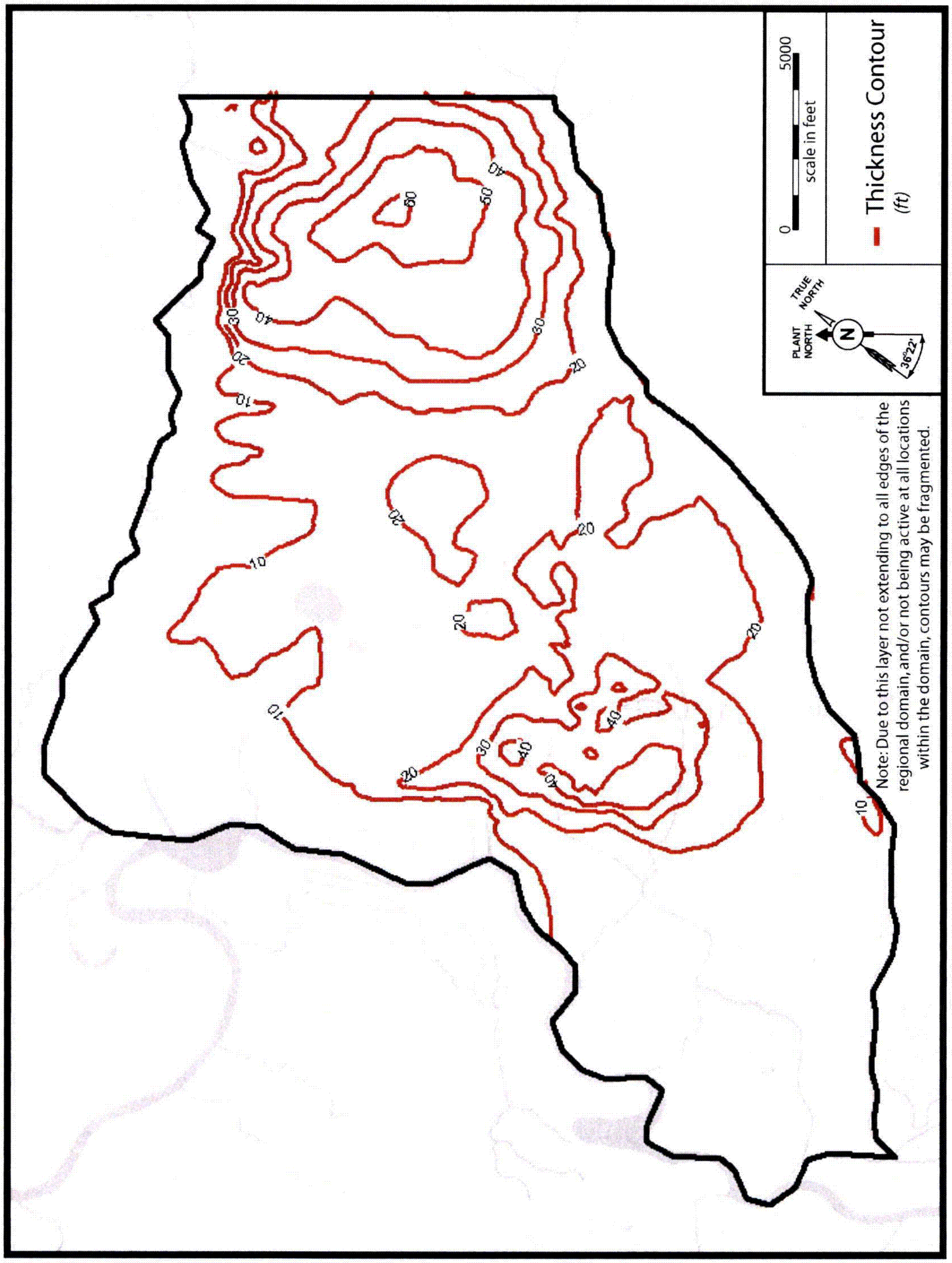

Figure 2-8. (con't) Regional Model Layer 3 (UTRA) Thickness and Top Elevation

(b) Layer Top Elevation (ft amsl)

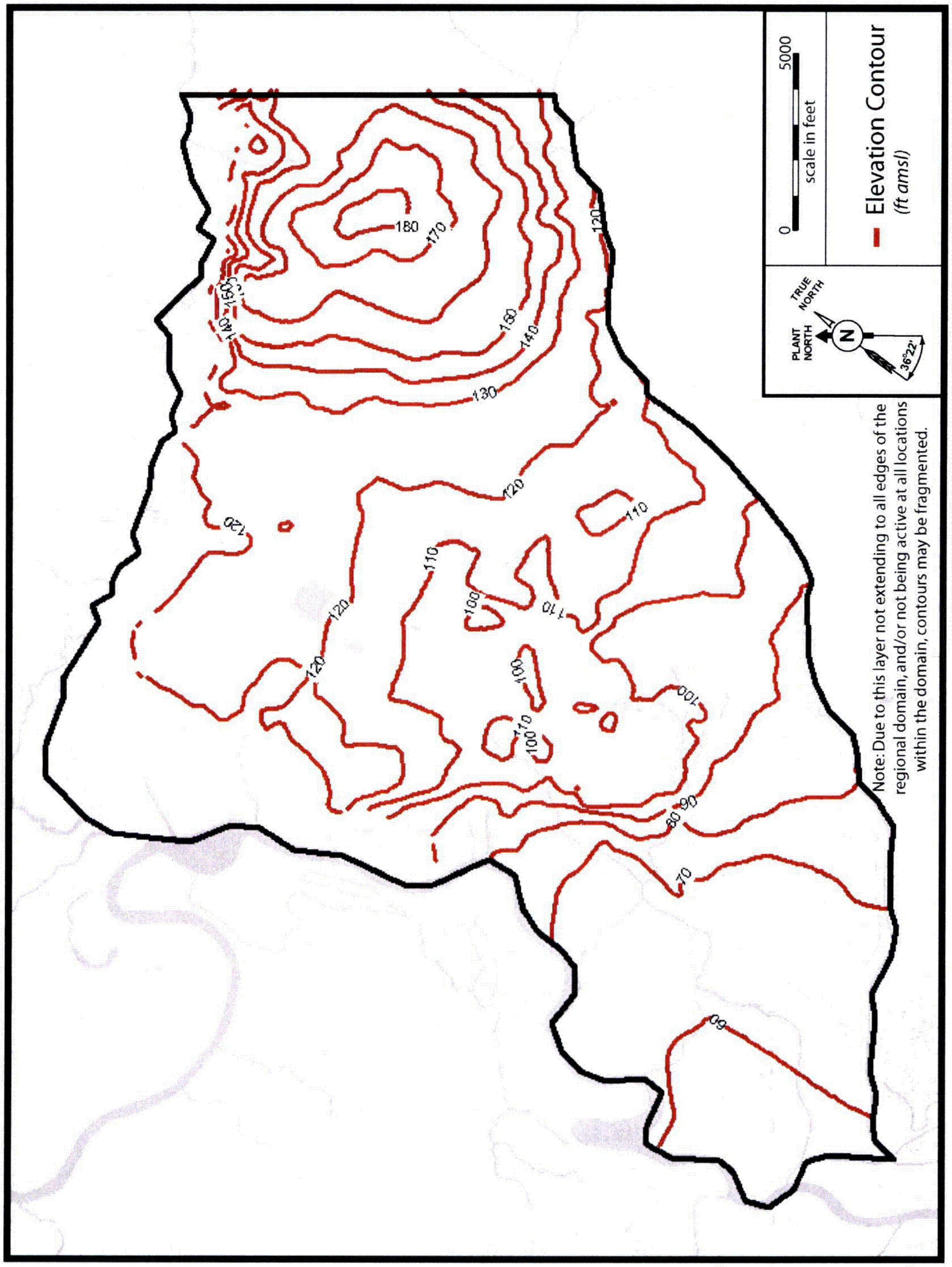

Figure 2-9. Regional Model Layer 4 (GCU) Thickness and Top Elevation

(a) Layer Thickness (ft)

Figure 2-9. (con't) Regional Model Layer 4 (GCU) Thickness and Top Elevation

(b) Layer Top Elevation (ft amsl)

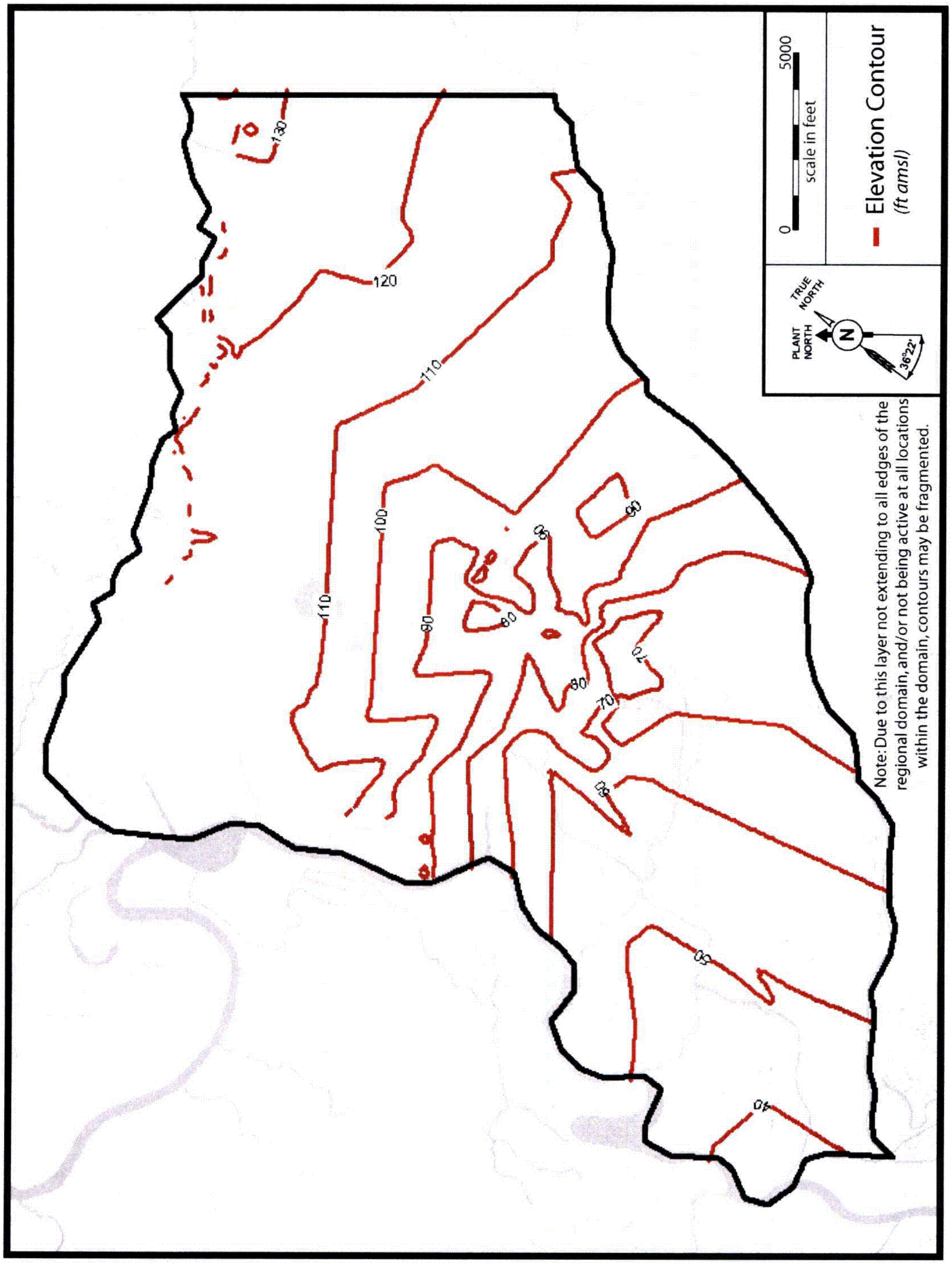

Figure 2-10. Regional Model Layer 5 (GA) Thickness and Top Elevation

(a) Layer Thickness (ft)

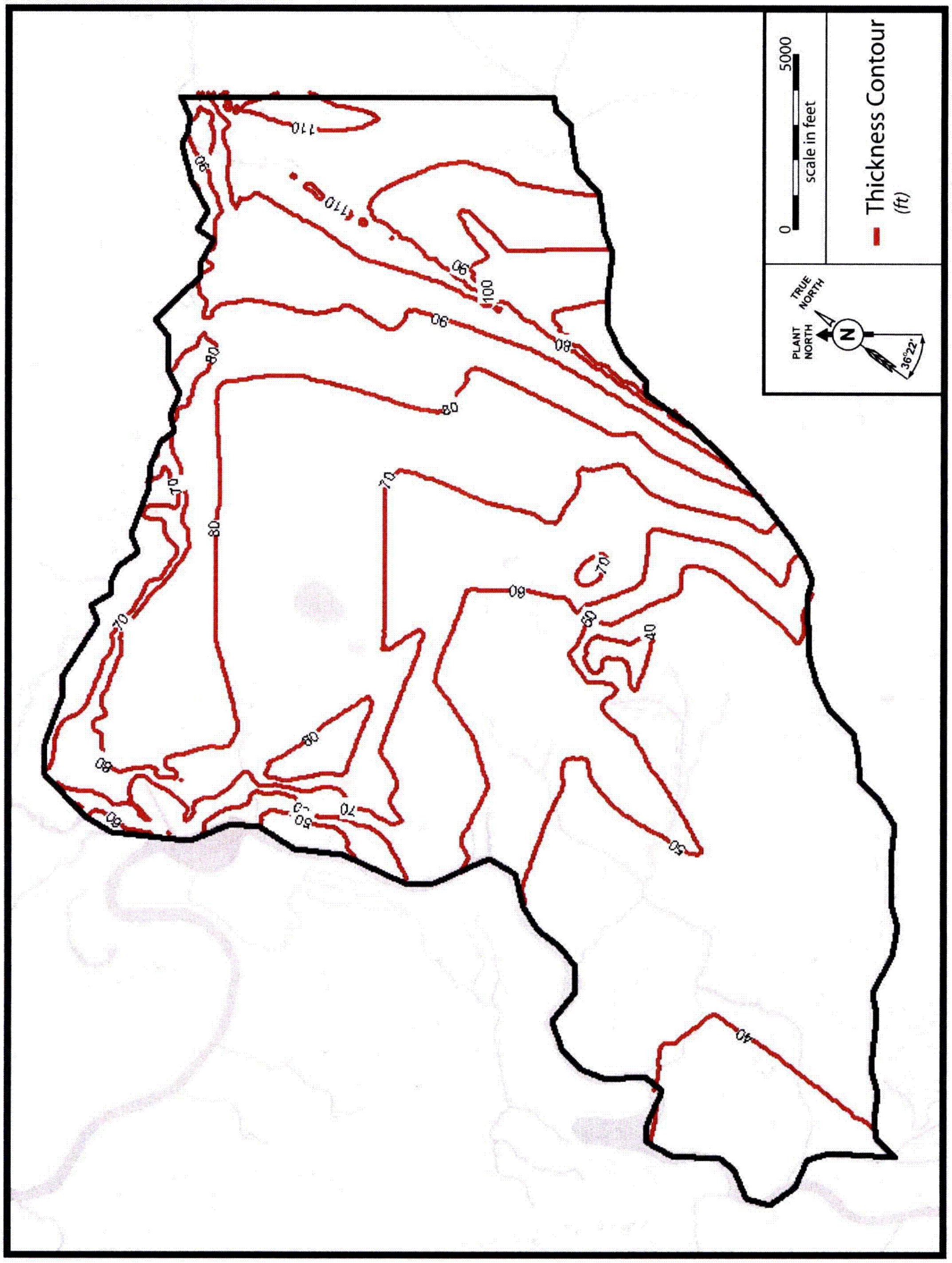

Figure 2-10. (con't) Regional Model Layer 5 (GA) Thickness and Top Elevation

(b) Layer Top Elevation (ft amsl)

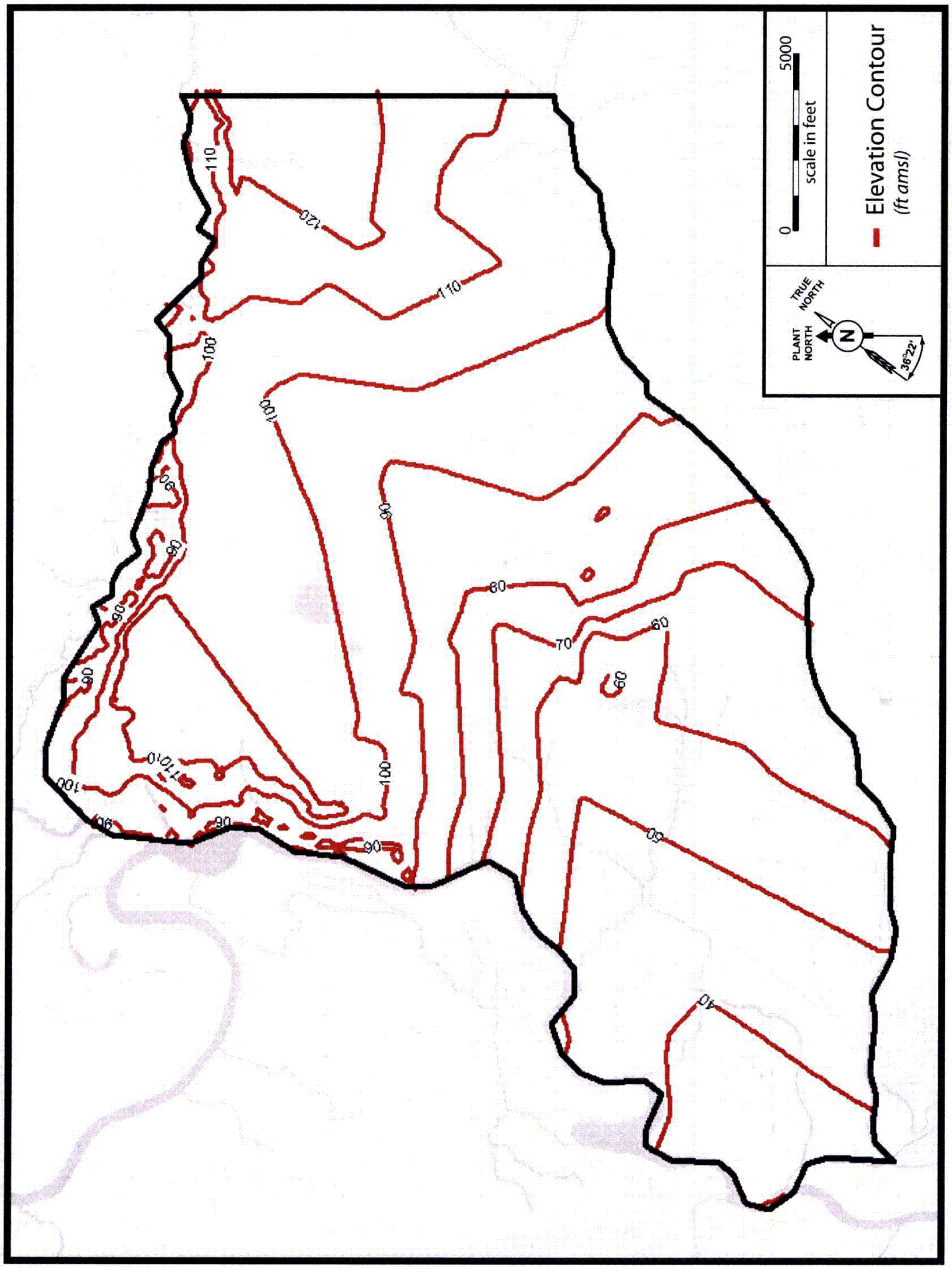

Figure 2-11. Regional Model Layer 1 (UTRA) Material Distribution

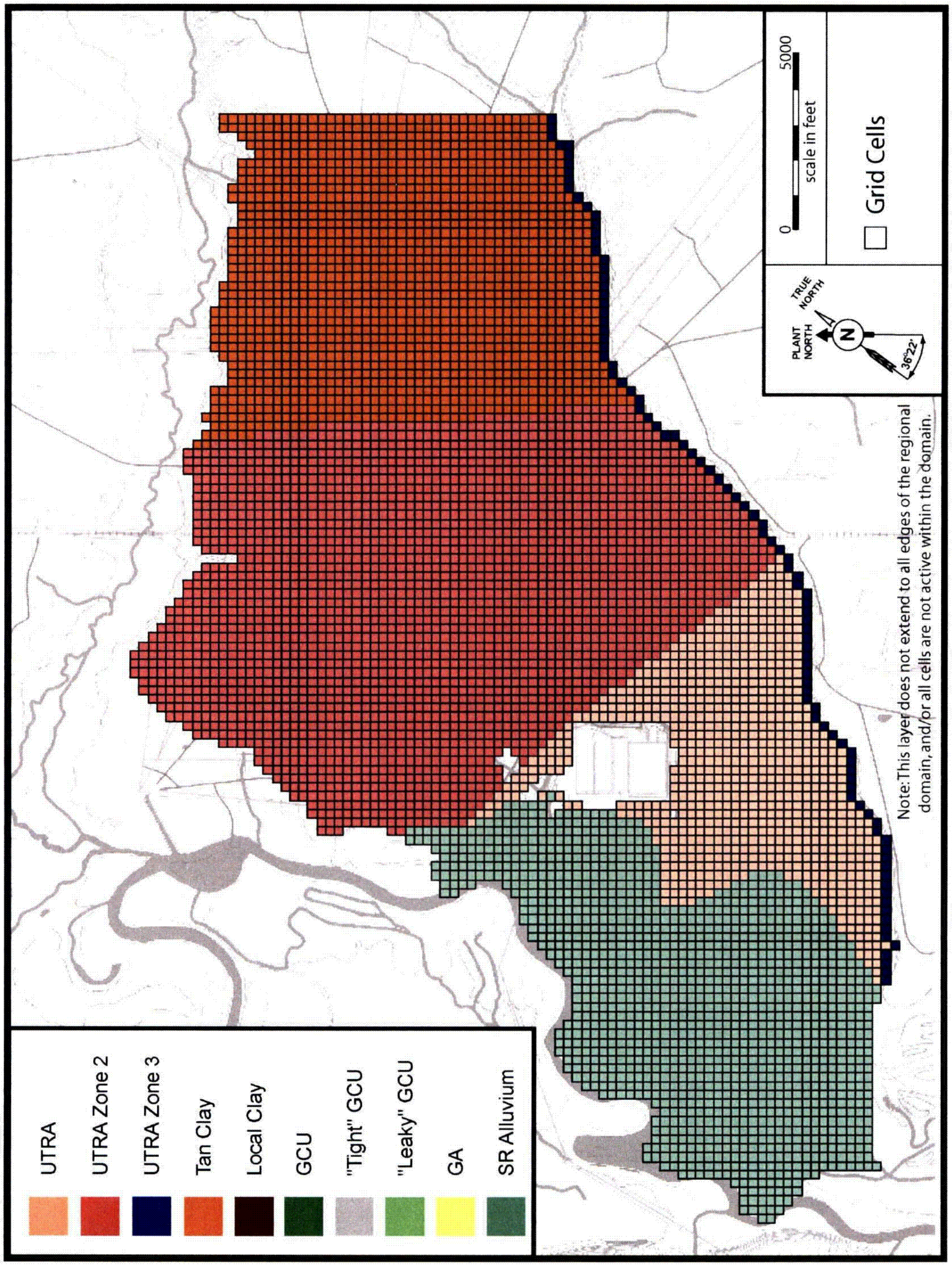

Figure 2-12. Regional Model Layer 2 (UTRA) Material Distribution

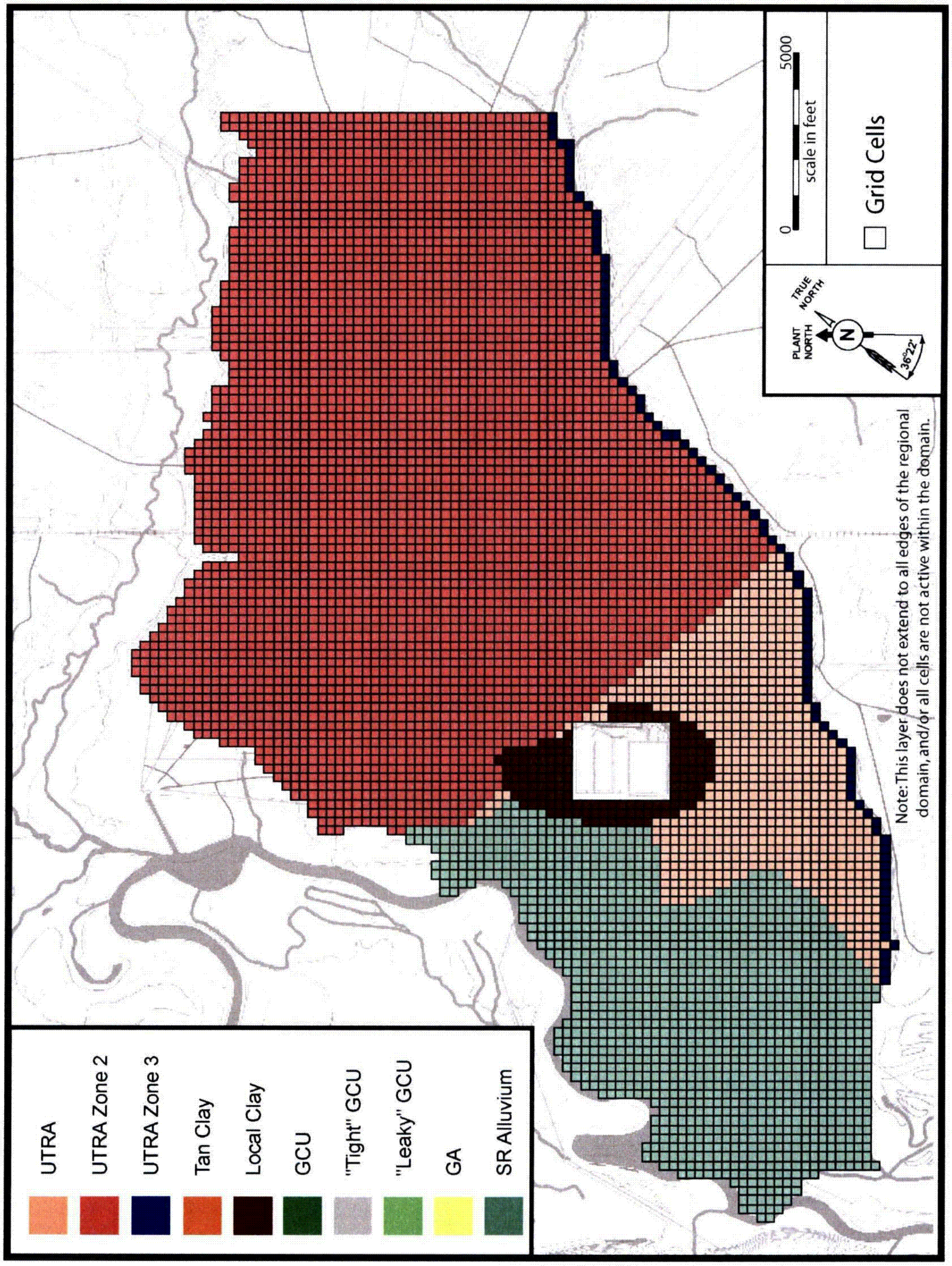

Figure 2-13. Regional Model Layer 3 (UTRA) Material Distribution

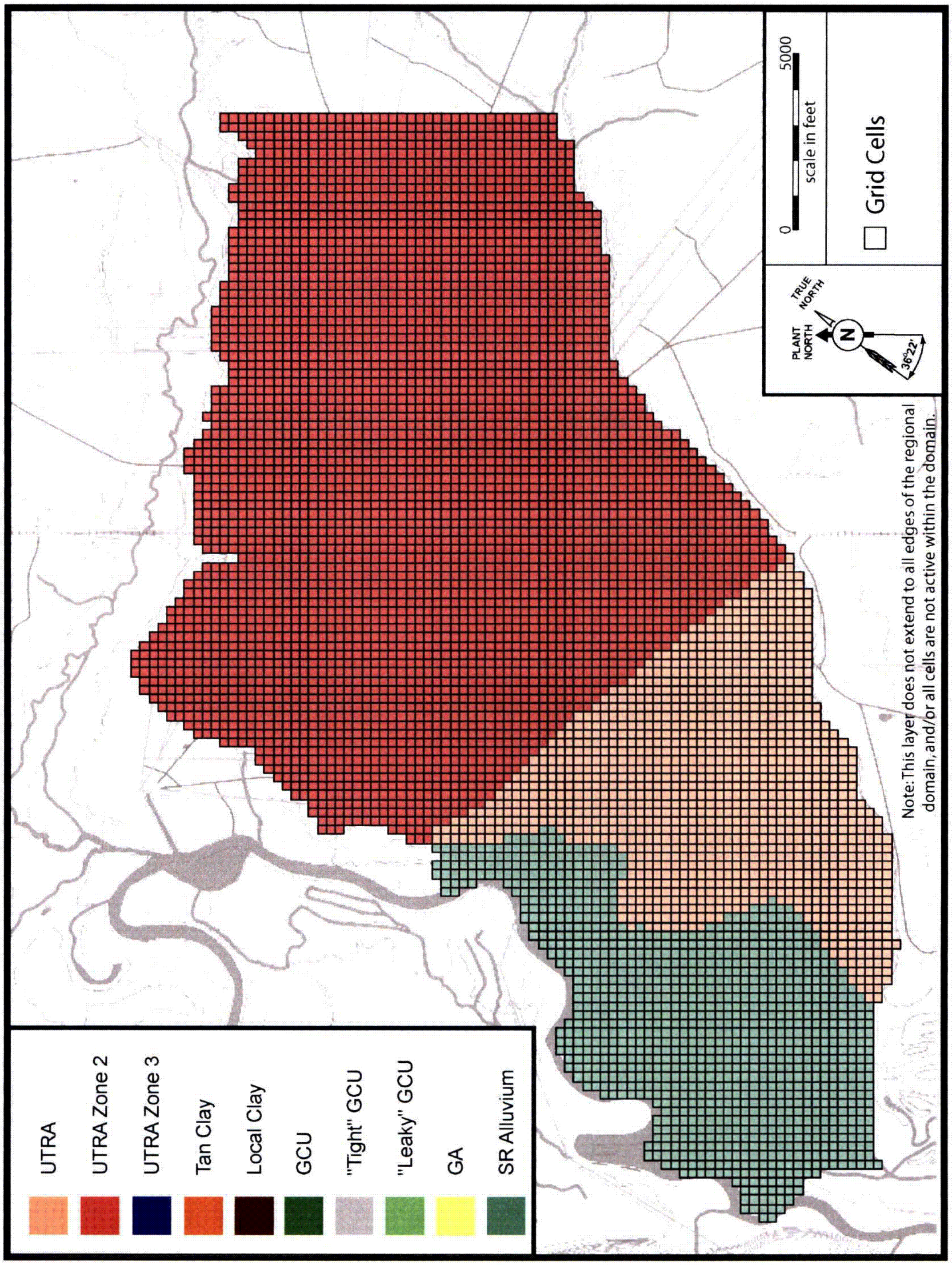

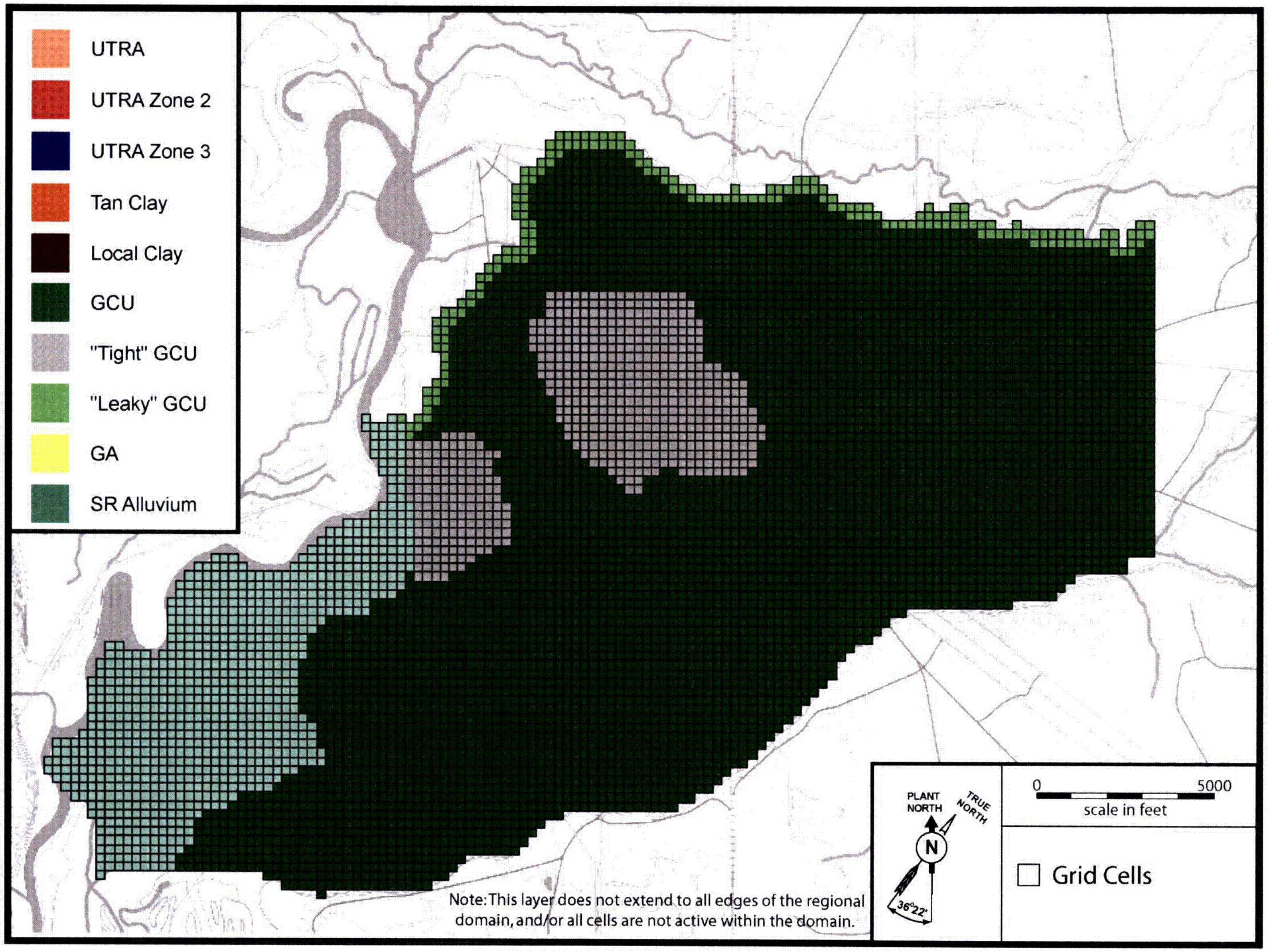

Figure 2-14. Regional Model Layer 4 (GCU) Material Distribution

Figure 2-15. Regional Model Layer 5 (GA) Material Distribution

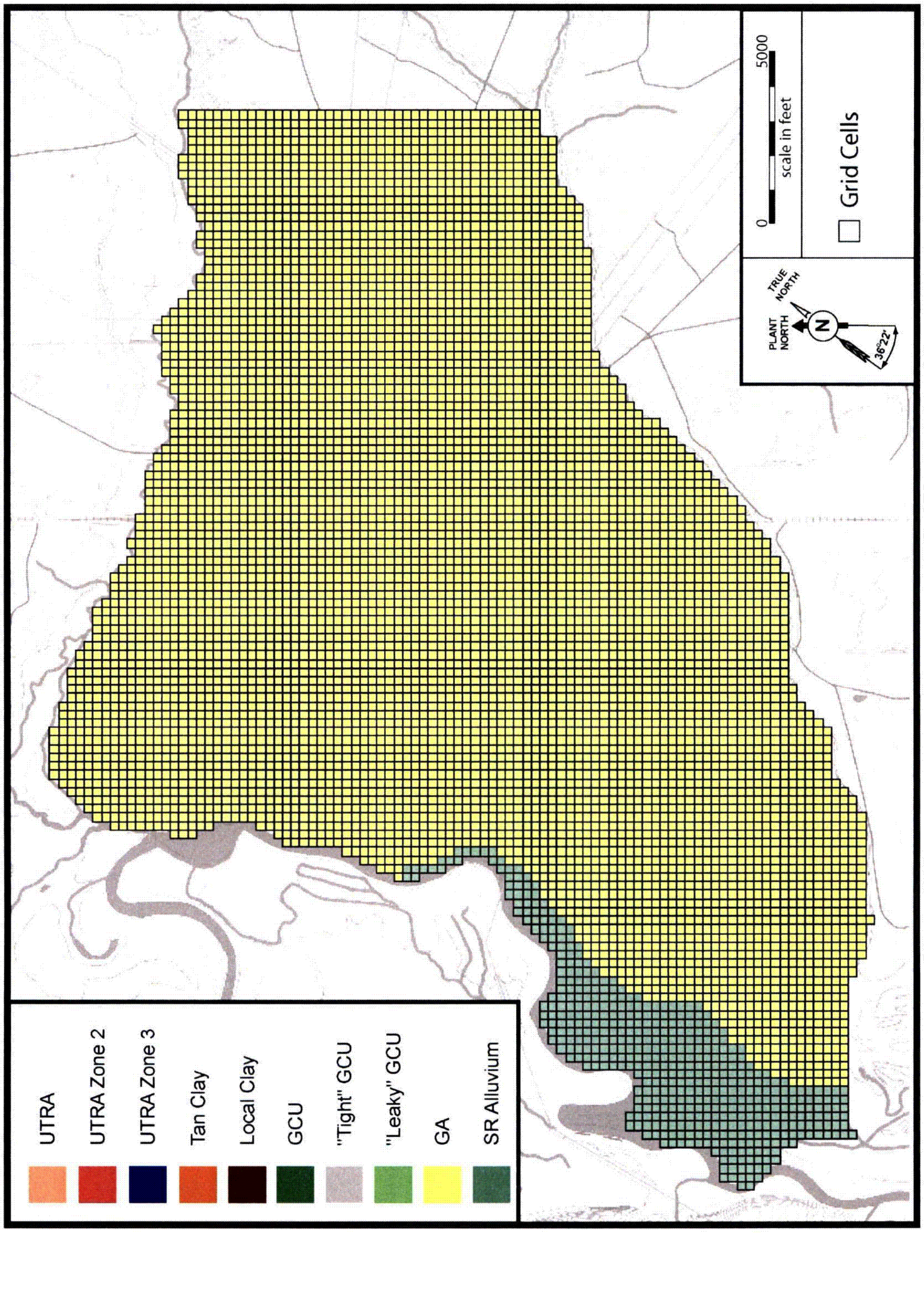

Figure 3-1. Regional Flow Model Grid

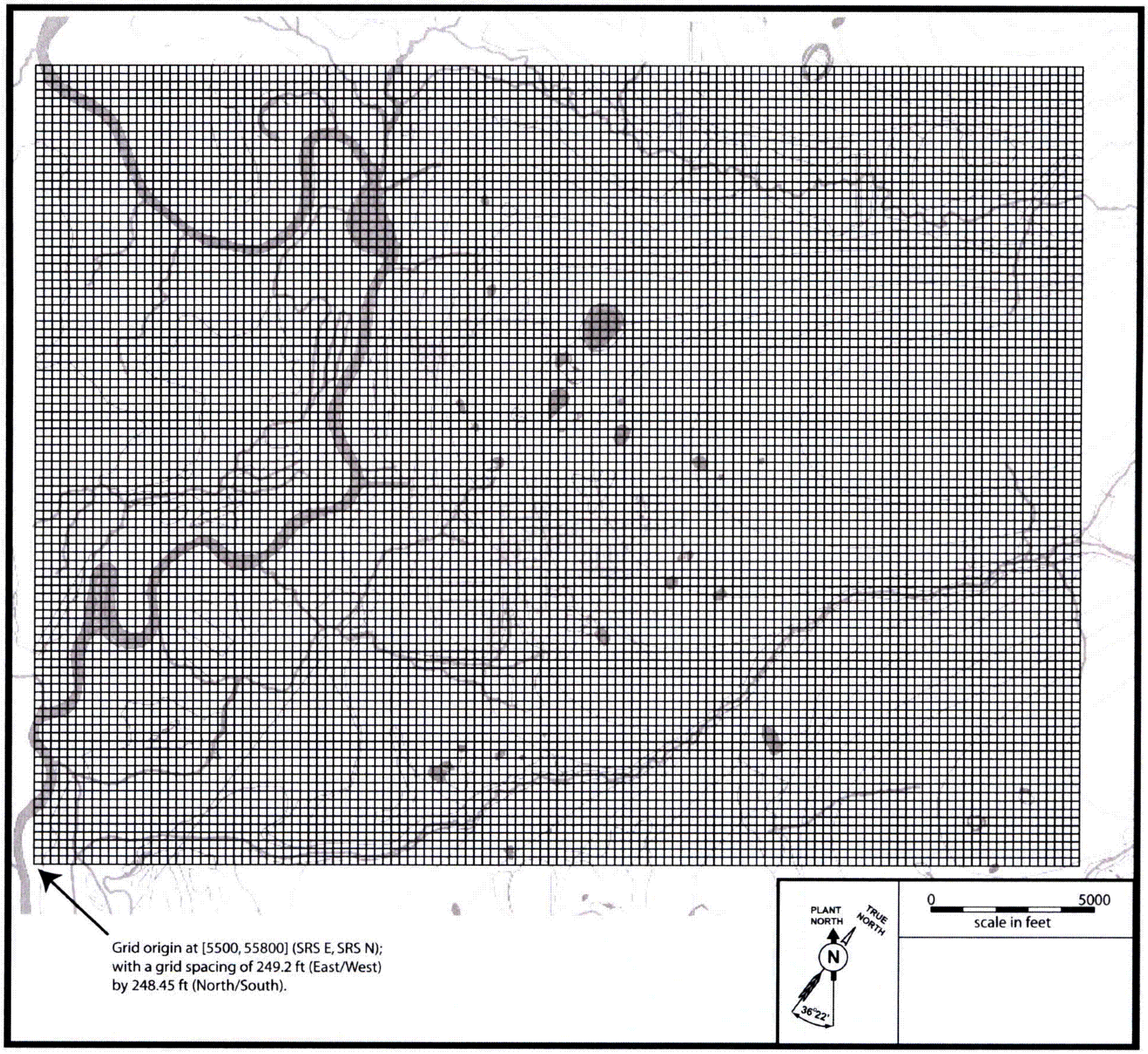

Figure 3-2. Layer 1 (UTRA) Boundary Conditions for Regional Flow Model

(a) Conceptual Arcs and Conditions

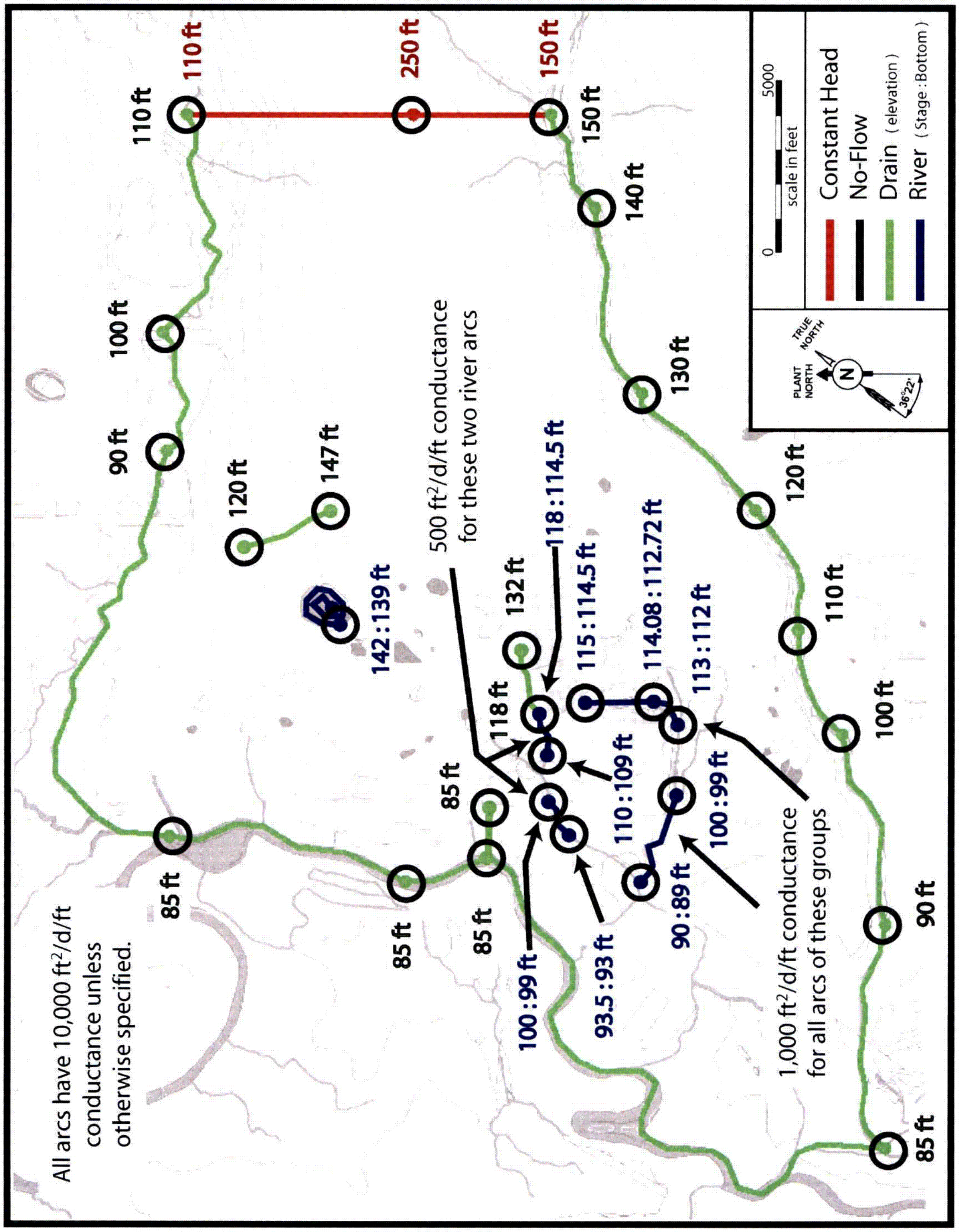

Figure 3-2. (con't) Layer 1 (UTRA) Boundary Conditions for Regional Flow Model

(b) Modflow Cell Designations

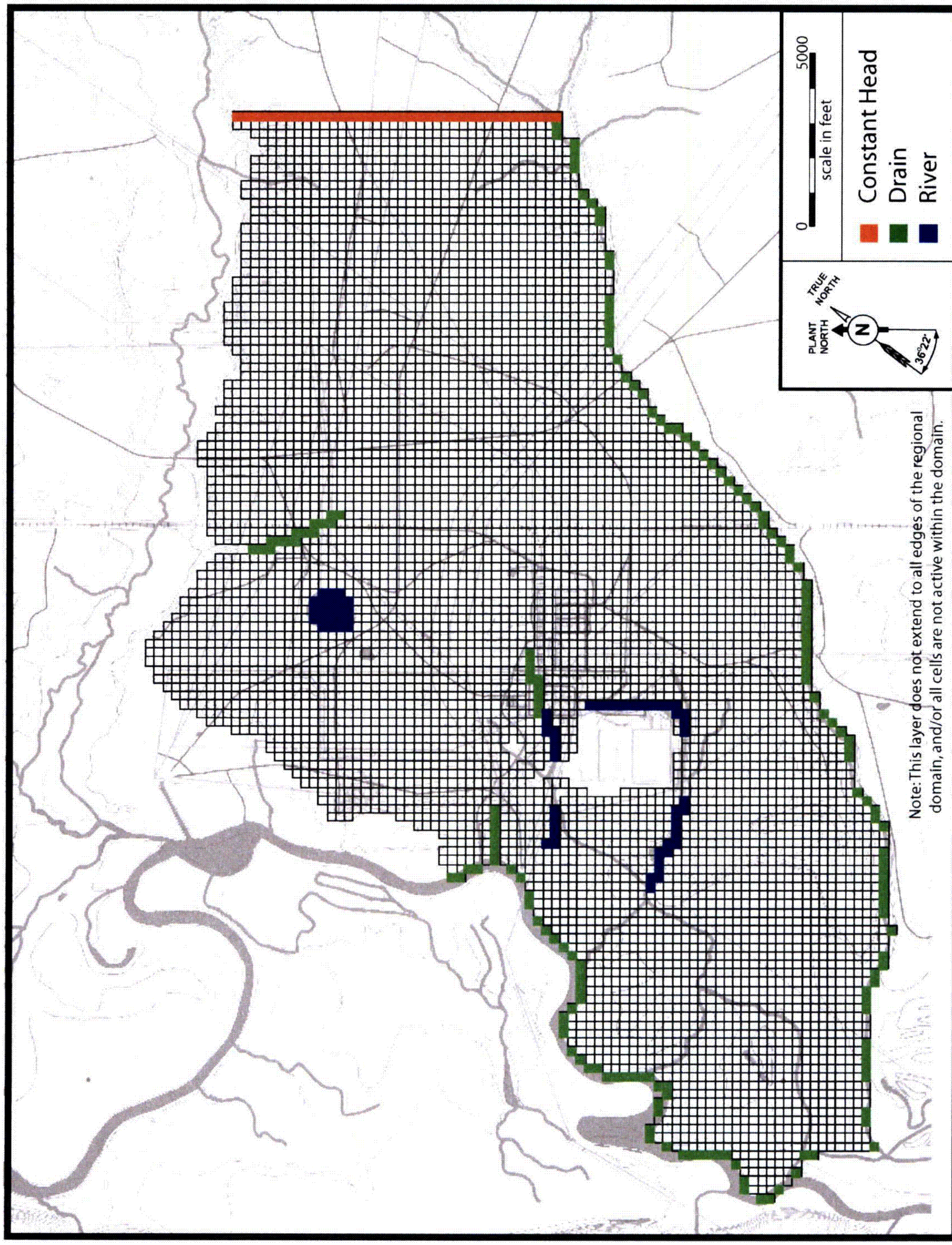

Figure 3-3. Layer 2 (UTRA) Boundary Conditions for Regional Flow Model

(a) Conceptual Arcs and Conditions

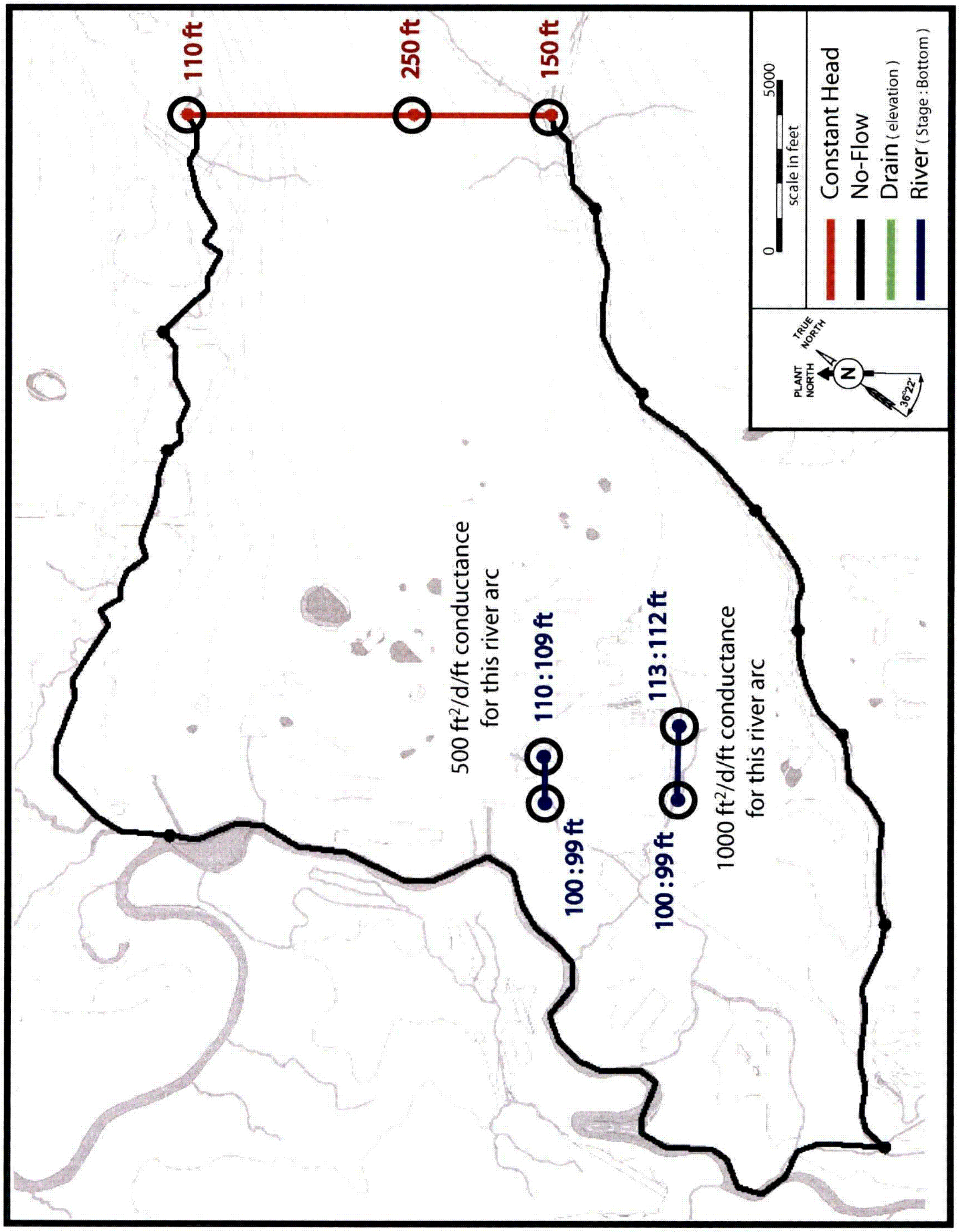

Figure 3-3. (con't) Layer 2 (UTRA) Boundary Conditions for Regional Flow Model

(b) Modflow Cell Designations

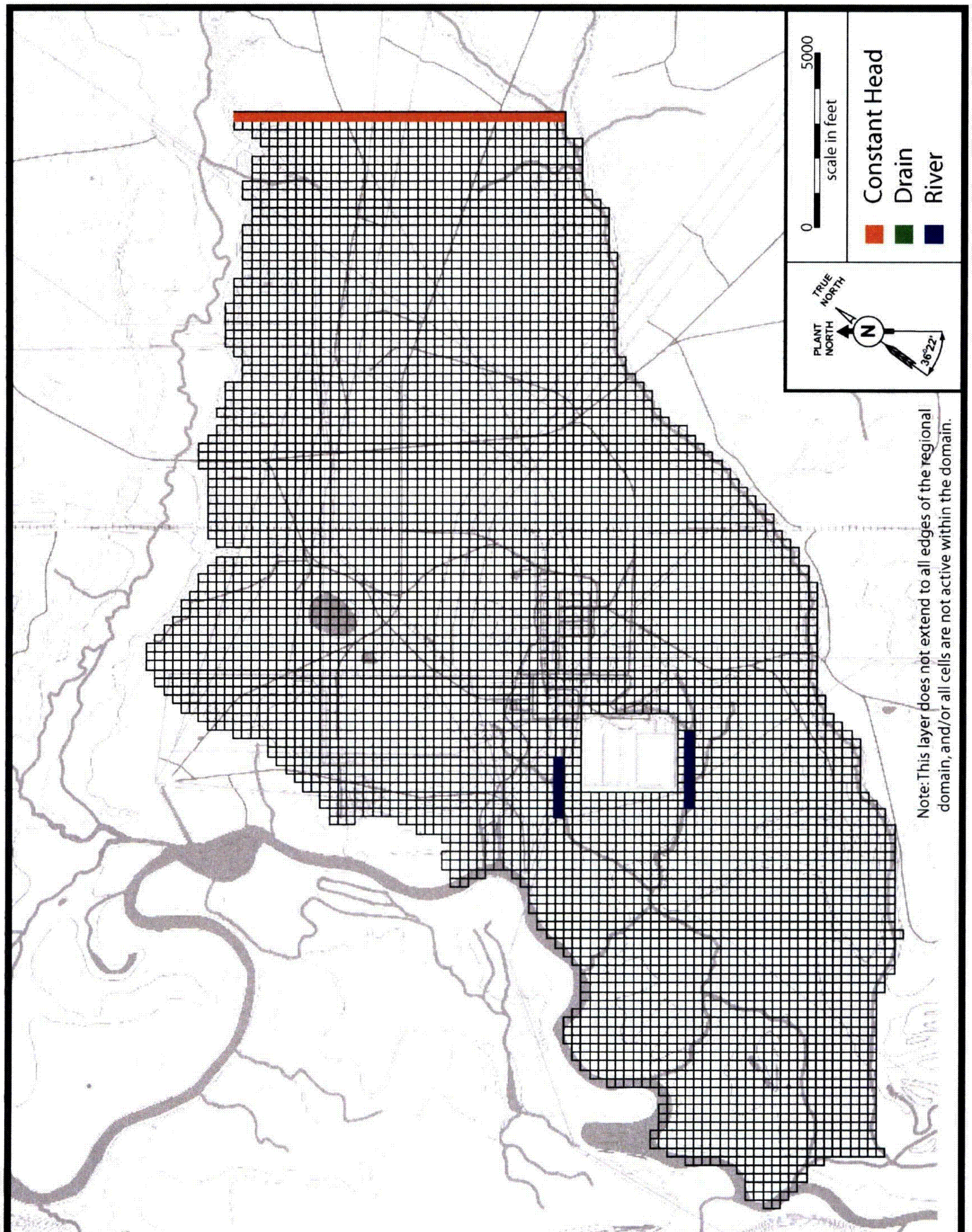

Figure 3-4. Layer 3 (UTRA) Boundary Conditions for Regional Flow Model

(a) Conceptual Arcs and Conditions

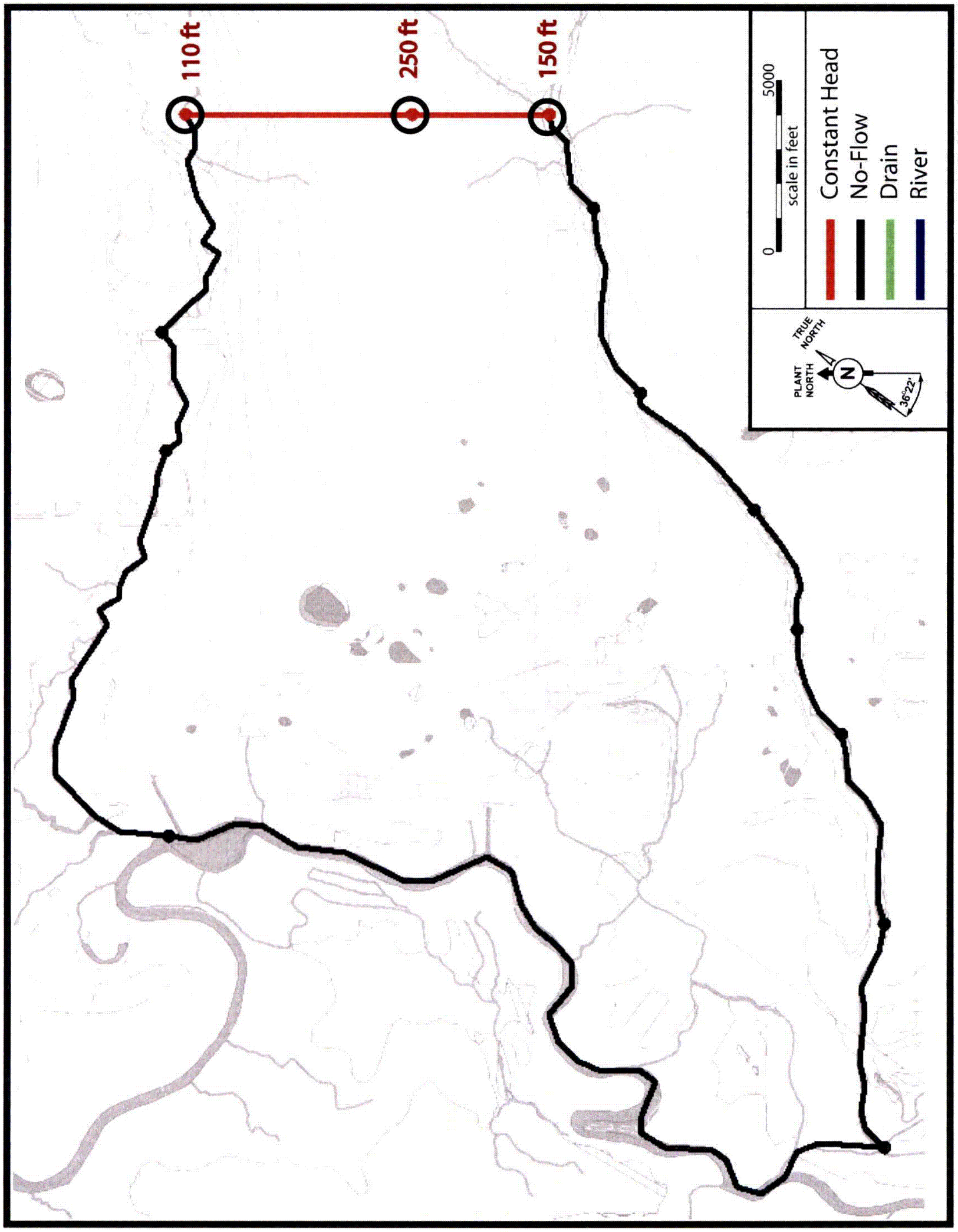

Figure 3-4. (con't) Layer 3 (UTRA) Boundary Conditions for Regional Flow Model

(b) Modflow Cell Designations

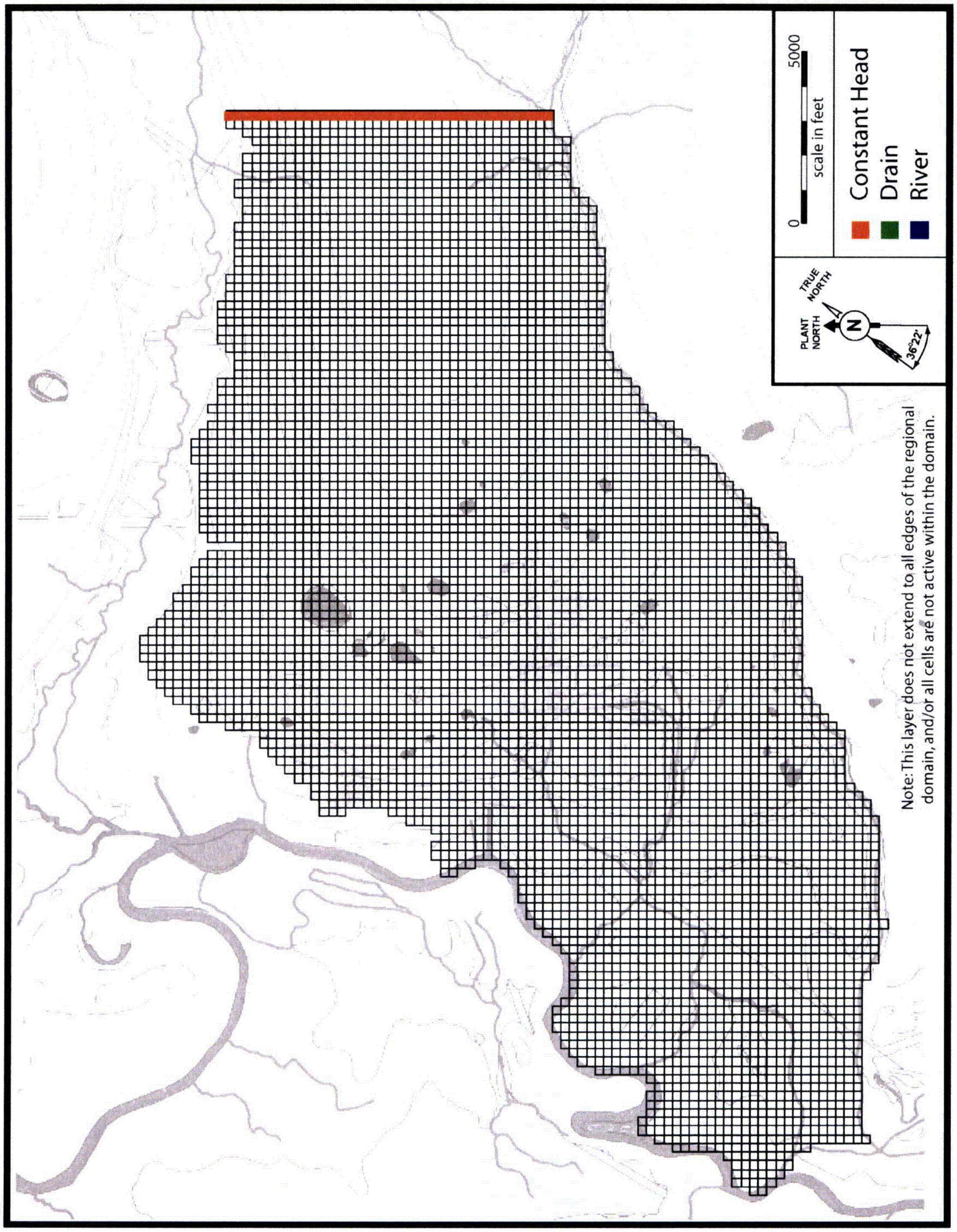

Figure 3-5. Layer 4 (GCU) Boundary Conditions for Regional Flow Model

(a) Conceptual Arcs and Conditions

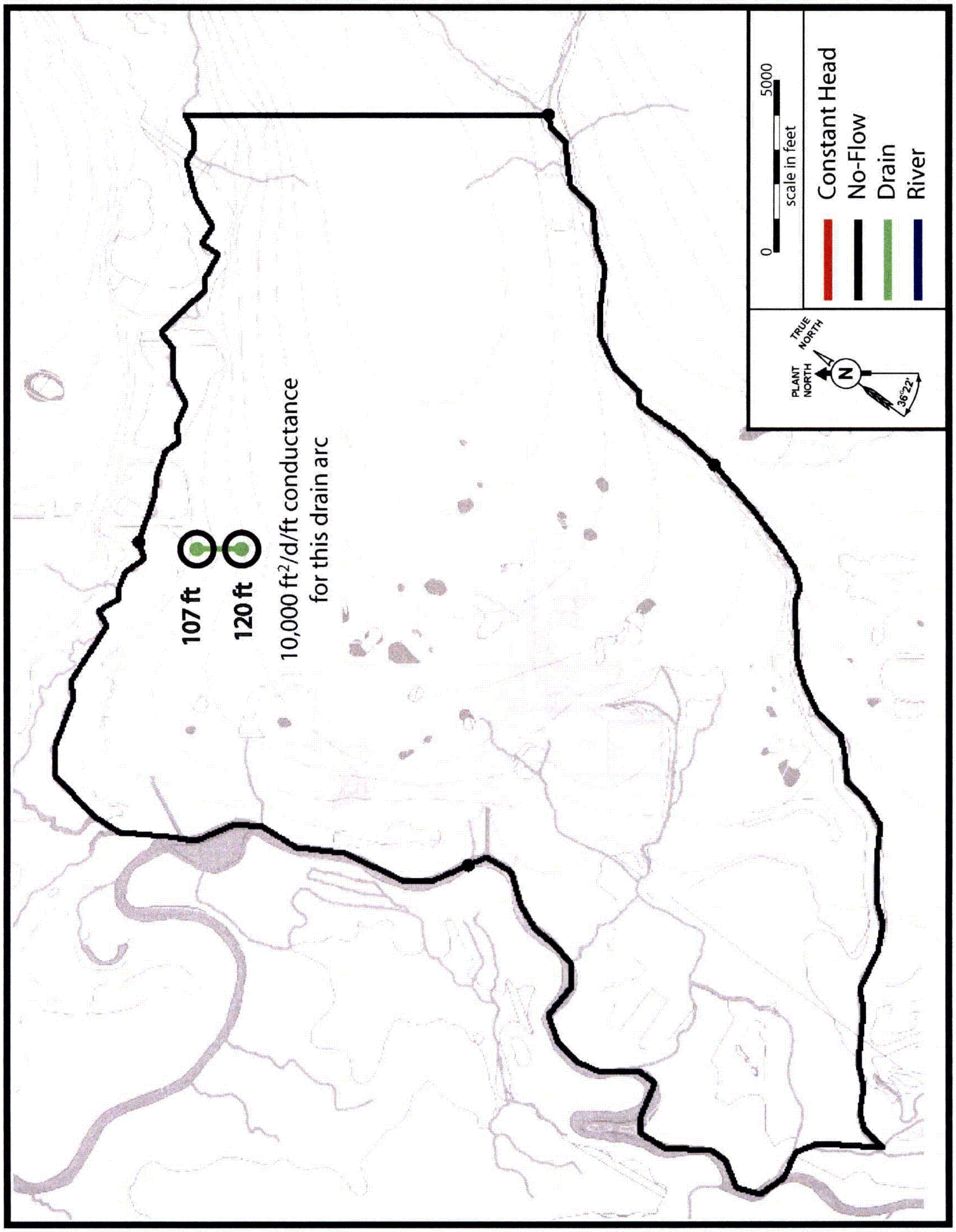

Figure 3-5. (con't) Layer 4 (GCU) Boundary Conditions for Regional Flow Model

(b) Modflow Cell Designations

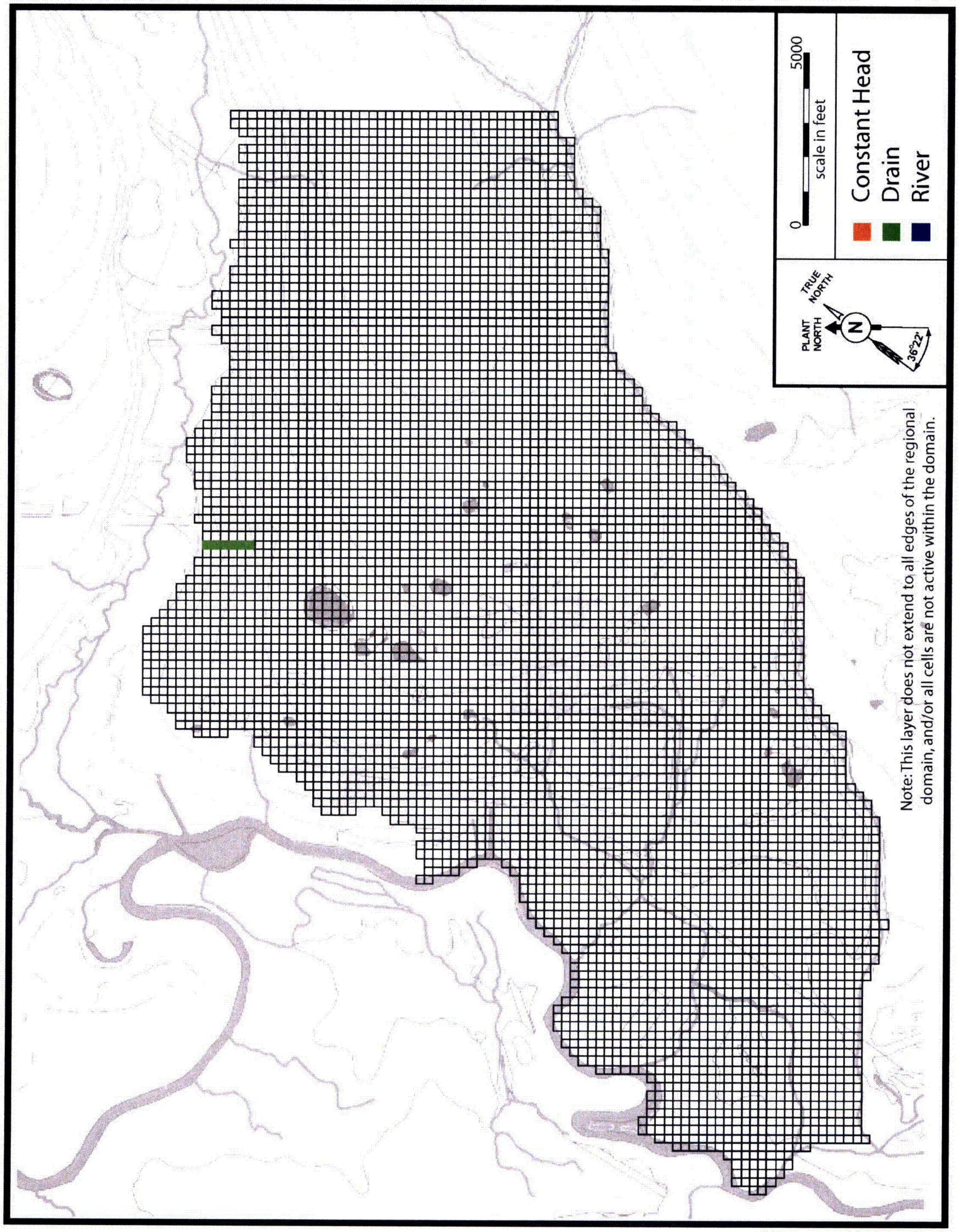

Figure 3-6. Layer 5 (GA) Boundary Conditions for Regional Flow Model

(a) Conceptual Arcs and Conditions

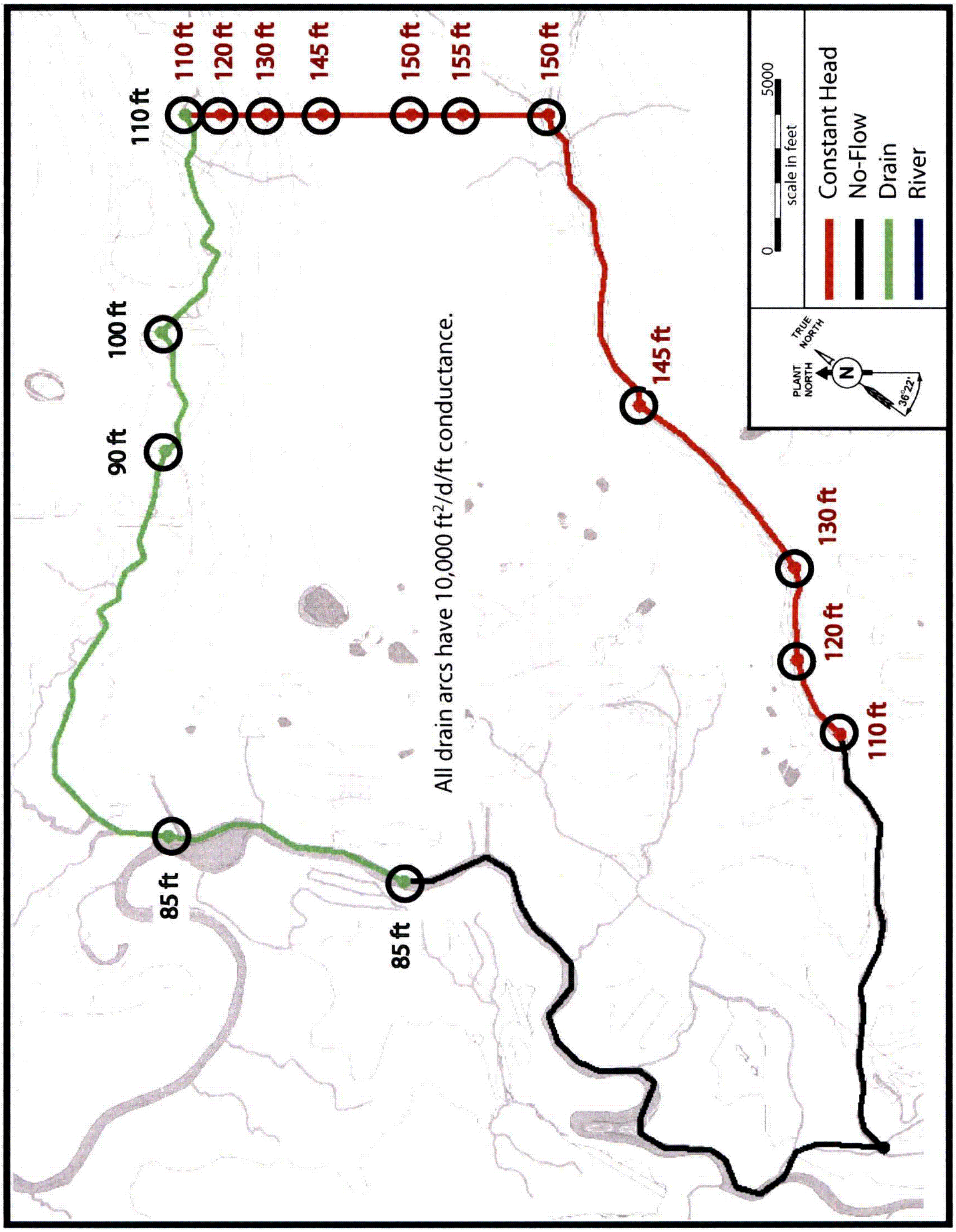

Figure 3-6. (con't) Layer 5 (GA) Boundary Conditions for Regional Flow Model

(b) Modflow Cell Designations

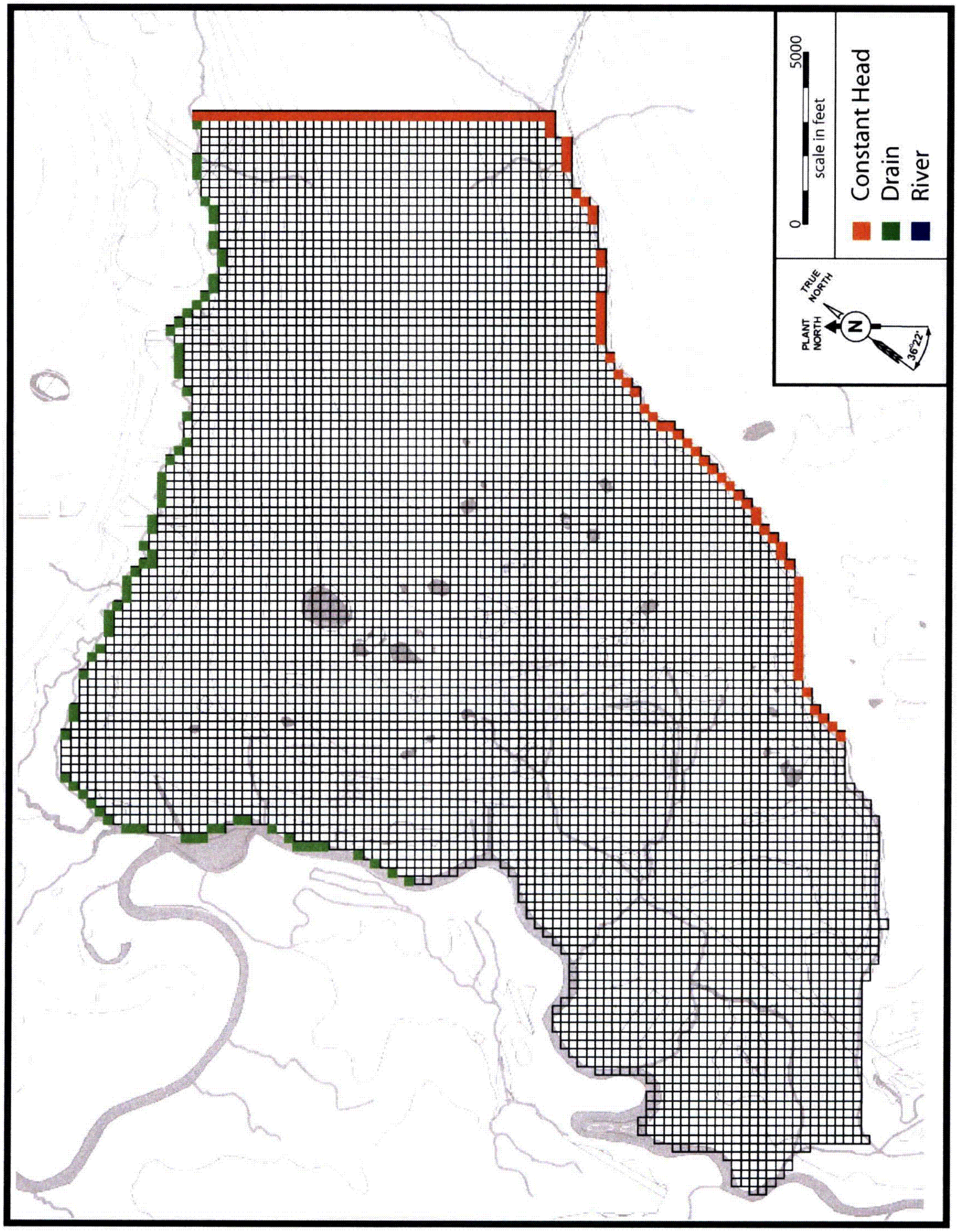

Figure 3-7. Conceptual Diagram of Stream Boundaries

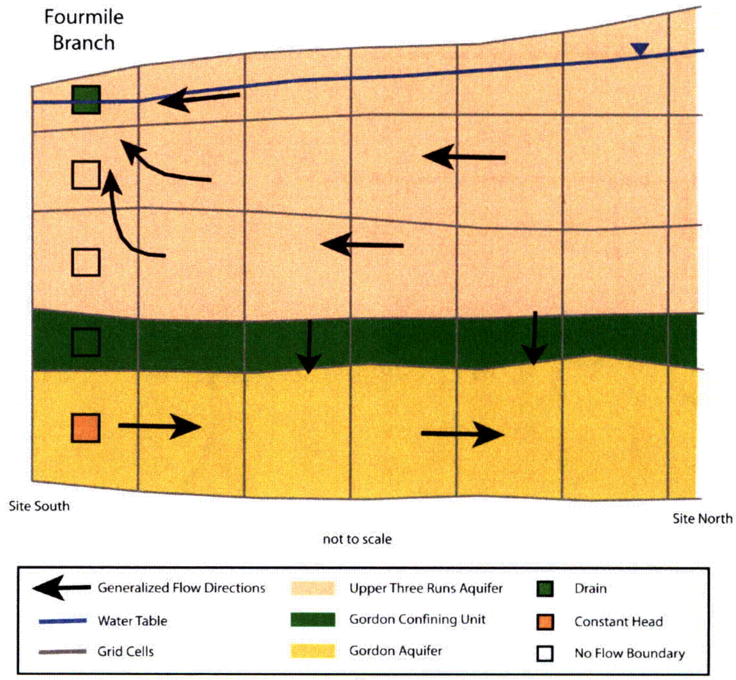

(a) Fourmile Branch

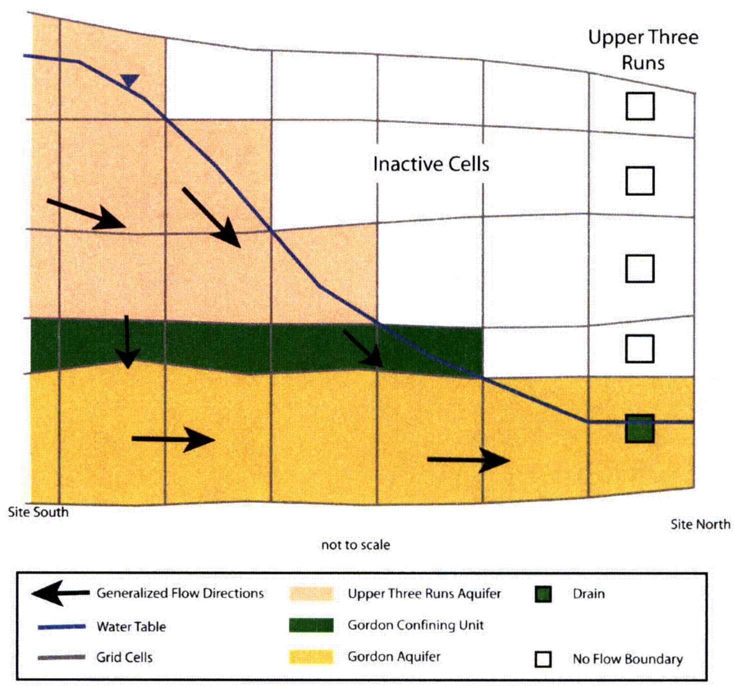

(b) Upper Three Runs

Figure 3-8. Regional Flow Model Recharge Zones

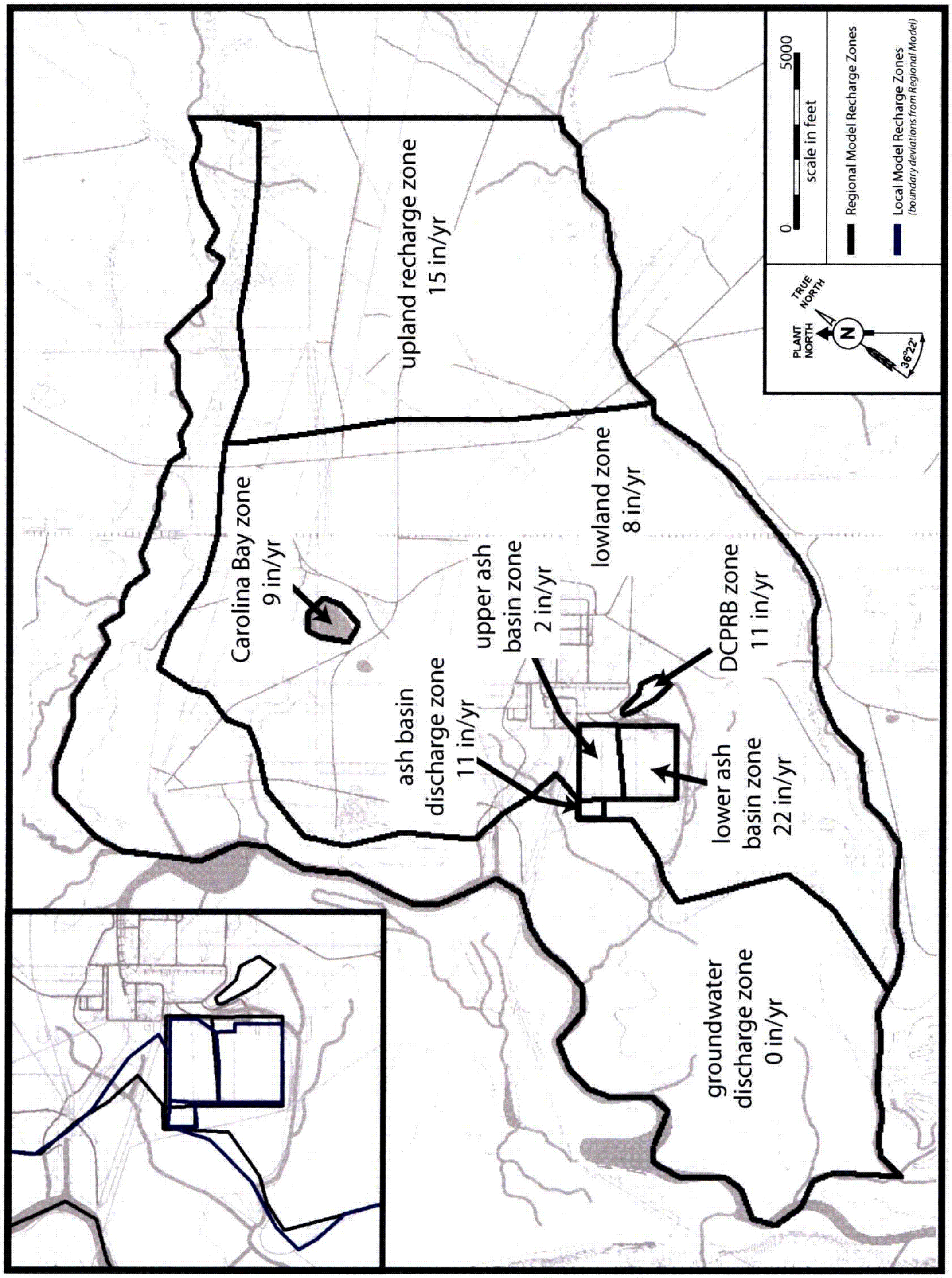

Figure 3-9. Qualitative Calibration Goals

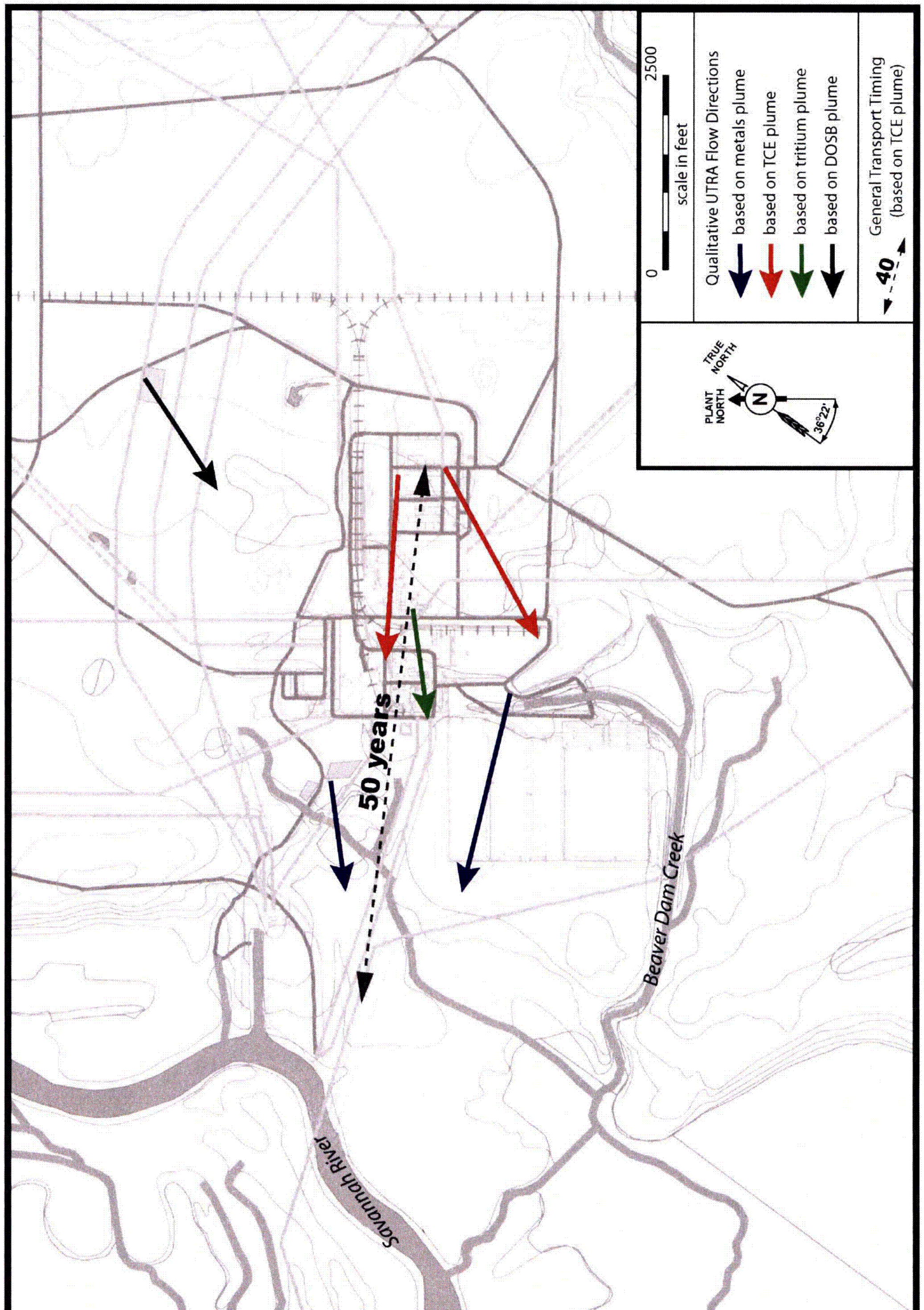

Figure 3-10. Sample Quarters for D-Area and TNX Monitoring Wells

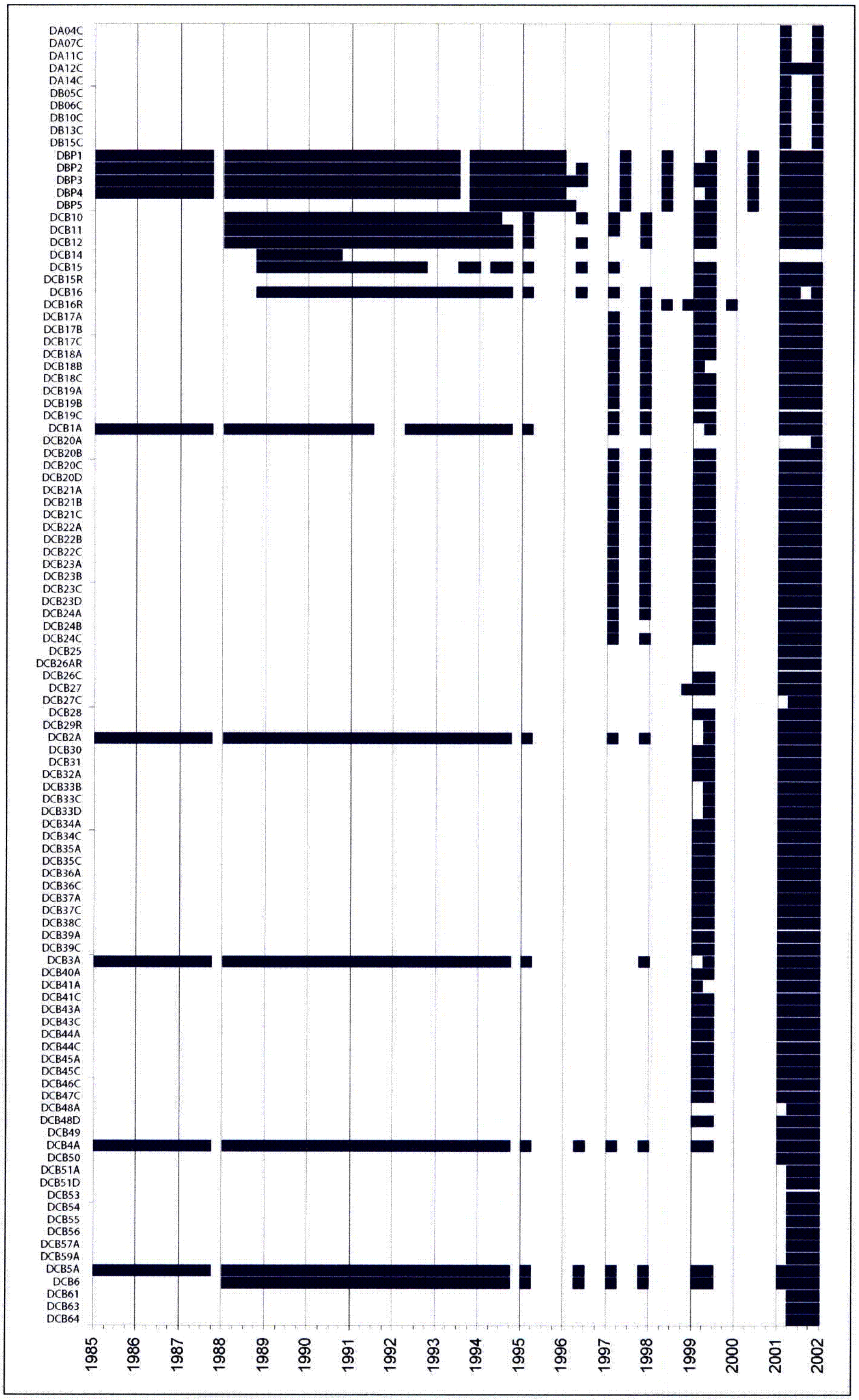

Figure 3-10 (con't). Sample Quarters for D-Area and TNX Monitoring Wells

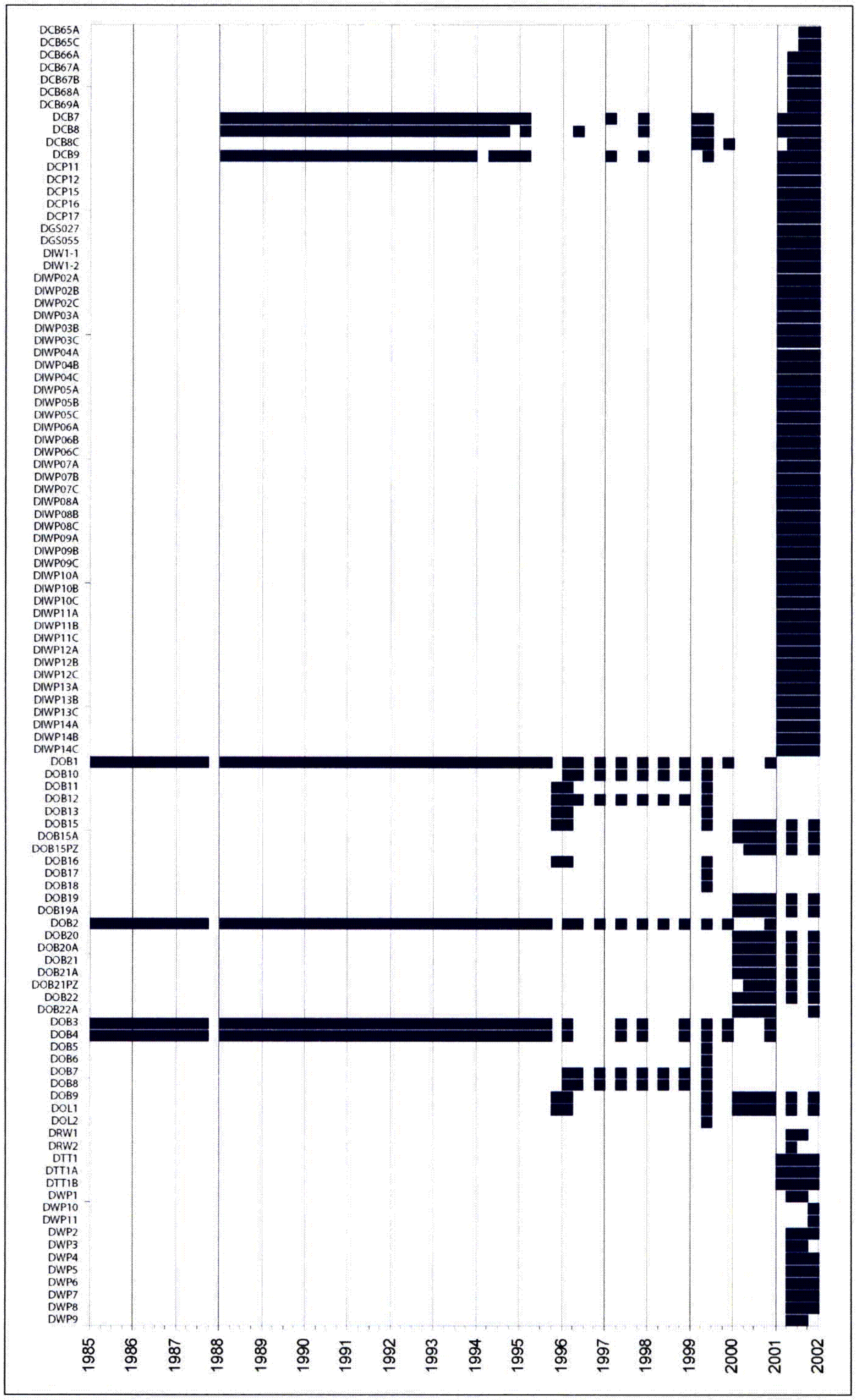

Figure 3-10 (con't). Sample Quarters for D-Area and TNX Monitoring Wells

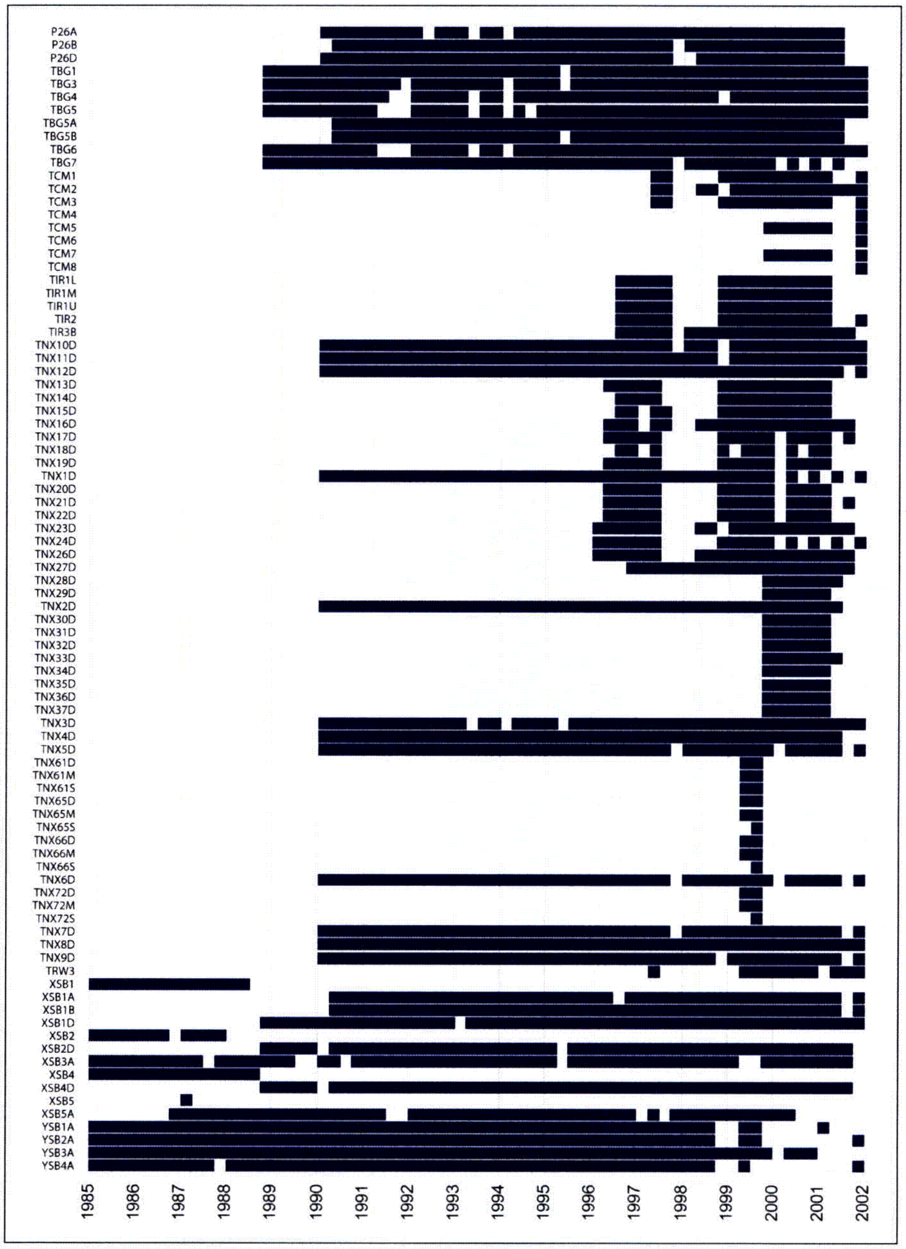

Figure 3-11. Groundwater Monitoring Data Density Map

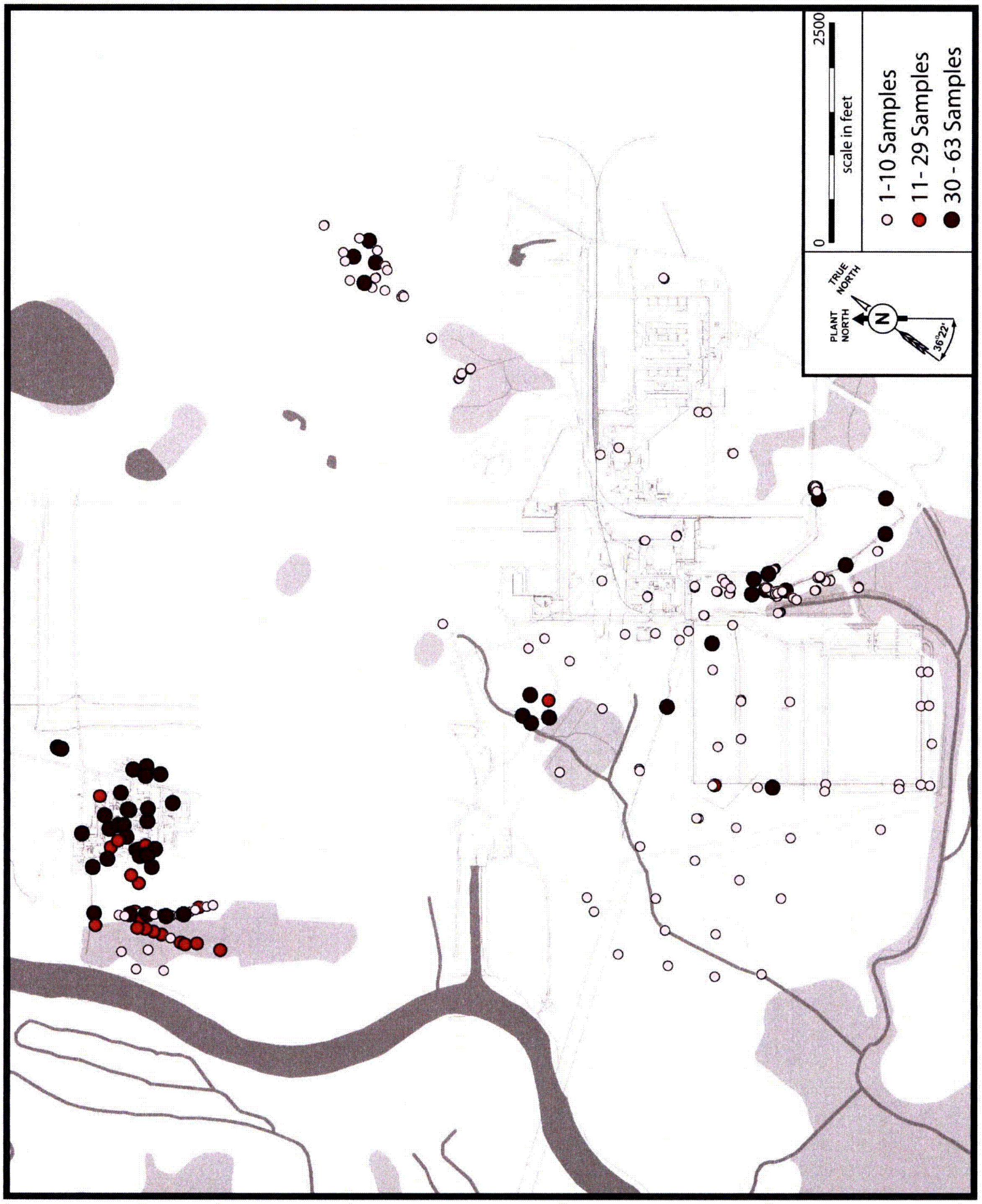

Figure 3-12. USGS Measured Streamflow at Upper Three Runs at Road A

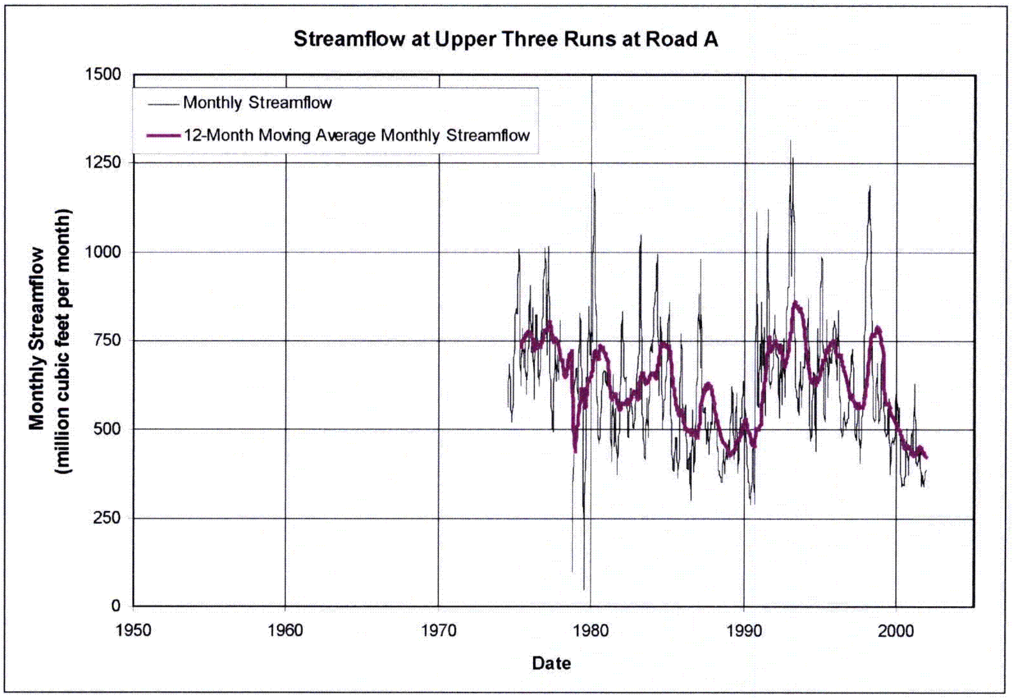

Figure 3-13. SRS Monthly Rainfall at A/M Area (Source: WSRC-TR-2001-00009-012)

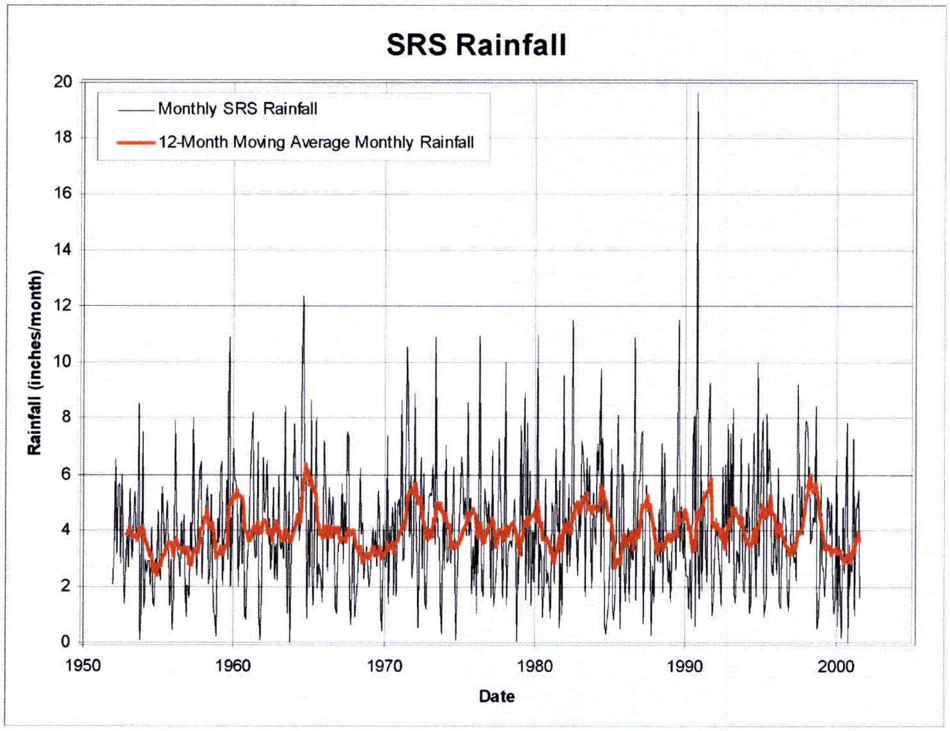

Figure 3-14. Comparison of Monthly Rainfall and Monthly Streamflow

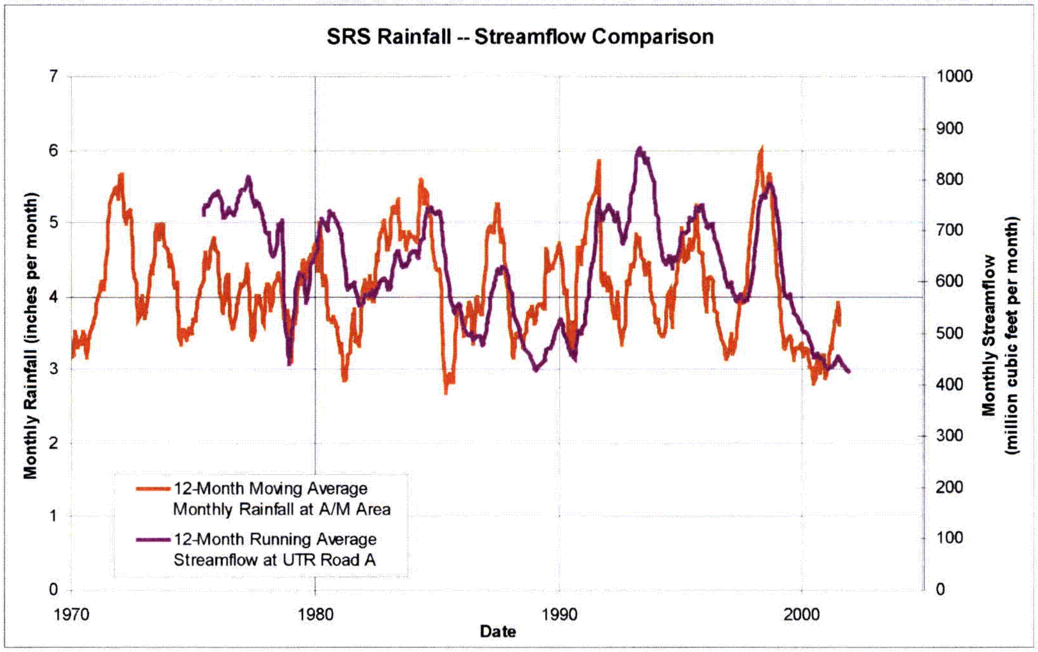

Figure 3-15. Comparison of Select Long-Term Monitoring Wells and Monthly Rainfall

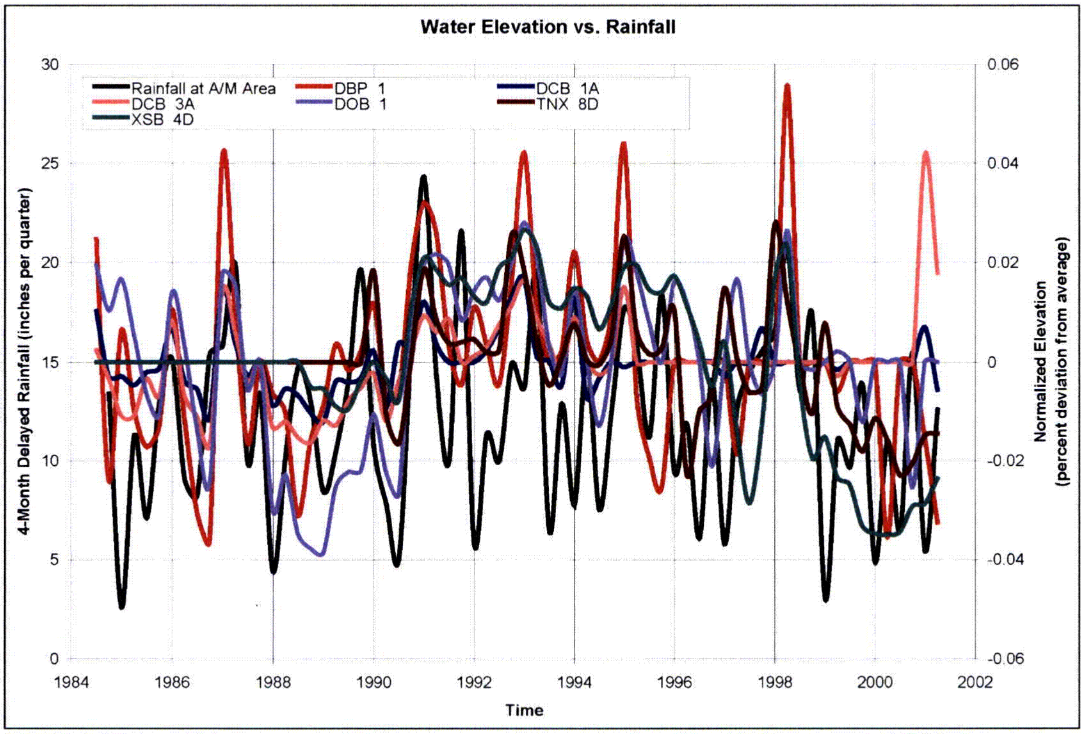

Figure 3-16. Southern Oscillation Index

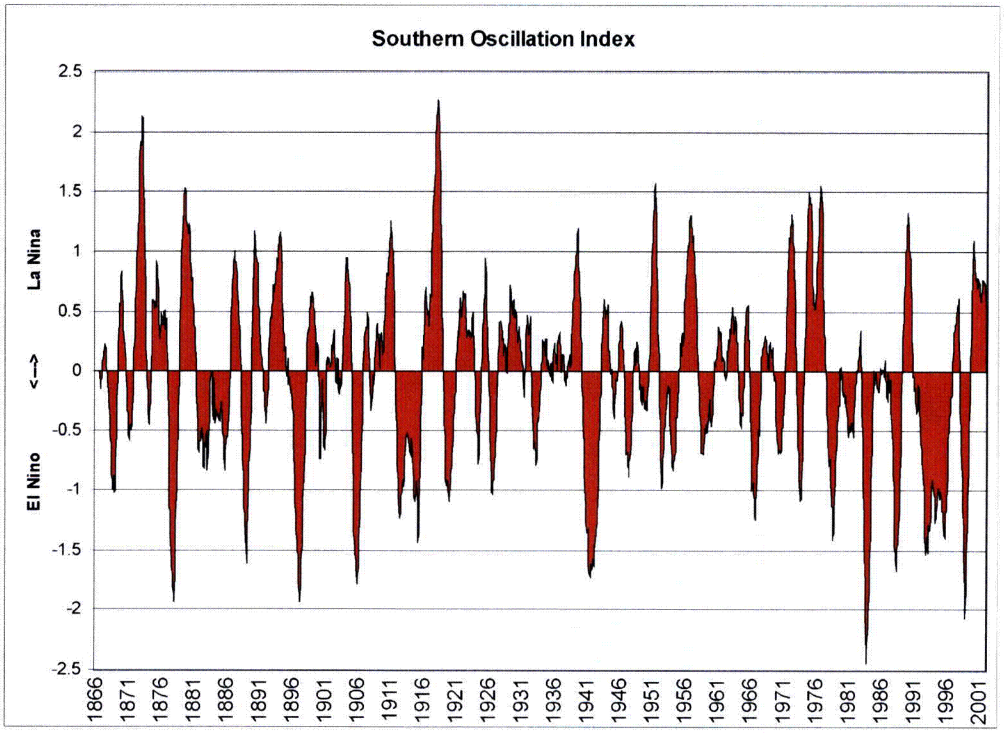

Figure 3-17. Comparison of Rainfall, Streamflow, and Southern Oscillation Index

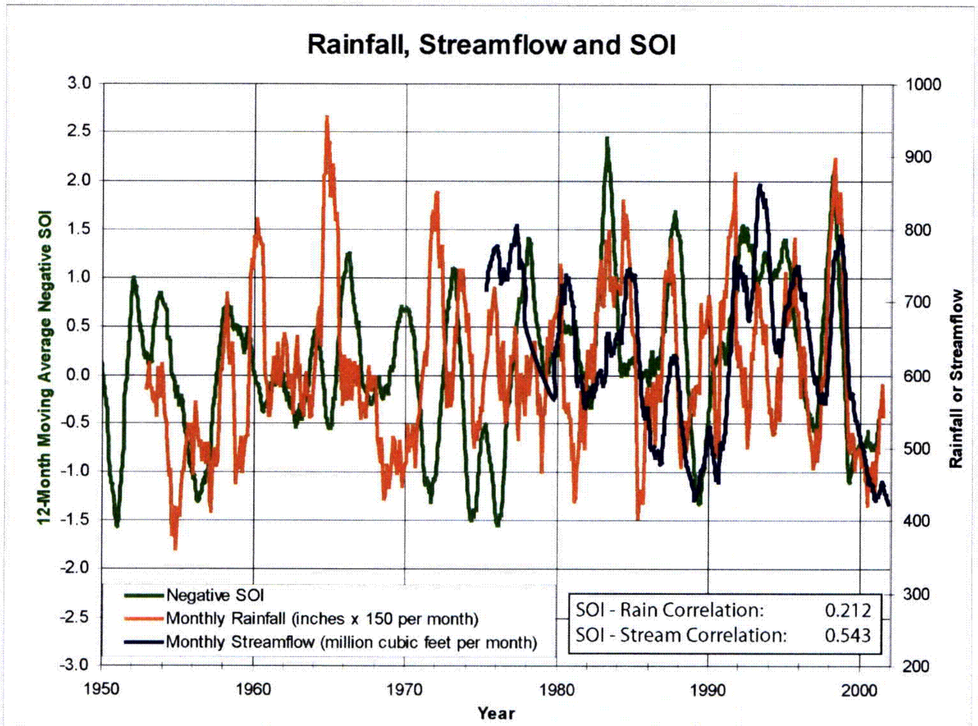

Figure 3-18. Regional Flow Model Calibration Target Locations

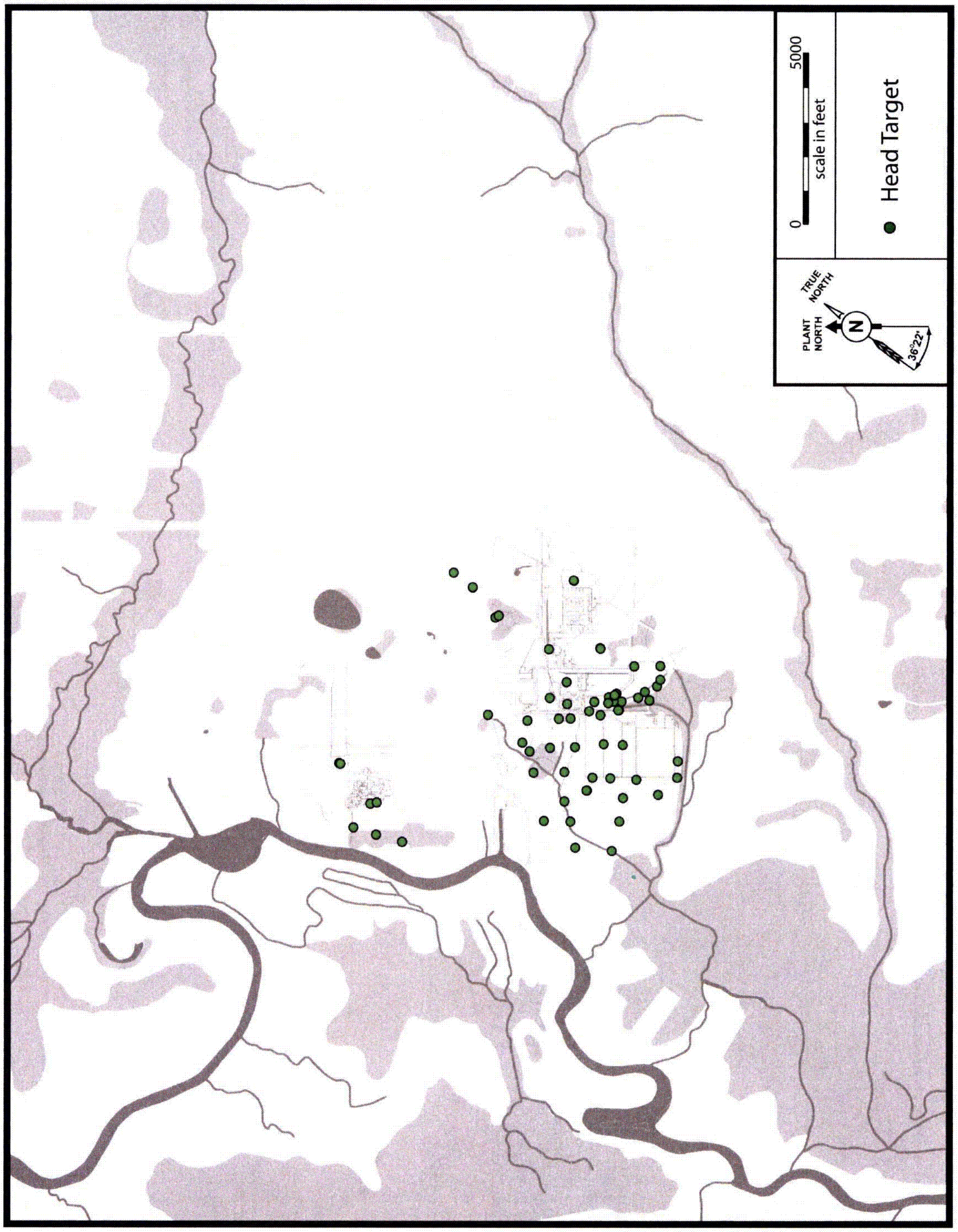

Figure 3-19. USGS Stream Gauge Locations used for Flux Baseflow

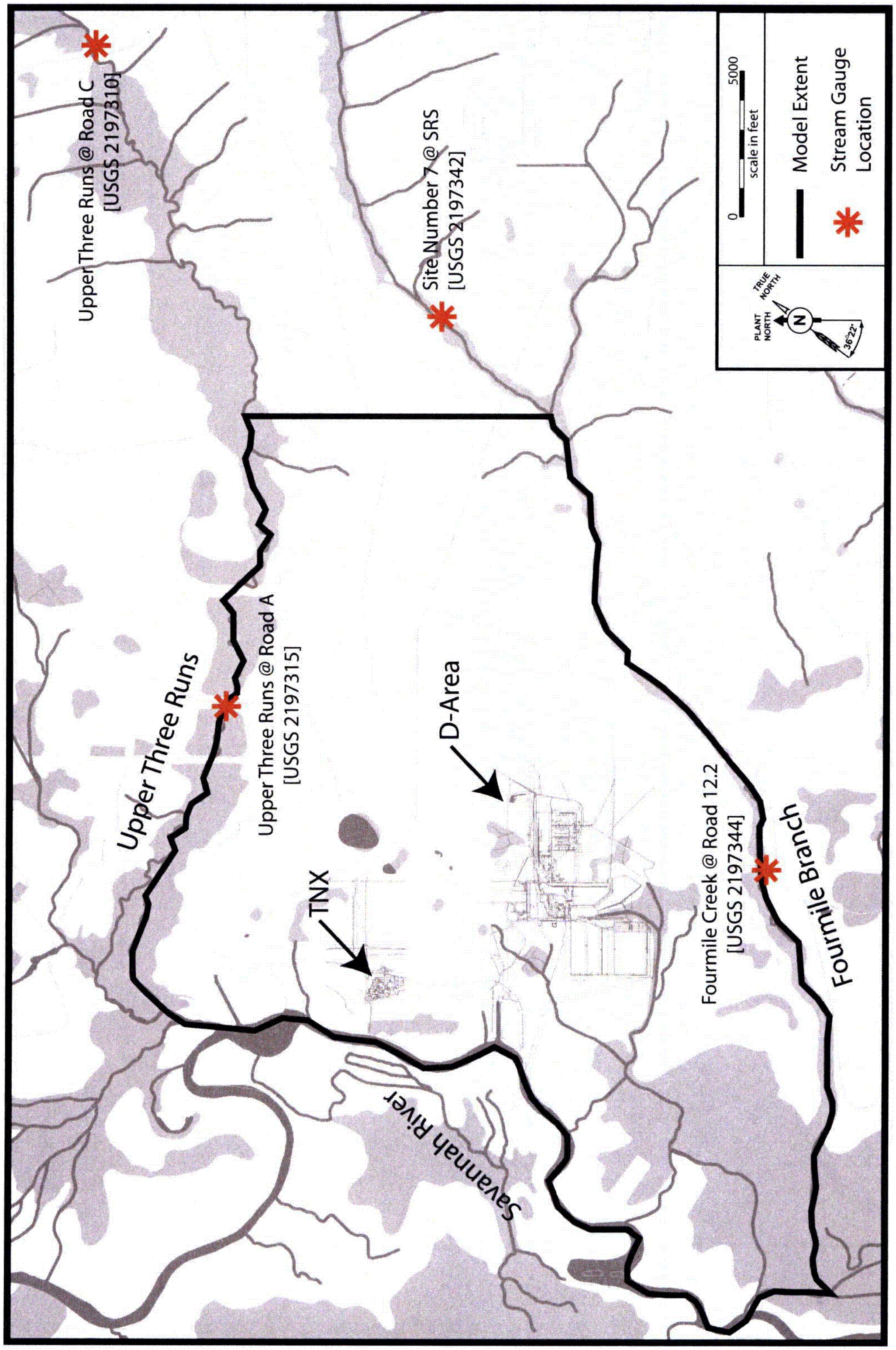

Figure 3-20. Regional Model Calibration Results – Observed versus Model Values

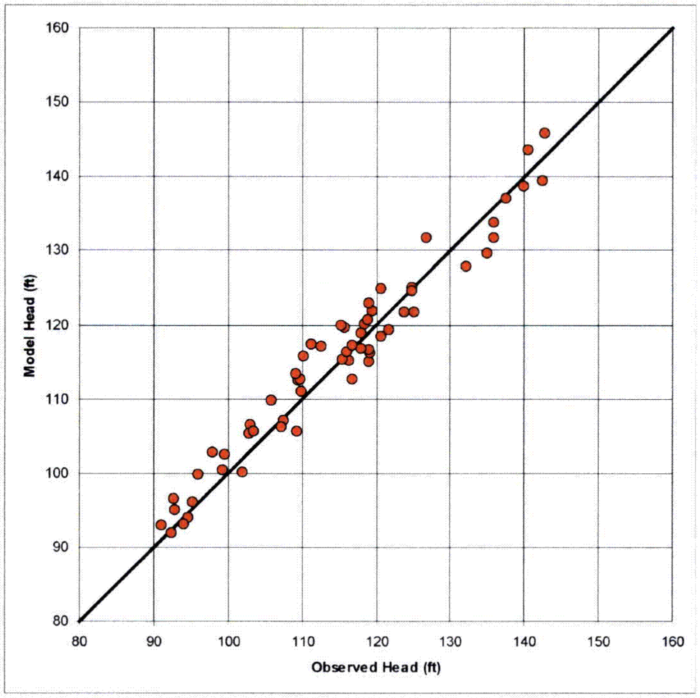

Figure 3-21. Regional Model Calibration Results – Observed versus Residual Values

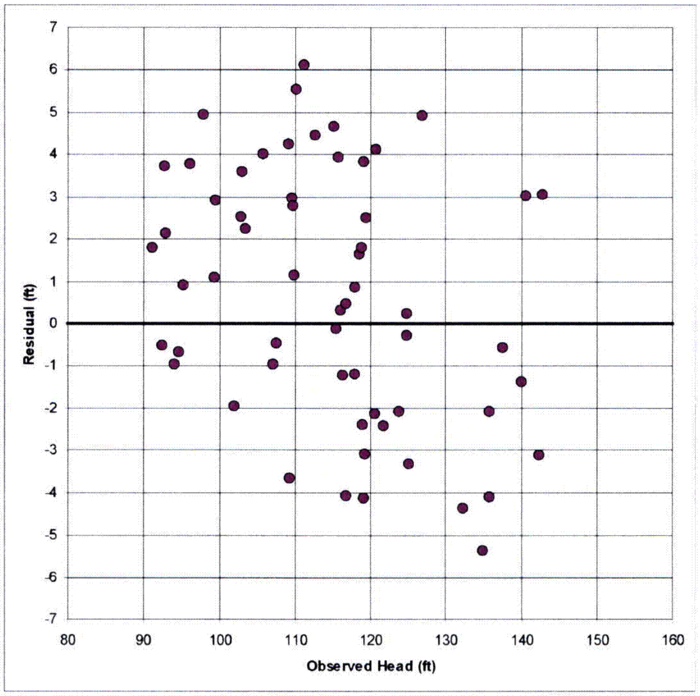

Figure 3-22. Regional Model Calibration Results – Spatial Distribution of Residual Values

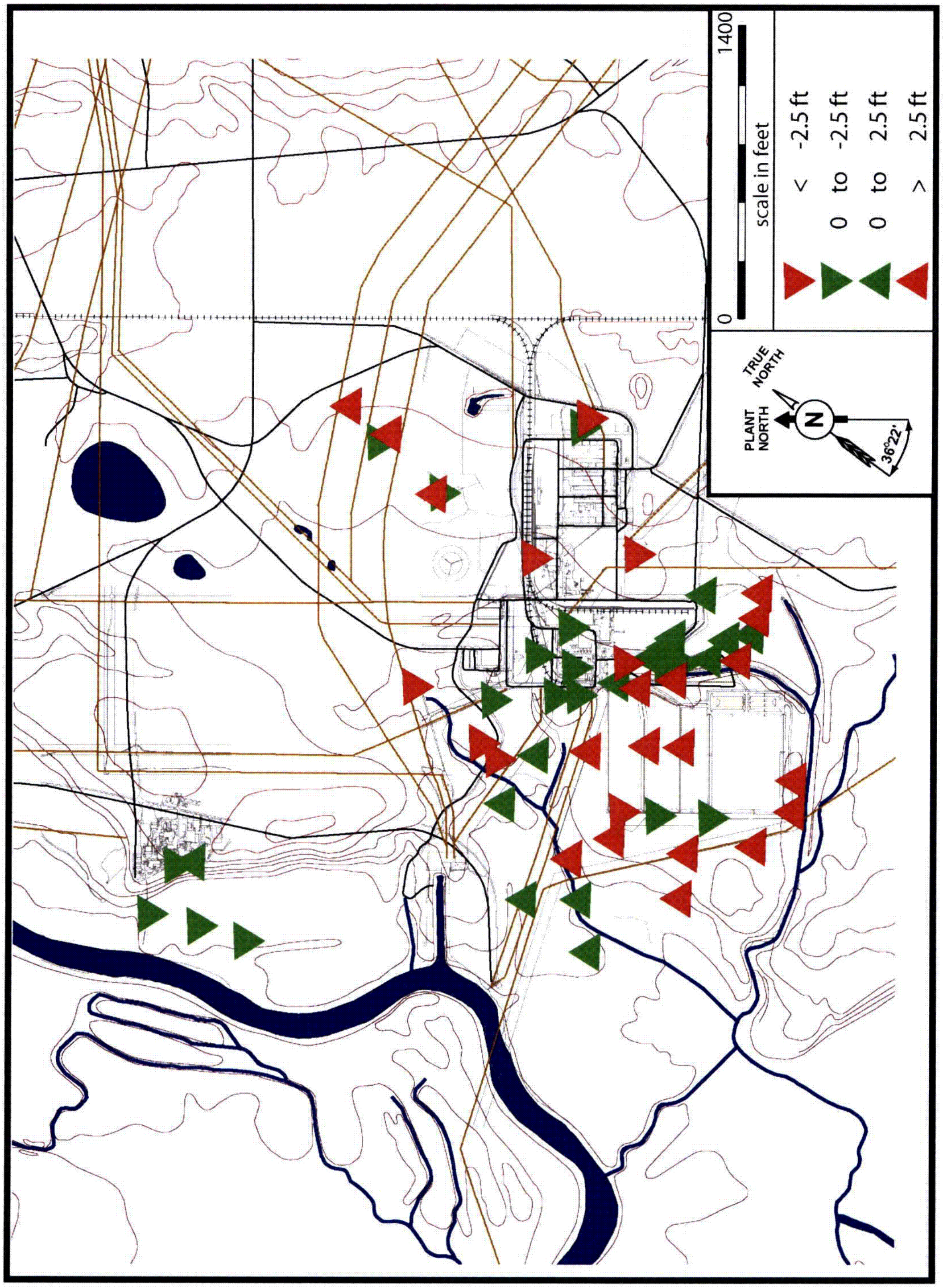

Figure 3-23. Regional Calibrated Model Heads – Layer 1 (UTRA)

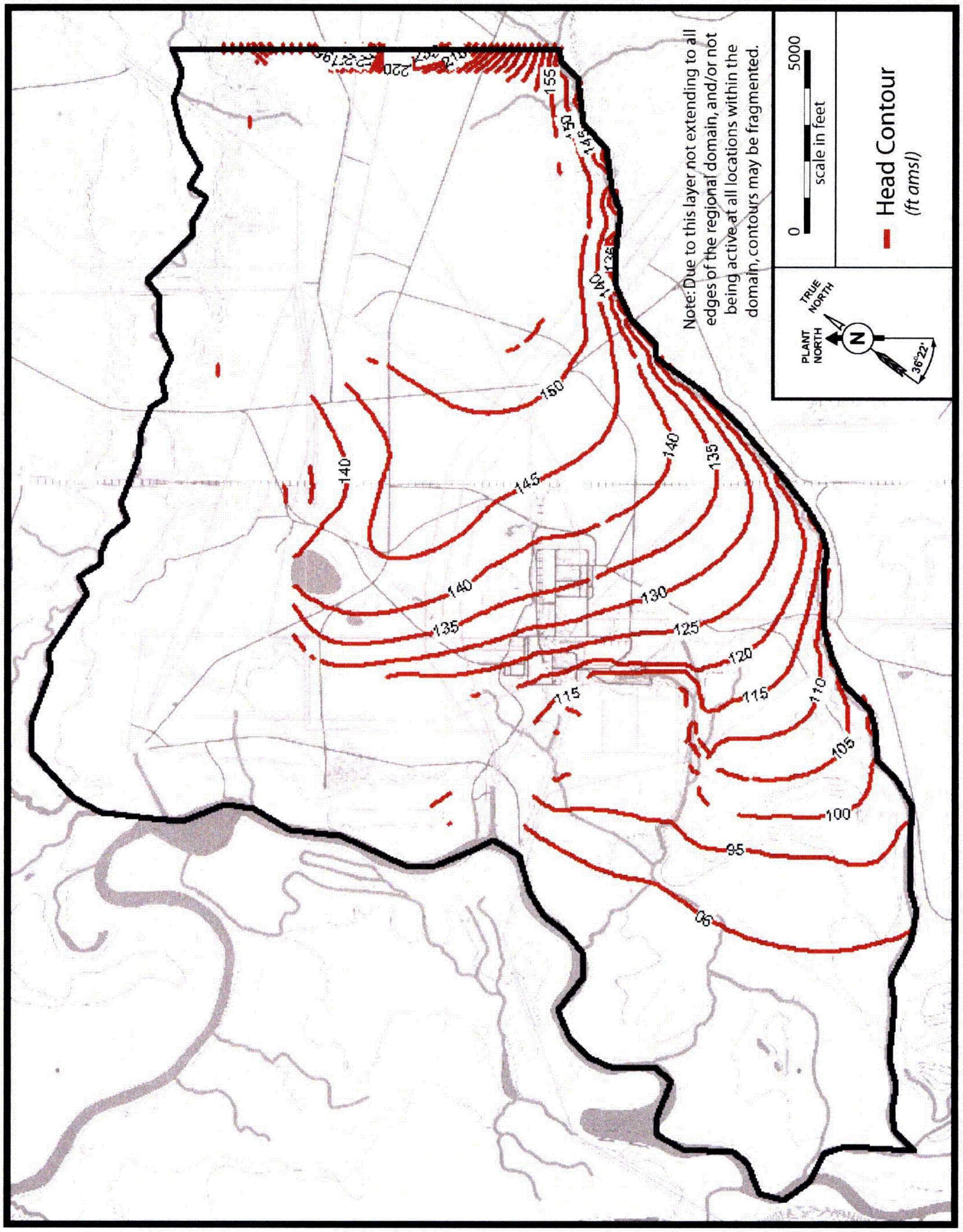

Figure 3-24. Regional Calibrated Model Heads – Layer 2 (UTRA)

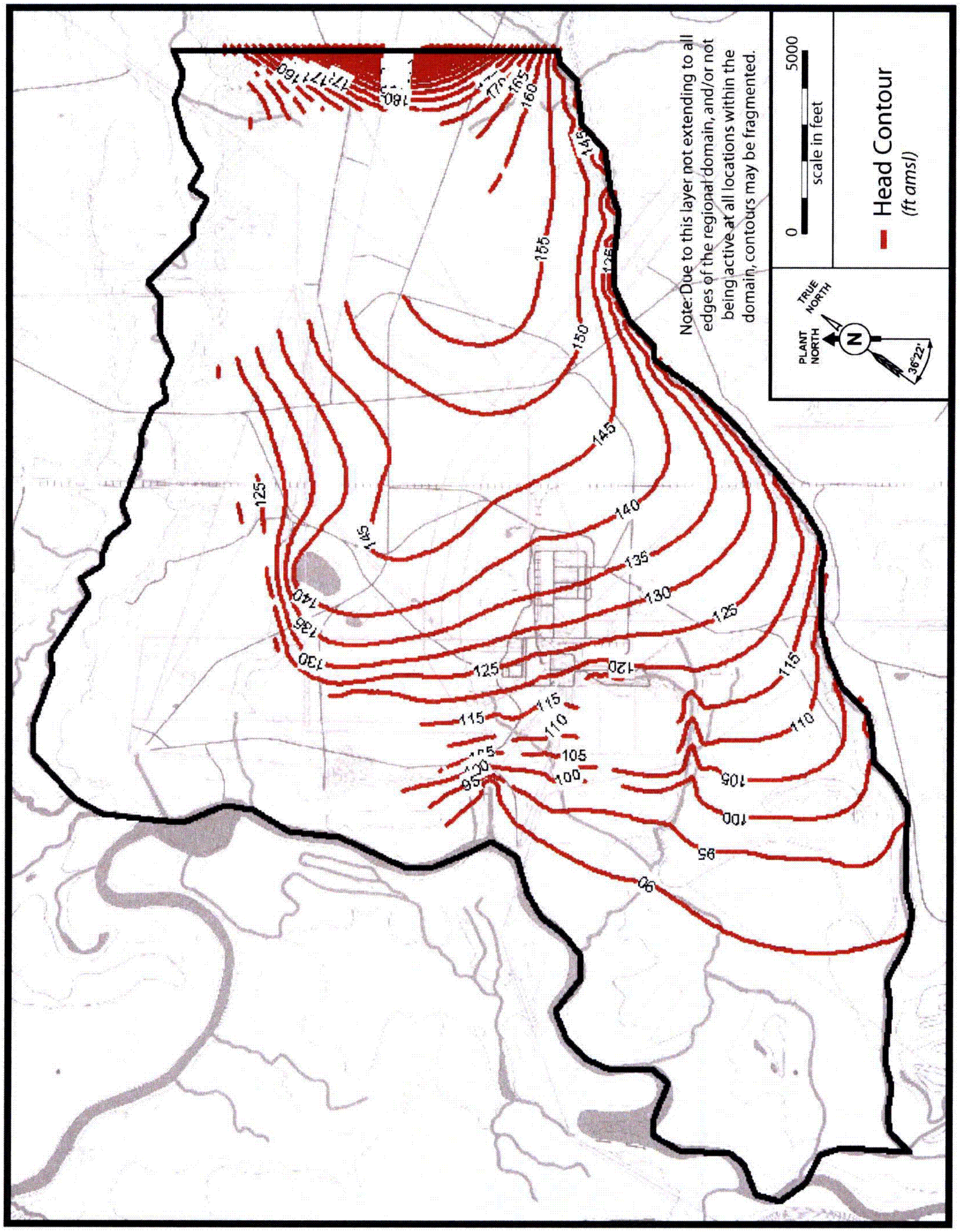

Figure 3-25. Regional Calibrated Model Heads – Layer 3 (UTRA)

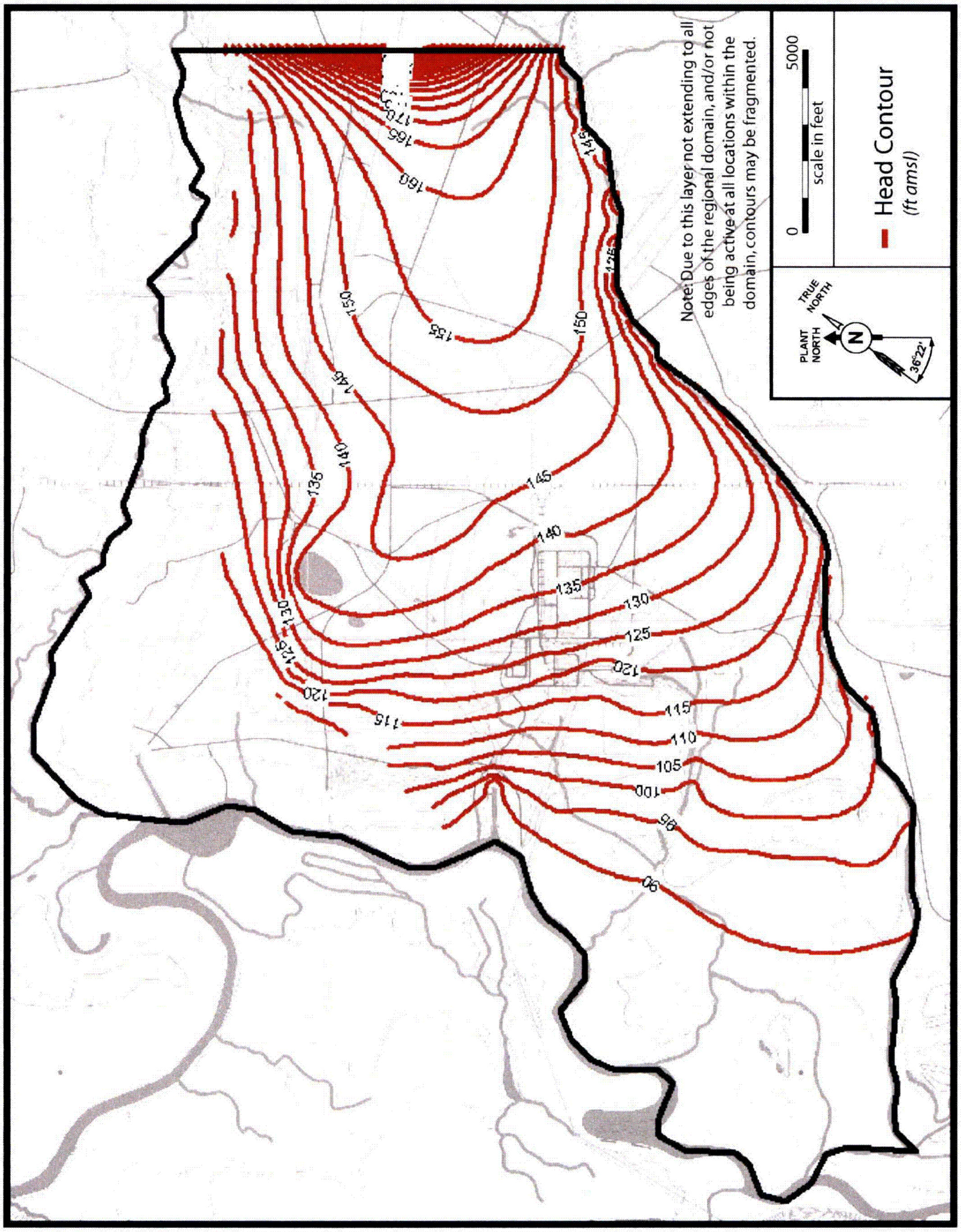

Figure 3-26. Regional Calibrated Model Heads – Layer 4 (GCU)

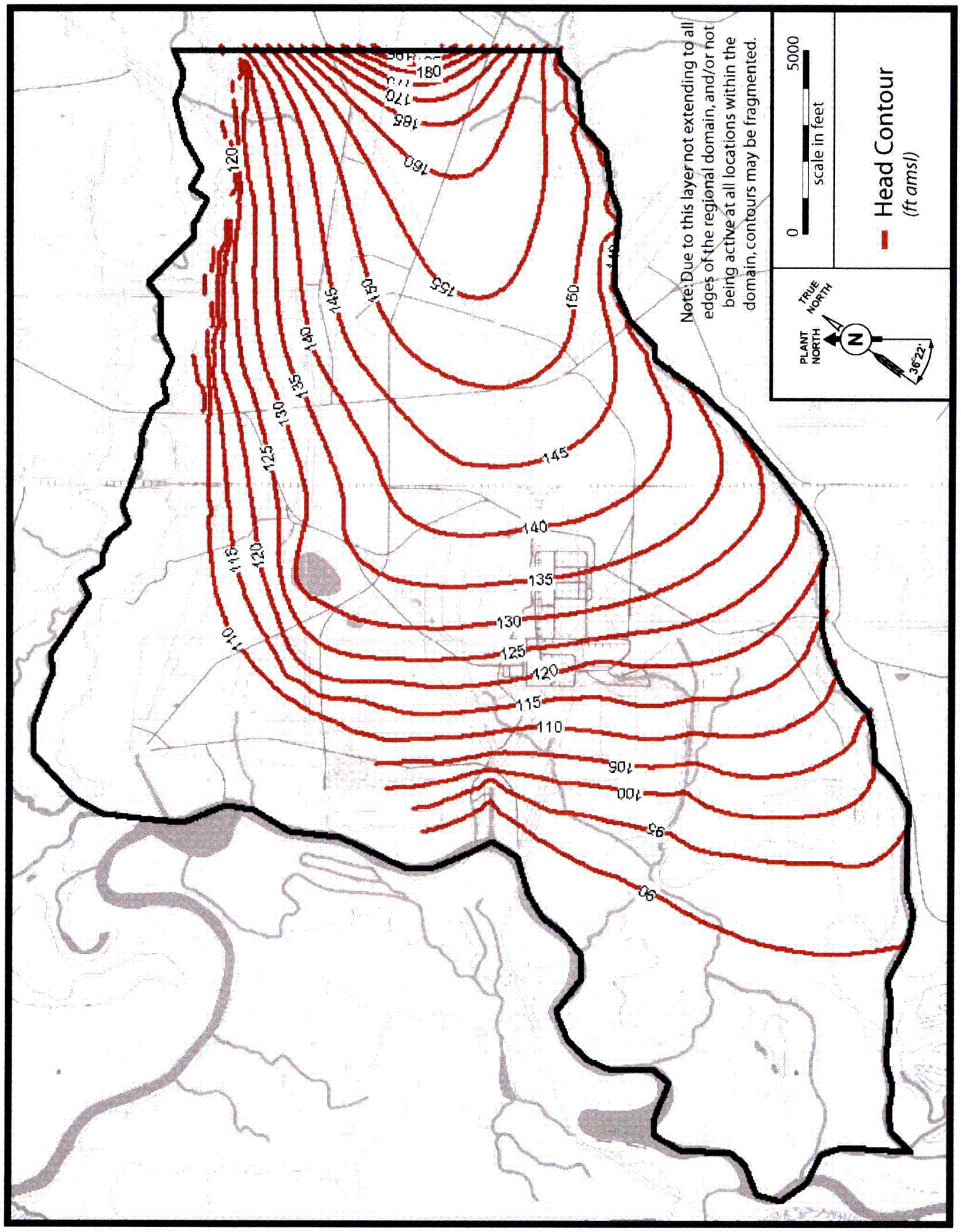

Figure 3-27.   Regional Calibrated Model Heads – Layer 5 (GA)

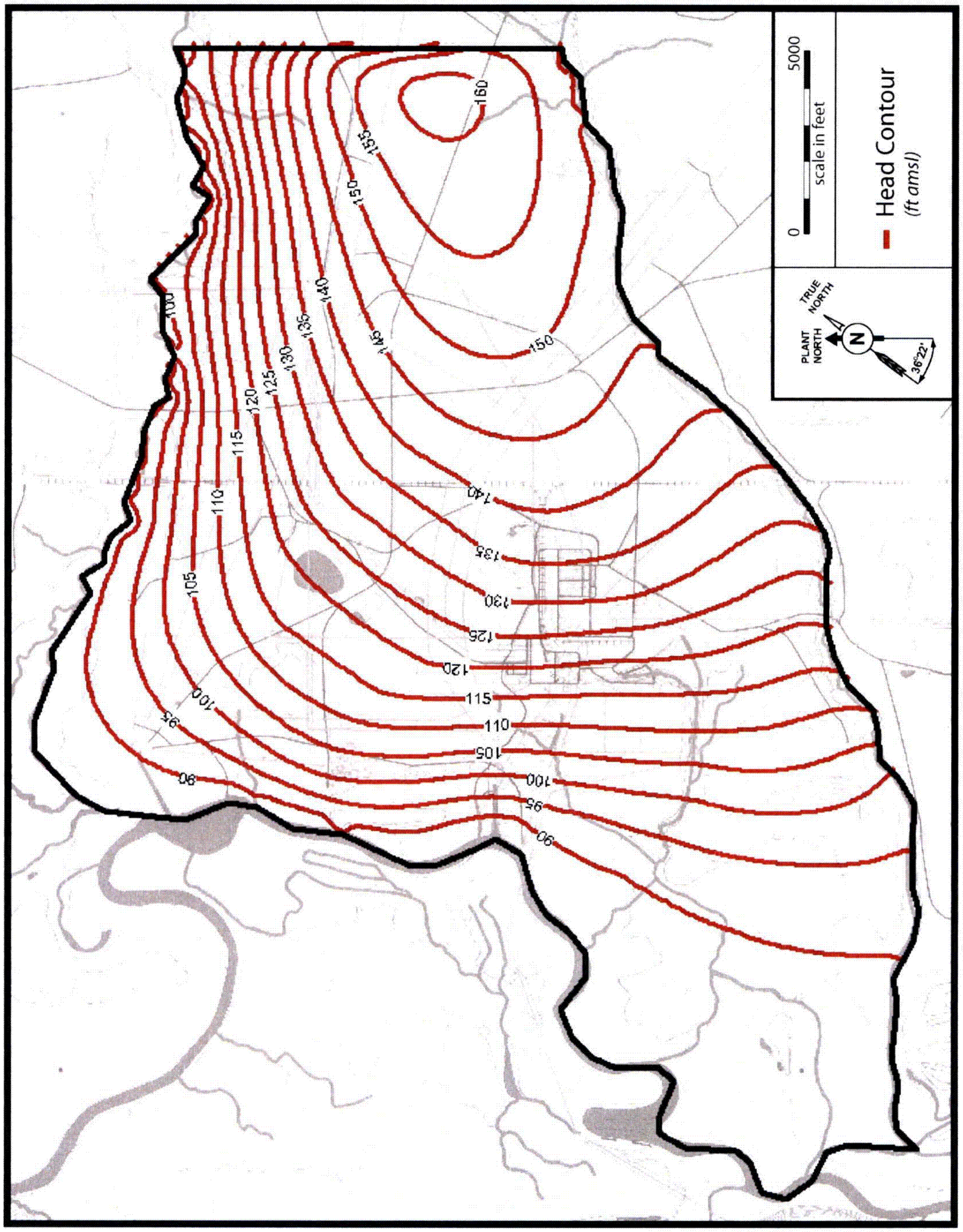

Figure 3-28. Regional Calibrated Model Heads – West-East Cross Section

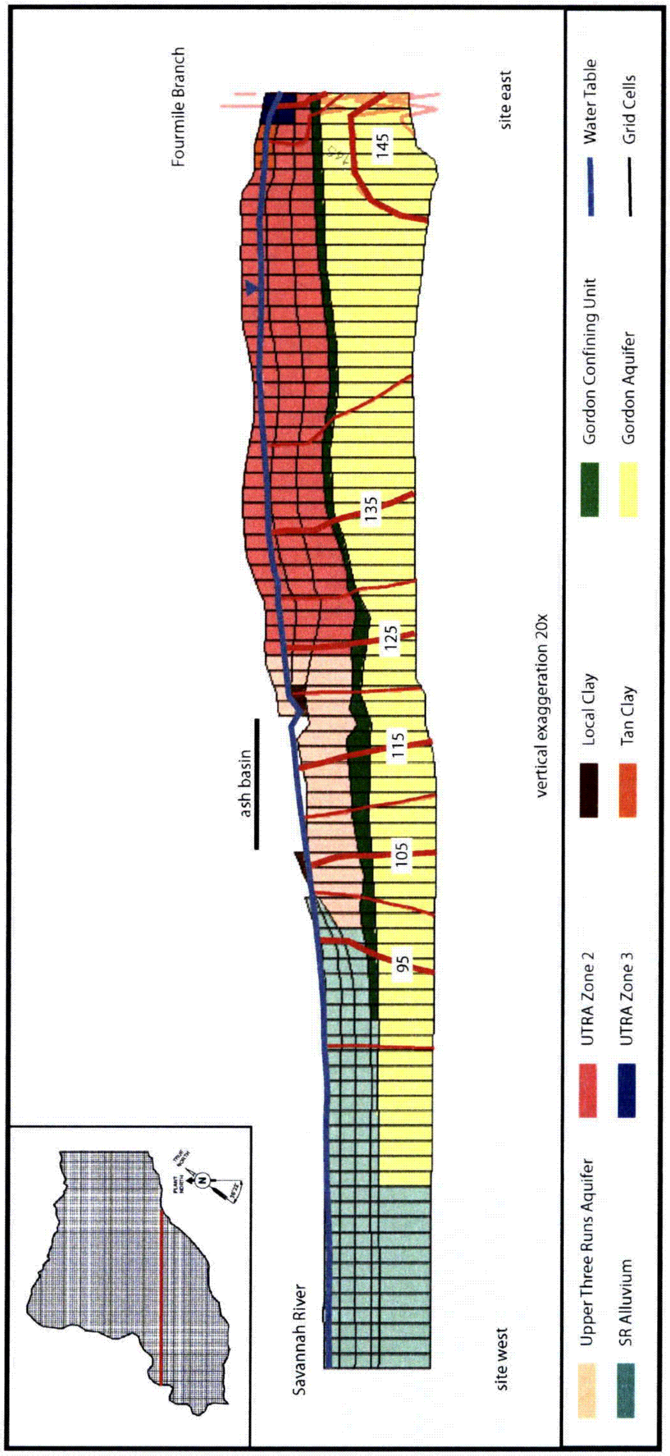

Figure 3-29. Regional Model Particle Tracks

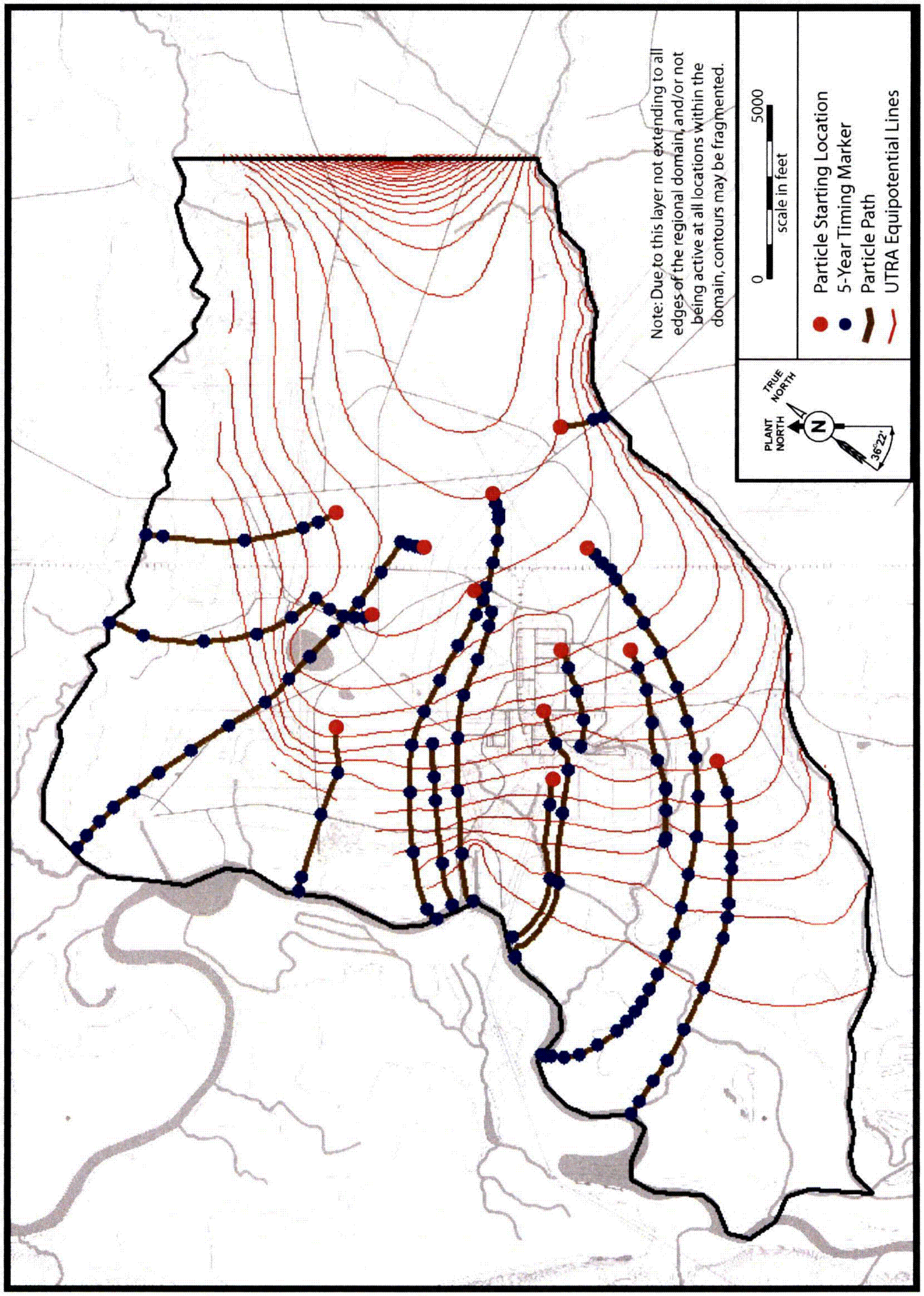

Figure 3-30. Regional Model Particle Tracks – West-East Cross Section

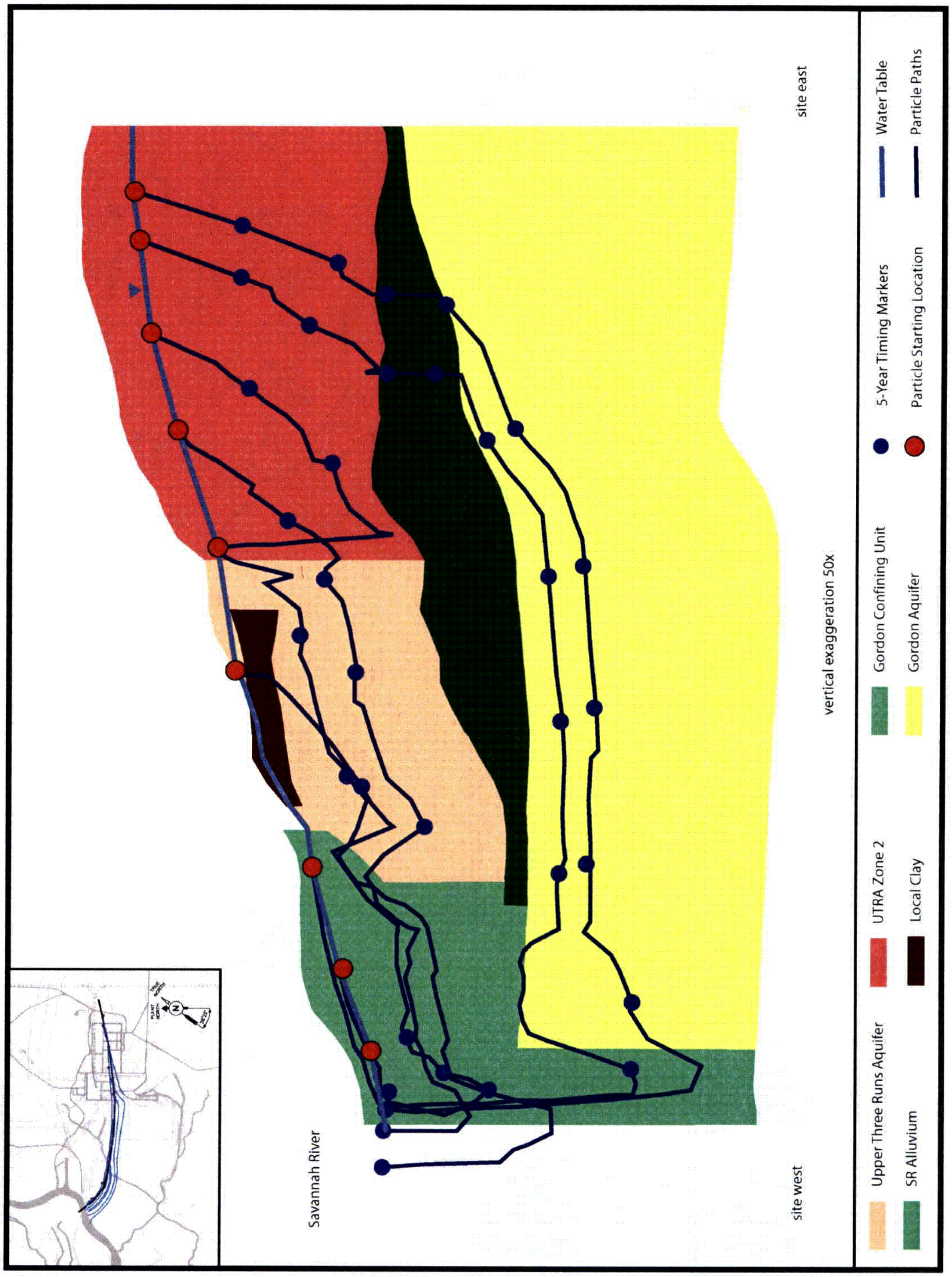

Figure 3-31. Regional Model Flow Budget Diagram

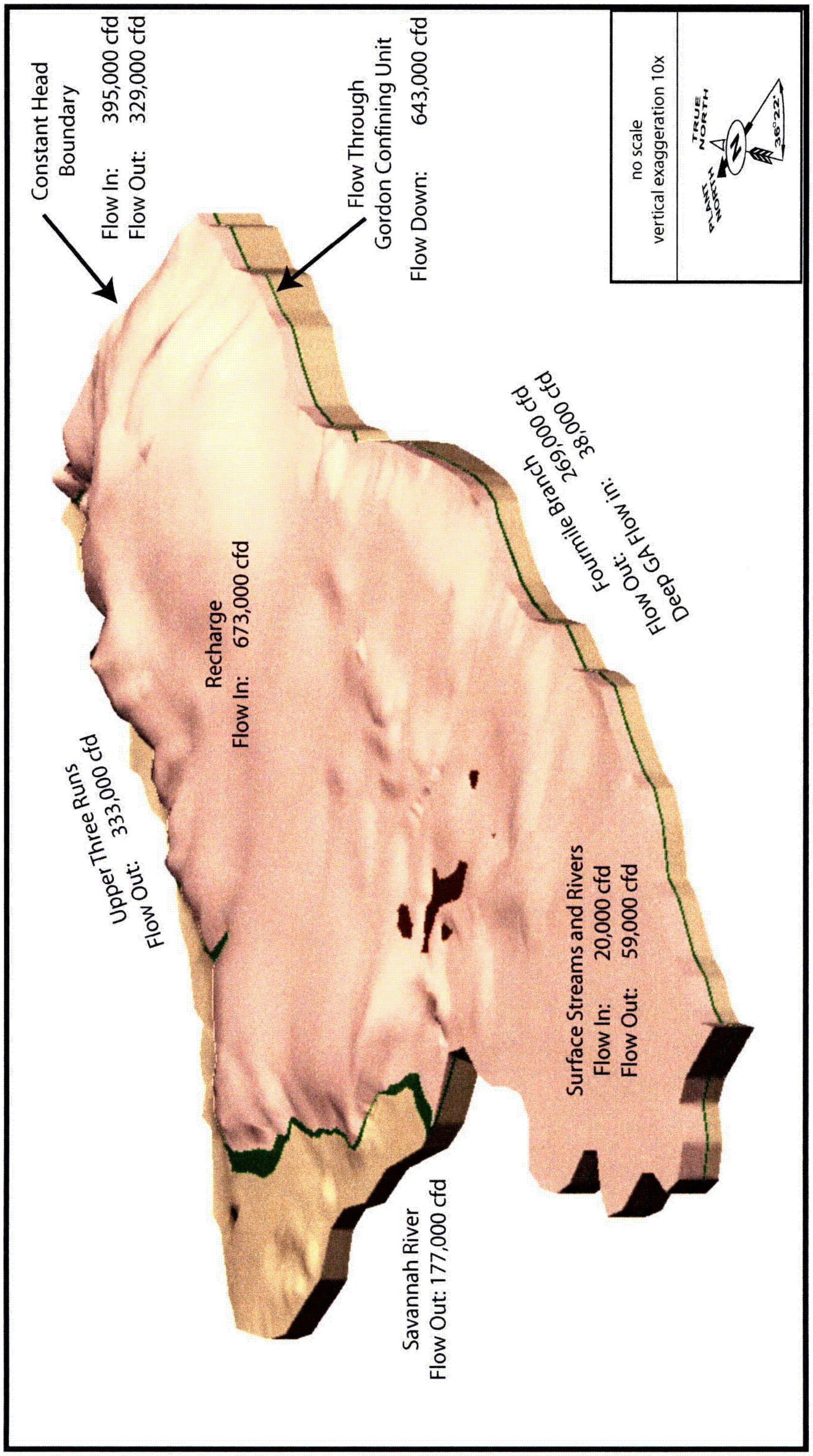

Figure 3-32. Regional Model Sensitivity Particle Track Starting Locations

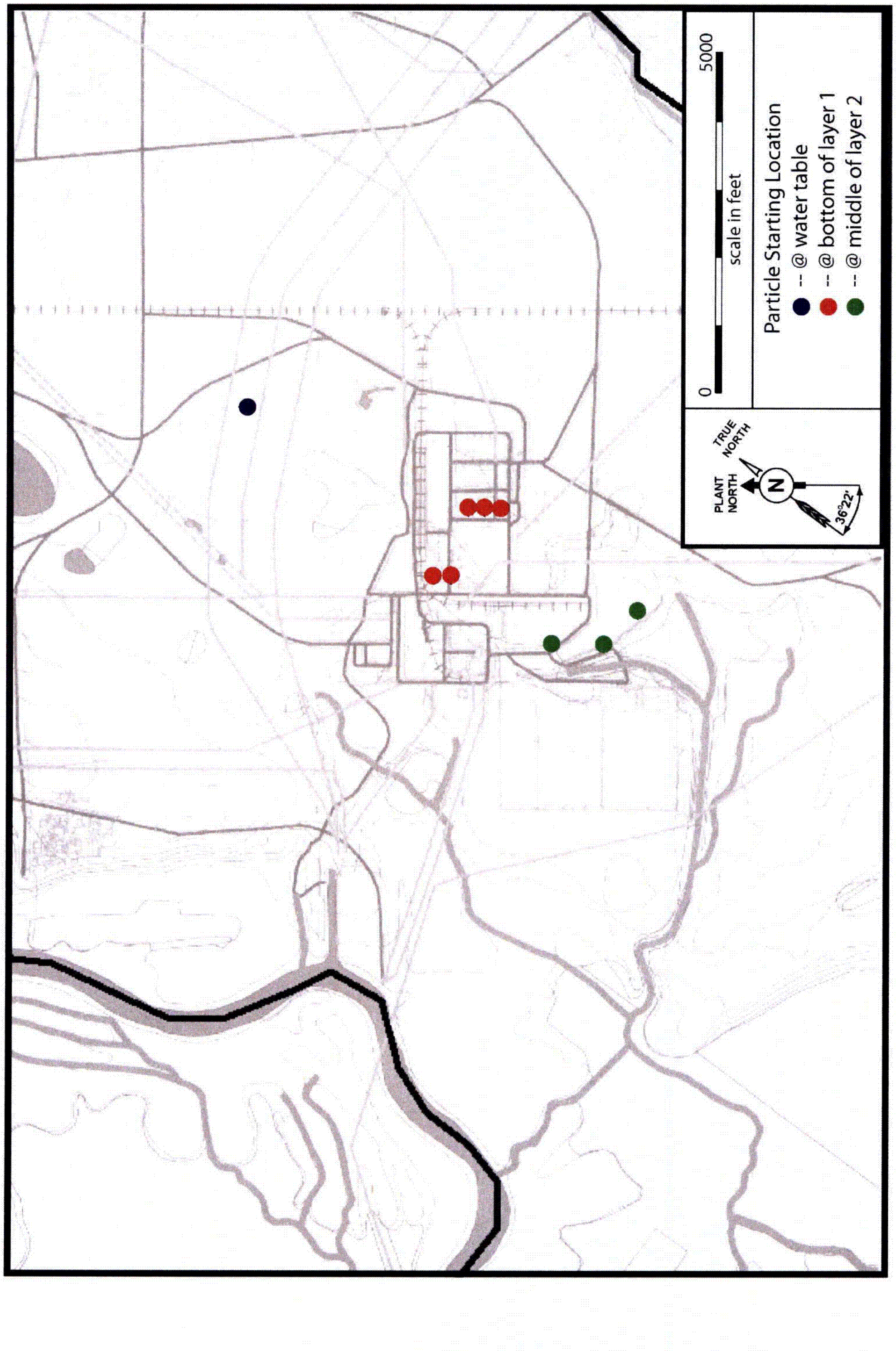

Figure 3-33. Regional Model Sensitivity Particle Track Results – Calibrated Model

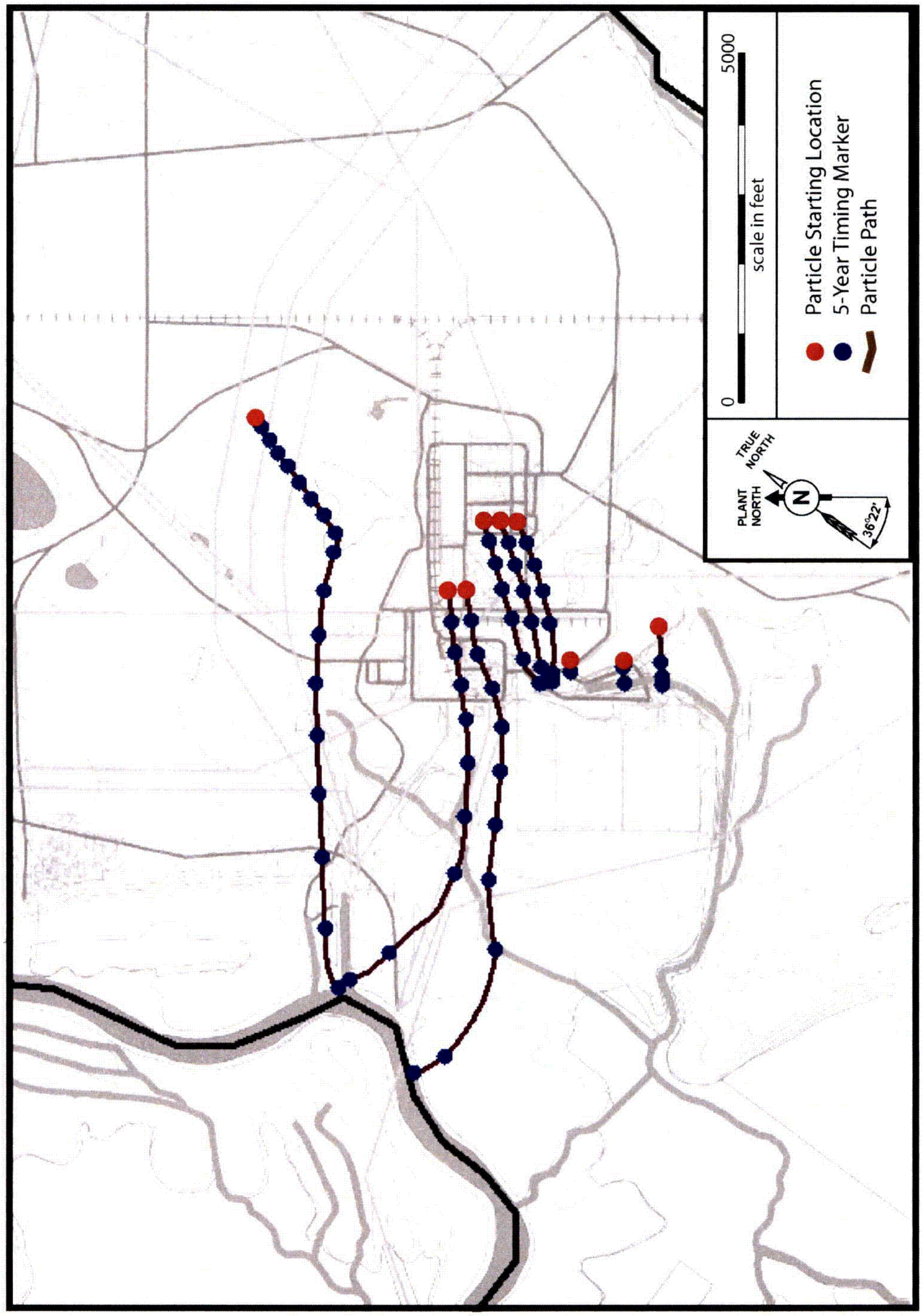

Figure 3-34. Regional Model Sensitivity Results for K_v Parameters

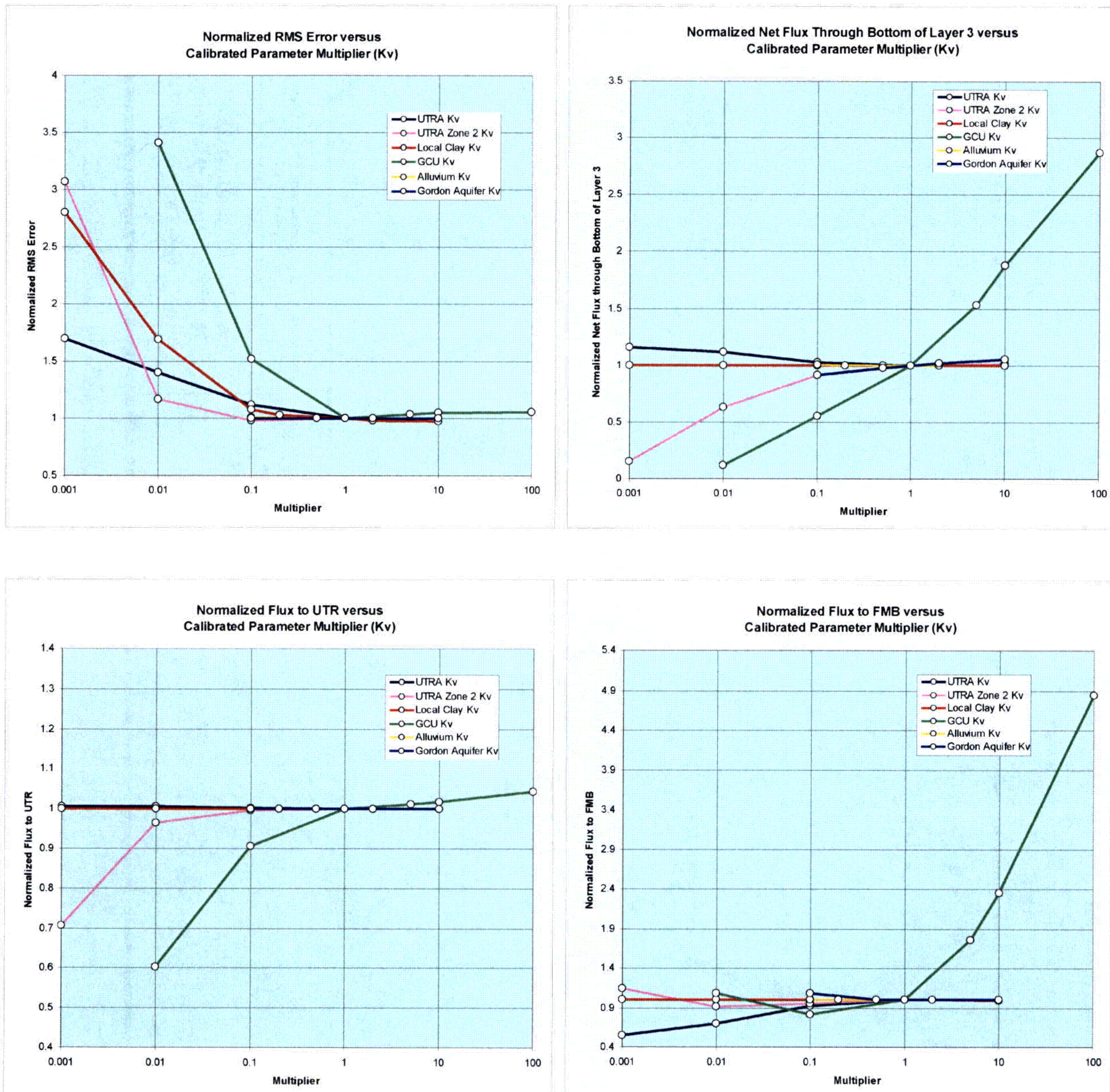

Figure 3-35. Regional Model Sensitivity Results for K_h Parameters

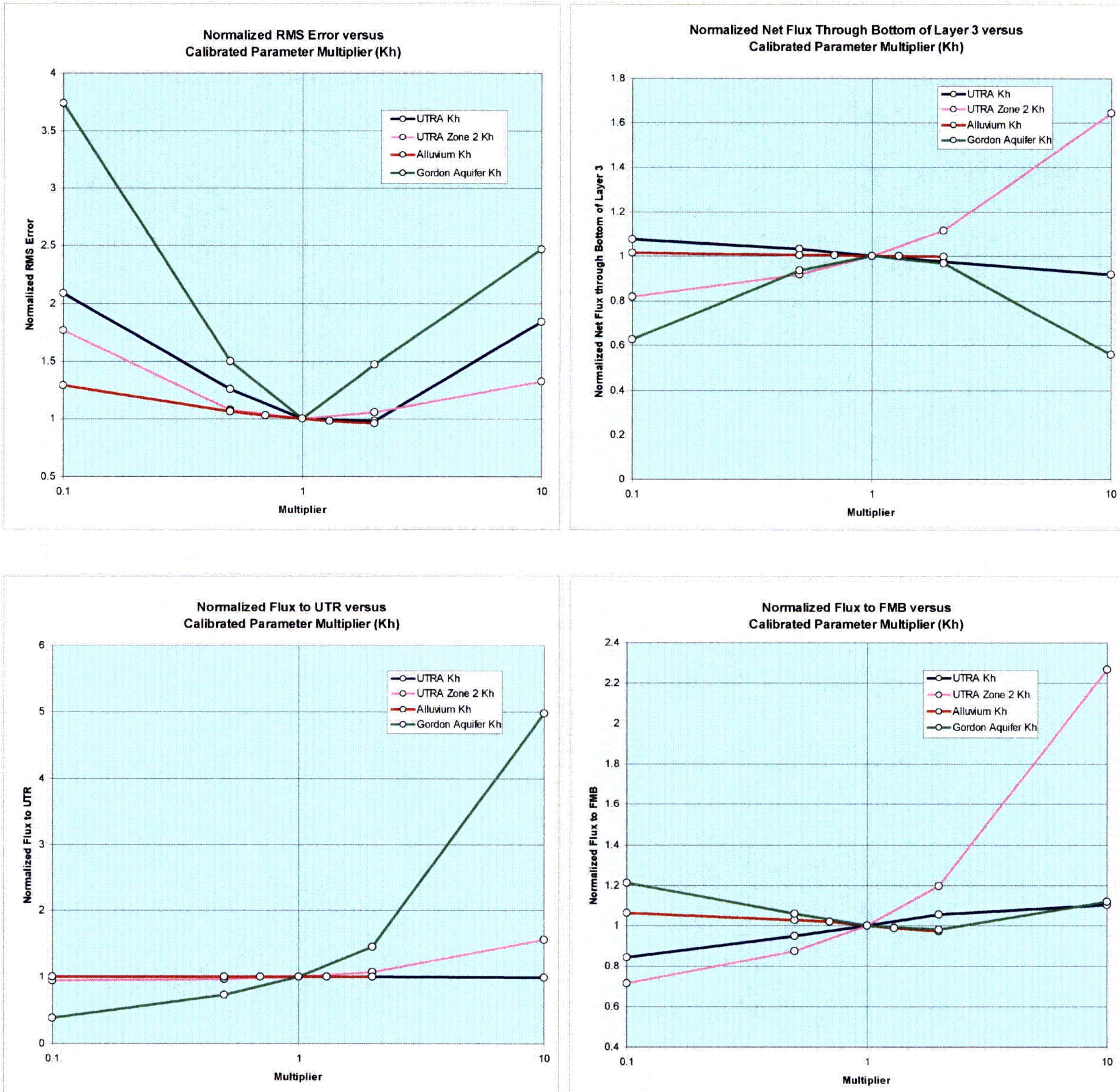

Figure 3-36. Regional Model Sensitivity Results for Recharge Parameters